INVESTIGATION OF DYSFUNCTIONAL AROMATIC AMINO ACID METABOLISM IN OESOPHAGO-GASTRIC CANCER AND LINK TO PHENOL PRODUCTION

Tom Wiggins MBChB MRCS (Eng)

Department of Surgery and Cancer, Imperial College London

St Mary's Hospital, London, UK

2017

A thesis submitted to Imperial College London for the degree of

Doctorate of Philosophy

Supervisors

Professor George B Hanna PhD FRCS

Department of Surgery and Cancer, Imperial College London,

St Mary's Hospital, London, UK

Professor Zoltan Takats PhD

Department of Computational and Systems Medicine, Imperial College London,

London, UK.

THESIS DECLARATION

I hereby declare that I am the sole author of this thesis and all work contained within it is my own. All individuals who collaborated on any sections of the work are appropriately credited.

Tom Wiggins Date: 02/09/2017

COPYRIGHT DECLARATION

The copyright of this thesis rests with the author and is made available under a Creative Commons Attribution Non-Commercial No Derivatives licence. Researchers are free to copy, distribute or transmit the thesis on the condition that they attribute it, that they do not use it for commercial purposes and that they do not alter, transform or build upon it. For any reuse or redistribution researchers must make clear to others the licence terms of this work.

ABSTRACT

Oesophago-gastric cancer is a significant health problem in the United Kingdom. Only 37.6% of patients can be treated with curative intent at the time of diagnosis. The development of non-invasive biomarkers aims to identify patients at early stages of the condition prior to disease spread. Phenol has been proposed as a potential marker of oesophago-gastric cancer in exhaled breath and urine. The nature of origin of this compound is unknown. The aim of this research was to investigate the link between aromatic amino acid metabolism and phenol production in oesophago-gastric cancer; the long term aim being to validate the use of phenol as a non-invasive marker of this disease.

Dried blood spot samples were analysed using nano-electrospray ionisation mass spectrometry to identify intermediary metabolites of aromatic amino acid metabolism. Homogentisate was identified at reduced concentrations in oesophago-gastric cancer patients. These results led to a targeted investigation of enzymes regulating this pathway using quantitative PCR and immunohistochemistry. Homogentisate 1,2 dioxygenase was found to be downregulated in oesophageal cancer tissues.

To investigate phenol production gastric content samples were analysed using gas-chromatography mass spectrometry. Phenol was consistently identified within gastric content samples, and addition of isotope labelled tyrosine indicated that phenol was produced from this aromatic amino acid in gastric juice. Bacterial sequencing identified the presence of phenol producing bacteria within the stomach. Phenol concentrations were significantly increased in the plasma of these patients, providing a transport mechanism for phenol produced in the tumour environment to be excreted by the lungs or kidneys. Urinary analysis also revealed increased concentrations of phenol relative to controls.

This work has indicated that the gastric microbiome may be responsible for conversion of tyrosine to phenol in oesophago-gastric cancer. The underlying mechanism responsible for aromatic amino acid dysfunction has also been identified.

By demonstrating the biological mechanism responsible for phenol production this project has validated the use of this compound as a non-invasive marker of this disease in exhaled breath or urine. These findings will help to introduce the clinical use of phenol as a non-invasive marker for oesophago-gastric cancer risk stratification, thereby increasing the proportion of patients diagnosed at early stages of disease and improving overall survival.

PRIZES, PRESENTATIONS AND PUBLICATIONS

Prizes

1. *December 2014* – 'Dried blood spot analysis for tyrosine metabolites in oesophago-gastric cancer – A pilot study', Division of Surgery 'Best Scientific Poster', Imperial College London.
2. *December 2015* – 'Dried blood spot analysis for targeted investigation of dysfunctional tyrosine metabolism in oesophago-gastric cancer', Division of Surgery 'Best Oral Presentation', Imperial College London.
3. *April 2016* – 'Dried blood spot analysis for targeted investigation of dysfunctional tyrosine metabolism in oesophago-gastric cancer' North East Thames Regional Presentation Day 'Best Oral Presentation', Whipps Cross University Hospital.

Presentations

1. *December 2014* - 'Dried blood spot analysis for tyrosine metabolites in oesophago-gastric cancer – A pilot study', Poster presentation at Division of Surgery Research Afternoon, Imperial College London.
2. *September 2015* – 'Phenol metabolism in oesophago-gastric cancer', Oral presentation at Division of Surgery Symposium, Imperial College London.
3. *December 2015* – 'Dried blood spot analysis for targeted investigation of dysfunctional tyrosine metabolism in oesophago-gastric cancer', Oral presentation at Division of Surgery Research Afternoon, Imperial College London.
4. *April 2016* – 'Dried blood spot analysis for targeted investigation of dysfunctional tyrosine metabolism in oesophago-gastric cancer', Oral presentation at North East Thames Regional Presentation Day, Whipps Cross University Hospital.
5. *September 2016* - 'Use of dried blood spot analysis to guide targeted molecular investigation of homogentisate 1,2 dioxygenase activity in esophageal cancer'. Poster presentation at International Society for Diseases of the Esophagus, Singapore.
6. *January 2017* – 'Dysfunctional tyrosine metabolism in oesophago-gastric cancer and link to phenol production', Oral presentation in Patey Prize Session, Society of Academic & Research Surgery, Dublin.

Publications

1. Wiggins T, Kumar S, Markar SR, Antonowicz S, Hanna GB, 'Tyrosine, Phenylalanine and Tryptophan in Gastroesophageal Malignancy: A Systematic Review', Cancer Epidemiol Biomarkers Prev. 2015 Jan; 24(1): 32-38.
2. Sovova K, Wiggins T, Markar SR, Hanna GB, 'Quantification of phenol in urine headspace using SIFT-MS and investigation of variability with respect to urinary concentration', *Analytical Methods*. 2015 Jun; 7(12): 5134-5141.

ACKNOWLEDGEMENTS

Throughout the period of undertaking this research project I have received support from a large number of individuals who have enabled me to complete this work. I would firstly like to express my gratitude to Professor George Hanna. His support and guidance over the course of this project have been fundamental to the successful completion of this work. I would also like to thank Professor Zoltan Takats who has guided me through complex principles of mass spectrometry and contributed greatly throughout this project. I am very grateful to Sacheen Kumar who has provided me with support and advice during the course of this work. I would also like to thank my fellow Clinical Research Fellows including Stefan Antonowicz, Sheraz Markar, Jeremy Huddy, Nima Abbassi-Ghadi, Hugh Mackenzie and Mina Adam who have all supported me at various stages of this project. I am extremely grateful to the other scientists who have worked with me including Zsolt Bodai, Krystina Sovova, Simon Cameron, Jocelyn Tilner and Verena Horneffer-van der Sluis who have each provided their time and expertise to support this work. I would also like to thank Professor Robert Goldin, Hiromi Kudo and Francesca Rossini for their assistance with the histopathology and immunohistochemistry aspects of this project.

Finally I would like to thank my wife Helen and children Sophie and James. Without the support and patience of my family this work would not have been possible, and I am extremely appreciative of the sacrifices each of them has had to make in order for me to ensure this project was successful.

CONTENTS

ABSTRACT 3
PRIZES, PRESENTATIONS AND PUBLICATIONS 4
LIST OF ABBREVIATIONS 10
LIST OF FIGURES 11
LIST OF TABLES 14
LIST OF SUPPLEMENTARY FIGURES 16
LIST OF SUPPLEMENTARY TABLES 16
CHAPTER 1 - INTRODUCTION 17
1.1 Oesophago-Gastric Cancer 18
1.2 Volatile Organic Compounds 21
1.3 Phenol Production 21
1.4 Aromatic Amino Acid Breakdown 22
1.5 Inborn Errors of Aromatic Amino Acid Metabolism 23
1.5.1 Phenylketonuria 23
1.5.2 Tyrosinaemia 23
1.5.3 Alkaptonuria 24
1.6 Systematic Review – Aromatic Amino Acids and Phenol in Oesophago-Gastric Cancer 25
1.6.1 Introduction 25
1.6.2 Methods 25
1.6.3 Results 27
1.6.4 Discussion 41
1.7 Conclusions from Systematic Review 45
1.8 Thesis Aims 46
CHAPTER 2 - METHOD DEVELOPMENT 47
2.1 Phenol GC-MS Method Development 48
2.1.1 Objective 48
2.1.2 Introduction 48
2.1.3 Method Development 50
2.1.4 Conclusions 61
2.2 Solid Phase Micro-Extraction Method Development for GC-MS 62
2.2.1 Objective 62
2.2.2 Introduction 62
2.2.3 Method Development 62
2.2.4 Conclusions 74
2.3 Direct Liquid Injection Method Development for GC-MS 75
2.3.1 Objective 75
2.3.2 Introduction 75
2.3.3 Method Development 76
2.3.4 Conclusions 92
2.4 LC-MS Method Development 93

2.4.1 Objective 93
2.4.2 Introduction 93
2.4.3 Method Development 95
2.4.4 Conclusions 114
CHAPTER 3 - AMINO ACID METABOLISM IN OESOPHAGO-GASTRIC CANCER 116
3.1 Nano-electrospray Ionisation Mass Spectrometry Dried Blood Spot Analysis 117
3.1.1 Objective 117
3.1.2 Introduction 117
3.1.3 Methods 118
3.1.4 Results 120
3.1.5 Discussion 134
3.1.6 Conclusion 137
3.2 In Silico Analysis 138
3.2.1 Objectives 138
3.2.2 Introduction 138
3.2.3 Methods 139
3.2.4 Results 139
3.2.5 Discussion 141
3.2.6 Conclusion 142
3.3 Quantitative PCR 143
3.3.1 Objectives 143
3.3.2 Introduction 143
3.3.3 Methods 144
3.3.4 Results 146
3.3.5 Discussion 153
3.3.6 Conclusions 154
3.4 Immunohistochemistry 155
3.4.1 Objectives 155
3.4.2 Introduction 155
3.4.3 Methods 155
3.4.4 Results 156
3.4.5 Discussion 161
3.4.6 Conclusions 163
3.5 Conclusions of Amino Acid Experimental Section 164
CHAPTER 4 - PHENOL METABOLISM IN OESOPHAGO-GASTRIC CANCER 169
4.1 Urine GC-MS 170
4.1.1 Objective 170
4.1.2 Introduction 170
4.1.3 Methods 171
4.1.4 Results 172
4.1.5 Discussion 181
4.1.6 Conclusion 183

4.2 Plasma GC-MS 184
4.2.1 Objective 184
4.2.2 Introduction 184
4.2.3 Methods 185
4.2.4 Results 186
4.2.5 Discussion 189
4.2.6 Conclusion 189
4.3 Tissue GC-MS 190
4.3.1 Objective 190
4.3.2 Introduction 190
4.3.3 Methods 191
4.3.4 Results 192
4.3.5 Discussion 192
4.3.6 Conclusion 193
4.4 Gastric Content Analysis 194
4.4.1 Objective 194
4.4.2 Introduction 194
4.4.3 Methods 195
4.4.4 Results 197
4.4.5 Discussion 201
4.4.6 Conclusion 203
4.5 Enrichment of Gastric Juice with Deuterated Tyrosine 204
4.5.1 Objective 204
4.5.2 Introduction 204
4.5.3 Methods 205
4.5.4 Results 206
4.5.5 Discussion 208
4.4.6 Conclusion 209
4.6 Identification of Phenol-Producing Bacteria within the Stomach. 210
4.6.1 Objectives 210
4.6.2 Introduction 210
4.6.3 Methods 211
4.6.4 Results 212
4.6.5 Discussion 212
4.6.6 Conclusions 214
4.7 Conclusions of Phenol Experimental Section 215
CHAPTER 5 - SUMMARY, CONCLUSIONS AND FUTURE WORK 216
APPENDIX 1: SUPPLEMENTARY FIGURES 230
APPENDIX 2: SUPPLEMENTARY TABLE 238
APPENDIX 3: ETHICAL APPROVALS 239

FUNDING STATEMENT

This research was funded by the Royal College of Surgeons One Year Research Fellowship (Freemason's Surgical Research Fund) – Value £58,372.

LIST OF ABBREVIATIONS

AQC – Aminoquinolyl-n-hydroxysuccinimidyl carbamate
CT – Computerised tomography
DNPH – 2,4-Dinitrophenylhydrazine
EDTA – Ethylenediaminetetraacetic acid
FAH – Fumarylacetoactate hydroxylase
g – Times gravity OR grams
GC-MS – Gas chromatography mass spectrometry
H & E – Hematoxylin and eosin stain
HCl – Hydrochloric acid
HGD – Homogentisate 1,2 dioxygenase
HPD – Hydroxyphenylpyruvate dioxygenase
HPLC – High-performance liquid chromatography
Hom – Homogentisate
HS – Head space.
Hydrox - Hydroxyphenylpyruvate
IHC – Immunohistochemistry
IQR – Inter-quartile range
LC-MS – Liquid chromatography mass spectrometry
LOD – Limit of detection
LOQ – Limit of quantification
MAAI – Maleylacetoacetate isomerase
ME – Matrix effect
MRM – Multiple Reaction Monitoring
MW – Molecular weight
m/z – Mass-to-charge ratio
MWU – Mann-Whitney U
NaCl – Sodium Chloride
NMR – Nuclear magnetic resonance
N.P.I –Normalised peak intensity
OGD – Oesophago-gastroduodenoscopy (upper gastrointestinal endoscopy)
PAH – Phenylalanine Hydroxylase
PE – Process efficiency
Phe - Phenylalanine
Ppbv – Parts per billion by volume
PTFE - Polytetrafluoroethylene
qPCR – Quantitative polymerase chain reaction
RE – Recovery of extraction process
ROC – Receiver operating characteristic
S/N – Signal to noise ratio
SIFT-MS – Selected ion flow tube mass spectrometry
SIR – Selected ion recording
SPE – Solid phase extraction
SPME – Solid phase micro-extraction
TAT – Tyrosine Aminotransferase
ToF – Time-of-flight
Tyr - Tyrosine
UPLC – Ultra-performance liquid chromatography
VOC – Volatile organic compound

LIST OF FIGURES

Figure 1: Phenylalanine and tyrosine metabolic pathway. **22**
Figure 2: PRISMA diagram for aromatic amino acid studies (A) and phenol studies (B) **28**
Figure 3: Assessment of risk of bias (A) and applicability concerns (B): **30**
Figure 4: Outline of a typical GC-MS system showing compounds entering the injector (A) then becoming retained upon the chromatographic column (B). As oven temperature is gradually increased compounds lose affinity for the column at a specific retention time and travel to the downstream mass spectrometer to be detected. **49**
Figure 5: Initial temperature programmes for GC-MS analysis. A - 20°C/min, B- 15°C/min, C-10°C/min **51**
Figure 6: Separation of all compounds on new column using above temperature methods. Compound elution times as follows: Phenol 6.60 minutes, 2-ethylphenol 6.80 minutes, p-cresol 6.88 minutes, m-cresol 6.92 minutes, 4-ethylphenol 7.28 minutes, 3-ethylphenol 7.32 minutes. **53**
Figure 7: Phenol and o-cresol eluting at 10.54 and 10.60. **54**
Figure 8: Optimised temperature programme. **54**
Figure 9: The full scan chromatogram for phenol peak is shown in A. When SIR for phenol m/z of 94 was used (B) peak shape was seen to improve and overall baseline is reduced. Although the mass spectrum for phenol in full scan mode (C) contained a greater number of ions the critical ions for phenol identification could still be assessed using SIR as shown in D. **57**
Figure 10: SIR scanning for the m/z of Phenol D6 (m/z 99; elution time 10.57) and phenol (m/z 94, elution time 10.58). **59**
Figure 11: A – Phenol calibration curve (94:99 ratio versus phenol concentration up to 20ug/ml phenol); B – P-Cresol calibration curve (107:99 ratio versus p-Cresol concentration up to 20ug/ml phenol). **60**
Figure 12: Phenol peak area with equilibration times of 10 minutes, 20 minutes and 30 minutes. **64**
Figure 13: Phenol peak area with increasing SPME extraction temperature at 30°C, 45°C and 60°C. **65**
Figure 14: Increasing phenol peak area with lengthening of SPME extraction time. **67**
Figure 15: Increasing phenol peak area with increasing salination of samples. **69**
Figure 16: Little change in phenol peak area with changes in pH. **71**
Figure 17: Greatly increased phenol peak area following urine hydrolysis. **72**
Figure 18: Schematic diagram of the SPE process. **76**
Figure 19: Best phenol recovery with BondElut PPL tubes (71% recovery). **79**
Figure 20: Percentage recovery and peak area for different elution solvents. **80**
Figure 21: Cumulative percentage recovery with increasing elution volume. **81**
Figure 22: Assessment of sample evaporation. **83**
Figure 23: Wash step optimisation. A – Optimisation with different quantities of methanol in wash. B – Optimisation by changing the pH in the wash. **85**
Figure 24: Phenol recovery at various starting concentrations. **86**
Figure 25: A: General LC-MS setup showing mobile phases (A & B), pumps to regulate mobile phase, autosampler where samples are introduced, column (including packing of stationary phase and mass spectrometer. B: During aqueous phase compounds become affixed to column. C: As proportion of organic phase (B) increases compounds gradually lose affinity for the column at different elution times. **94**
Figure 26: A – Details of mobile phase gradient. B-E: Chromatograms for phenylalanine (B), tyrosine (C), hydroxyphenylpyruvate (D) and homogentisate (E). **98**
Figure 27: A: Details of mobile phase gradient. B: Visual representation of gradient. **100**
Figure 28: Chromatography with good separation of all compounds. **101**
Figure 29: Optimisation of capillary voltage with 2kV providing the largest peak area for all compounds. **102**
Figure 30: Demonstrating effect of desolvation temperature on peak area with 600°C providing the largest peak area for three out of four compounds. **103**
Figure 31: Desolvation flow of 1000L/hour providing the largest peak area for all compounds except phenylalanine. **104**
Figure 32: Variable peak areas with changes in cone flow, but greatest homogentisate peak area with cone flow of 150L/hr. **105**
Figure 33: Linear calibration curves for all compounds. **106**
Figure 34: Distortion of tyrosine peak shape when injecting from methanol. **109**

Figure 35: Linear calibration curve for tyrosine quantification (using D4 tyrosine as internal standard) up to 50µM. **111**
Figure 36: Peak at 6.28 minutes when scanning for m/z 301 in hydroxyphenylpyruvate standards and plasma derivitised with DNPH. **114**
Figure 37: Phenylalanine peak at m/z 164.0702. ..... **120**
Figure 38: Correlation of peak intensity to punch size demonstrated linearly increasing peak intensity with increasing punch size indicating phenylalanine was a true peak. **121**
Figure 39: Tyrosine peak visible at m/z 180.0653. ..... **121**
Figure 40: Good correlation between peak intensity and punch size for tyrosine. **122**
Figure 41: Homogentisate peak visible at 167.0336. ..... **122**
Figure 42: Homogentisate peak intensity to punch size correlation demonstrated R-squared above 0.8. ..... **123**
Figure 43: Peak at m/z 179.0336. ..... **123**
Figure 44: No correlation between peak intensity and punch size for hydroxyphenylpyruvate. **124**
Figure 45: A - Calculation of peak area via peak integration. B – Good correlation for phenylalanine between peak area and intensity. **125**
Figure 46: Poor correlation between punch weight and patient haematocrit. **127**
Figure 47: Boxplots of median normalised peak intensities for phenylalanine and homogentisate in control and cancer samples. **129**
Figure 48: Boxplot of homogentisate normalised peak intensities for control samples and cancer patients pre- and post-chemotherapy. **130**
Figure 49: Boxplot of homogentisate normalised peak intensity for oesophageal and gastric adenocarcinoma patients separately. **131**
Figure 50: Boxplot of normalised homogentisate intensity for cancer patients divided according to early stage disease (T1/2) or later stage disease (T3/4). **132**
Figure 51: Fold change in OE33 and OE19 cell enzyme activity expressed relative to HET-1A cell enzyme activity. PAH – Phenylalanine hydroxylase; TAT – tyrosine aminotransferase; HPD – 4-Hydroxyphenylpyruvate dioxygenase; HGD – Homogentisate 1,2 dioxygenase; MAAI – maleylacetoacetate isomerase; FAH – fumarylacetoacetate isomerase. **147**
Figure 52: Boxplot of relative fold change for each enzyme. Green line represents a value of 1 indicating expression of normal mucosa for that enzyme relative to which cancer sample fold change was calculated. **149**
Figure 53: Boxplot of relative fold change for each enzyme related to aromatic amino acid breakdown. **151**
Figure 54: Homogentisate 1,2 dioxygenase activity in oesophageal and gastric tissues demonstrated contrasting findings with up-regulation in oesophageal cancer and down-regulation in gastric cancer. **153**
Figure 55: Representative staining for each enzyme in an oesophageal cancer case. **157**
Figure 56: Boxplots of H-score for TAT, HPD and HGD in oesophageal cancer with representative staining. **159**
Figure 57: Boxplot of HPD in gastric cancer with representative staining. **161**
Figure 58: Correlation between qPCR fold change results and immunohistochemistry H-score analysis for each relevant enzyme in oesophageal cancer. Representative staining is also presented. **162**
Figure 59: Correlation between qPCR fold change results and immunohistochemistry H-score analysis for each relevant enzyme in gastric cancer. Representative staining also presented. **163**
Figure 60: Findings in oesophageal cancer patients with reduced phenylalanine and homogentisate on dried blood spot analysis. Tyrosine aminotransferase and homogentisate 1,2 dioxygenase were up-regulated in qPCR and immunohistochemistry and hydroxyphenylpyruvate dioxygenase down-regulated on immunohistochemistry. **165**
Figure 61: Gastric cancer patients also had reduced phenylalanine and homogentisate on dried blood spot analysis. All pathway enzymes after hydroxyphenylpyruvate dioxygenase were down-regulated on qPCR but this was only cross-validated in hydroxyphenylpyruvate dioxygenase on immunohistochemistry. **165**
Figure 62: Urinary phenol and p-cresol in control and cancer cohorts. **175**
Figure 63: Urinary phenol and p-cresol concentrations in oesophageal and gastric cancer patients separately. **177**
Figure 64: Results for neoadjuvant naïve patients (Pre-Chemo) compared to those who had completed chemotherapy and control patients. **178**
Figure 65: Results divided by tumour stage. **179**

Figure 66: ROC curves for oesophago-gastric cancer patients versus all controls (A – Area under curve 0.687) and against healthy volunteers only (B – Area under curve 0.755). **180**
Figure 67: Boxplot of plasma phenol concentration across the three groups. **188**
Figure 68: Boxplot showing no difference in median phenol concentration in cancer and control samples. **199**
Figure 69: A: When all samples were included there appeared to be a weak correlation between tyrosine and phenol concentration. B: When the sample beyond the dynamic range of tyrosine LC-MS method was excluded this relationship was lost. There appeared to be no clear correlation between tyrosine and phenol concentration. **200**
Figure 70: Conversion of D4 tyrosine to D4 phenol. **205**
Figure 71: A – Selected ion recording for m/z 98 demonstrated no peak in unenriched samples. B – Peak visible at 10.44 minutes (m/z 98) in D4 tyrosine enriched samples indicating the presence of D4 phenol. **207**

LIST OF TABLES

Table 1: Summary table of included studies investigating aromatic amino acid metabolism. **32**
Table 2: Details of studies included in phenolic compound review. **38**
Table 3: Results of exhaled breath analysis by Kumar et al.[25] **41**
Table 4: Details of SIR including compound of interest, elution time, scan time, and m/z to be scanned. **56**
Table 5: Finalised SIR method incorporating scanning for 99 ion of phenol D6 and reduced number of m/z values in each SIR period to improve peak shape. **59**
Table 6: Phenol peak area results with changes in equilibration time. **64**
Table 7: Phenol peak area with SPME extraction temperature of 30°C, 45°C and 60°C. **65**
Table 8: Phenol peak area increasing with increasing extraction time. **67**
Table 9: Changes in phenol peak area with salination of samples. **69**
Table 10: Effect of pH changes upon phenol extraction from gastric content. **71**
Table 11: Greatly increased phenol peak area with hydrolysis of urine samples. **72**
Table 12: Results of intra- and inter-day accuracy and precision for phenol quantification. **73**
Table 13: Details of solvent expansion and safe injection volume for methanol, acetone and dichloromethane. **77**
Table 14: Phenol recovery with variety of SPE tubes. **79**
Table 15: Results of assessing various elution solvents. **80**
Table 16: Recovery with sequential 1ml aliquots of acetone with a final total elution volume of 5ml. 99.33% of phenol recovered using 3ml acetone. **81**
Table 17: Phenol peak area with and without sample evaporation. 3ml acetone for elution followed by evaporation to 1ml provided the largest peak area. **83**
Table 18: Assessment of wash step. **84**
Table 19: Assessment on changes in pH upon effectiveness of wash step. **85**
Table 20: Phenol recovery at various starting concentrations. **86**
Table 21: Results of intra- and inter-day accuracy and precision for phenol quantification using direct injection method. **88**
Table 22: Results of addition of various quantities of beta-glucuronidase for phenol deconjugation. **89**
Table 23: Results of varying incubation time at 37°C for phenol deconjugation with 20µL beta-glucuronidase. **90**
Table 24: Assessment of different solvent for tissue homogenisation showed little variation. **91**
Table 25: Mass transitions, cone voltage and collision energy for each compound. **96**
Table 26: Mass transitions selected for quantification purposes. **97**
Table 27: Intra-day and inter-day accuracy results for the LC-MS method. **107**
Table 28: Matrix effect, recovery, and process efficiency for analysis of tyrosine in gastric content. **110**
Table 29: Results of gastric content experiments for accuracy of tyrosine quantification. **111**
Table 30: Matrix effect, recovery, and process efficiency in plasma samples. **112**
Table 31: Details of homogentisate peak areas and stability (relative to standard solution) with different sample treatments. Addition of formic acid provided the greatest stability. **113**
Table 32: Demographic details for patients from who dried blood spot samples were collected. **128**
Table 33: Overall normalised peak intensities (N.P.I.) for cancer and control cohorts. **129**
Table 34: Sub-group analysis of patient who had not received any neoadjuvant chemotherapy (pre-chemo) and those who had completed chemotherapy (post-chemo). **130**
Table 35: Sub-group analysis of oesophageal and gastric patients separately. **131**
Table 36: Patients divided by T-stage. **132**
Table 37: Patients separated according to the presence or absence of spread to lymph nodes. **133**
Table 38: Patients divided according to the presence or absence of metastatic spread. **133**
Table 39: Fold change analysis (relative to normal squamous oesophageal mucosa) for oesophageal adenocarcinoma samples in each relevant dataset. **140**
Table 40: Fold change analysis (relative to normal gastric mucosa) for gastric adenocarcinoma samples in each relevant dataset. **141**
Table 41: Fold change for OE33 and OE19 cells relative to HET1A. **146**
Table 42: Details of qPCR fold-change results for oesophageal adenocarcinoma patients. **148**
Table 43: Normal oesophageal mucosa and oesophageal adenocarcinoma results presented as expression per 1000 GAPDH. **150**
Table 44: Relative fold change results for gastric adenocarcinoma tissue compared to healthy gastric mucosa. **151**

Table 45: Normal gastric mucosa and gastric adenocarcinoma results presented as expression per 1000 GAPDH. **152**
Table 46: H-score assessment of each enzyme in normal oesophageal mucosa and oesophageal adenocarcinoma. **158**
Table 47: H-Score assessment of each enzyme in normal gastric mucosa and gastric adenocarcinoma **160**
Table 48: Demographic details for patients included in urinary analysis. **173**
Table 49: Phenol and p-cresol concentrations in control and cancer patient cohorts. **174**
Table 50: Comparison of phenol and p-cresol concentration in healthy volunteers, symptomatic benign controls and cancer patients. **176**
Table 51: Results divided by disease type. **177**
Table 52: Urinary phenol and p-Cresol concentration subdivided according to whether patients had received neo-adjuvant chemotherapy. **178**
Table 53: Results divided according to tumour stage. **179**
Table 54: Results sub-divided according to nodal involvement. **180**
Table 55: Demographic details of control and cancer patients undergoing plasma analysis. **187**
Table 56: Details of phenol concentration in the control, oesophageal cancer and gastric cancer groups. **188**
Table 57: Details of demographic details of each patient group demonstrating no significant differences between the demographics of the control or cancer patient groups. **198**
Table 58: Details of results of D4 phenol production from D4 tyrosine in each patient. D4 phenol was below the limit of detection for all unenriched samples but visible in all samples enriched with D4 tyrosine. **208**

LIST OF SUPPLEMENTARY FIGURES

Supplementary Figure 1: Peak shape for phenol with temperature ramp set to 20°C per minute (A), 15°C per minute (B) and 10°C per minute (C). **230**
Supplementary Figure 2: Peak shape for phenol with temperature ramp set to 45°C per minute (A), 40°C per minute (B) and 30°C per minute (C). **231**
Supplementary Figure 3: Peaks of phenol (5.22) and p-cresol (5.65) on this temperature programme. **232**
Supplementary Figure 4: p and m-cresol eluting together at 5.64 minutes on this temperature programme. **232**
Supplementary Figure 5: p and m-cresol still eluting together at 6.14/5 minutes. **232**
Supplementary Figure 6: Phenolic compound elution for 40°C/min ramp (A), 30°C/min ramp (B), and 20°C/min ramp (C). **233**
Supplementary Figure 7: Phenol peak shape on full scan mode with scan time of A: 0.4s; B: 0.2s; C: 0.1s; D: 0.08s. **234**
Supplementary Figure 8: A – Peak shape when scanning for all four m/z on SIR (65,94,107,108); B – Scanning for 94 ion only; C – Scanning for m/z 94,107 and 108; D – Reduced dwell-time to 0.02s. **235**
Supplementary Figure 9: A: Mobile phase gradient details for analysis with phenyl-hexyl column. B: Representative chromatogram showing lack of retention of phenylalanine with this column. **236**
Supplementary Figure 10: Poor peak shape with methanol as mobile phase B. **237**

LIST OF SUPPLEMENTARY TABLES

Supplementary Table 1: Mobile phase gradient details for assessment of HILIC column. 238

CHAPTER 1 - INTRODUCTION

1.1 Oesophago-Gastric Cancer

Cancer is a leading cause of death worldwide with an estimated 14.1 million new cancer cases and 8.2 million cancer deaths worldwide in 2012[1]. Cancer of the gullet (oesophagus) and stomach (together termed oesophago-gastric cancer) represent a significant health issue worldwide with 400,200 deaths related to oesophageal cancer in 2012, and 723,100 attributed to gastric cancer[1].

The highest rates of oesophageal cancer are found in Eastern Asia as well as Eastern and Southern Africa. This disease is around 3 to 4 times more common in men than women[1]. Oesophageal cancer is divided into two major histological subtypes. Squamous cell carcinoma is more common within Central and South-East Asia whereas oesophageal adenocarcinoma is much more prevalent in Western Countries. In 2012 there were 398,000 cases of squamous cell carcinoma worldwide and 52,000 cases of oesophageal adenocarcinoma[2]. Oesophageal adenocarcinoma is a particular issue in the United Kingdom, which has the highest incidence of oesophageal adenocarcinoma worldwide (affecting 5,800 patients per year)[1–3]. The incidence of oesophageal adenocarcinoma in the United Kingdom is 7.2 per 100,000 men and 2.7 per 100,000 women. This compares to an overall global incidence of 0.7 per 100,000 (1.1 per 100,000 in men and 0.3 per 100,000 in women)[2].

Oesophageal adenocarcinoma typically develops in the lower third of the oesophagus and can originate from an area of Barrett's mucosa (defined as intestinal metaplasia within the distal oesophagus). Step-wise progression from metaplastic change leads to dysplasia, and finally invasive cancer. Although Barrett's oesophagus is a major risk factor for oesophageal adenocarcinoma the annual risk of progression to invasive cancer is only 0.12%[4]. Despite Barrett's oesophagus being a potential risk factor around 95% of patients receiving a diagnosis of oesophageal cancer are not previously known to suffer with Barrett's oesophagus[5–7]. This indicates that current endoscopic screening programmes of known Barrett's oesophagus patients are not effective for preventing oesophageal adenocarcinoma development in the general population. One major risk factor for development of both Barrett's oesophagus and oesophageal adenocarcinoma is gastro-oesophageal reflux disease[8,9]. Chronic reflux produces chronic inflammation within the oesophagus causing oxidative stress, leading to DNA damage and increased mutation rates, subsequently being

responsible for tumour formation[10]. The increasing incidence of oesophageal adenocarcinoma in the United Kingdom is believed to be in part related to increasing rates of obesity which is strongly related to risk of oesophageal adenocarcinoma, Barrett's oesophagus, and gastro-oesophageal reflux disease[11–13].

The Incidence of stomach cancer is generally highest in eastern Asia (particularly Korea, Mongolia, Japan and China), Central and Eastern Europe, and South America, whilst being lowest in Northern America and most parts of Africa[1]. Large differences in the incidence of gastric cancer exist geographically with an incidence of up to 26.9 per 100 000 among males in Asia, compared to 3.4 per 100 000 among females of North America[14]. Chronic infection with *Helicobacter Pylori* is the strongest risk factor for stomach cancer with 89% of non-cardia gastric cancer cases attributed to infection with this bacteria[15].

Oesophageal and gastric cancer have overall five-year survival rates of only 15% and 19% respectively in the United Kingdom[3]. This compares unfavourably with 5-year survival for other malignant diseases including breast cancer (87%), bowel cancer (59%), bladder cancer (54%) and ovarian cancer (46%)[16]. At the time of clinical presentation the majority of oesophago-gastric cancer cases have advanced disease and only 37.6% can be treated with curative intent[3]. Late diagnosis is in part due to the non-specific symptoms associated with oesophageal and gastric cancer. Patients with oesophageal cancer attend their primary care physician on average 22 days after first noticing symptoms compared to 2-3 days for bladder and renal cancer and 7 days for brain or breast cancer[17]. In addition to poor patient awareness of alert symptoms[18], the diagnosis of oesophageal cancer can be challenging in primary care with around 25% of oesophageal cancer patients visiting their primary care physician three or more times prior to referral for further investigation[19]. There is also known to be a paucity of symptoms in early stages of the gastric cancer[20]. Despite these factors current national guidelines from the National Institute for Health and Care Excellence focus upon the presence of alarm symptoms such as dysphagia, unintentional weight loss, persistent vomiting, iron deficiency anaemia or an epigastric mass. The guidance also states that endoscopic investigation is not necessary in patients less than 55 years old in the absence of alarm symptoms[21]. Evidence has

suggested this leads to a longer referral time for patients under the age of 55 with oesophago-gastric cancer[22].

At present there are no national screening programmes for oesophageal cancer largely because the incidence is relatively low, the gold-standard diagnostic test (endoscopy) is expensive, and due to the invasive nature of this test it is associated with significant potential risks to patients. In the Japanese population the national screening programme for gastric cancer helps facilitates early detection of disease and contributes towards better oncological outcomes[23]. It has been suggested there is a need in Western Countries to screen patients with symptomatic reflux, but it is not currently feasible to use endoscopy-based screening with the available health care resources[24]. There is a clear need to better delineate those patients suffering with non-specific upper gastrointestinal symptoms (such as reflux or dyspepsia) that are at sufficiently high-risk to justify endoscopic investigation. Use of non-invasive biomarkers may allow for risk-stratification of symptomatic patients to streamline access to endoscopy services for those at greatest risk.

Analysis of volatile organic compounds within exhaled breath or urine of oesophago-gastric cancer patients has been proposed as one potential method of risk stratification prior to endoscopy[25–27].

1.2 Volatile Organic Compounds

The utilisation of breath analysis as a medical test has long been established, with Hippocrates describing *fetor oris* and *fetor hepaticus* in his treatise on breath aroma and disease[28] In 1971 Linus Pauling used gas-liquid partition chromatography to establish that exhaled breath was a complex mixture of over 250 volatile organic compounds (VOC's) whilst there were also 280 VOC's within the headspace of urine samples[29]. Since this time VOCs have been of great interest to researchers as a potential method to identify human disease states. Particular focus has been upon identifying a link between specific VOCs and cancer. Previous studies have shown links between the levels of VOCs and lung[30–32], bladder[33], breast[34] and oesophago-gastric cancer[26,35,36].

1.3 Phenol Production

Phenol can be produced from five main precursors including tyrosine, 4-hydroxybenzoate, phenylboronic acid, salicylic acid and benzene[37,38]. Production of phenol from tyrosine is of particular interest in oesophago-gastric cancer as tyrosine concentrations have previously been shown to be elevated within the gastric juice of gastric cancer patients[39,40]. Tyrosine is converted to phenol via the action of the bacterial enzyme *tyrosine phenol-lyase*. This reaction was first discovered in bacterial cultures by Kakihara & Ichihara[41]. The role of gut bacteria in phenol production has long been established[42].

Cresols (methylphenols) are also a product of bacterial fermentation of tyrosine[42]. Cresols have three different isomeric forms depending upon the position of the methyl-group. These are o-cresol (2-methylphenol), m-cresol (3-methylphenol), and p-cresol (4-methylphenol).

1.4 Aromatic Amino Acid Breakdown

Phenylalanine is an essential amino acid in the human diet which is required for the production of the non-essential amino acid tyrosine. The production of tyrosine from phenylalanine was first discovered by Womack and Rose in 1934[43]. This conversion is catalysed by the enzyme phenylalanine hydroxylase, which predominantly functions within the liver, but has been shown to be active in other body tissues including the kidney, pancreas and brain[44]. It has been demonstrated that phenylalanine hydroxylase activity can be altered in inflammation or malignancy[45,46]. Tyrosine can be converted to phenol via the action of *tyrosine phenol* lyase, or can enter the aromatic amino acid breakdown pathway which leads to the citrate cycle via a series of intermediary metabolites (hydroxyphenylpyruvate, homogentisate, maleyl-acetoacetate and fumaryl-acetoacetate). The full metabolic pathway of these aromatic amino acids is shown in Figure 1. Enzymes responsible for regulating this pathway can be affected by a series of inborn errors of metabolism.

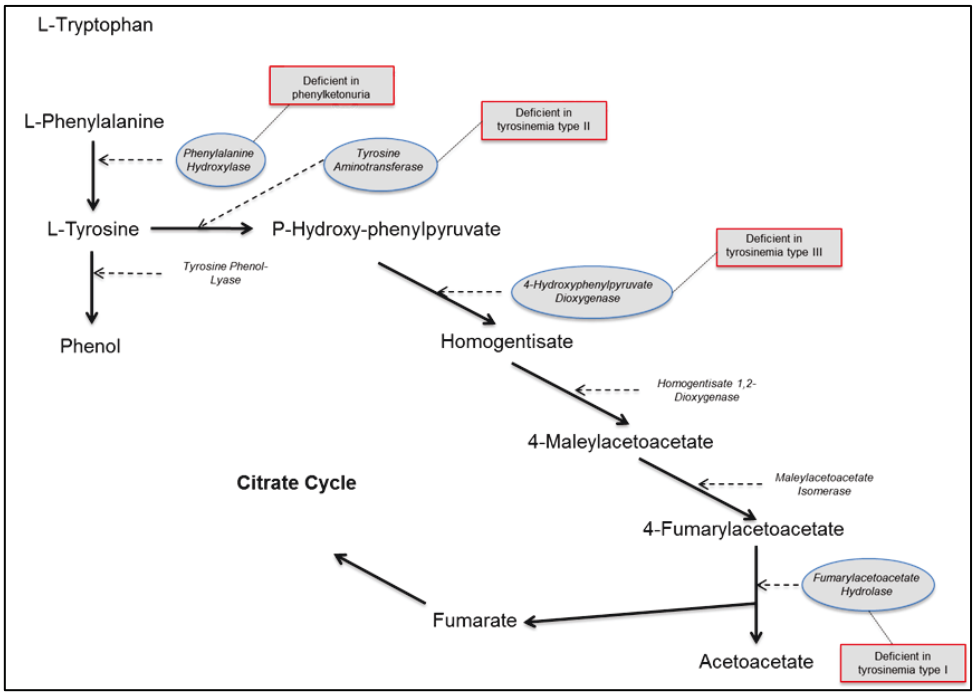


Figure 1: Phenylalanine and tyrosine metabolic pathway.

1.5 Inborn Errors of Aromatic Amino Acid Metabolism

Analytical techniques for quantification of aromatic amino acids have previously been developed for the purposes of newborn screening for inborn errors of aromatic amino acid metabolism. These conditions are caused by deficiency of specific enzymes which regulate aromatic amino acid breakdown. Inborn errors of aromatic amino acid metabolism are discussed in this section due to the relevance of these changes in enzyme activity to the pathway under investigation in this thesis.

1.5.1 Phenylketonuria

Phenylketonuria is an autosomal recessive condition caused by mutations in the phenylalanine hydroxylase gene leading to deficiency of this enzyme[47]. Incidence varies widely around the world and it affects around one case per 10,000 births in Caucasians, with the highest incidence being in Northern Europe[48]. Diagnosis is usually made through new-born screening programmes and clinical features result from accumulation of excess phenylalanine which may cause severe intellectual disability if left untreated. Other clinical features include autistic behaviours, motor deficits, eczematous rash and seizures[47]. There is no cure for phenylketonuria and treatment focusses upon dietary restriction of phenylalanine to the minimum required for normal growth[47].

1.5.2 Tyrosinaemia

Tyrosinaemia is divided into three separate types[49]:

- Tyrosinaemia Type 1: Caused by deficiency of fumarylacetoacetate hydrolase.
- *Tyrosinaemia Type 2:* Due to deficiency of tyrosine aminotransferase.
- *Tyrosinaemia Type 3:* Extremely rare disorder of absence of 4-hydroxyphenylpyruvate dioxygenase.

Tyrosinaemia Type 1

Tyrosinaemia type 1 is the most severe form of tyrosinaemia and has a prevalence of around 1 in 100,000 births. It is caused by deficiency of fumarylacetoacetate hydrolase[49]. Biochemical findings

typically include increased concentrations of succinylacetone, tyrosine, methionine and phenylalanine in blood, as well as increased urinary excretion of toxic metabolites such as succinylacetone and delta-aminolevulinic acid[50,51]. Left untreated patients develop liver failure and renal tubular involvement. Treatment involves the use of nitisinone (2-(2-nitro-4-trifluoromethylbenzoyl)-1,3-cyclohexanedione (NTBC)) which acts as an inhibitor of 4-hydroxyphenylpyruvate dioxygenase[52]. This prevents the accumulation of succinylacetone but can lead to increased plasma tyrosine concentration[53] which can be managed with dietary restriction of tyrosine and phenylalanine.

Tyrosinaemia Type 2

Tyrosinaemia Type 2 is an autosomal recessive disorder which causes a deficiency of tyrosine aminotransferase. It is generally a less severe condition than tyrosinaemia type 1 and clinical manifestations include skin lesions with hyperkeratotic plaques upon the feet and palms of hands and eye symptoms with photophobia and scleral inflammation[49]. Treatment with low protein diet is usually successful at resolving both eye and skin symptoms.

Tyrosinaemia Type 3

Tyrosinaemia type 3 is an extremely rare condition caused by deficiency of 4-hydroxyphenylpyruvate dioxygenase. The clinical symptoms include severe learning difficulties and neurological symptoms[54].

1.5.3 Alkaptonuria

Alkaptonuria is a rare autosomal recessive disorder which was first described by Garrod in 1902[55]. This disorder is caused by a deficiency of the enzyme homogentisate 1,2 dioxygenase within the liver[56], and leads to excretion of large quantities of homogentisate within the urine[57]. The incidence of alkaptonuria is around 1 case per 250,000 to 1,000,000 live births[58]. Deficiency of homogentisate 1,2 dioxygenase leads to accumulation of homogentisate or benzoquinones (products of homogentisate oxidation), which can form melanin-like polymers. Deposition of these compounds within connective tissues leads to ochronosis with darkening of cartilaginous tissues and bone, arthritis, joint destruction and deterioration of cardiac valves[59–62]. Treatment options include the use of nitisinone to inhibit 4-hydroxyphenylpyruvate dioxygenase activity and thereby cease the production of homogentisate[58].

1.6 Systematic Review – Aromatic Amino Acids and Phenol in Oesophago-Gastric Cancer

1.6.1 Introduction

Amino acids are compounds that have been muted as potential biomarkers of malignant disease. A previous review demonstrated that tryptophan was the metabolite with the most frequently altered concentrations across several cancer types[63]. Patients with oesophageal cancer have reduced plasma levels of 14 separate amino acids including tyrosine, phenylalanine and tryptophan[64]. Cancer patients suffering with anorexia and malnutrition have the most distinctive changes in the plasma amino acid profile[64]. Due to the obstructive nature of advanced oesophageal cancer up to 79% of patients develop a degree of malnutrition prior to diagnosis[65,66].

Phenolic compounds are potential markers of oesophago-gastric cancer with altered concentrations previously observed within exhaled breath[36], urine[67], and gastric content[35].

Therefore a combination of investigating aromatic amino acid and phenol profiles may yield suitable clinical assays to assess a patient's risk of having oesophago-gastric cancer. This systematic review has investigated the current published literature to evaluate concentrations of tyrosine, phenylalanine and tryptophan within the biofluids and tissues of oesophago-gastric cancer patients, and assess their potential as biomarkers of this disease. It has also investigated the role of phenolic compounds (namely phenol, cresol (also known as methyl-phenol) and ethylphenol) as potential biomarkers of gastrointestinal cancer.

1.6.2 Methods

A literature search (title and abstract) was performed using Ovid Medline® (1948-2016), Embase® (1974-2016), Web of Science® and PubMed® electronic databases up to and including 10th September 2016. This search was used to identify relevant studies that had measured tyrosine, phenylalanine or tryptophan within tissues or biofluids of patients with oesophago-gastric cancer. The

search also identified studies which measured phenolic compounds in gastrointestinal cancer patients. Only studies which had compared results to a control group of healthy individuals (either healthy volunteers or those with benign disease of the upper gastrointestinal tract) were included. For aromatic amino acids the search was undertaken using the terms *Tyrosine* OR *Phenylalanine* OR *Tryptophan* AND (*Cancer* OR *malignancy* OR *neoplasm)* AND (*Gastric* OR *Stomach* OR *Oesophageal* OR *Esophageal*) as well as the medical subject headings (MeSH), *Tyrosine* OR *Phenylalanine* OR *Tryptophan AND* (*stomach neoplasms* OR *esophageal neoplasms*). A second search was performed using the terms (*phenol* OR *methylphenol* OR *cresol* OR *ethylphenol*) AND (*Cancer* OR *malignancy* OR *neoplasm)* AND (*Gastric* OR *Stomach* OR *Oesophageal* OR *Esophageal*) as well as MeSH terms (*stomach neoplasms* OR *esophageal neoplasms*). Due to the small number of studies investigating phenol metabolism in oesophago-gastric cancer the search was extended to include colorectal cancer by addition of the search terms '*Colon* OR *Rectum',* and MeSH subject heading '*Colorectal neoplasms'.*

The electronic search was supplemented by a hand-search of published abstracts from relevant conference proceedings (2010 – 2016). Two reviewers independently screened titles and abstracts of studies identified via the electronic search. Full texts were retrieved for all potentially relevant articles. Searching of reference lists of appropriate texts identified further potentially relevant studies. Inclusion criteria were any study measuring tyrosine, phenylalanine or tryptophan in oesophago-gastric cancer patients or phenol, cresol (also known as methyl-phenol) or ethylphenol in gastrointestinal cancer, via any appropriate analytical method comparing biological samples from cancer patients and suitable controls. Exclusion criteria were any studies without an appropriate control group or animal studies. Studies that reported the same patient population in multiple publications were also excluded, except for the most recent or complete publication.

The two reviewers independently extracted data from the selected studies including: number and types of specimen; analytical platform; amino acid/phenol concentrations in cancer and control groups. The hypothesis under investigation was whether concentrations of aromatic amino acids and phenolic compounds would be significantly different between cancer and control samples. The QUADAS-2 tool was used to assess the quality of the included studies[68]. This model consists of four

domains including patient selection, index test, reference standard and flow of patients through the study. The reference standard is defined as the best available method to establish the presence or absence of the target condition[69], which in this review was considered to be histological confirmation of the diagnosis. Each domain is assessed in terms of bias and the first three are also assessed in terms of concerns regarding applicability.

1.6.3 Results

Twenty-two studies were included in this review. Sixteen studies investigated aromatic amino acid metabolism in oesophago-gastric cancer, and six studies investigated phenol production in gastrointestinal cancer. PRISMA flow diagrams for each section are shown in Figure 2A and 2B.

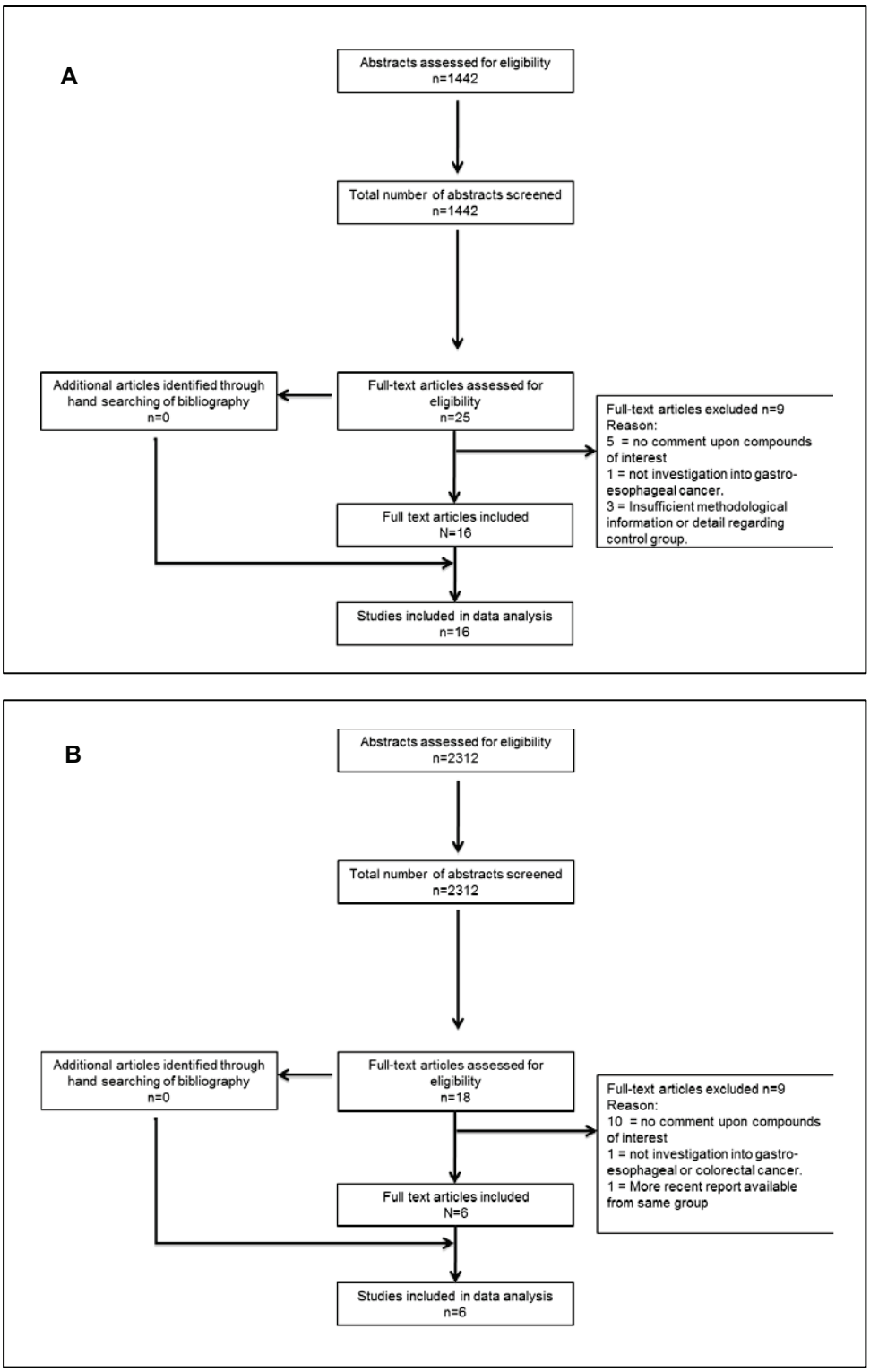
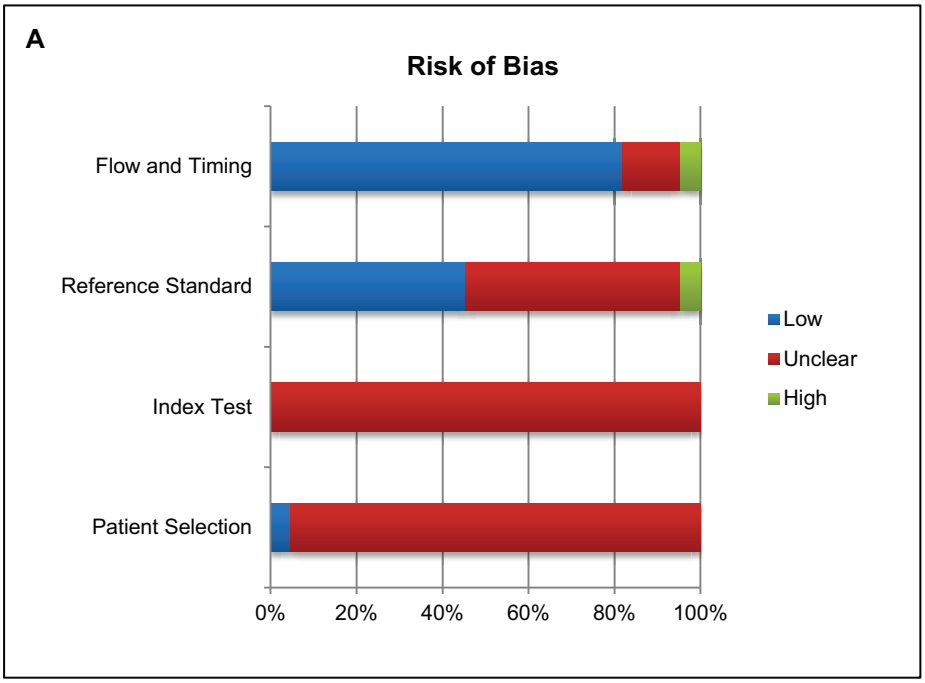


Figure 2: PRISMA diagram for aromatic amino acid studies (A) and phenol studies (B)

Quality Assessment of Studies

Details of the QUADAS-2 study quality assessment are shown in Figures 3A and 3B. Unclear risk of bias in patient selection was recorded in all but one study due to a lack of information regarding patient recruitment, as it was not specified whether consecutive patients were included or if any patients were excluded. The risk of bias for the index test was unclear due to lack of information regarding blinding of assessors. Several papers had a high risk of bias with regard to patient flow as not all of the controls received the reference standard investigation (histological examination). Twenty three percent of studies had an unclear or high risk of applicability concerns due to cancer and control groups not being appropriately matched.



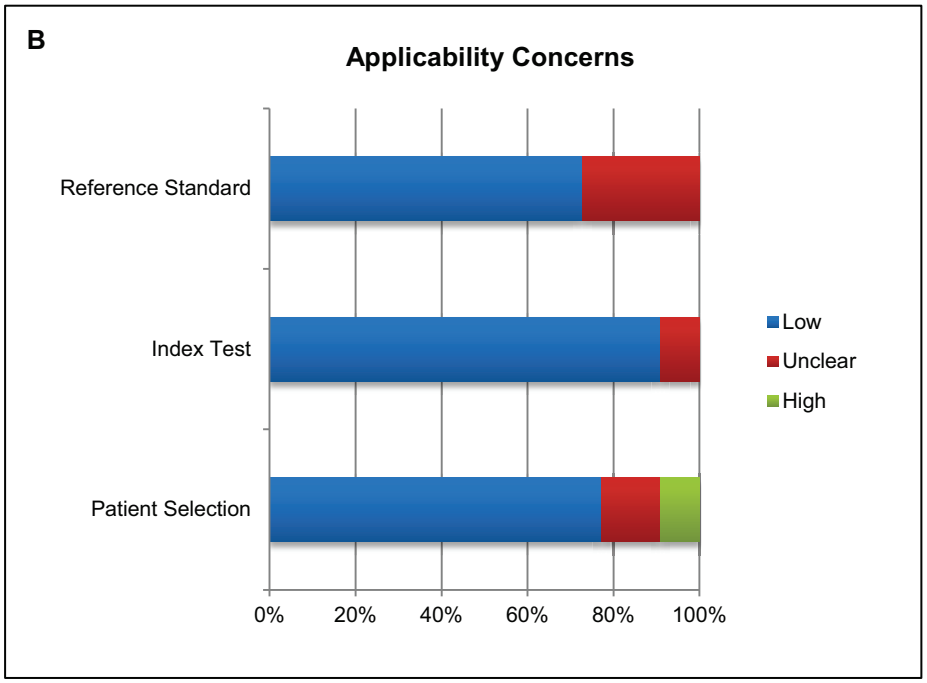


Figure 3: Assessment of risk of bias (A) and applicability concerns (B):

1.6.3.1 Aromatic Amino Acid Metabolism in Oesophago-Gastric Cancer

There were 16 studies investigating aromatic amino acid metabolism in oesophago-gastric cancer that met the inclusion criteria for this systematic review[39,40,70–83].

Summary Table

Please see table 1.

Author and Year	Sample Type	Amino Acids Investigated	Cancer Type	Platform	n Cancer	n Control	Tyr (Cancer vs Control)	Phe (Cancer vs Control)	Trp (Cancer vs Control)
Serum-Based Studies									
Zhang X 2013[70]	Serum	Tyr, Phe, Trp	Oesophageal	NMR LC-MS	25	25	↓*	↑*	↓*
Zhang J 2012[71]	Serum	Tyr, Trp	Oesophageal	LC-MS + NMR	67	BE 3 HGD 9 HC 34	-	N/A	↓
Miyagi 2011[72]	Serum	Tyr, Phe, Trp	Gastric	LC-MS	199	985	↓**	↓**	↓**
Ikeda 2011[73]	Serum	Tyr, Phe, Trp	Gastric and oesophageal	GC-MS	Oes n=15 Gas n=11	HC =12	-	-	-
Naini 1988[74]	Plasma	Phe, Trp	Oesophageal	Amino acid analyzer	11	Hiatus hernia n=9	N/A	-	↓* (free trp levels)
Norton 1985[75]	Plasma	Tyr, Phe	Oesophageal	Amino acid analyzer	6	14	↓*	↓*	N/A
Gastric Juice Based Studies									
Deng 2012[39]	Gastric juice	Tyr, Phe, Trp	Gastric	LC-MS	EGC n=49 AGC n=66	BGD N=70	↑**	↑**	↑**
Lian 2012[76]	Gastric juice	Trp	Gastric	LC-MS	38	48 (BGD)	N/A	N/A	↑
Deng 2011[40]	Gastric juice	Tyr, Phe, Trp	Gastric	LC-MS NMR	33	68 (mix HC and BGD)	↑*	↑*	↑*
Segawa 1985[77]	Gastric juice	Tyr, Phe	Gastric	LC-MS	16	40 (mix HC and BGD)	↑	↑	N/A
Abasov 1969[78]	Gastric juice	Tyr, Phe, Trp	Gastric	Chroma-tography	100	140 (HC + BGD)	↑	↑	↑
Urine Based Studies									
Hasim 2012[79]	Urine	Tyr, Phe	Oesophageal	NMR	108	40	↑	↑	N/A
Davis 2012[80]	Urine	Tyr	Oesophageal	NMR	44	44	↑	N/A	N/A
Tissue Based Studies									
Song 2011[81]	Tissue	Phe	Gastric	GC-MS	30	30	N/A	↑	N/A
Wu 2009[82]	Tissue	Tyr, Phe	Oesophageal	GC-MS	20	20	↑**	-	N/A
Hirayama 2009[83]	Tissue	Tyr, Phe, Trp	Gastric	CE-TOF-MS	12	12	↑**	↑**	↑*

Table 1: Summary table of included studies investigating aromatic amino acid metabolism.

Key: ↑=raised levels in cancer patients; ↓=decreased levels in cancer patients; - =No difference shown; N/A = Not reported; * = p<0.05; ** p<0.001. (Tyr = tyrosine; Phe=Phenylalanine; Trp = Tryptophan; LC-MS=Liquid chromatography mass spectrometry; GC-MS=Gas chromatography mass spectrometry; NMR=Nuclear magnetic resonance; CE-TOF-MS=Capillary electrophoresis time-of-flight mass spectrometry; EGC=Early gastric cancer; AGC=Advanced gastric cancer; HC=Healthy controls; BGD=Benign gastric disease; BE=Barrett's oesophagus;)

Study Characteristics

Seven studies involved the investigation of patients with oesophageal cancer[70,71,74,75,79,80,82], eight studies investigated gastric cancer patients[39,40,72,76–78,81,83] and one study investigated both cancer types[73]. In total there were 524 patients with gastric cancer and 296 oesophageal cancer patients included over these 16 studies. Six studies investigated blood levels of these aromatic amino acids (four oesophageal cancer, one gastric cancer and one for both cancers), five studies investigated gastric content (all gastric cancer patients), two investigated urinary concentrations in oesophageal cancer patients, and three studies analysed concentrations of these amino acids in cancer tissues (one oesophageal and two gastric). Several analytical platforms were utilised for analysis including liquid chromatography mass spectrometry (LC-MS) (n=7), gas chromatography mass spectrometry (GC-MS) (n=3), nuclear magnetic resonance (NMR) spectroscopy (n=5), capillary electrophoresis mass spectrometry (CE-MS) (n=1), automated amino acid analyser (n=2), and ascending chromatography (n=1). Some studies utilised more than one analytical platform.

Tyrosine

Tyrosine was measured in 13 of the studies included (five serum based, four gastric content, two urine based and two in tissue).

Miyagi *et al.* investigated concentrations of plasma free amino acids in various cancer types using high performance liquid chromatography electrospray ionisation mass spectrometry[72]. This study included 199 gastric cancer cases and 985 healthy controls. Results from this study showed a significantly decreased tyrosine concentration in gastric cancer cases compared to controls ($p<0.01$). This difference was apparent in early (Stage I) as well as late (stage IV) stages of disease. Zhang X *et al.* demonstrated that serum tyrosine concentrations were decreased in oesophageal cancer patients (n=25) compared to healthy controls (n=25) ($p<0.002$)[70], a finding which was also reported by Norton *et al.* ($p<0.05$)[75]. However other studies by Zhang J *et al.*[71] and Ikeda *et al.*[73] showed no significant difference in serum tyrosine concentrations in oesophageal and gastric cancer patients compared to controls.

Deng *et al*. have performed two studies to investigate levels of amino acids within gastric content[39,40]. The initial study compared concentrations within gastric content of gastric cancer patients (n=33) to a control group (n=68) using NMR spectroscopy and LC-MS. The median concentration of tyrosine in the cancer group was 54.9±11.0μg/mL, compared to 8.7±2.6μg/mL in the control group ($p<0.05$)[40]. Another study by the same group compared cases of early gastric cancer (n=49), advanced gastric cancer (n=66) and a control group of patients with non-neoplastic gastric disease (n=70). This study showed that median gastric content tyrosine concentrations in the early gastric cancer group was 19.4μg/mL (5.8-72.4), compared to 18.3μg/mL (6.4-52.3) in advanced gastric cancer patients and 3.8μg/mL (1.7-7.5) for the control group. A Receiver Operator Characteristic (ROC) curve analysis for the utilisation of tyrosine concentrations to distinguish early gastric cancer from controls showed an area under the curve of 0.790 (95% CI, 0.703-0.877, $p<0.001$). This finding of increased tyrosine concentrations within gastric content is supported by an early study by Abasov *et al.* which utilised one-dimensional ascending chromatography to detect the presence of aromatic amino acids in the gastric content of gastric cancer cases (n=100)[78]. These patients were compared to a control group containing healthy volunteers and benign gastric disease patients (n=140). This study detected tyrosine in 65% of cancer cases compared to 46% of controls. Segawa *et al.* also showed that overall concentrations of amino acids (including tyrosine and phenylalanine) were higher in the gastric content of gastric cancer patients (n=16) compared to controls (n=40)[77].

Hasim *et al.* investigated concentrations of tyrosine in the urine of oesophageal cancer patients (n=108) compared to controls (n=40) using NMR spectroscopy[79]. They demonstrated that tyrosine concentrations were increased within the urine of oesophageal cancer patients (Correlation co-efficient -0.32). Davis *et al.* found tyrosine concentrations were increased in urine of oesophageal cancer patients (n=44) compared to healthy controls (n=44) although this difference did not reach statistical significance[80]. This study also investigated urinary concentrations of tyrosine and tryptophan in Barrett's oesophagus patients (n=31) compared to a healthy control group (n=31) but no significant differences were observed. Two studies investigated concentrations of tyrosine within gastric cancer tissue compared to normal controls. Wu *et al.* used paired tissue samples (cancer and healthy mucosa) from 20 oesophageal cancer patients and utilised GC-MS to establish concentrations of tyrosine[82]. This showed significantly increased concentrations of tyrosine in cancer

tissue compared to normal mucosa. Hirayama *et al.* used capillary electrophoresis mass spectrometry and showed that concentrations of tyrosine were significantly increased in gastric cancer tissues compared to normal tissue ($p<0.001$)[83].

Phenylalanine

Phenylalanine concentrations were measured in 13 included studies (five blood based studies, four gastric content based studies, one urine based, and three tissue studies).

Miyagi *et al*.[72] and Norton *et al.*[75] respectively demonstrated that serum phenylalanine concentrations were decreased in gastric, and oesophageal cancer patients. However, Zhang X *et al.* had conflicting results with raised serum phenylalanine concentrations in oesophageal cancer patients relative to healthy controls ($p=0.004$)[70]. Ikeda *et al.* compared phenylalanine concentrations in gastric and oesophageal cancer patients (n=15, and n=11 respectively) to healthy controls (n=12) but observed no significant difference[73]. Naini *et al.* also showed no significant change in plasma phenylalanine concentrations[74].

Deng *et al.* demonstrated that median concentrations of phenylalanine in gastric content were 54.3±11 μg/mL in the gastric cancer group, compared to 8.8±2.1μg/mL in the control group ($p<0.05$)[40]. In a second study by Deng *et al.*, the area under the ROC curve using gastric content phenylalanine concentrations to discriminate early gastric cancer cases from controls was 0.831 (95% CI, 0.750-0.911, $p<0.001$)[39]. The area under the ROC curve for the advanced gastric cancer cases compared to controls was 0.858 (95% CI, 0.794-0.922, $p<0.001$). Abasov *et al.* demonstrated that phenylalanine was detected in 80% of cancer cases and 56% of controls[78]*. Hasim et al.* observed increased phenylalanine concentrations in the urine of oesophageal cancer patients compared to controls (Correlation co-efficient -0.45)[79].

In the tissue-based studies, Hirayama *et al.* showed significantly higher concentrations of phenylalanine in gastric cancer tissues compared to controls ($p<0.001$)[83]. However, Wu *et al.* demonstrated no significant differences in phenylalanine concentrations between oesophageal cancer

tissue and normal mucosa[82]. Song *et al*. reported a trend towards increased phenylalanine concentrations in gastric cancer tissues but this observation was not statistically significant[81].

Tryptophan

Tryptophan concentrations were investigated in 10 studies (five blood-based, four in gastric content, and one in tissue).

Zhang J *et al*. measured fasting tryptophan concentrations in 67 oesophageal cancer patients and a control group including three patients with Barrett's oesophagus, nine patients with high-grade dysplasia and 34 healthy volunteers[71]. This study demonstrated that tryptophan concentrations were significantly reduced in oesophageal cancer patients compared to controls (p=<0.001; fold change -1.2). This finding was supported by other groups including Zhang X *et al.*[70] and Naini *et al.*[74], who reported decreased serum concentrations of tryptophan in these patients (Zhang X VIP 3.35, p<0.001; Naini p<0.05 reduction for free tryptophan concentrations (However, total tryptophan levels showed no significant change in concentration therefore this significance of this result is unclear)). Miyagi *et al.* also demonstrated significantly decreased plasma tryptophan concentrations in gastric cancer cases compared to controls (p<0.01)[72]. However, Ikeda *et al.* found no significant difference in tryptophan between esophageal or gastric cancer patients when compared to healthy controls[73].

Lian *et al.* demonstrated that tryptophan concentrations of greater than 6.0µg/mL were found within the gastric content of 52.6% of gastric cancer patients (n=38) compared to 22.9% of controls with benign gastric disease (n=48) (p<0.05)[76]. This finding was further supported by Deng *et al* who showed that median concentrations of tryptophan in gastric content of gastric cancer patients was 19.4±4.7µg/mL, compared to 2.7±1.0µg/mL in controls (p<0.05)[40]. The second study by Deng *et al.* showed that the area under the ROC curve for gastric content tryptophan concentrations was 0.819 (95% CI, 0.739-0.900, p<0.001) to discriminate gastric cancer from controls[39]. Abasov *et al.* reported that tryptophan was identified in 23% of cancer cases compared to 13% of controls[78]. Hirayama *et al.* found significantly increased tryptophan concentrations in gastric tissues compared to controls (p <0.05)[83].

1.6.3.2 Phenol Metabolism in Cancer

A total of six studies met the inclusion criteria for systematic review[25,26,35,67,84,85].

Study Characteristics

Types of cancers investigated in these studies were oesophago-gastric (n=3) and colorectal (n=3). In total there were 112 patients with oesophago-gastric cancer and 173 patients with colorectal cancer included across these studies. Urine was used as the sample type in four studies (three investigating colorectal cancer, and one oesophago-gastric). Gastric content was the biological matrix analysed in one study on oesophago-gastric cancer, and the final study measured exhaled breath from oesophago-gastric cancer patients. The analytical platform used was selective ion flow tube mass spectrometry (SIFT-MS) in three studies, GC-MS in two studies and one study used both GC-ToFMS (Gas-chromatography coupled to Time-of-Flight Mass Spectrometry) and UPLC-QToFMS (Ultra Performance Liquid Chromatography with Quadrapole Time-of-Flight Mass Spectrometry). Details of the included studies are shown in table 2.

Author and Year	Sample Type	Cancer Type	Platform	n Cancer	n Control	Phenol (Cancer vs Control)	Cresol (Cancer vs Control)	Ethyl-Phenol (Cancer vs Control
Urine-Based Studies								
Y Cheng 2012[67]	Urine	Colon	GC TOFMS UPLC-QTOFMS	101	103	↓**	↓**	N/A
Qiu 2010[84]	Urine	Colon	GC-MS	60	63	N/A	↑	N/A
Silva 2011[85]	Urine	Colon	GC-MS	12	21	-	↑*	N/A
Huang 2013[26]	Urine	Oesophago-gastric	SIFT-MS	12	48	↓*	-	-
Gastric Juice Based Studies								
Kumar 2013[35]	Gastric content	Oesophago-gastric	SIFT-MS	19	20	N/A	↑*	N/A
Exhaled Breath								
Kumar 2015[25]	Breath	Oesophago-gastric	SIFT-MS	81	129	↑**	↑**	↑**

Table 2: Details of studies included in phenolic compound review.

*Key: ↑=raised levels in cancer patients; ↓=decreased levels in cancer patients; - =No difference shown; N/A = Not reported; * = p<0.05; ** p<0.001.*

Urine Based Studies

Four studies investigated phenolic compound concentrations within the urine of cancer patients (three colorectal, one oesophago-gastric) against healthy controls[26,67,84,85].

All studies involved the sampling of a single urine sample rather than 24 hour collection. Three of these studies involved collection of an early morning urine specimen after overnight fasting[67,84,85], and one study involved patient fasting for at least six hours prior to collection[26]. Phenol concentrations were recorded in three of these studies, cresols (methylphenols) were measured in all four studies and ethylphenols measured in one study.

The largest study[67] included results from 101 colorectal cancer patients compared to 103 healthy controls and measured concentrations of both phenol and p-cresol. Concentrations of phenol and p-

cresol (4-methylphenol) were found to be significantly decreased within the urine of colorectal cancer patients compared to healthy controls. Phenol concentrations showed a fold change of -3.13 between cancer and control patients (MWU p<0.001). P-cresol concentrations were also reduced in cancer patients with a fold change of -3.57 compared to healthy controls (MWU p<0.001).

The other two urine studies investigating colorectal cancer patients[84,85] also provided data on concentrations of p-cresol. Qiu et al[84] successfully identified p-cresol within the urine of colorectal cancer patients although there was no significant difference between cancer patients (n=63) and healthy controls (n=60) (Fold change +1.4; p=0.096 (*Student T-Test)).* This study also produced a rat model of colorectal cancer (using intra-peritoneal injection of 1,2-dimethylhydrazine for rats in the cancer group, or sham injection of intra-peritoneal saline for the control group)[84]. Urine from these rats was analysed and demonstrated decreased p-cresol concentrations in the cancer group versus the controls (fold change -2.2 p<0.0001 (*Student t-test*)). This was in the opposite expression direction to clinical samples from this study (Patient samples fold change: +1.4; Rat cancer model fold change: -2.2).

The study by Silva et al[85] analysed urine from patients with multiple cancer types (colorectal (n=12), lymphoma (n=7), leukaemia (n=14)) compared to healthy controls (n=21). There was significantly increased concentrations of p-cresol in the urine of colorectal cancer patients with a 216.5% change of mean peak area compared to healthy controls (p=0.001). When all three cancer types were considered together for analysis in the same paper[85], urinary p-cresol concentrations was significantly elevated across all cancer types (Percentage Increase vs Controls: Colorectal Cancer – +216.5%; Lymphoma – +40.9%; Leukaemia – +89.4% (p=0.014 (*Fishers LSD test)).*

The final urine-based paper by Huang et al[26] compared urinary phenol measurements in patients with oesophago gastric cancer (n=12) with positive control patients (n=14) (defined as patients with non-cancerous disease of the upper gastrointestinal tract), and healthy controls (n=34) (defined as patients with entirely normal upper gastrointestinal tracts as assessed at endoscopy). Results demonstrated significantly reduced concentrations of phenol in the urine of cancer patients (IQR [9-20ppbv]) compared to positive controls (IQR [11-35ppbv]) and healthy controls (IQR [28-50ppbv]).

When the cancer and healthy control groups were directly compared these results were statistically significant (MWU p=0.027). There was no significant difference in cresol (methyl phenol) or ethyl phenol concentrations across these patient groups.

Gastric Content Based Studies

The study which investigated phenolic compounds in gastric content involved collection of intra-gastric fluid at the time of patient endoscopy after a minimum period of six-hour fasting[35]. Patients were grouped into those with gastric cancer (n=19) positive controls (n=9), and healthy controls (n=11). Samples were collected in a disposable suction jar and analysed via SIFT-MS within one-hour of collection. Cancer patients were found to have the highest median methyl phenol concentration (16 ppbv), followed by the positive control group (11 ppbv) and the healthy group (9ppbv) (Kruskal-Wallis test p=0.027).

Breath Sample Based Studies

In the study investigating exhaled breath[36], all breath samples were collected from patients who had been fasted for a minimum of six-hours. Samples were collected in the same room where the patient had been resting for a minimum of 20 minutes. Sampling was performed using a system which comprised a Nalophan (Kalle UK Ltd., Witham UK) bag via a 1mL Luer lok syringe (Terumo Europe, Leuven, Belgium) via a standardised technique. This sampling method was validated in a prior publication[36]. All samples were analysed using the SIFT-MS platform immediately following collection. Patients were divided into three groups consisting of a cancer, positive control and healthy control group via the same method described in the previous studies from the same group[26,35].

In this study concentrations of phenol, cresol (methyl-phenol) and ethyl-phenol were measured. All of these compounds were found to have statistically significant concentration differences between the exhaled breath of oesophago-gastric cancer patients and non-cancer controls as shown in table 3[25].

Compound	Gastric Cancer (n= 33)		Oesophageal Cancer (n=48)		Benign Controls (n=62)		Healthy Controls (n=51)		Cancer vs non-cancer
	Median (ppbv)	***IQR***	***Median (ppbv)***	***IQR***	***Median (ppbv)***	***IQR***	***Median (ppbv)***	***IQR***	***MWU***
Phenol	10	6-25	9	6-18	5	2-8	4	3-7	<0.001
Cresol	8	3-10	7	4-13	4	2-6	3	2-5	<0.001
Ethyl-Phenol	12	7-21	8	4-14	5	2-8	4	2-6	<0.001

Table 3: Results of exhaled breath analysis by Kumar et al.[25] (ppbv = parts per billion by volume; IQR = inter-quartile range).

This study also demonstrated that oesophago-gastric cancer disease stage (either early (Stage I) or late (Stage II and III)), did not significantly affect concentration of these phenolic compounds in exhaled breath[25].

1.6.4 Discussion

The results of this systematic review suggest that the three aromatic amino acids under investigation (tyrosine, phenylalanine, and tryptophan) appear to be increased within the gastric content and tissues of patients with oesophago-gastric cancer. Tyrosine and phenylalanine concentrations were also increased in the urine of these patients. The majority of studies investigating serum (or plasma) concentrations demonstrate that levels of these amino acids are decreased in the serum (or plasma) of oesophago-gastric cancer patients.

Investigation of phenolic compounds has demonstrated that phenol and cresol (methyl-phenol) concentrations appear to be altered in the urine of patients with gastrointestinal cancer with two studies demonstrating increased concentrations of phenol and p-cresol in the urine of cancer patients, and a further two studies demonstrating reduced concentrations of these compounds. One potential limitation of the urine-based studies included in this review is that results were not normalised to urinary creatinine concentration or osmolality[86,87]. Patient hydration status has a significant affect

upon absolute concentrations of urinary metabolites and this may have been a confounding factor for the results of these studies. In addition these studies only measured concentrations of unbound ('free') phenol. Large amounts of phenol are conjugated to glucuronic acid or sulphate in urine, and it would be necessary to deconjugate these prior to analysis in order to take into account total urinary phenol concentrations[87]. These factors may in part explain the conflicting results regarding phenol and p-cresol concentrations in urine. Studies upon exhaled breath and gastric content have demonstrated increased concentrations of phenolic compounds for oesophago-gastric cancer patients within these biological samples.

The causes for these changes in aromatic amino acid and phenol profiles remain unknown. Malnourishment may be a contributing factor to the reduced concentrations of plasma amino acids. Malnourished patients develop a hypermetabolic state with increased hepatic gluconeogenesis and protein catabolism. However, cachexia and malnutrition does not appear to be the primary factor contributing to decreased serum amino acid concentrations in oesophago-gastric cancer patients; this hypothesis is supported by Miyagi *et al.*, who observed decreased plasma free amino acid levels in both early stage disease (stage I) as well as stage IV disease patients[72]. Kawamura *et al.* have also demonstrated that in tumour bearing rats, there are increased hepatic protein synthetic rates and increased muscle catabolism, particularly during later stages of disease[88]. They concluded that development of cachexia in cancer patients was not only related to reduced dietary intake, but is linked to increased whole-body protein turnover. This particularly occurs during the late stages of disease where skeletal muscle protein is mobilised for increased tumour synthesis. Increased protein requirement in the tumour-bearing state reduces the availability of plasma amino acids[64]. Increased demand and overutilisation of amino acids by tumour tissue may account for the reduced concentration of serum amino acids[79]. The changes in blood levels of phenylalanine are of particular interest. Two studies in this review demonstrated reduced concentrations in oesophago-gastric cancer patients and another identified increased concentrations. Previous work has demonstrated that activity of phenylalanine hydroxylase (which converts phenylalanine to tyrosine) is dysfunctional in inflammatory or malignant disease states[45,46]. This raises the possibility that blood phenylalanine levels could be altered in oesophago-gastric cancer patients due to reduced action of this enzyme. Reduction in activity of this enzyme could also account for the decreased tyrosine concentrations

observed by Zhang X *et al.*[70], due to reduced conversion of phenylalanine to tyrosine. However, the biological mechanism responsible for these alterations in amino acid concentrations in cancer patients remains unclear and further investigation is required to identify specific changes within this metabolic pathway of aromatic amino acid breakdown.

The increased levels of aromatic amino acids within gastric content may be an especially important finding as this could potentially link changes in aromatic amino acid profile to phenol production[39,40,42]. Various mechanisms have been proposed to account for increased concentrations of these aromatic amino acids within gastric content. One possibility involves increased production of enzymes by invasive cancer cells which degrade the basement membrane and extracellular matrix[89]. Specific matrix metalloproteinase enzymes have been shown to be up-regulated by aggressive cancer cells[90]. This degradation may release aromatic amino acids into the gastric content causing increased concentrations of these compounds[40]. Other postulated mechanisms to explain this phenomenon include increased protein synthesis within rapidly growing malignant tissues thereby releasing these aromatic amino acids into the gastric content.

These increased amino acid concentrations in gastric content can be linked to phenol production via the process of proteolytic fermentation due to the action of the bacterial enzyme *tyrosine phenol-lyase*. Once tyrosine has been released into the gastric content the action of *tyrosine phenol-lyase* from the gut microbiota could convert tyrosine to phenol causing increased concentrations of this compound within gastric content. This is in keeping with the findings of the study by *Kumar et al.* demonstrating increased phenolic compound concentrations within gastric content of oesophago-gastric cancer patients[35].

The study by *Qiu et al.* proposed that the opposite expression direction for p-cresol in the rat cancer model (down regulated) and patient samples (up regulated) may be explained by differences in the colonic microbiome relating to the development of colorectal cancer. In particular the action of the *Clostridium* was felt to be one potential mechanism for this change as this species is known to be responsible for p-cresol production[91]. Certain subgroups of *Clostridium* have been previously demonstrated to show increased diversity in colorectal cancer patients[92]. These changes in gut flora

may have a causative effect for the changes in p-cresol profile seen in the studies included in this review, and explain the variation in direction of change for this compound (up-regulated in two studies, down regulated in two studies and one animal model).

Although a large amount of research has been focussed upon the makeup of the colonic microbiome, little work has been completed to investigate the bacterial species present within the stomach. The presence of *Helicobacter Pylori* has long been recognised as a causative factor for the development of gastric cancer[93,94]. Recent advances in bacterial sequencing have allowed the characterisation of the bacterial ecosystem within the stomach beyond simply the presence or absence of *H. Pylori.* Studies have established that the predominant bacterial phyla present within the stomach are *Proteobacteria, Firmicutes, Actinobacteria, Bacteriodetes* and *Fusobacteria*[95–98]. Bacteria which are known to contain the *tyrosine phenol lyase* enzyme include *Fusobacteria*[37,38]*, Clostridium*[91]*, and Escherichia*[99]*.* Each of these bacteria have been identified within the stomach at a genus level[95–98], indicating the potential of stomach bacteria to convert tyrosine to phenol. There is also significant overlap between the bacterial composition of the stomach and distal oesophagus, with *Fusobacteria, Clostridium* and *Escherichia* all having been identified within areas of normal squamous oesophageal tissue[100–102]. *Fusobacterium* has been observed to be more prevalent in areas of reflux oesophagitis or Barrett's oesophagus than normal mucosa, and this change in microbial makeup relating to disease may be an influencing factor in phenol production[101].

This hypothesis of bacterial conversion of tyrosine within the upper gastro-intestinal tract provides a potential explanation for increased phenol concentrations identified in the exhaled breath of oesophago-gastric cancer patients[25]. Based upon the findings of *Kumar et al. p*henol is a potentially valuable biomarker of oesophago-gastric cancer in exhaled breath[25]. This study established that not only were phenol, cresol (methylphenol) and ethyl-phenol significantly different between cancer and control patients, but these increased concentrations were also present within the exhaled breath of patients with early stage cancer (Stage I). This highlights the potential of this diagnostic test to identify patients with oesophago-gastric cancer at early-stages of the condition when the patient can still be offered curative surgery. Phenol, methyl-phenol and ethyl-phenol were included as part of a diagnostic model (along with nine other compounds) which was able to differentiate oesophago-

gastric cancer patients from non-cancer controls with an area under the ROC curve of 0.92[25]. Development of a non-invasive exhaled breath test to assess oesophago-gastric cancer risk could help to increase the number of patients with this disease who can be treated with curative intent (currently only 37.6% of cases[3]) and thereby improve survival.

1.7 Conclusions from Systematic Review

Tyrosine, phenylalanine and tryptophan concentrations appear to be altered within the biofluids and tissue of oesophago-gastric cancer patients; these compounds represent promising biomarker targets in oesophago-gastric cancer and hence further studies are needed to investigate the underlying cause of dysfunctional aromatic amino acid metabolism in oesophago-gastric cancer.

These alterations in aromatic amino acid metabolism are potentially related to phenol production in these patients via the activity of bacteria within the stomach which contain the *tyrosine phenol lyase* enzyme. Phenol has been identified as a potential biomarker or oesophago-gastric cancer in exhaled breath[36], urine[67], and gastric content[35].

Although aromatic amino acid metabolism has been demonstrated to be dysfunctional in oesophago-gastric cancer the biological mechanism responsible for these changes remains unclear and no detailed investigation of the enzymes regulating aromatic amino acid breakdown in these patients has been performed. The potential link between aromatic amino acid breakdown and phenol production in these patients has not been previously examined and this may provide a biological explanation for increased phenol production in oesophago-gastric cancer patients.

1.8 Thesis Aims

The primary aims of this thesis are to:

1. Investigate the underlying mechanism responsible for dysfunctional aromatic amino acid metabolism in oesophago-gastric cancer.
2. Undertake a thorough investigation of phenol production in these patients and how this may be linked to aromatic amino acid breakdown via *tyrosine phenol lyase* activity.

The long term aims of this work are to provide a greater understanding of how phenol is produced in oesophago-gastric cancer patients. The use of breath or urine analysis as non-invasive tests for the diagnosis of oesophago-gastric cancer will not be widely adopted by the clinical community unless it is possible to explain the underlying mechanism responsible for the changes seen. Establishing the cause of increased phenol production will help to introduce these non-invasive methods for stratification of oesophago-gastric cancer risk into clinical practice, and thereby allow for streamlining the use of endoscopy services to those at greatest risk of this disease. It is hoped this would lead to an increase rate of diagnosis at early-stages of disease before symptoms of more advanced disease such as dysphagia develop. This would lead to more patients being treated with curative intent and thereby improve survival.

CHAPTER 2 - METHOD DEVELOPMENT

2.1 Phenol GC-MS Method Development

2.1.1 Objective

This section aimed to develop a gas-chromatography mass spectrometry (GC-MS) method for analysis of phenolic compounds including phenol, cresols (methyl-phenols), and ethyl-phenols. This method has been utilised in later sections for quantification of phenolic compounds within urine, gastric content, serum and tissues.

2.1.2 Introduction

Previous studies using selected ion flow tube mass spectrometry (SIFT-MS) have identified phenol, cresol (methyl-phenol) and ethyl-phenol as potential markers of oesophago-gastric cancer in exhaled breath, urine and gastric content[25,26,35]. SIFT-MS utilises chemical ionisation of volatile compounds in air/vapour samples for direct mass spectrometry analysis[103]. This enables accurate real-time quantification of volatile compounds. However, due to the lack of chromatographic separation using this analytical technique, compound identification is reliant upon characteristic product ion patterns stored within the internal reference library. This can create difficulties with overlaps between multiple product ions leading to challenges in compound identification. Of particular relevance to this work are potential overlaps between the product ions of phenol and dimethyl-disulphide[86].

Gas-chromatography mass spectrometry (GC-MS) overcomes these issues with compound identification via the use of chromatographic separation, and is generally considered the 'gold-standard' in analysis of volatile compounds. This analytical technique involves samples being introduced into an injector at high temperature, and then passing onto the chromatographic column (typically held initially at low temperature within an oven) via a carrier gas (usually helium). Upon entering the column different compounds within a mixed sample are separated according to their relative affinity for the stationary-phase of the column. As the temperature of the chromatographic column gradually rises compounds lose their affinity to the column (elute) at different times (known as retention time) and then can be detected by the downstream mass spectrometer. A schematic diagram outlining the principle of a typical GC-MS system is shown in figure 4.

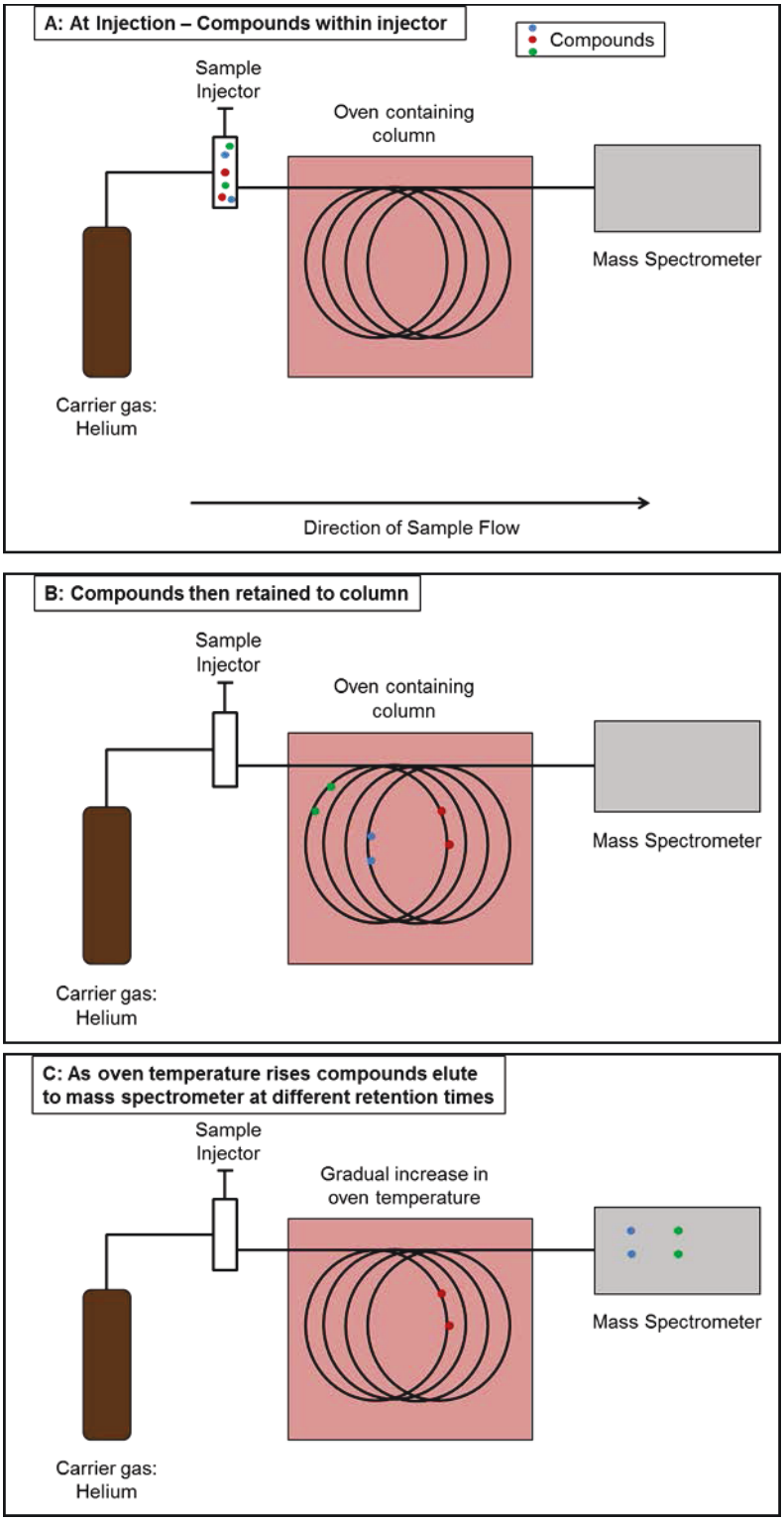


Figure 4: *Outline of a typical GC-MS system showing compounds entering the injector (A) then becoming retained upon the chromatographic column (B). As oven temperature is gradually increased compounds lose affinity for the column and travel to the downstream mass spectrometer to be detected at a specific retention time (C).*

This section of method development aimed to produce a targeted GC-MS method to chromatographically separate and quantify phenolic compounds (phenol, o-cresol (2-methylphenol), m-cresol (3-methylphenol), p-cresol (4-methylphenol), 2-ethylphenol, 3-ethylphenol, and 4-ethylphenol).

2.1.3 Method Development

These experiments were performed using a Clarus 580-SQ8 GC-MS® (Perkin Elmer, Seer Green, BUCKS, UK) equipped with a CTC autosampler® (PAL systems, Zwingen, Switzerland). Columns assessed included an RXi5ms® (crossbond diphenyl dimethyl polysiloxane) column followed by a Stabilwax DA® polyethyleneglycol column (both Restek, Bellefonte, PA, USA). Both columns used were 30m in length, with an internal diameter of 0.25mm and thickness of 0.25µm. Headspace analysis of standard solutions (Phenol, p-cresol, m-cresol, o-cresol, 2-ethylphenol, 3-ethylphenol, 4-ethylphenol (All Sigma Aldrich, Gillingham, Dorset, UK)) was undertaken via solid phase micro-extraction (SPME) using a carboxen/polydimethysiloxane solid phase microextraction (SPME) fibre (Supelco, Bellefonte, PA, USA). SPME conditions were constant for all experiments with the incubator temperature of 60°C, a sample equilibration time of 20 minutes within the incubator, followed by an extraction time of 40 minutes.

During all experiments the injector temperature was 230°C with a helium carrier gas flow of 1ml/min. Splitless time and amount of split were adjusted during the experiment to optimise compound peak shape but was initially 20ml/minute after a splitless time of 1 minute.

The temperature programs produced for initial analysis are shown in figure 5. These methods were later adjusted to optimise compound elution and peak shape.

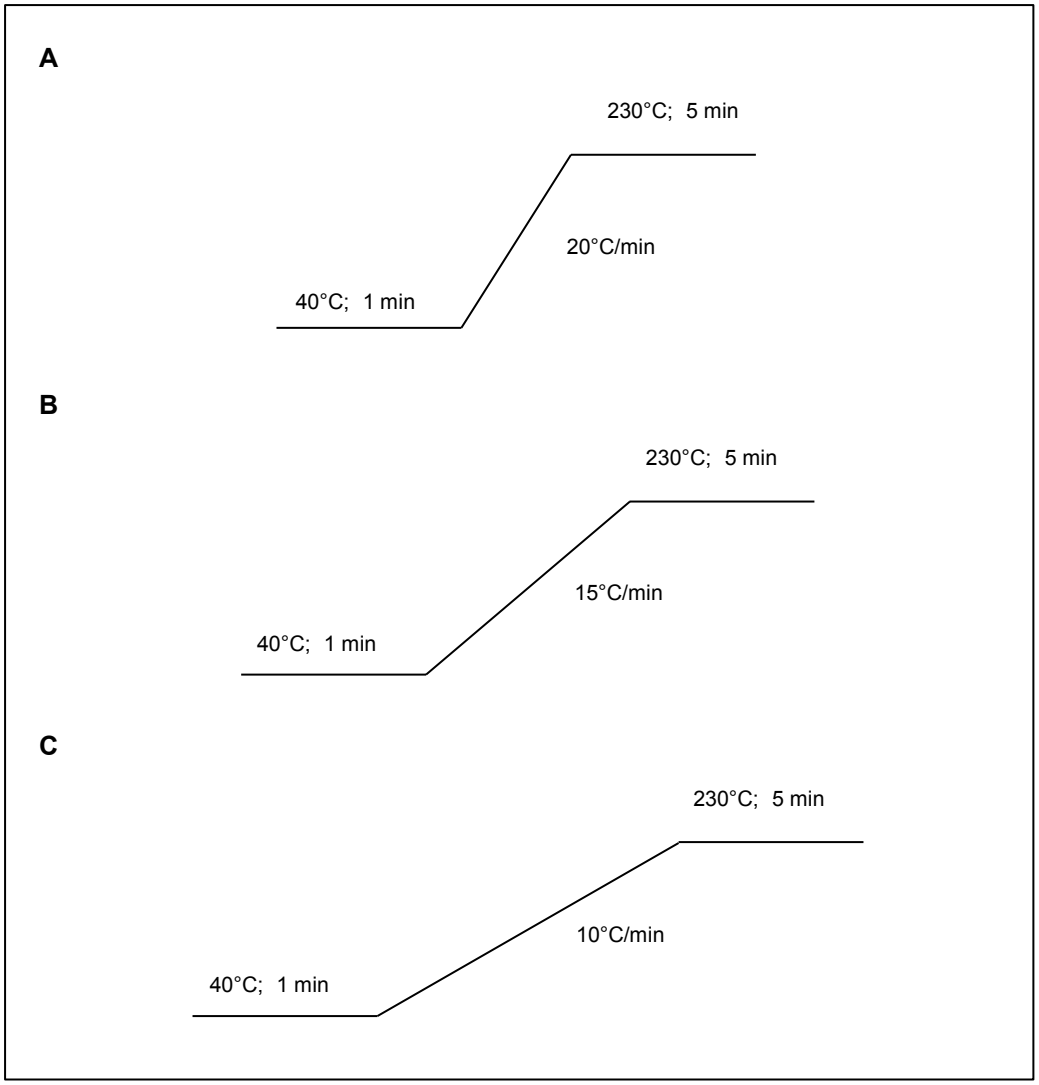


Figure 5: Initial temperature programmes for GC-MS analysis. A - 20°C/min, B- 15°C/min, C- 10°C/min

Standard solutions were initially analysed at a concentration of 2µg/ml. Five millilitre aliquots of standard solutions (All Sigma Aldrich, Gillingham, Dorset, UK) were added to 20ml glass vials with magnetic caps and PTFE septum (Chromacol, Welwyn Garden City, HERTS, UK).

Column Selection

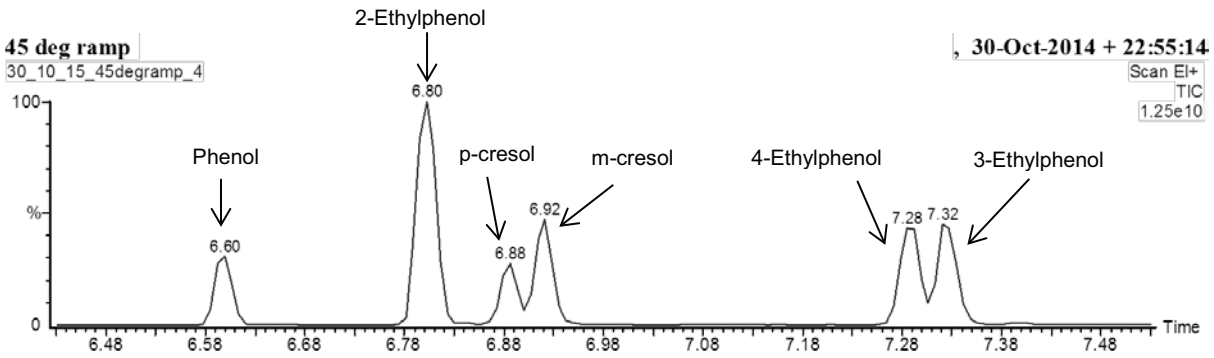
Initial analysis was performed using an RXi5ms® column. Standard solutions of 2µg/ml phenol were analysed according to the conditions described above using temperature programmes with a ramp of

20°C per minute, 15°C per minute and 10°C per minute. Chromatograms are shown in Supplementary figures 1 A-C.

The peak shape of phenol was poor using this temperature programme and column combination with a large amount of peak tailing. Therefore the speed of the temperature ramp was increased in an attempt to improve peak shape. Supplementary figure 2 (A-C) shows results when the temperature protocol was adjusted to a temperature increase of 45°C per minute, 40°C per minute, and 30°C per minute. The best peak shape was identified with a temperature ramp of 40°C per minute.

p-Cresol was then added to the solution at the same concentration as phenol (both 2µg/mL) and the resulting chromatogram is shown in supplementary figure 3. m-Cresol was then analysed with p-cresol to establish if these isomers could be separated. The same temperature programme was used as above. As shown in supplementary figure 4 it was not possible to separate these isomers and therefore an isothermic temperature hold at 180°C was added to the temperature programme to establish if this change would facilitate separation of these isomers. As shown in supplementary figure 5 it was still not possible to separate these isomers.

Due to the difficulties in separating these isomers of cresol the GC column was changed to a Stabilwax© DA polyethylene glycol column. The length of this column was 30m with an internal diameter of 0.25mm. Analysis using a temperature programme with a 45°C ramp is shown below in figure 6.



<u>Figure 6:</u> Separation of all compounds on new column using above temperature methods. Compound elution times as follows: Phenol 6.60 minutes, 2-ethylphenol 6.80 minutes, p-cresol 6.88 minutes, m-cresol 6.92 minutes, 4-ethylphenol 7.28 minutes, 3-ethylphenol 7.32 minutes.

On this alternative column it was possible to separate these isomers of cresol (p and m) as well as phenol, and all isomers of ethyl-phenol eluted separately. Temperature ramps of 40°C per minute, 30°C per minute, and 20°C per minute were tested and results are shown in supplementary figure 6:

This demonstrated that separation was similar with temperature ramps of 40°C, 30°C, and 20°C. As there was little difference in analysis time (40°C – 10 minutes; 30°C – 12 minutes; 20°C – 14 minutes) the 20°C per minute ramp was selected to be utilised as part of further analysis. This was because this slightly slower temperature ramp would reduce co-elution of phenolics with other compounds within the sample matrix. As there was no difference in phenolic compound separation or peak shape and analysis time was only a few minutes longer with the 20°C per minute ramp the faster temperature protocols did not offer any significant benefits.

o-Cresol standards were then added to the analysis. Elution time for o-cresol on this temperature programme was very close to that for phenol (10.54 o-cresol; 10.60 phenol).

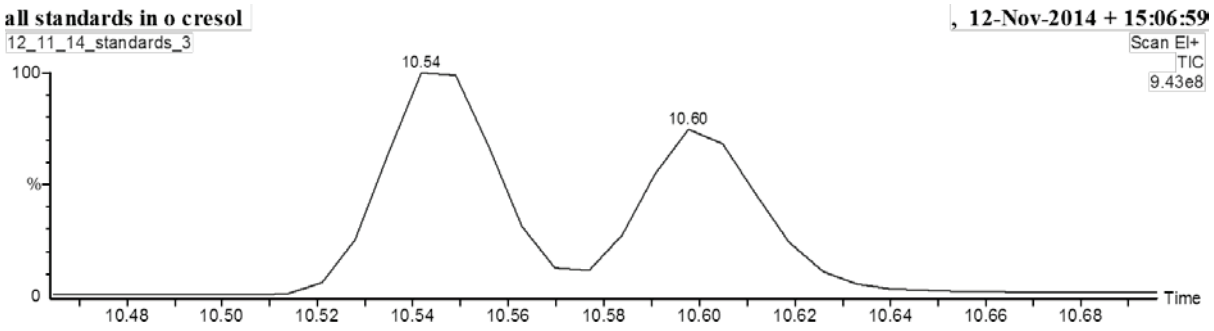


Figure 7: Phenol and o-cresol eluting at 10.54 and 10.60.

Alternative temperature ramps were trialled in an attempt to further separate these two compounds but this was not possible. Therefore, the temperature programme shown below was taken forward as the finalised temperature protocol:

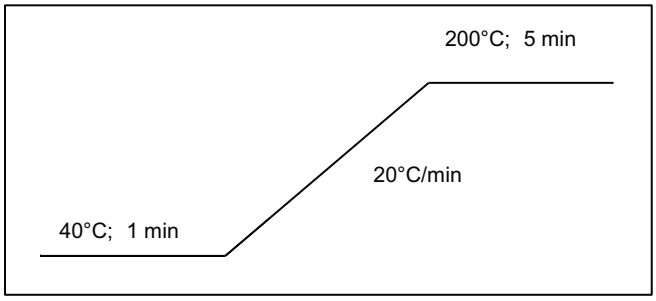


Figure 8: Optimised temperature programme.

Adjustment of Split Time

The splitless time and split amount was adjusted to establish if this could improve peak shape further.

The following split parameters were used:

1. 50mL split after 2 minutes.
2. 30mL split after 2 minutes.
3. 20mL split after 2 minutes.
4. 50mL split after 1 minute.
5. 30mL split after 1 minute.
6. 20mL split after 1 minute.
7. 50mL split after 30 seconds.
8. 30mL split after 30 seconds.
9. 20mL split after 30 seconds.

These results showed similar peak shapes with these split time but a split of 30mL after a splitless time of 30 seconds appeared to demonstrate the best peak shape.

Development of Mass Spectrometry Method

The above experiments were performed using a basic mass spectrometry (MS) method which only included full scan data acquisition without any selected ion recording (SIR). The scan time on this original method was 0.4 seconds.

In order to optimise phenolics analysis it was necessary to develop an SIR method so that the mass-to-charge ratio (m/z) of the compounds of interest are specifically captured during the elution period for that compound. The first step in developing the SIR method was to establish the scan period for the various m/z values needed based upon the elution time and mass spectrum of the relevant compound. Details are shown below in table 4.

Compound	Elution Time(min)	Scan Time (min)	m/z (Da)
o-cresol and Phenol	10.58 & 10.60	10.30 – 10.80	65, 94, 95, 107, 108.
2-ethylphenol	11.10	10.90 – 11.19	123, 122, 107.
p & m-cresol	11.26 & 11.34	11.20 – 11.50	79, 107, 108.
4 & 3-ethylphenol	12.25 & 12.35	12.10 – 12.50	107, 122, 123

Table 4: Details of SIR including compound of interest, elution time, scan time, and m/z to be scanned.

The above SIR method was created with a dwell time of 0.05 seconds and inter-channel delay of 0.02 seconds. This was created to run alongside the full scan mass spectrometry method which would run throughout the whole analysis time.

The use of SIR assisted the analysis of these phenolic compounds as the mass spectrometer quadrapole specifically selected the chosen m/z during that scan period. Using phenol as an example the difference in chromatogram and mass spectrum using full scan and SIR is detailed in figure 9 A-D.

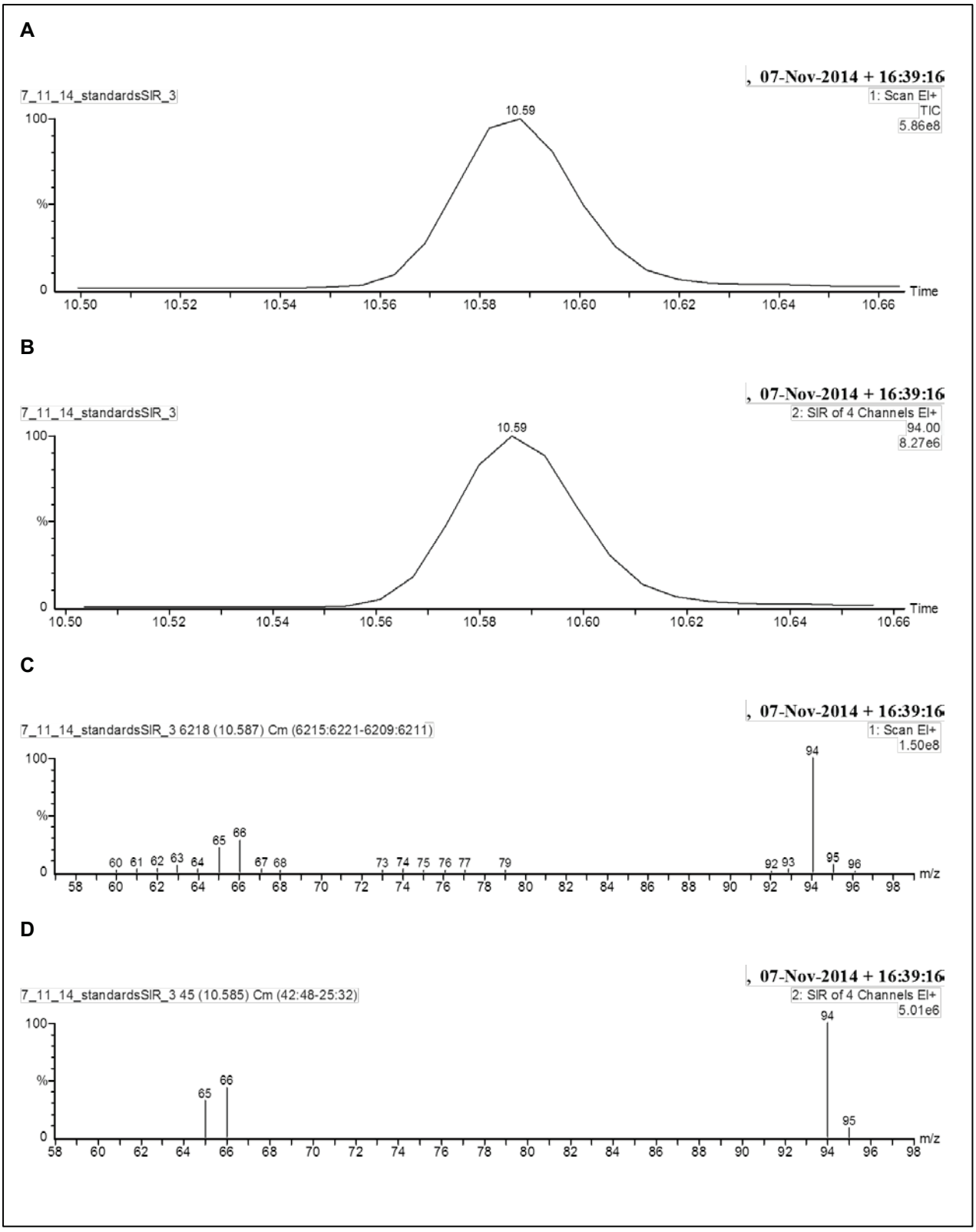


Figure 9: The full scan chromatogram for the phenol peak is shown in A. When SIR for phenol m/z of 94 was used (B) peak shape was seen to improve and overall baseline is reduced. Although the mass spectrum for phenol in full scan mode (C) contained a greater number of ions the critical ions for phenol identification could still be assessed using SIR as shown in D.

The full scan mode scan time was initially 0.4 seconds with an inter-scan delay of 0.02 seconds. The addition of the SIR method alongside the full scan mode increased the length of time between each full scan capture data point. This significantly affected peak shape. To improve peak shape various scan times were trialled with a constant inter-scan delay of 0.02 seconds. It was aimed to capture a minimum of 8 data points for the phenol peak. These results are shown in supplementary figure 7.

Scan times of 0.4 and 0.2 seconds did not provide adequate data points. The scan times of 0.1 and 0.08 seconds did provide greater than eight data points and peak shape was good with these scan times. A full scan mode scan time of 0.1 seconds was therefore selected.

During the first SIR section there were initially four m/z's being scanned with a dwell time of 0.05 seconds and inter-channel delay of 0.02s. This lead to poor peak shapes for the 94 m/z ion. When the 94 m/z ion was scanned alone the peak shape was greatly improved. However in order to also measure o-cresol it was also necessary to scan for the 107 and 108 m/z ions. Phenol peak shape when scanning for all three of these ions was adequate. Finally, the dwell time for each m/z was reduced to 0.02 seconds and this produced good peak shape. All chromatograms are shown in supplementary figure 8.

From these results it appeared that a dwell time of 0.02 seconds provided an adequate peak shape (with a minimum of 8 data points per peak) when it was necessary to scan for three m/z's during SIR. As full scan mode was being analysed alongside SIR the full scan chromatogram could be utilised for compound identification where other m/z ions (outside of the SIR method) were required.

Addition of Isotope Labelled Phenol D6

Phenol D6 was selected as isotope labelled internal standard to facilitate quantification of phenolic compounds. Phenol D6 had the same elution time as phenol on the current temperature programme (10.57 vs 10.58). Multiple different temperature programmes were attempted but it was not possible to separate phenol D6 and phenol. The SIR method was adjusted to include scanning for the largest ion of phenol D6 (m/z 99) to allow for separate analysis of phenol D6 and phenol as shown in figure 10.

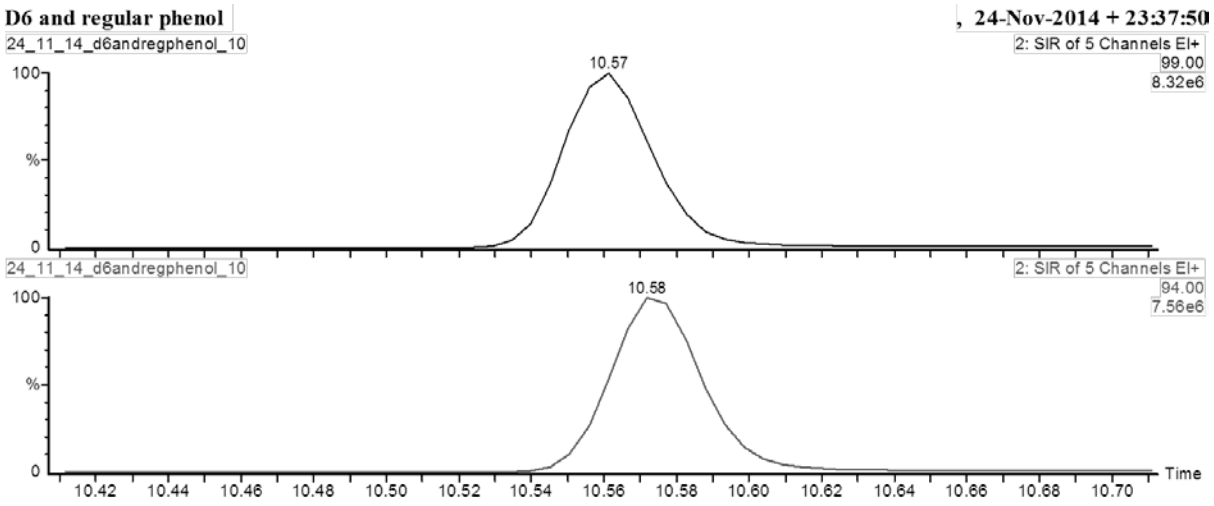


Figure 10: SIR scanning for the m/z of Phenol D6 (m/z 99; elution time 10.57) and phenol (m/z 94, elution time 10.58).

The revised SIR method to incorporate scanning for phenol D6 is shown below in table 5.

Compound	**Elution Time (min)**	**Scan Time (min)**	**m/z (Da)**
o-cresol, Phenol & Phenol D6	10.58, 10.58-10.60 and 10.57	10.30 – 10.80	94, 99, 108.
2-ethylphenol	11.10	10.90 – 11.19	123, 122.
m & p-cresol	11.26 & 11.34	11.20 – 11.50	107, 108.
4 & 3-ethylphenol	12.25 & 12.35	12.10 – 12.50	122, 123

Table 5: Finalised SIR method incorporating scanning for 99 ion of phenol D6 and reduced number of m/z values in each SIR period to improve peak shape.

Calibration Curve

In order to quantify phenol within biological samples it was necessary to produce a calibration curve. As isotope labelled D6 phenol was being utilised as internal standard the calibration curve was produced to compare the ratio of phenolic compounds to D6 phenol. The concentration of D6 phenol remained constant with 2.5µg being added to each 5mL sample (as a 10µl spike of 250µg/ml

concentration D6 phenol in HPLC grade water) to give a final concentration of 0.5µg/ml. The following phenolic compound concentrations were used: 0.05µg/ml, 0.1µg/ml, 0.25µg/ml, 0.5µg/ml, 1µg/ml, 2µg/ml, 5µg/ml, 10µg/ml, 15µg/ml, and 20µg/ml. All calibration points were measured in technical triplicates. Calibration curves for phenol and p-cresol are shown in figure 11:

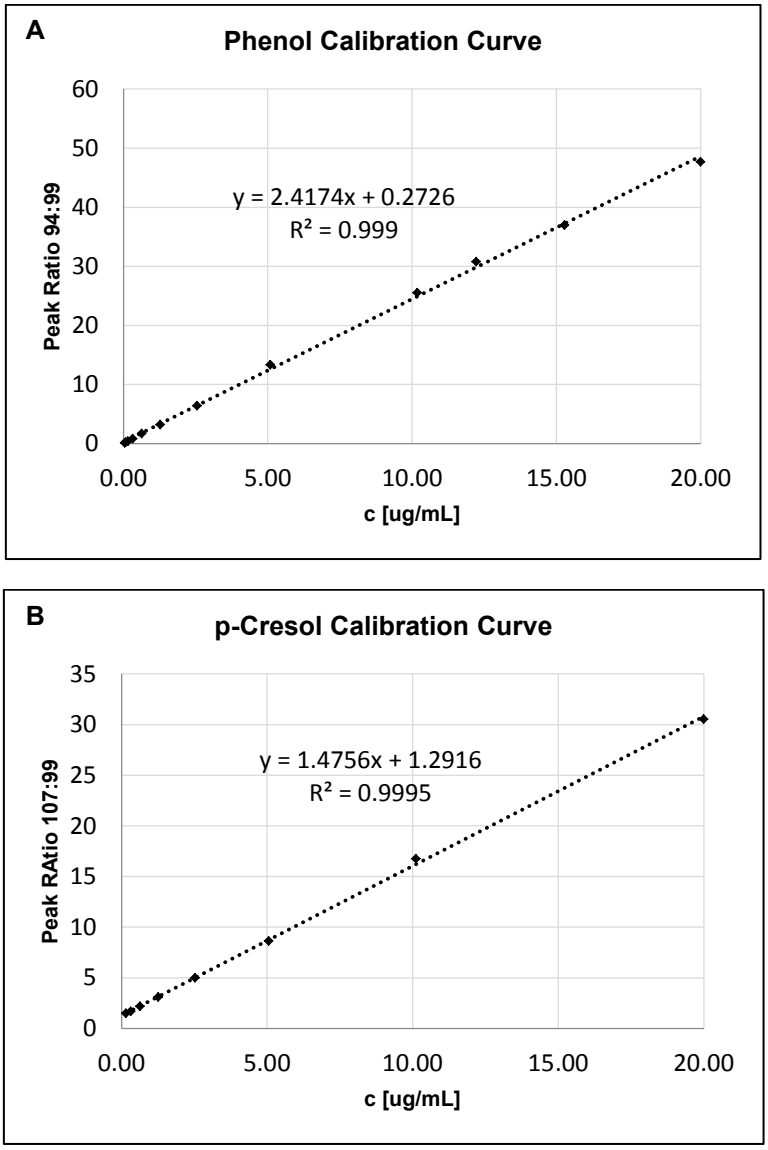


Figure 11: A – Phenol calibration curve (94:99 ratio versus phenol concentration up to 20ug/ml phenol); B – P-Cresol calibration curve (107:99 ratio versus p-Cresol concentration up to 20ug/ml phenol).

These calibration curves demonstrated good linearity between for phenol and p-cresol calibration up to 20µg/ml concentration. As it was not anticipated the concentrations would be higher than this it was not felt necessary for higher phenol and p-cresol concentrations to be examined.

2.1.4 Conclusions

This work has produced a GC-MS method to identify and quantify phenol, o-cresol, p-cresol, m-cresol, 2-ethylphenol, 3-ethylphenol, and 4-ethylphenol. These compounds were separated chromatographically by the method produced and peak shapes optimised.

Having established the GC-MS chromatography method to be used for analysis it was then necessary to optimise sample extraction using solid-phase micro-extraction (SPME) or solid-phase extraction (for direct liquid injection analysis).

2.2 Solid Phase Micro-Extraction Method Development for GC-MS

2.2.1 Objective

This section aimed to optimise a head-space solid phase microextraction (HS-SPME) method for extraction of phenol from patient samples (urine and gastric content) for analysis using the GC-MS method developed in Section 2.1.

2.2.2 Introduction

Solid phase microextraction (SPME) was developed in the 1990's by Professor Janusz Pawliszyn[104]. This technique utilises a fused-silica fibre coated with an appropriate stationary phase housed within a protective needle[105]. SPME can be used to extract analytes from biological samples either via directly immersing the fibre within the sample matrix, or by extracting analytes from the headspace above the sample (head-space solid phase micro-extraction (HS-SPME)[106]. Following extraction the fibre is placed within the inlet of the analytical instrument being utilised, and has been routinely coupled to GC-MS[107]. The benefits of this method of extraction for volatile analytes include the limited amount of sample preparation steps required, lack of solvent use, and the potential to concentrate analytes and improve detection limits[107]. Solid phase microextraction coupled to GC-MS has previously been successfully utilised for measurement of phenol concentrations from drinking water[108].

2.2.3 Method Development

These optimisation experiments were performed using a CTC autosampler® (PAL systems, Zwingen, Switzerland) coupled to the Clarus 580-SQ8 GC-MS® (Perkin Elmer, Seer Green, BUCKS, UK) with an SPME liner (internal diameter 1mm) (Supelco, Bellefonte, PA, USA).

All samples were agitated by the autosampler during equilibration and SPME extraction performed at 500rpm (on time 5 seconds followed by 2 seconds off time). This agitation remained constant throughout all optimisation experiments.

During this section the following parameters were investigated in order to establish their effect upon the extraction of the phenolic compounds via HS-SPME in urine and gastric content:

- SPME Fibre type.
- Equilibration time.
- Solid phase micro-extraction (SPME) temperature.
- SPME time.
- Salination of samples.
- pH alteration of gastric content samples.
- Hydrolysis of urine samples.

Pooled samples of urine and gastric content were produced from the available samples and each of these different parameters was evaluated using a separate aliquot of the same pooled sample. Each variable to be evaluated was analysed in triplicate to reduce the risk of an error in sample preparation or analysis influencing results.

SPME Fibre Type

A carboxen/polydimethysiloxane (CAR-PDMS) SPME fibre was tested against a polydimethylsiloxane/Divinylbenzene (PDMS/DVB) fibre (both Supelco, Bellefonte, PA, USA). Extraction appeared increased using the CAR-PDMS fibre and this was selected for further analysis.

Equilibration Time

Prior to SPME extraction each sample required time for headspace equilibration at increased temperature. Longer time prior to the beginning of SPME could improve headspace equilibration but would prolong sample analysis time. In this section of the experiment the following headspace equilibration times were assessed:

- 10 minutes
- 20 minutes
- 30 minutes

All other variables (except equilibration time) remained constant during this analysis. Equilibration temperature was 60°C.

The phenol peak area with an equilibration time of 10 minutes was similar to that for a 20 minute and 30 minute equilibration time (see table 6 and figure 12). This indicated that headspace equilibration was adequate using a pre-SPME equilibration time of 10 minutes and therefore this was selected for further experimentation.

Equilibration Time (Mins)	**Urine (Phenol peak Area)**	**Gastric Content (Phenol Peak Area)**
10	3204 ± 295	229581 ± 48179
20	3668 ± 267	237864 ± 43239
30	3971 ± 891	237566 ± 31598

Table 6: Phenol peak area results with changes in equilibration time.

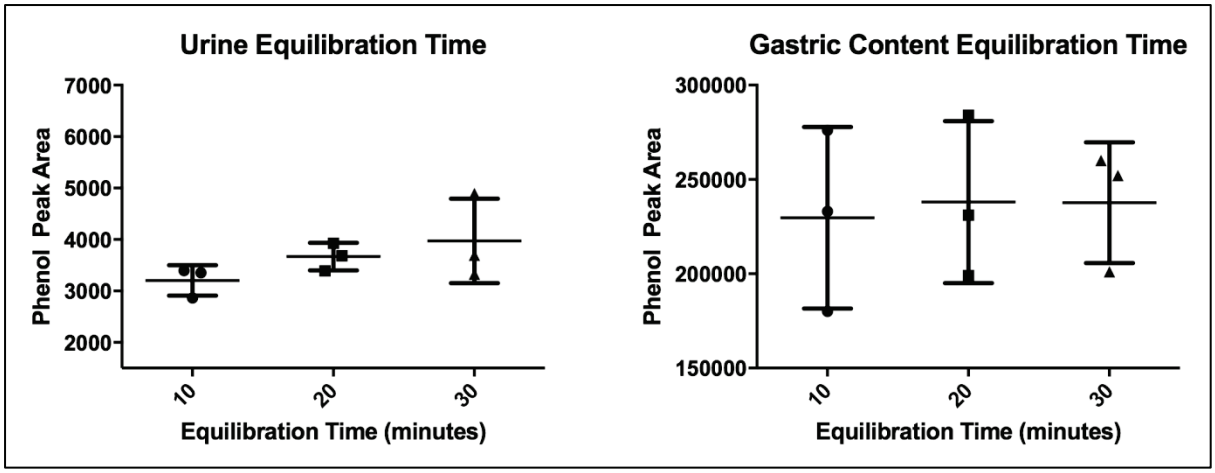


Figure 12: Phenol peak area with equilibration times of 10 minutes, 20 minutes and 30 minutes.

SPME Temperature

The temperature at which SPME was performed would also influence the headspace equilibration. Raising the temperature of SPME could increase the release of phenolic compounds into the sample

headspace and therefore improve extraction. During this section the following SPME extraction temperatures were evaluated:

- 30°C
- 45°C
- 60°C

Again, all other parameters remained constant and aliquots from the same pooled sample were utilised for each different temperature point.

Increasing temperature of SPME extraction showed an increasing phenol peak area. Phenol peak area at 30°C extraction was low and increased substantially when extraction temperature was increased to 45°C and then even further at 60°C. For this reason a SPME extraction temperature of 60°C was selected for further experimentation.

Extraction Temp (Degrees Celsius)	**Urine (Phenol peak Area)**	**Gastric Content (Phenol Peak Area)**
30°C	866 ± 178	13352 ± 8686
45°C	1634 ± 92	103754 ± 4418
60°C	3204 ± 296	249814 ± 34369

Table 7: Phenol peak area with SPME extraction temperature of 30°C, 45°C and 60°C.

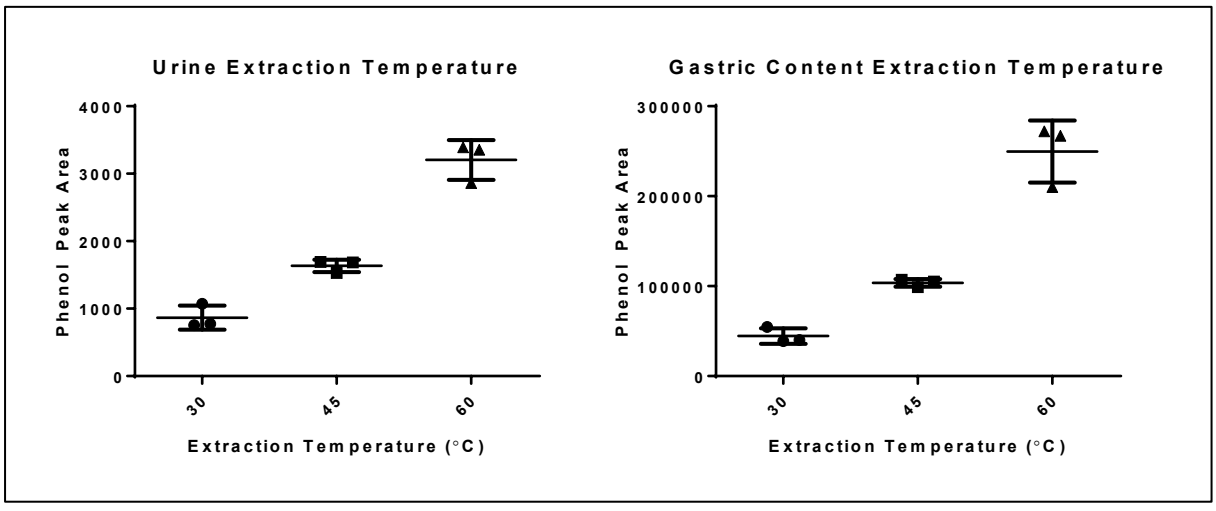


Figure 13: Phenol peak area with increasing SPME extraction temperature at 30°C, 45°C and 60°C.

SPME Time

Increasing extraction time could be expected to increase the absorption of phenol onto the SPME fibre and therefore increase the peak area of phenol identified on GC-MS analysis. However, increasing the extraction time would increase the sample analysis time. The following SPME times were assessed (while all other parameters remained constant):

- 20 minutes.
- 40 minutes.
- 60 minutes.

During evaluation of SPME extraction time there was an increasing phenol peak area from 20 minutes to 40 minutes, and 60 minutes. As the phenol peak area was largest with 60 minutes extraction this was selected as the best SPME extraction time for this method. Longer SPME times were not considered for the final method due to prolonged analysis times.

Extraction Time (Mins)	Urine (Phenol peak Area)	Gastric Content (Phenol Peak Area)
20	2091 ± 309	136775 ± 20155
40	3204 ± 295	262841 ± 3744
60	7622 ± 1533	348234 ± 33334

Table 8: Phenol peak area increasing with increasing extraction time.

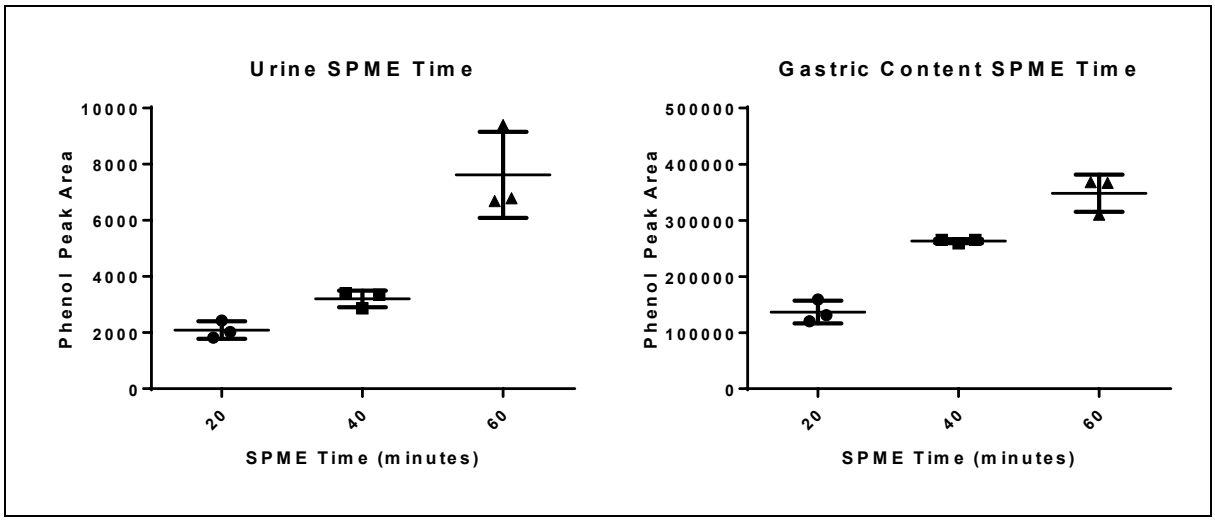


Figure 14: Increasing phenol peak area with lengthening of SPME extraction time.

Based upon these results a 60 minute SPME extraction time was selected as the optimum extraction time and was therefore used in all further experiments.

Salination of Samples

Salination of biological samples has been shown to increase release of volatile compounds into the headspace for extraction. This 'salting out' effect occurs as the presence of salt decreases the solubility of other compounds in water (as water molecules preferentially solvate the salt ions)[109]. This reduction in solubility shifts the equilibrium by forcing more analyte ions (in this case phenol) into the headspace, and therefore increasing the amount extracted onto the SPME fibre. In this section of the experiment differing quantities of sodium chloride (NaCl - Sigma Aldrich, Gillingham, Dorset, UK) were

added to different aliquots of the same pooled sample to evaluate the affect this has upon phenol extraction. SPME temperature (60°C) and extraction time (60 minutes) were kept constant. The quantities of NaCl to be added to each 5ml sample were:

- 0g.
- 0.2g.
- 0.4g.
- 0.6g.

As increasing quantities of NaCl were added the phenol peak area increased. However, when 0.6g of NaCl was added to each sample the salt did not adequately dissolve within the 5ml sample. These samples were therefore not analysed. It was selected that 0.4g of NaCl would be added to each of the samples for analysis. These results of large increases in sample extraction with increasing salt addition are consistent with results from previous studies where salination produced a 5.5 factor increase in phenol extraction[109].

NaCl Added (Grams)	Urine (Phenol peak Area)	Gastric Content (Phenol Peak Area)
0	3204 ± 295	115655 ± 12632
0.2	6046 ± 478	152824 ± 30694
0.4	8483 ± 543	195469 ± 40538

Table 9: Changes in phenol peak area with salination of samples.

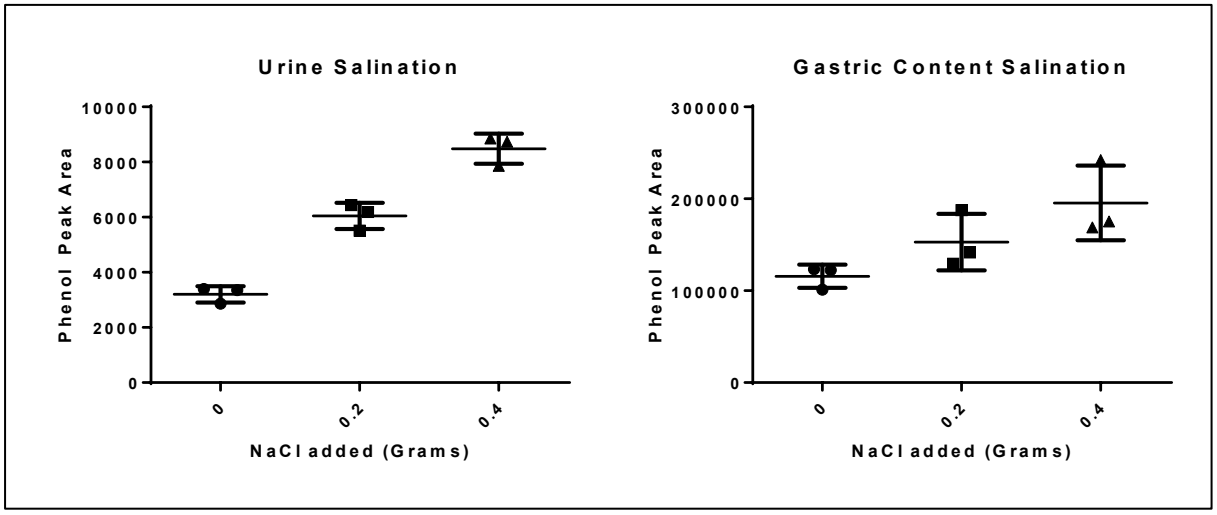


Figure 15: Increasing phenol peak area with increasing salination of samples.

Effect of pH

The acidity of samples has been shown to influence the release of volatile compounds into headspace, with increased volatility as pH is lowered. This phenomenon occurs because at neutral pH analytes are largely in their ionic form. By lowering the sample pH the acid-base equilibriums of these compounds shifts towards their neutral form. This provides a greater affinity for the SPME fibre and increases the amount extracted[109]. Samples were buffered to the following pH values using sodium hydroxide and hydrochloric acid (both Sigma Aldrich, Gillingham, Dorset, UK) where necessary. The following pH points were assessed using the same pooled gastric content sample:

- pH 2
- pH 4
- pH 6
- pH 8

Effect of pH was not analysed for urine samples as all urine samples were buffered to pH 2 to as phenol is conjugated to glucuronic acid or sulphate in urine and it was necessary to deconjugate this prior to analysis[87]. This procedure is discussed in the next section.

Alteration of pH showed little difference in the peak area of phenol from gastric content. This was consistent with previous findings where buffering samples to pH 2 produced no significant change in phenol extraction (factor change of 0.9;)[109]. When combined with salination of samples, acidification produced a factor change of 6.0 (factor change of 5.5 for salination alone)[109]. Therefore, along with salination with 0.4g of NaCl all samples would be buffered to a pH of 2 prior to analysis.

pH	Urine (Phenol peak Area)	Gastric Content (Phenol Peak Area)
2	N/A	127069 ± 30719
4	N/A	150749 ± 23264
6	N/A	143284 ± 21502
8	N/A	136269 ± 28822

Table 10: Effect of pH changes upon phenol extraction from gastric content.

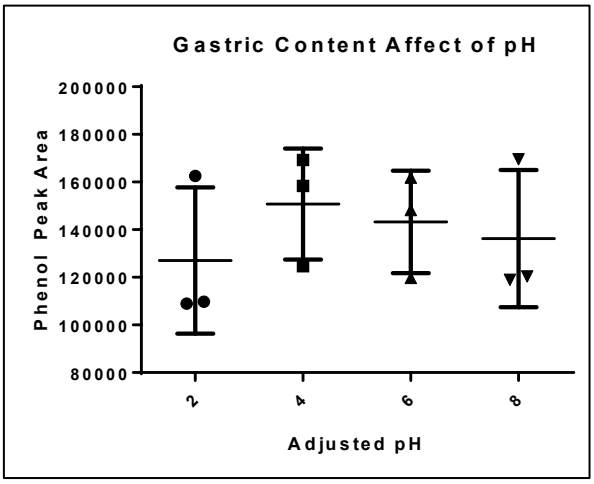


Figure 16: Little change in phenol peak area with changes in pH.

Hydrolysis of Urine Samples

As urinary phenol is conjugated to glucuronic acid or sulphate in urine, it was necessary to hydrolyse samples prior to analysis in order to measure total phenol concentrations[87]. This process deconjugates phenol from glucuronic acid or sulphate and can be performed via an enzymatic process or acidification and heating[110]. For urine samples it was chosen to use acidification and heating.

Unhydrolysed samples were analysed directly without addition of acid or heating. 0.4g NaCl was added to 5ml of urine and they were analysed as above. For hydrolysed samples 5ml of urine was acidified with 80µL concentrated hydrochloric acid (to buffer to pH 2) and 0.4g of NaCl added prior to

heating. Vials were sealed using screw caps with polytetrefluroethylene inserts (Chromacol, Welwyn Garden City, UK) then heated to 90°C for 90 minutes for hydrolysis. Samples were allowed to cool and remained sealed until analysis.

	Urine **(Phenol peak Area)**
Unhydrolysed	196 ± 29
Hydrolysed	3204 ± 295

Table 11: Greatly increased phenol peak area with hydrolysis of urine samples.

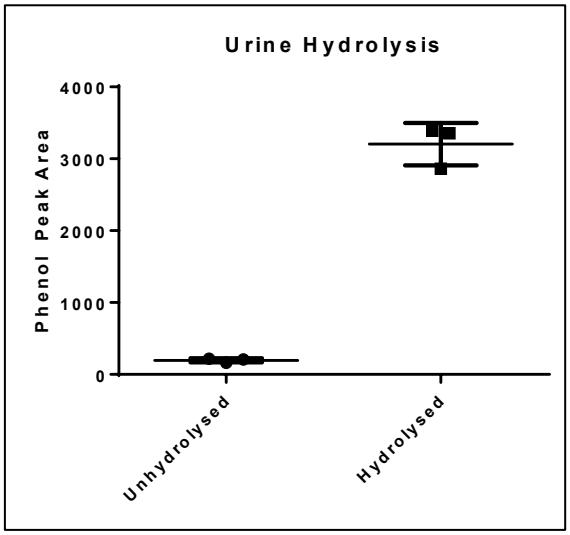


Figure 17: Greatly increased phenol peak area following urine hydrolysis.

These results demonstrated that a large quantity of phenol is conjugated to glucuronic acid or sulphate in urine, and hydrolysis allows for measurement of total phenol, rather than the unbound (free) component). Therefore, all urine samples underwent hydrolysis prior to analysis.

Calculation of Limit of Detection and Limit of Quantification

Using this HS-SPME protocol with the GC-MS method developed in Section 2.1 the limit of detection (LOD) was calculated as the concentration at which the signal-noise (S/N) ratio was more than 3. The LOD for this method was 0.005ug/ml.

Limit of quantification (LOQ) was defined as the lowest concentration at which the S/N ratio was greater than 10 and standard error less than 10%. The LOQ for this method was 0.01ug/ml.

Intra-Day and Inter-Day Accuracy

The intra-day and inter-day accuracy were calculated for phenol by repeated analysing of stock solutions (0.5ug/ml & 1ug/ml). The accuracy was expressed as the ratio of the quantified concentration to the known concentration of the stock solution. The error (or precision) was calculated as the relative standard deviation (%) of the replicates[111].

Intra-day accuracy results were calculated from three individual samples analysed on the same day. Inter-day accuracy results were calculated from three individual samples analysed on non-consecutive days. Results are shown in table 12.

Concentration (µg/ml)	**Recovered (Mean±SD, µg/ml)**		**Accuracy (%)**		**Error (%)**	
	Intra-Day	**Inter-Day**	**Intra-Day**	**Inter-day**	**Intra-Day**	**Inter-Day**
0.5	0.50 ± 0.02	0.50 ± 0.01	99.82	99.13	3.81	1.57
1	1.02 ± 0.01	1.00 ± 0.02	101.70	100.20	1.38	1.73

Table 12: Results of intra- and inter-day accuracy and precision for phenol quantification.

2.2.4 Conclusions

This series has developed an optimised SPME extraction method for gastric content and urine analysis using the following parameters:

- Equilibration time – 10 minutes.
- SPME temperature - 60°C
- SPME time – 60 minutes.
- 0.4g NaCl added to each sample.
- All gastric content samples buffered to pH 2.
- Gastric content samples analysed without filtration.
- All urine samples hydrolysed via acidification and heating prior to analysis.

2.3 Direct Liquid Injection Method Development for GC-MS

2.3.1 Objective

This section aimed to produce a direct liquid injection method for phenol analysis in plasma and tissue samples. These experiments optimised each phase of sample preparation including plasma preparation, tissue homogenisation and solid-phase extraction.

2.3.2 Introduction

Although HS-SPME can be utilised for analysis of phenol from urine and gastric content it is not necessarily suitable for all biological matrices.

During the current project HS-SPME was initially tested for plasma samples but heating of plasma samples (necessary for SPME extraction) caused the plasma protein to solidify (even when samples were diluted with water) and very little signal was identified. De-proteination of samples would require the use of organic solvents (not easily compatible with SPME) so a direct injection method was required for plasma analysis.

SPME can be adapted for direct insertion into tissues[112,113], and has also been previously used to measure headspace directly from stomach cancer tissues[114]. However, this study by *Buszewski et al.* used tissues which were around two grams in weight[114]. As the available sample-set consisted of tissue samples of 10-30mg it was felt SPME would not be suitable in this instance. Due to the small sample size available tissue would require homogenisation in organic solvent prior to analysis using direct liquid injection.

For these reasons it was necessary to develop a direct liquid injection method for introduction of analytes for GC-MS analysis. This method utilised solid-phase extraction to remove contaminants from plasma and tissue samples prior to injection.

The principles of solid-phase extraction (SPE) involve four main stages[115]:

1. **Condition** – Passing organic solvents through the SPE tube wets the surface of the sorbent and penetrates bonded alkyl phases, allowing water to wet the silica surface efficiently.
2. **Load –** The sample is passed through the tube and analytes become adhered to the packing.
3. **Wash –** Unwanted and contaminants are washed from the packing, whilst the compounds of interest are retained.
4. **Elute –** An elution solvent is used to rinse the packing and elute the compounds of interest for further analysis.

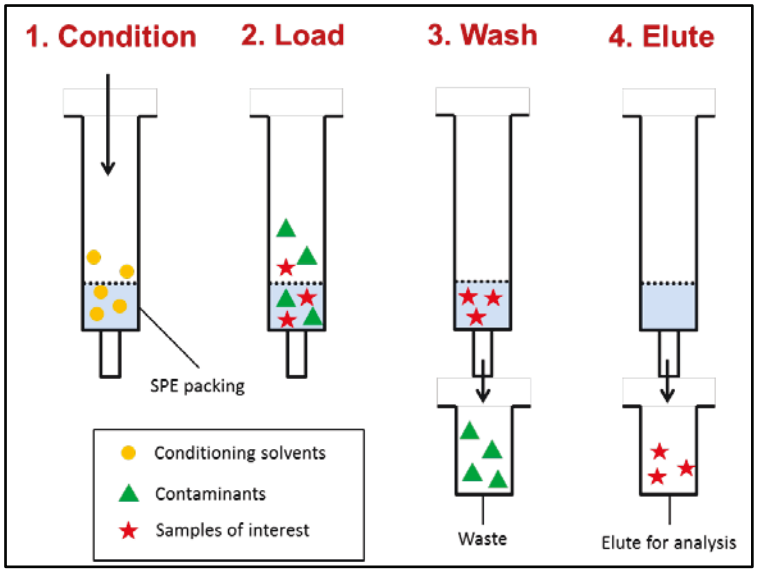


Figure 18: Schematic diagram of the SPE process.

2.3.3 Method Development

2.3.3.1 GC-MS Analysis

GC-MS analysis was performed using the same column and temperature protocol as developed in Section 2.1. A direct injection attachment was installed on the CTC direct injection autosampler (PAL systems, Zwingen, Switzerland) with a 1.2µL Hamilton Syringe (Hamilton Company, Reno, NV, USA). A quartz wool direct injection liner (Length - 86.2mm; internal diameter – 2mm; effective volume 135µL) (Supelco, Bellefonte, PA, USA) was utilised with the injector temperature remaining at 230°C. Safe injection volumes for each injection solvent were calculated using the Restek Vapor Solvent

Expansion Calculator (Restek, Bellefonte, PA, USA)[116]. These volumes were used to ensure the vapour cloud volume was smaller than the effective liner volume and prevent backflash and contamination of the injector septum.

Elution Solvent	Liner Volume (µL)	Injector Temperature (°C)	Head Pressure (psig)	Safe injection volume (µL)	Vapour Cloud (µL)
Methanol	135	230	10	0.2	121
Acetone	135	230	10	0.3	100
Dichloromethane	135	230	10	0.3	129

Table 13: Details of solvent expansion and safe injection volume for methanol, acetone and dichloromethane.

2.3.3.2 Solid Phase Extraction Optimisation

The first stage of developing the tissue extraction methodology was to optimise the process of solid phase extraction (SPE). A previous method using SPE for measurement of phenol in drinking water has been produced by the U.S Environmental Protection Agency[117].

Optimisation was undertaken by investigating the effect of the following variables upon SPE process efficiency:

i. SPE tube selection (C18, DVB, Oasis, Charcoal)
ii. Elution solvent (dichloromethane, methanol, acetone – All Sigma Aldrich, Gillingham, Dorset, UK).
iii. Elution volume.
iv. Elute evaporation.
v. Wash step.

Standards Preparation

For SPE optimisation standard solutions of 1µg/ml of phenol and phenol D6 were made up in methanol. Prior to loading on SPE tubes 1ml of this solution was added to a volumetric flask and diluted in 46ml of HPLC grade water plus 3ml of 0.05M HCl (final volume 50ml, pH 2). These samples were then loaded onto the SPE tubes.

SPE Tube Types

The following SPE tubes were evaluated: Empore C18-SD (Sigma Aldrich, Gillingham, Dorset, UK), BondElut PPL (Agilent Technologies, Santa Clara, CA, USA), Oasis Prime HLB (Waters, Milford, MA, USA) and Supelclean Coconut Charcoal SPE Tubes (Sigma Aldrich, Gillingham, Dorset, UK). All SPE was undertaken on an SPE manifold.

The tube conditioning process for C18, BondElut PPL and charcoal tubes consisted of passing 3ml of dichloromethane through each SPE tube, then 3ml of methanol followed by 3ml of water with 0.05M HCl. Oasis tubes were conditioned using 5ml of methanol, 5ml of acetonitrile and 5ml of water. Samples were then loaded onto the SPE tube and then eluted using methanol as initial elution solvent. It was ensured that the tubes did not run-dry at any point during the process.

Peak areas from the GC-MS analysis of elute from each of the different tube types are shown in table 14 (peak areas compared to that for a standard of 1µg/ml phenol).

Tube Type	Phenol Peak Area	D6 Phenol Peak Area	Percentage Recovery
Standard (1µg/ml)	1361 ± 347	625 ± 170	N/A
C18	140 ± 52	55 ± 20	10 %
BondElut PPL	973 ± 43	886 ± 66	71%
Oasis	624 ± 61	330 ± 23	46%
Charcoal	64 ± 10	9 ± 3	5%

Table 14: Phenol recovery with variety of SPE tubes.

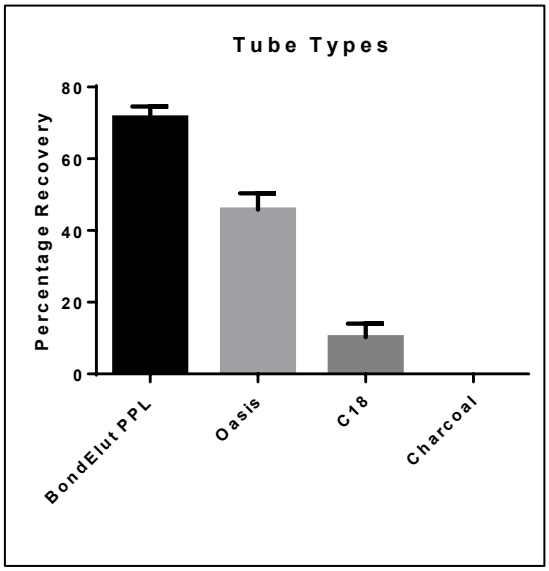


Figure 19: Best phenol recovery with BondElut PPL tubes (71% recovery).

On the basis of these results BondElut PPL tubes were used for further optimisation steps. These are the same tubes that were selected for the U.S Environmental Protection Agency method[117].

Elution Solvent

Dichloromethane, methanol and acetone were all assessed as elution solvents from BondElut PPL tubes. All results were compared to phenol standards (1µg/ml) in the same solvent (dichloromethane, methanol or acetone).

Results for peak area from these elutes is shown in table 15.

Elution Solvent	Phenol Peak Area	Phenol D6 Peak Area	Percentage Recovery
Phenol Standard (DCM)	1361 ± 347	625 ± 170	Not applicable
DCM Elute	973 ± 43	886 ± 66	71%
Phenol Standard (Methanol)	858 ± 156	446 ± 96	Not applicable
Methanol Elute	542 ± 55	232 ± 29	63%
Phenol Standard (Acetone)	1633 ± 101	834 ± 54	Not applicable
Acetone Elute	1028 ± 36	469 ± 25	63%

Table 15: Results of assessing various elution solvents.

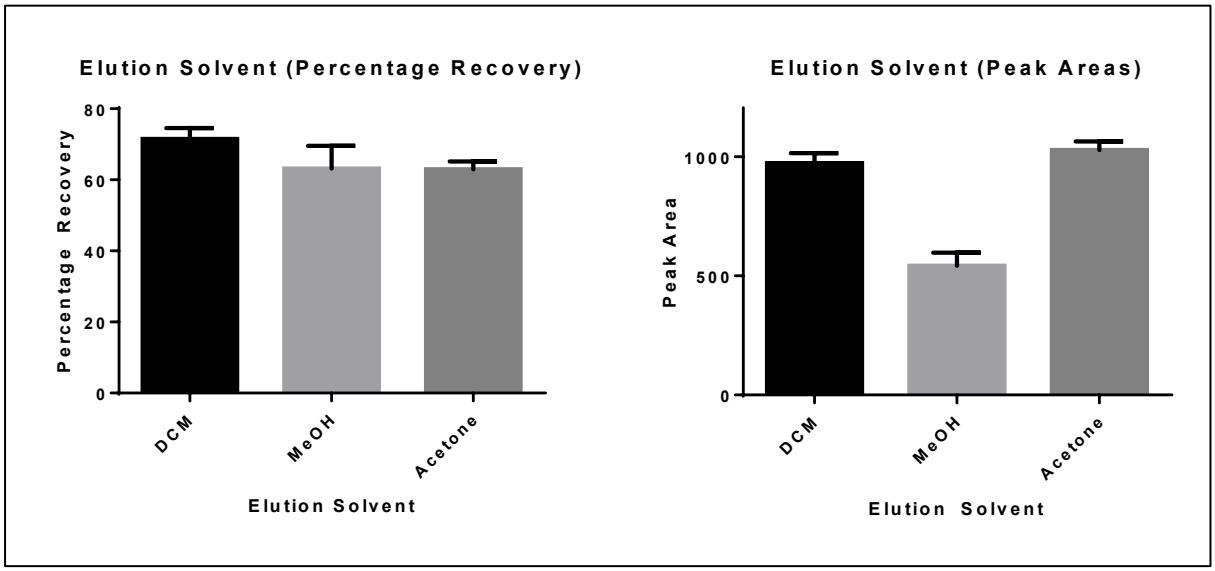


Figure 20: Percentage recovery and peak area for different elution solvents.

Elution with acetone provided the largest peak area response. Although the percentage recovery with acetone (63%) was inferior to dichloromethane (71%) the difference was relatively small. Due to the increased peak area response (both with acetone elute and phenol standards in acetone) it was felt this would improve the LOD and LOQ for this method and this was selected as elution solvent.

Elution Volume

Elution volume was tested with 1ml, 2ml, 3ml, 4ml, and 5ml of acetone to establish at which point all phenol had been completely eluted from the solid-phase extraction tubes. Results are demonstrated below:

Total Elution Volume	**Mean Phenol Peak Area**	**Mean D6 Phenol Peak Area**	**Cumulative percentage phenol recovery**
1ml	1166 ± 32	523 ± 13	69%
2ml	502 ± 64	217 ± 33	98%
3ml	21 ± 8	6 ± 3.8	99%
4ml	5 ± 2	0	100%
5ml	6 ± 0.6	0	100%

Table 16: Recovery with sequential 1ml aliquots of acetone with a final total elution volume of 5ml. 99.33% of phenol recovered using 3ml acetone.

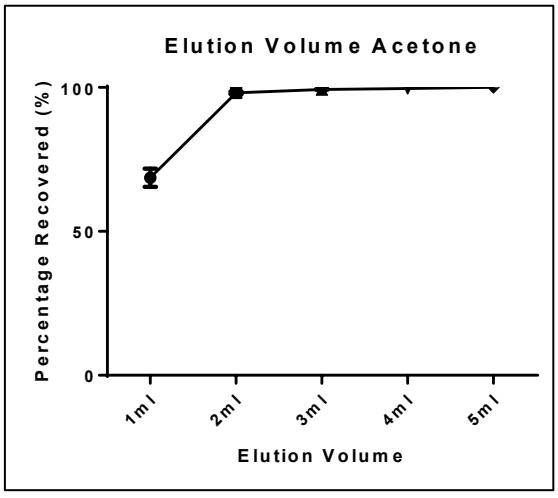


Figure 21: Cumulative percentage recovery with increasing elution volume.

From these results a large proportion of phenol (69%) was eluted with 1ml of acetone. Following 3ml acetone nearly all phenol (99%) was eluted successfully from the SPE tube. It was planned to assess

the effect of elute evaporation upon concentration prior to deciding whether to utilise 1ml or 3ml as elution volume.

Elute Evaporation

Acetone elutes could be evaporated under nitrogen to increase phenol concentration via volume reduction. However, due to the volatile nature of phenol evaporation to dryness could lead to phenol loss[117]. All samples were spiked with 1µg/ml phenol and phenol D6 and the following elution and evaporation parameters were compared when investigating the effect of elute evaporation:

1. 1ml acetone elute (no evaporation)
2. 3ml acetone elute (no evaporation)
3. 3ml acetone elute (evaporated to 1ml)
4. 3ml acetone elute (evaporated to dryness then reconstituted with 1ml acetone).

Sample elution and Evaporation	Mean Phenol Peak Area	Mean D6 Phenol Peak Area
1µg/ml Phenol standard	1704 ±74	735 ±18
1ml elute (no evaporation)	630 ±23	252 ±14
3ml elute (no evaporation)	425 ±162	163 ±67
3ml elute (evaporated to 1ml)	1412 ±146	597 ±73
3ml elute (evaporated to dryness)	335 ±108	116 ±15

Table 17: Phenol peak area with and without sample evaporation. 3ml acetone for elution followed by evaporation to 1ml provided the largest peak area.

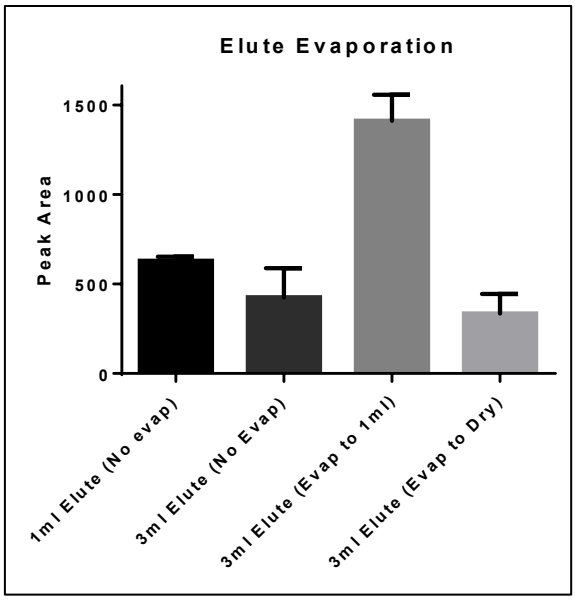


Figure 22: Assessment of sample evaporation.

The optimal phenol peak area was seen when a 3ml elute was dried to 1ml volume. The phenol peak area with this method showed good compound recovery when compared to the peak area in the standard solution of 1µg/ml (peak area 1412 vs 1704 (83% total recovery). Use of 3ml acetone for elution followed by drying under nitrogen to 1ml was utilised for further analysis.

Wash Step Optimisation

Wash step optimisation was performed by testing the use of 3ml of one of the following potential wash solutions:

i. Water
ii. 5% methanol
iii. 20% methanol
iv. 50% methanol.

Results are shown in table 18:

Wash Step	**Mean Phenol Peak Area**	**Mean D6 Phenol Peak Area**
Water wash	1806 ± 17	747 ± 17
5% Methanol	1539 ± 211	656 ± 92
20% Methanol	897 ± 322	379 ± 141
50% Methanol	1162 ± 91	506 ± 34

Table 18: Assessment of wash step.

Although water wash provided the largest phenol peak area, 5% methanol was selected as this would provide greater wash of unwanted contaminants whilst retaining large quantities of phenol upon the SPE cartridge.

Effect of changing the pH of the wash step was assessed by using:

i. 5% methanol
ii. 5% methanol with 0.1% formic acid.
iii. 5% methanol with 0.1% ammonium hydroxide.

Results are shown in table 19:

Wash Step	Mean Phenol Peak Area	Mean D6 Phenol Peak Area
5% Methanol	1231 ± 126	488 ± 41
5% methanol with 0.1% formic acid	1212 ± 41	552 ± 14
5% methanol with 0.1% ammonium hydroxide	1124 ± 304	490 ± 137

Table 19: Assessment on changes in pH upon effectiveness of wash step.

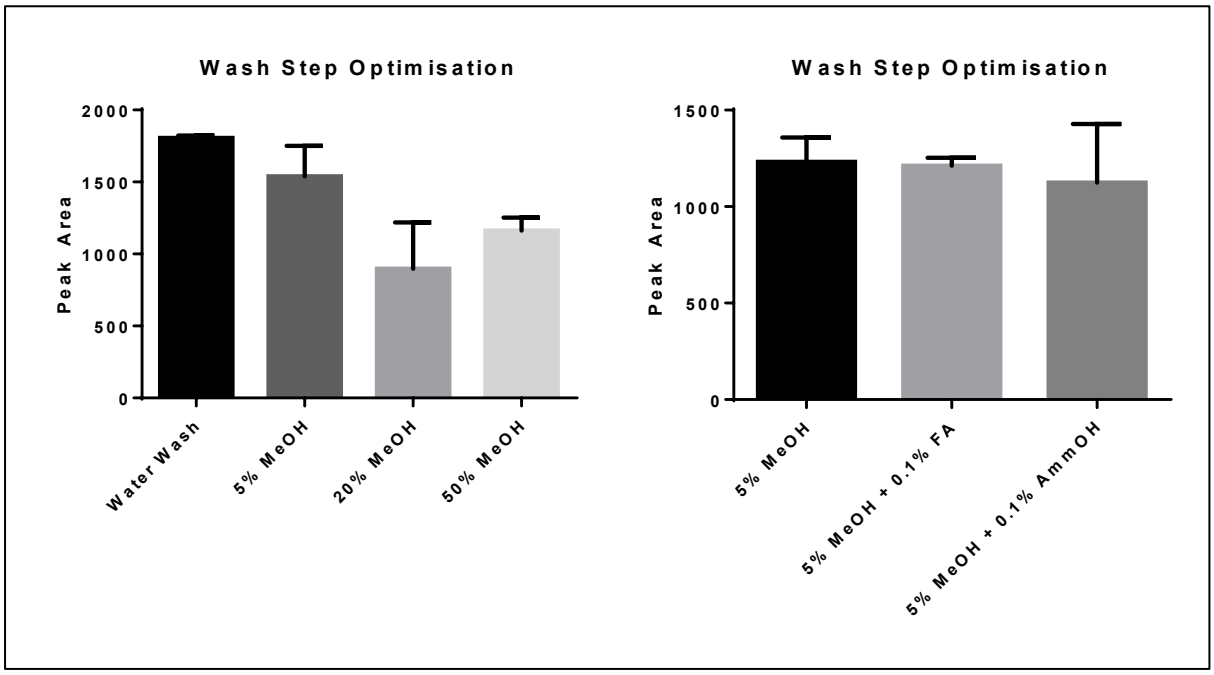


Figure 23: Wash step optimisation. A – Optimisation with different quantities of methanol in wash. B – Optimisation by changing the pH in the wash.

As changing the pH of the wash step did not seem to affect the phenol peak area 5% methanol without pH adjustment was used as the wash step solution.

Recovery at Different Concentrations

Phenol recoveries at various concentrations were tested to ensure that these SPE tubes would provide a good percentage recovery within the predicted concentration range for phenol within plasma and tissue samples (0.5-1µg/ml). Results are shown below:

Concentration (µg/ml)	Mean Standard Phenol Peak Area	Mean Phenol Peak Area post SPE	Percentage Recovery following SPE
0.5	439±35	312±49	71%
1	778±175	697±14	90%
2	1485±395	828±96	56%
5	4698±490	1778±562	38%
10	10562±1750	3120±518	30%

Table 20: Phenol recovery at various starting concentrations.

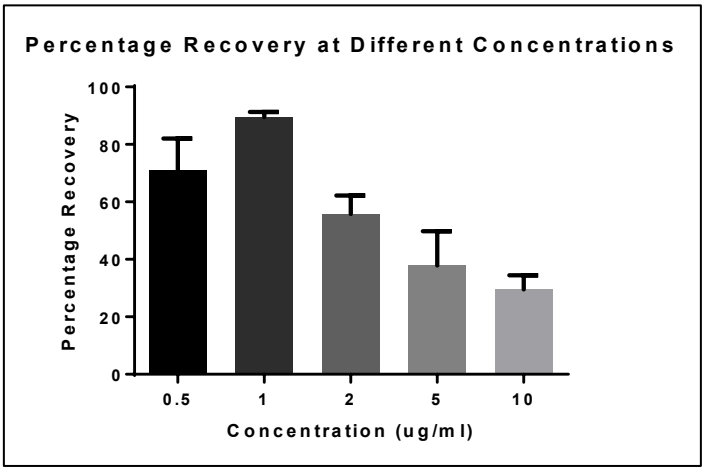


Figure 24: Phenol recovery at various starting concentrations.

Phenol recovery was good at a concentration of 0.5µg/ml and 1µg/ml (70.93% and 89.52% respectively). However, recovery decreased with increasing concentration with a recovery of only 29.54% at 10µg/ml. Given the anticipated range of phenol concentration in extracted serum and

tissue samples would be below 1µg/ml these SPE tubes and method would be suitable to utilise in phenol recovery.

Solid Phase Extraction Protocol

These optimisation steps have developed the following solid phase extraction protocol:

- 1ml sample (in methanol) added to 3mL 0.05M HCL and 46mL water (final volume 50ml, pH 2).
- Bond-Elut PPL SPE tubes (Agilent Technologies, Santa Clara, CA, USA) used on SPE manifold.
- Condition: 3ml dichloromethane; 3ml methanol; 3ml 0.05M HCL in water.
- Load: 50ml sample loaded to tube.
- Wash: Tube washed in 3ml 5% methanol.
- Elute: Phenol eluted with 3ml acetone.
- Evaporate: Sample evaporated to 1ml prior to analysis.
- Direct injection analysis on GC-MS (Acetone injection volume 0.3µl).

2.3.3.2 Calculation of Limit of Detection and Limit of Quantification

Using this direct injection method (using 0.3µl of acetone for injection) with the GC-MS method developed in Section 2.1 the limit of detection (LOD) was calculated as the concentration at which the signal-noise (S/N) ratio was more than 3. The LOD for this method was 0.005µg/ml.

Limit of quantification (LOQ) was defined as the lowest concentration at which the S/N ratio was greater than 10 and standard error less than 10%. The LOQ for this method was 0.01µg/ml.

2.3.3.3 Intra-Day and Inter-Day Accuracy

The intra-day and inter-day accuracy were calculated for phenol by repeated analysing of stock solutions (0.5µg/ml & 1µg/ml). The accuracy was expressed as the ratio of the quantified

concentration to the known concentration of the stock solution. The error (or precision) was calculated as the relative standard deviation (%) of the replicates[111].

Intra-day accuracy results were calculated from three injections of the same sample analysed on the same day. Inter-day accuracy results were calculated from three injections of the same sample analysed on non-consecutive days. Results are shown in table 21:

Concentration (µg/ml)	**Recovered (Mean ± SD, µg/ml)**		**Accuracy (%)**		**Error (%)**	
	Intra-Day	**Inter-Day**	**Intra-Day**	**Inter-day**	**Intra-Day**	**Inter-Day**
0.5	0.48 ± 0.02	0.52 ± 0.04	96.0	104.4	3.4	7.5
1	1.02 ± 0.01	0.99 ± 0.03	101.2	99.0	1.2	3.2

Table 21: Results of intra- and inter-day accuracy and precision for phenol quantification using direct injection method.

2.3.3.4 Plasma Preparation and Phenol Deconjugation

As phenol is transported in blood bound to glucuronic acid or sulphate phenol deconjugation was necessary prior to plasma analysis[110]. 1ml plasma samples were spiked with 1µg of phenyl-glucuronide (Sigma Aldrich, Gillingham, Dorset, UK) and different quantities of beta-glucuronidase (also Sigma Aldrich, Gillingham, Dorset, UK) were added. Beta-glucuronidase produced from *Helix* pomatia was selected as this would also provide sulfatase activity. Various incubation times were also tested.

Quantity of beta-glucuronidase or hydrochloric acid was initially assessed by adding:

i. No beta-gluuoronidase and incubate at 37°C for 30 minutes.
ii. 5µl beta-glucuronidase and incubate at 37°C for 30 minutes.
iii. 10µl beta-glucuronidase and incubate at 37°C for 30 minutes.
iv. 20µl beta-glucuronidase and incubate at 37°C for 30 minutes.

Each of the above samples were prepared and analysed in triplicate. Following the above deconjugation plasma samples were spiked with 1µg/ml of phenol D6 as internal standard. Protein was then precipitated using methanol. Initial testing demonstrated that a 1:3 plasma:methanol ratio was necessary for complete precipitation of protein. 400µl of plasma was added to 1200µl methanol and centrifuged at 18000g for 10 minutes. 1ml supernatant was extracted and underwent SPE (as per Section 2.3.3.2) followed by injection on GC-MS via direct injection. Results are shown below:

Beta-glucuronidase added	**Phenol (µg/mL)**
None	0.01 ±0.002
5µL	0.02 ± 0.002
10µL	0.07 ± 0.009
20µL	0.18 ± 0.002

Table 22: Results of addition of various quantities of beta-glucuronidase for phenol deconjugation.

These results demonstrated an increase in quantity of phenol deconjugated when 20µL of beta-glucuronidase was added to a 1mL plasma sample and incubated at 37°C for 20 minutes.

It was then necessary to establish the effect of incubation time on phenol deconjugation. 1ml serum samples again had 1µg of phenyl-glucuronide added and were incubated at 37°C with 20µL of beta-glucuronidase for 15 minutes, 30 minutes and 60 minutes. Samples were then deproteinated with methanol and analysed following SPE as above.

Results are shown in table 23:

Incubation Time (mins)	Phenol (µg/mL)
15	0.14 ± 0.024
30	0.18 ± 0.003
60	0.19 ± 0.018

Table 23: Results of varying incubation time at 37°C for phenol deconjugation with 20µL beta-glucuronidase.

These results demonstrated that although there was an increase in phenol deconjugation when incubating samples at 37°C for 30 minutes (0.18µg/ml) rather than 15 minutes (0.14µg/ml), there was little benefit for incubation times greater than 30 minutes (60 minutes – 0.19µg/ml).

These results led to the following protocol for plasma sample preparation for GC-MS analysis:

- 20µL beta-glucuronidase added to 1ml plasma sample and incubated for 30 minutes at 37°C.
- 400µL of plasma (following deconjugation) added to 1200µL methanol and centrifuged at 18000g for 10 minutes.
- Solid phase extraction (as per Section 2.3.3.1) performed on 1ml of deproteinated plasma sample.
- Sample analysed on GC-MS using direct injection as per Sections 2.1 and 2.3.3.1

2.3.3.5 Tissue Homogenisation and Extraction

To optimise tissue homogenisation porcine gastric mucosa samples were weighed and then crushed in liquid nitrogen (in order to retain volatile compounds) using a pestle and mortar. Crushed samples were then added to a 2ml vial with 1ml of one of the following solvents:

i. Methanol.
ii. Methanol:Water (50:50).
iii. Acetonitrile.

Each tested homogenisation solvent was analysed as an unspiked tissue sample and as a separate sample having been spiked with 1µg/ml of phenol. All samples were spiked with 1µg/ml of phenol D6 as internal standard. Each of the above samples were prepared and analysed in triplicate. Each sample had a ball-bearing added and further homogenisation occurred using a tissue homogeniser (Retsch, Dusseldorf, Germany) at 25 revolutions per second for 3 minutes. 200mg of sodium chloride was then added to each vial and centrifuged at 18000g for 10 minutes. The supernatant was then retrieved and SPE performed according to the optimised protocol followed by GC-MS analysis.

Results are shown below:

	Unspiked (Phenol µg/mL)	**Spiked (Phenol µg/mL)**
Methanol	0.10 ± 0.03	1.37 ± 0.02
Methanol:Water	0.09 ± 0.01	1.53 ± 0.13
Acetonitrile	0.08 ± 0.01	1.49 ± 0.21

Table 24: Assessment of different solvent for tissue homogenisation showed little variation.

These results demonstrated little difference in phenol extraction for unspiked and spiked tissue samples using different homogenisation solvents. Adequacy of homogenisation was similar for all solvents but appeared slightly improved with methanol and this was therefore selected as the solvent for tissue homogenisation.

In unspiked samples phenol concentration was around the limit of quantification for this method (0.01µg/ml). This may have been due to volatile loss during tissue processing which is why initial homogenisation of tissues was undertaken in liquid nitrogen. However, as this method development was undertaken using porcine stomach it was necessary to further assess presence of phenol within human stomach tissues, and in particular gastric carcinoma tissues. This has been undertaken in Section 4.3.

2.3.4 Conclusions

Optimisation of solid phase extraction, plasma deproteination plus deconjugation, and tissue homogenisation has produced a sample preparation method for phenol analysis in plasma and tissues using direct liquid injection GC-MS.

2.4 LC-MS Method Development

2.4.1 Objective

This section aimed to develop a liquid-chromatography mass spectrometry (LC-MS) method to measure phenylalanine, tyrosine and intermediary metabolites of aromatic amino acid breakdown. This method was to be utilised specifically to quantify homogentisate in plasma samples and tyrosine in gastric content samples.

2.4.2 Introduction

Liquid chromatography mass spectrometry is widely used for analysing non-volatile compounds and is generally considered the 'gold-standard' analytical technique for non-volatiles. The principles of chromatographic separation are similar to those used in GC-MS but are achieved in a different fashion. GC-MS uses a constant mobile phase (helium gas) and increasing the temperature of the column elutes compounds. LC-MS utilises a constant column temperature, with changes in mobile phase composition from aqueous to organic eluting compounds during reversed-phase chromatography. The initial mobile phase consists of large quantities of the aqueous phase (water). This leads to compounds becoming fixed to the stationary phase within the column. As the proportion of organic phase (typically methanol or acetonitrile) increases analytes lose affinity for the column at different intervals creating chromatographic separation. Once compounds elute from the column they travel to the downstream mass spectrometer for detection. A schematic diagram of an LC-MS setup is shown in figure 25.

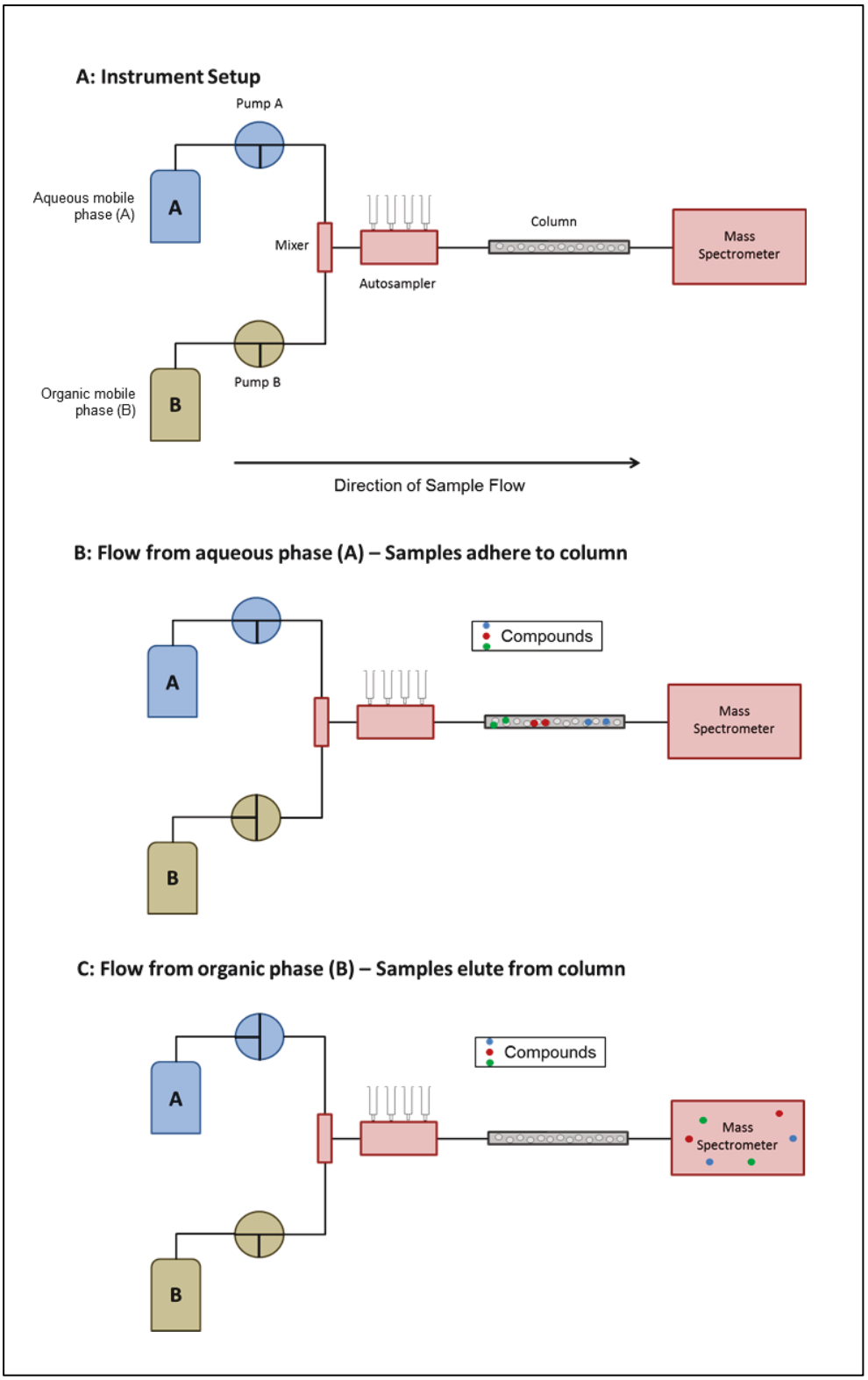


Figure 25: A: General LC-MS setup showing mobile phases (A & B), pumps to regulate mobile phase flow, autosampler where samples are introduced, column (including packing of stationary phase) and mass spectrometer. B: During aqueous phase compounds become retained on column. C: As proportion of organic phase (B) increases compounds gradually lose affinity for the column at different elution times.

Although GC-MS can be used for analysis of amino acids this requires derivitisation with chloroformates in order to make the compounds volatile for analysis[118]. Most amino acids require chemical derivitisation prior to analysis and AQC (6-aminoquinolyl-n-hydroxysuccinimidyl carbamate) is commonly used as a derivitisation agent for analysis with LC-MS or other analytical methods[119–122]. However, it is possible to determine aromatic amino acids without the need for derivitisation[123]. Underivitised analysis has previously been successfully reported in gastric content of gastric cancer patients[39,40]. The intermediary metabolites of tyrosine metabolism (hydroxyphenylpyruvate, homogentisate, maleylacetoacetate, and fumarylacetoacetate) lack the functional group required for AQC derivitisation meaning if this derivitisation method was used it would not be possible to measure these compounds simultaneously. As it was proposed that this method would simultaneously measure intermediary metabolites of tyrosine metabolism (primarily hydroxyphenylpyruvate and homogentisate) it was decided to analyse all compounds in an underivitised form. Homogentisate and tyrosine have previously been measured simultaneously using LC-MS in underivitised form in serum and urine of alkaptonuria patients[124,125]. For gastric content experiments it was planned to only measure tyrosine concentrations using this LC-MS method. This facilitated a correlation between tyrosine concentrations in gastric content (measured with LC-MS) and phenol concentration in the same samples (measured using GC-MS).

2.4.3 Method Development

All analysis was undertaken using an Aquity® UPLC binary solvent manager, sample manager and column thermostat (Waters, Milford, MA, USA) interfaced with a triple quadrapole (TQ-Micro) mass spectrometer (Waters, Milford, MA, USA).

Standards of phenylalanine, tyrosine, hydroxyphenylpyruvate and homogentisate (All Sigma Aldrich, Gillingham, Dorset, UK) were used to produce stock solutions of 5mM concentration. Standards for other intermediary metabolites of tyrosine breakdown (maleylacetoacetate and fumarylacetoacetate) were not commercially available. Isotope labelled standards of D5 phenylalanine, D4 tyrosine (both Sigma Aldrich, Gillingham, Dorset, UK) and $C_{13}6$ homogentisate (Toronto Research Chemicals, Toronto, Canada) were also purchased and 5mM stock solutions produced.

Standards and Mass Transitions

Standard solutions (100µM) of each compound and isotope labelled standards were analysed using the Intellistart® system (Waters, Milford, MA, USA) to establish the MRM (Multiple Reaction Monitoring) transitions and optimal cone voltage and collision energy for each compound and isotope labelled standard. Results are shown below in tables 25.

Compound	ESI Mode	Parent Ion	Daughter Ion	Dwell Time (s)	Cone Voltage (V)	Collision Energy (eV)
Phenylalanine	Positive	166.1	77.1	0.025	58	34
Phenylalanine	Positive	166.1	93.1	0.025	58	24
Phenylalanine	Positive	166.1	103.1	0.025	58	20
Phenylalanine	Positive	166.1	120.1	0.025	58	28
D5 Phenylalanine	Positive	171.1	80.1	0.025	2	46
D5 Phenylalanine	Positive	171.1	106.4	0.025	2	22
D5 Phenylalanine	Positive	171.1	125.2	0.025	2	12
Tyrosine	Positive	182.0	91.1	0.025	18	22
Tyrosine	Positive	182.0	95.1	0.025	18	36
Tyrosine	Positive	182.0	119.1	0.025	18	18
Tyrosine	Positive	182.0	123.1	0.025	18	18
D4 Tyrosine	Positive	186.0	94.1	0.025	2	24
D4 Tyrosine	Positive	186.0	127.1	0.025	2	20
D4 Tyrosine	Positive	186.0	140.2	0.025	2	18
Homogentisate	Negative	167.0	108.0	0.025	10	22
Homogentisate	Negative	167.0	122.1	0.025	10	28
Homogentisate	Negative	167.0	123.2	0.025	10	20
C_{13}6 Homogentisate	Negative	173.0	114.0	0.025	10	22
C_{13}6 Homogentisate	Negative	173.0	128.1	0.025	10	28
C_{13}6 Homogentisate	Negative	173.0	129.1	0.025	10	20
Hydroxy-phenylpyruvate	Negative	178.9	106.9	0.025	16	14
Hydroxy-phenylpyruvate	Negative	178.9	107.0	0.025	16	10
Hydroxy-phenylpyruvate	Negative	178.9	151.1	0.025	16	8

Table 25: Mass transitions, cone voltage and collision energy for each compound.

The above mass transitions and cone voltage and collision energies were used to produced separate mass spectrometry methods for positive and negative ion modes. Phenylalanine, tyrosine, D5 phenylalanine and D4 tyrosine were all measured in positive ion mode whilst hydroxyphenylpyruvate, homogentisate and $C_{13}6$ homogentisate were measured in negative ion mode.

The transitions shown below in table 26 were used for primary quantification.

Compound	ESI Mode	Parent Ion	Daughter Ion	Dwell Time (s)	Cone Voltage (V)	Collision Energy (eV)
Phenylalanine	Positive	166.1	77.1	0.025	58	34
D5 Phenylalanine	Positive	171.1	125.2	0.025	2	12
Tyrosine	Positive	182.0	119.1	0.025	18	18
D4 Tyrosine	Positive	186.0	140.2	0.025	2	18
Homogentisate	Negative	167.0	122.1	0.025	10	28
$C_{13}6$ Homogentisate	Negative	173.0	128.1	0.025	10	28
Hydroxy-phenylpyruvate	Negative	178.9	107.0	0.025	16	10

Table 26: Mass transitions selected for quantification purposes.

Column Selection

Columns assessed for suitability included HSS T3 (2.1 x 100mm, 1.8µm column), phenyl-hexyl (2.1 x 50mm, 1.7µm) and HILIC (2.1 x 50mm, 1.6µm) columns (all Waters, Milford, MA, USA).

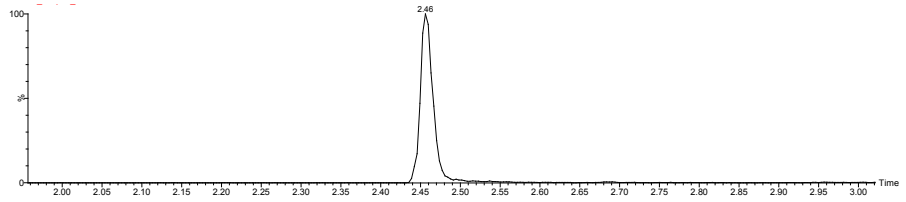
Initial mass spectrometer settings were capillary voltage 2kV, desolvation temperature 600°C, desolvation gas flow 600L/hour, cone gas flow 150L/hour. These parameters were optimised once the final chromatography method had been established.

The HSS T3 column was assessed initially. This was performed using water as mobile phase A and acetonitrile in mobile phase B. As the HSS T3 column is designed to withstand 100% water during chromatography this proportion of starting mobile phase A was utilised initially followed by a gradient. Flow rate was 0.3ml/min. A 10µM solution containing all standards in water was injected onto the column (injection volume 5µl). Details of the chromatographic conditions and representative chromatograms are shown in figure 26.

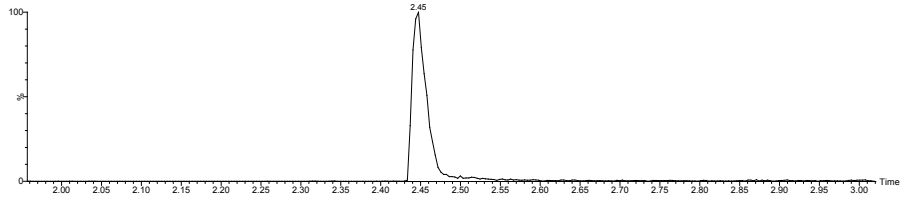
A

Time (min)	Flow rate (ml/min)	A (%)	B (%)
0	0.3	100	0
1	0.3	100	0
3	0.3	10	90
5	0.3	10	90
5.3	0.3	100	0
8	0.3	100	0

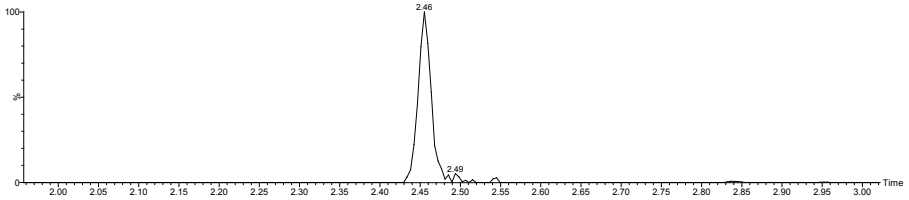
B



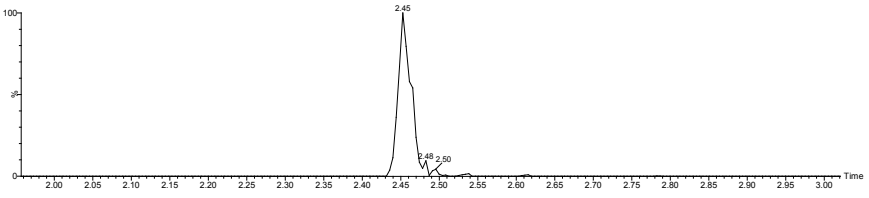
C



D



E



<u>Figure 26:</u> A – Details of mobile phase gradient. B-E: Chromatograms for phenylalanine (B), tyrosine (C), hydroxyphenylpyruvate (D) and homogentisate (E).

These chromatograms demonstrated reasonable peak shapes of three of these compounds on initial testing of this HSS T3 column. However, there was no chromatographic separation on this initial method.

The phenyl-hexyl column was then assessed. The same 10uM solution was injected onto the column and chromatography details and a representative chromatogram for phenylalanine is shown in supplementary figure 9. There was a lack of retention of phenylalanine with this column with a large humped chromatogram. Chromatographic appearances for all other compounds of interest were similarly poor.

Finally the HILIC column was tested. Samples were injected from acetonitrile. Water was again utilised as mobile phase A and acetonitrile as mobile phase B. Chromatographic conditions are shown in supplementary table 1. With this HILIC column phenylalanine and tyrosine eluted together at 4.00 and 4.01 minutes. Peak shape was adequate but not as good as with the HSS T3 column. Peak shape of homogentisate was poor and hydroxyphenylpyruvate was not visible.

On the basis of these initial column assessments it was decided to continue analysis using the HSS T3 column as this had demonstrated the most promising results.

Mobile Phase Selection

The chromatograms using the HSS T3 column shown in figure 26 were obtained using water and acetonitrile as mobile phases. Methanol was also assessed for use as mobile phase B in place of acetonitrile, but this solvent appeared to demonstrate inadequate compound elution from the column and chromatography was poor, as shown in supplementary figure 11. Therefore, acetonitrile was used as mobile phase B rather than methanol.

Chromatographic Separation

Peak shapes using this chromatographic method appeared adequate but there was a lack of chromatographic separation. Various adaptations of this chromatographic method were utilised and eventually the following method was established:

A

Time (min)	Flow rate (ml/min)	A (%)	B (%)
0	0.3	100	0
1	0.3	100	0
3	0.3	85	15
6	0.3	10	90
8	0.3	10	90
8.3	0.3	100	0
10	0.3	100	0

B

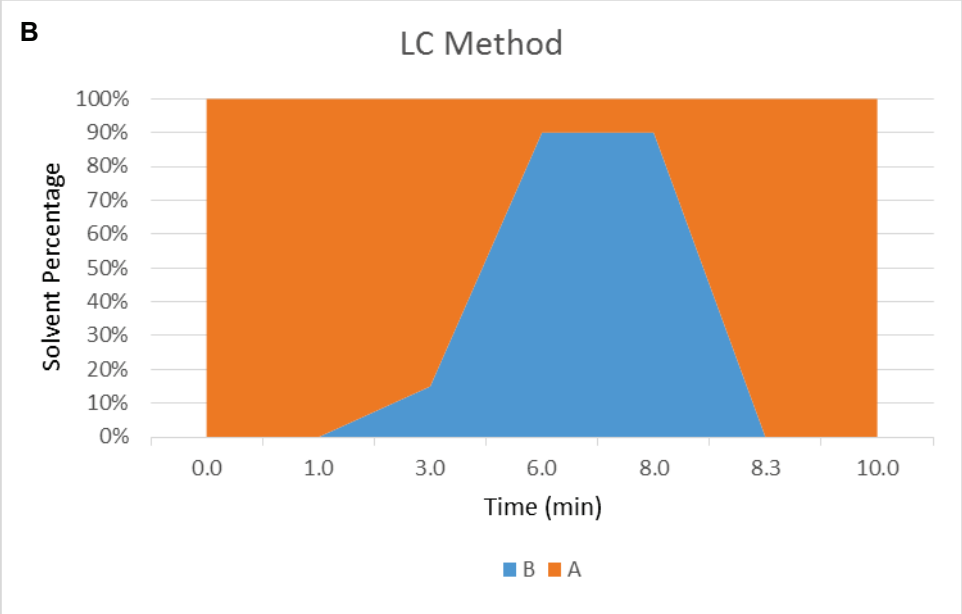


Figure 27: A: Details of mobile phase gradient. B: Visual representation of gradient.

This chromatographic method provided some peak separation but it was necessary to achieve greater separation. To achieve this addition of 0.1% acetic acid and 0.1% formic acid to the mobile phases were tested individually to establish if either of these would improve compound separation. This was intended to make the retention of the positive ion mode compounds shorter and negative ion mode compounds longer. Compound peak shape and separation was best with the addition of 0.1% acetic acid and the chromatography is demonstrated below:

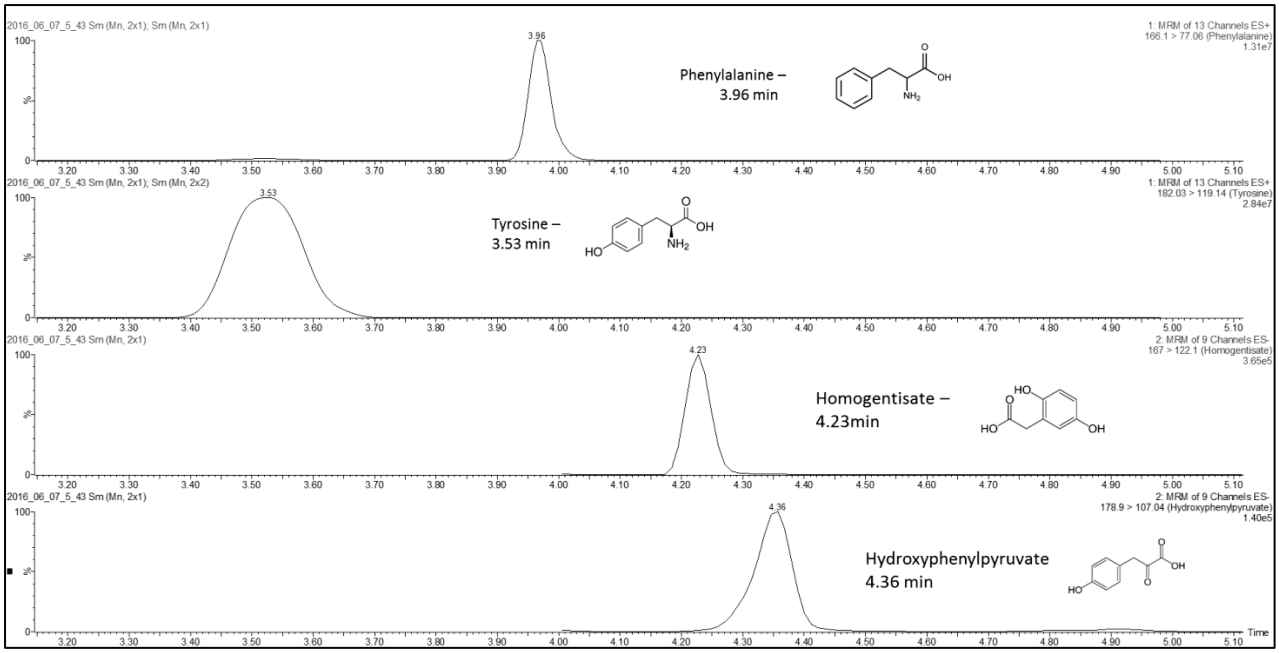


Figure 28: Chromatography with good separation of all compounds.

Needle Wash Selection

Weak needle washes were tested and the use of 500µl of water containing 20mM ammonium formate coupled with a strong wash of 50:50 water:isopropanol provided adequate needle cleaning between analytical runs.

Ion Source Optimisation

The mass spectrometer ion source parameters were further optimised by adjusting the following settings:

1. Capillary voltage (1.5kV, 2kV, 2.5kV).
2. Desolvation temperature (400°C, 500°C, 600°C).
3. Desolvation gas flow (400L/hr 600L/hr, 800L/hr, 1000L/hr).
4. Cone gas flow (150L/hr, 200L/hr, 300L/hr, 400L/hr).

Capillary Voltage

As demonstrated in figure 29 a capillary voltage of 2kV appeared to provide the largest peak area for all compounds.

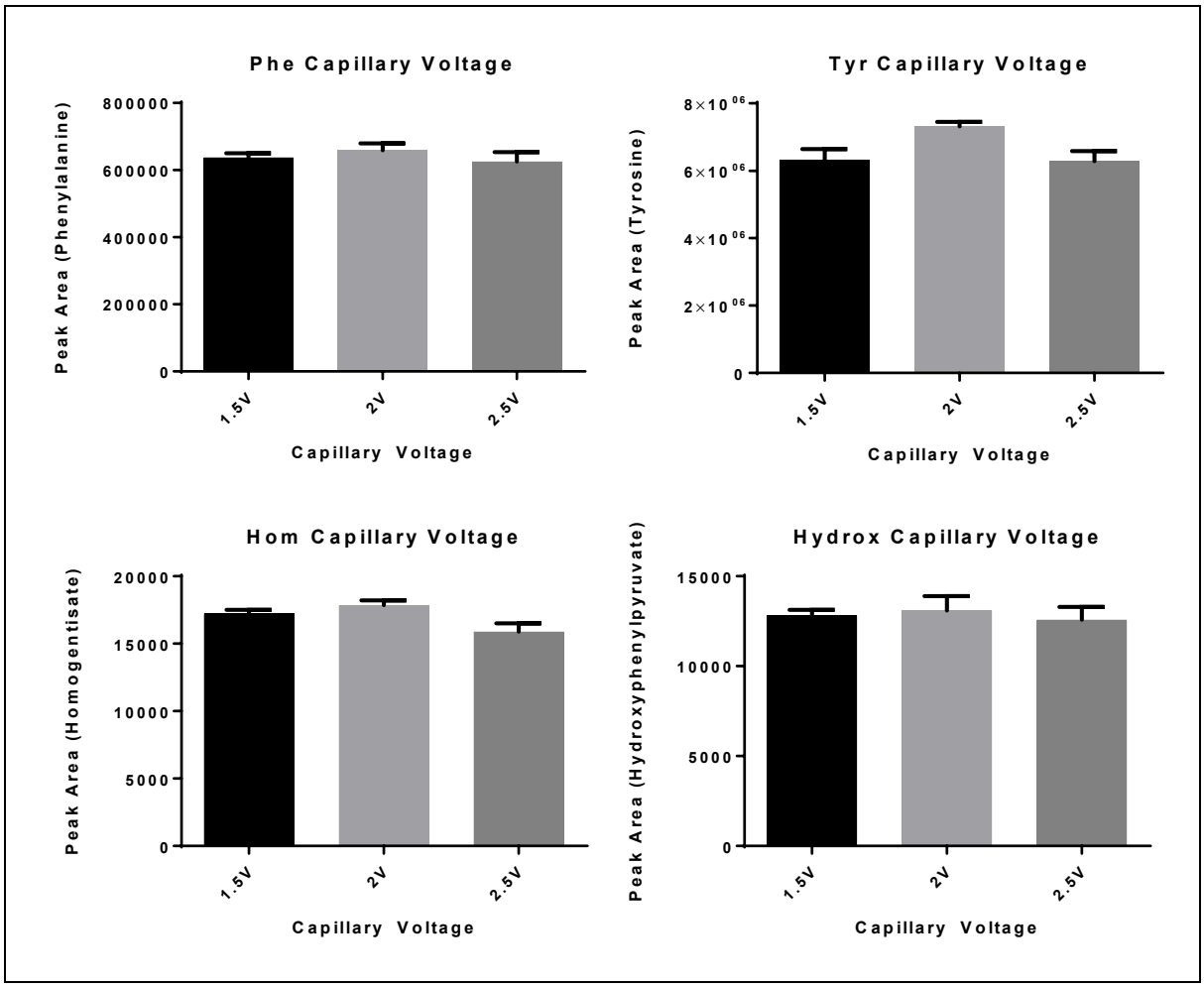


Figure 29: Optimisation of capillary voltage with 2kV providing the largest peak area for all compounds.

Desolvation Temperature

Desolvation temperature of 600°C provided the largest peak area for all compounds except hydroxyphenylpyruvate. As this provided the largest peak area for three out of four compounds this temperature was utilised as desolvation temperature.

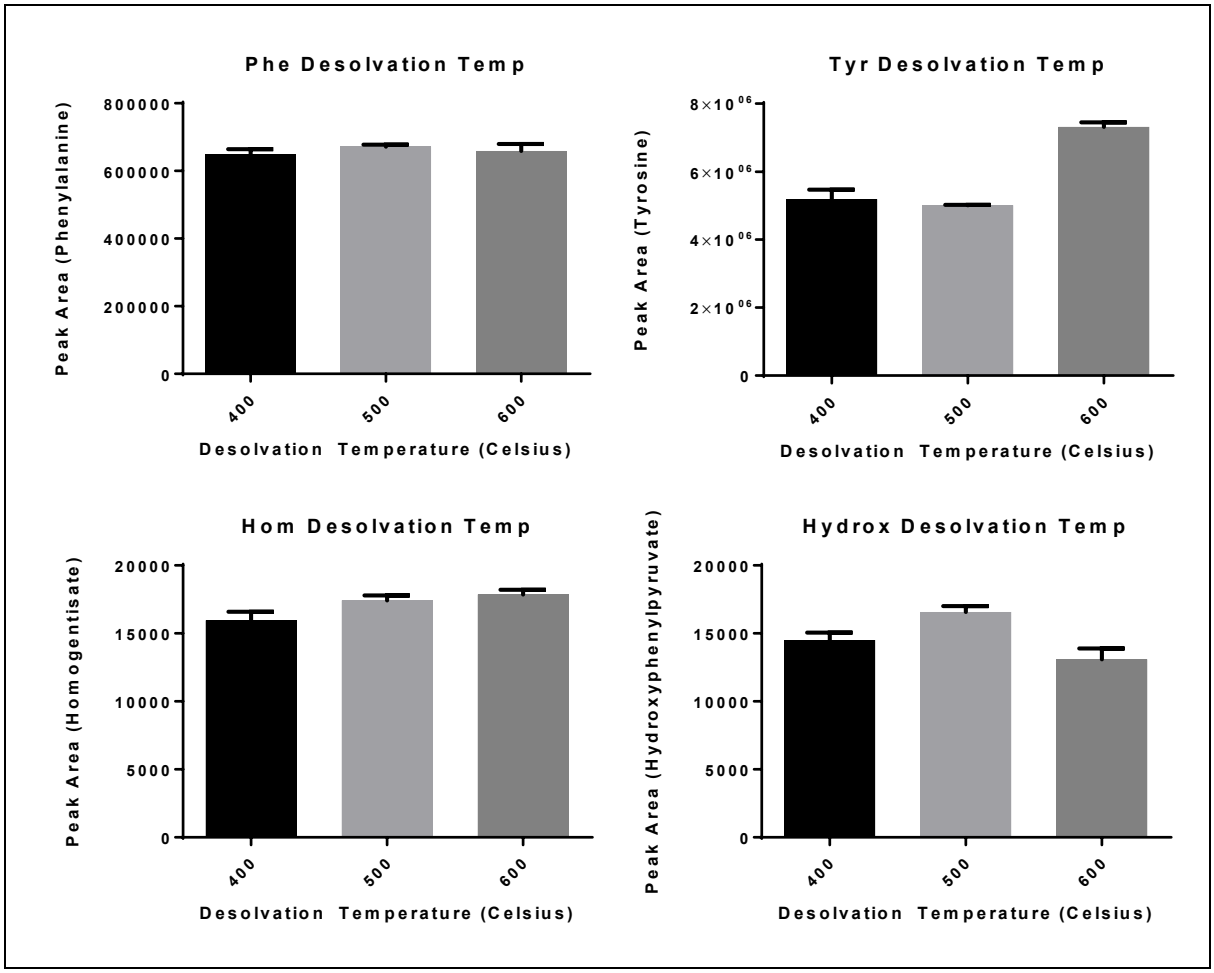


Figure 30: Demonstrating effect of the desolvation temperature on peak area with 600°C providing the largest peak area for three out of four compounds.

Desolvation Flow

Desolvation flow of 1000L/hour provided the largest peak area for all compounds except phenylalanine. This was selected as desolvation flow.

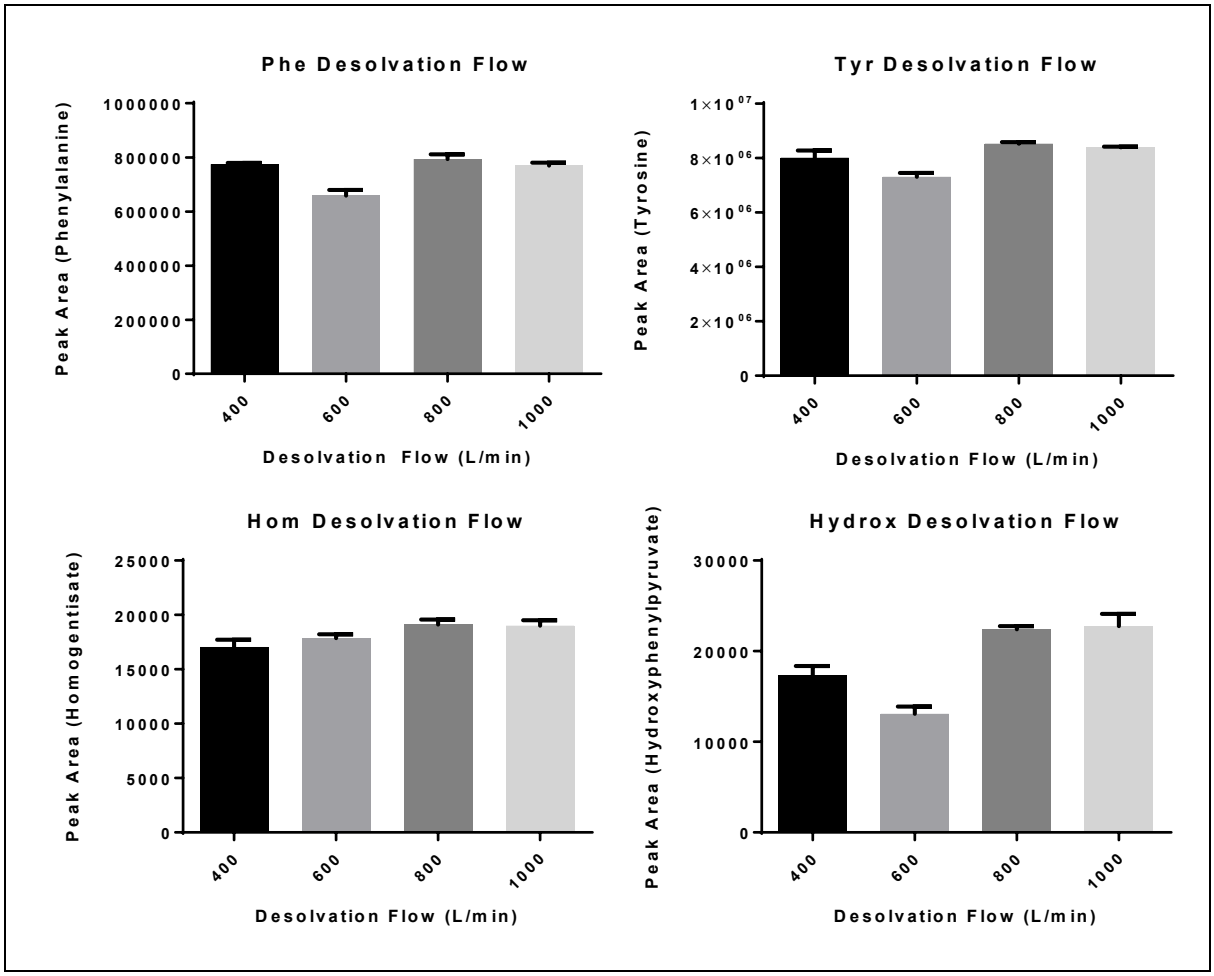


Figure 31: Desolvation flow of 1000L/hour providing the largest peak area for all compounds except phenylalanine.

Cone Flow

Cone flow showed some differences between compounds. Phenylalanine peak area became larger with increasing cone flow, whereas homogentisate and tyrosine peak area reduced with increasing cone flow. Hydroxyphenylpyruvate areas appeared variable. The method was optimised on the basis of changes in homogentisate peak areas and a low cone flow of 150L/hour was selected.

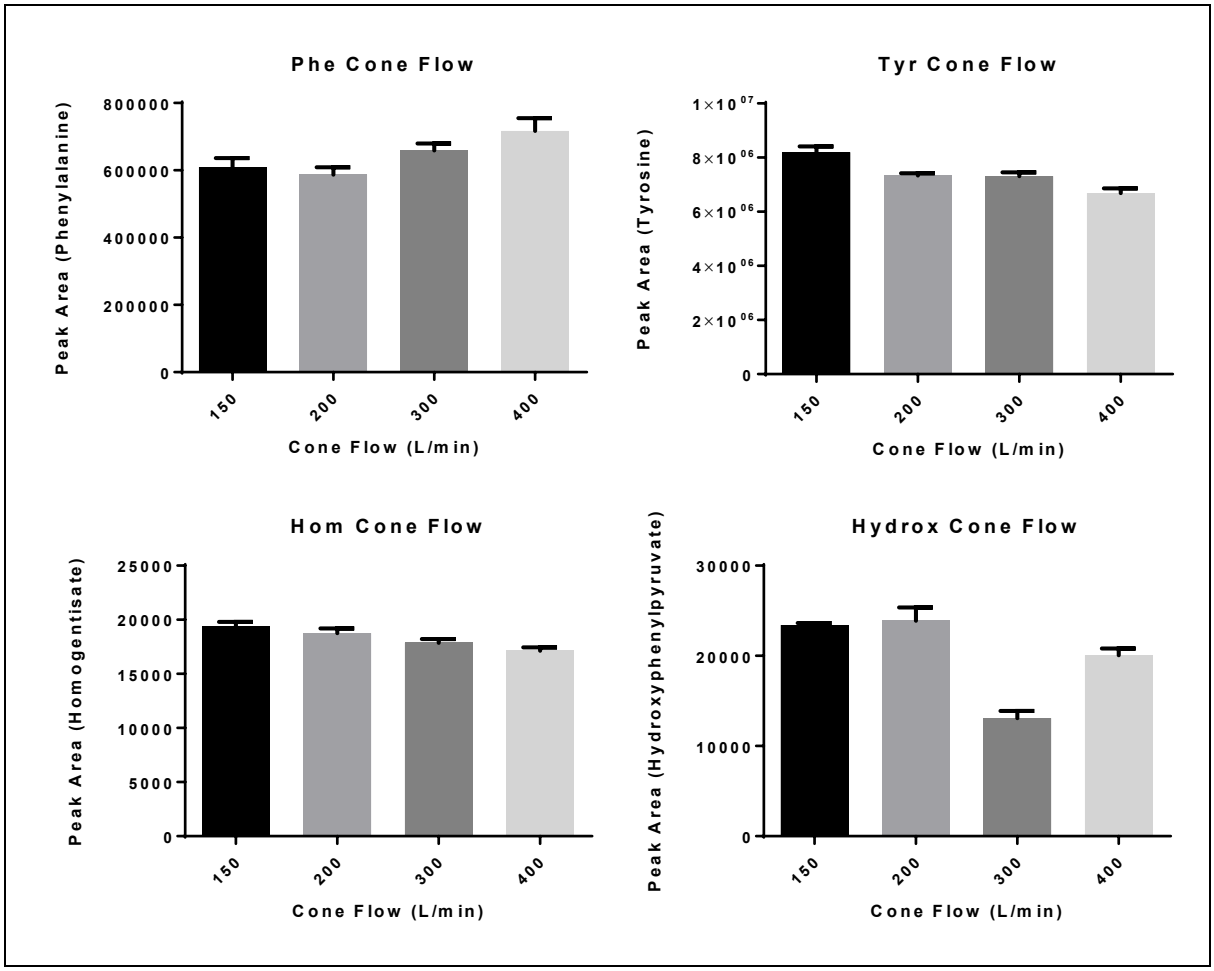


Figure 32: Variable peak areas with changes in cone flow, but greatest homogentisate peak area with cone flow of 150L/hr.

Optimised Mass Spectrometer Parameters

The optimised mass spectrometer ion source parameters were as follows:

1. Capillary voltage: 2kV.
2. Desolvation temperature 600°C.
3. Desolvation gas flow 1000L/hr.
4. Cone gas flow 150L/hr.

Calibration Curves

Calibration curves for all compounds were linear using this method up to 10µM. Calibration points were 0.01µM, 0.05µM, 0.1µM, 0.25µM, 0.5µM, 1µM, 2.5µM, 5µM and 10 µM. All samples were analysed as technical triplicates. Linearity beyond this concentration would be assessed later once the required dynamic range for samples was established.

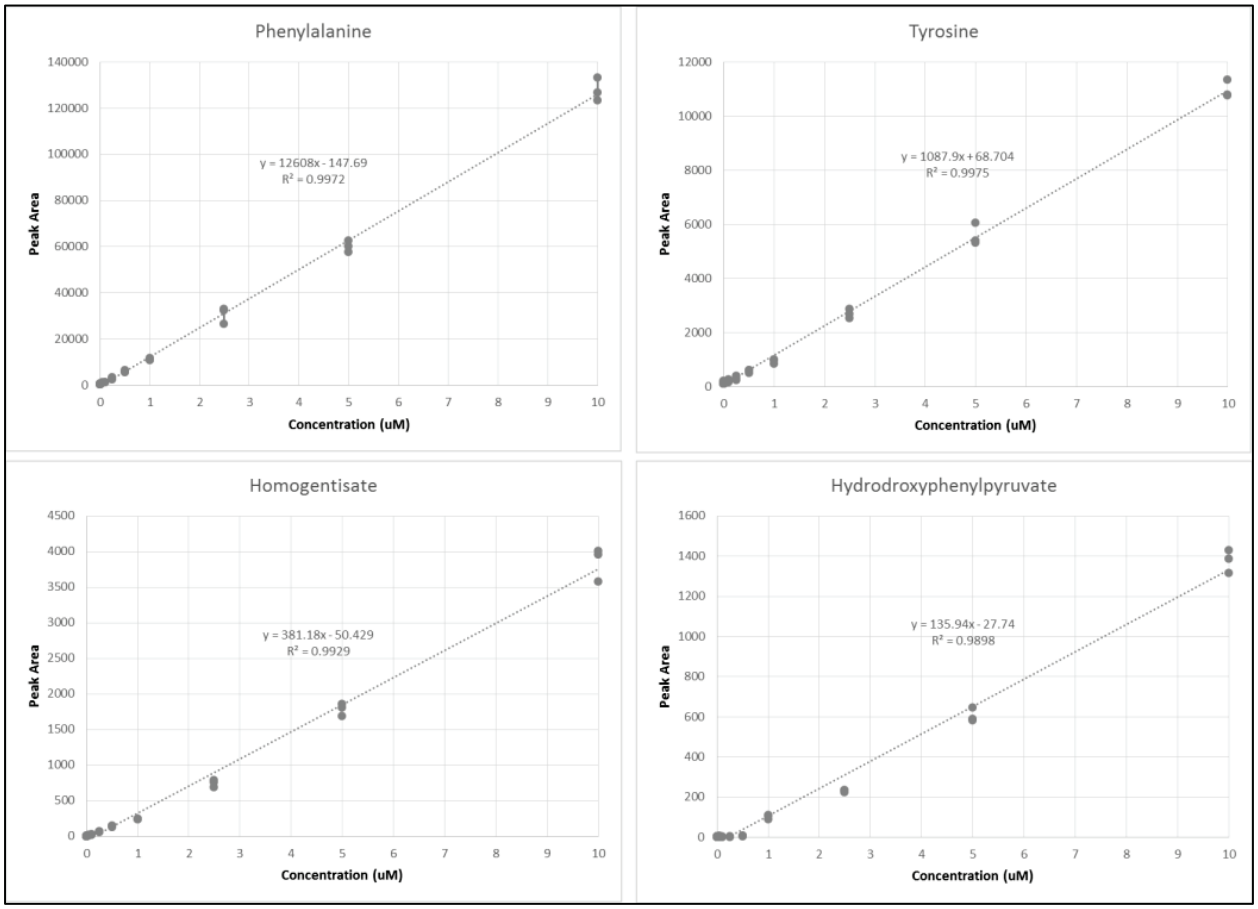


Figure 33: Linear calibration curves for all compounds.

Calculation of Limit of Detection and Limit of Quantification

Limit of detection (LOD) and limit of quantification (LOQ) were established using the above chromatography and mass spectrometry settings with an injection volume of 5µl.

Limit of detection was calculated for each compound as:

1. Phenylalanine – 0.05μM (0.008μg/ml).
2. Tyrosine – 0.5μM (0.09μg/ml).
3. Homogentisate – 1μM (0.168μg/ml).
4. Hydroxyphenylpyruvate – 1μM (0.18μg/ml).

Limit of quantification was calculated for each compound as:

1. Phenylalanine – 0.1μM (0.017μg/ml).
2. Tyrosine – 1μM (0.18μg/ml).
3. Homogentisate – 2.5μM (0.420μg/ml).
4. Hydroxyphenylpyruvate – 5μM (0.9μg/ml).

Intra-Day and Inter-Day Accuracy

Intra-day and inter-day accuracy were established by measuring each compound from three injections of a 5μM concentration standard solution either on the same day for intra-day accuracy or on non-consecutive days for inter-day accuracy.

Compound	**Recovered (Mean ± SD, μM)**		**Accuracy (%)**		**Error (%)**	
	Intra-Day	**Inter-Day**	**Intra-Day**	**Inter-day**	**Intra-Day**	**Inter-Day**
Phenylalanine	4.77±0.2	5.01±0.3	95.5	99.5	4.2	4.2
Tyrosine	5.06±0.4	4.96±0.3	101.2	99.2	7.4	5.4
Homogentisate	4.80±0.2	5.14±0.4	96.1	102.8	4.9	7.2
Hydroxy-phenylpyruvate	4.65±0.3	4.61±0.7	93.1	92.2	5.5	14.9

Table 27: Intra-day and inter-day accuracy results for the LC-MS method.

These results demonstrated good accuracy and precision for all compounds. Hydroxy-phenylpyruvate demonstrated the lowest accuracy and precision of all the compounds and had an inter-day error of 14.9%. Although this was higher than other compounds analysed it was within the acceptable limit of 20%.

Sample Preparation

Plasma and gastric content samples required deproteination prior to analysis. This was initially attempted using dichloromethane (DCM) in a 1:2 sample to DCM ratio (500µl sample and 1000µl DCM). These were vortex mixed and centrifuged at 18000g for 10 minutes. 200µl supernatant was removed and tested for effectiveness of protein precipitation by adding 600µl methanol. This demonstrated that this DCM-based method was not effective in precipitating protein from plasma.

Methanol-based protein precipitation was therefore used. The effective ratio of plasma to methanol necessary for complete precipitation of all protein in plasma was 1:3 (250µl plasma to 750µl methanol). These were vortex mixed and centrifuged at 18000g for 10 minutes. 200µl supernatant was removed and tested for effectiveness of protein precipitation by again adding 600µl methanol. This demonstrated that all protein had been precipitated from plasma and gastric content using this 1:3 plasma to methanol precipitation ratio.

Plasma and gastric content samples were spiked with 10µM of all standards and methanol precipitation performed as detailed above. The supernatant was analysed directly using the LC-MS method developed above with a 5µl injection volume. Injection from this methanol/water mix produced significant distortion of all peak shapes (in particular tyrosine).

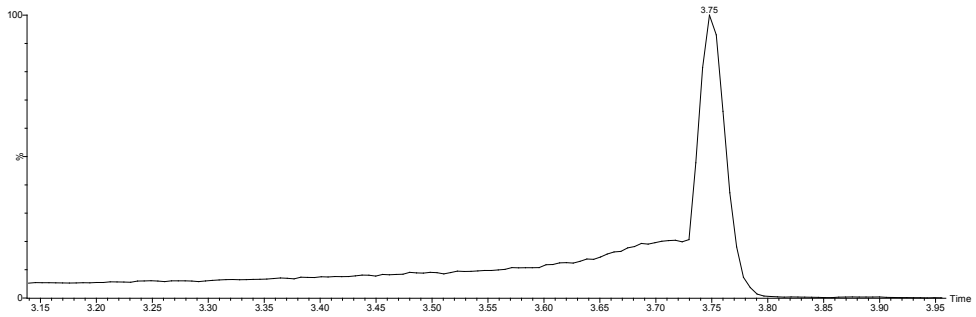


Figure 34: Distortion of tyrosine peak shape when injecting from methanol.

To solve this issue samples were evaporated following precipitation and then reconstituted in water prior to injection. This was undertaken by spiking samples with 10µM of all standards and completing the methanol precipitation as detailed above. 200µl supernatant was placed into a 2ml vial and evaporated to dryness in a centrifuge whilst being heated under vacuum. Samples were heated to 37°C for 40 minutes to achieve complete evaporation. Samples were then reconstituted with HPLC grade water (200µl for plasma and 1000µl for gastric content) and thoroughly mixed followed by being centrifuged at 13,000 rpm for 10 minutes. LC-MS analysis of these samples reconstituted in water demonstrated improved peak shapes.

The matrix effect, recovery of the extraction process, and overall process efficiency were then assessed. Assessment of matrix effect is necessary to account for ion suppression which may occur within the sample matrix due to the presence within the mixture of a large number of different compounds. These may affect the efficiency of analyte droplet formation, and the amount of analyte ions in the gas phase which reach the detector[126]. Assessment of matrix effect, recovery and process efficiency was undertaken using the previously described methods[127,128]. This utilises three different forms of sample (all analysed as technical triplicates):

A. Spike of standard solution in water (10µM).
B. Plasma sample spiked with 10µM standards following methanol extraction (post-spike sample).
C. Plasma sample spiked with 10µM standards before methanol extraction (pre-spike sample).

The percentages for matrix effect (ME), recovery of the extraction process (RE) and overall process efficiency (PE) are calculated as follows[127,128]:

- ME (%): (Post spike sample (B) ÷ Standard solution (A)) x 100; (B ÷ A)*100.
- RE (%): (Pre-spike sample (C) ÷ Post spike sample (B)) x 100; (C ÷ B)*100.
- PE (%): (Pre-spike sample (C) ÷ Standard solution (A)) x 100; (C ÷ A)*100.

Gastric Content

Results of ME, RE, and PE related to tyrosine in gastric content are demonstrated in table 28:

Gastric Content	Tyr
Matrix Effect (%)	235.85
Recovery (%)	88.25
Process Efficiency (%)	208.14

Table 28: Matrix effect, recovery, and process efficiency for analysis of tyrosine in gastric content.

Although there was ion enhancement with increased tyrosine intensity (236%) the use of isotope-labelled tyrosine standards (D4 Tyrosine) as internal standard should correct for this effect.

Analysis of a pooled unspiked gastric content sample revealed a mean tyrosine concentration of 10.32µM ± 0.16 (1.87µg/ml). This was far above the LOD and LOQ for tyrosine in this method (0.5 µM and 1µM respectively).

Accuracy was then calculated by spiking gastric content samples with various tyrosine concentrations (5µM, 10µM and 20µM). The accuracy was expressed as the ratio of the quantified concentration to

the known concentration of the stock solution following subtraction of the tyrosine peak area from the unspiked sample. The error (or precision) was calculated as the relative standard deviation (%) of the triplicates. Results and the calibration curve (to 50μM) are shown below.

Spike	Tyr (μM)	Accuracy (%)	Error (%)
5μM	4.62±0.94	92.4	20.5
10μM	9.35±1.09	93.5	11.7
20μM	17.60±0.78	88.0	4.46

Table 29: Results of gastric content experiments for accuracy of tyrosine quantification.

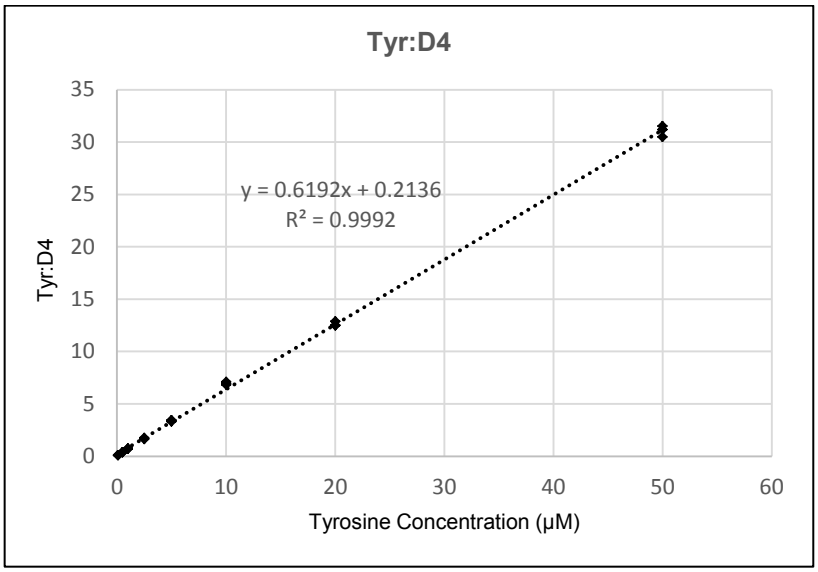


Figure 35: Linear calibration curve for tyrosine quantification (using 10 μM D4 tyrosine as internal standard) up to 50μM.

These results demonstrated good results for tyrosine quantification in gastric content using this method.

Plasma

Results of ME, RE and PE of these compounds in plasma are demonstrated below:

Plasma	Phe	Tyr	Hom	Hydrox
Matrix Effect (%)	59.99	235.85	2.50	91.21
Recovery (%)	121.85	88.25	N/A	1.69
Process Efficiency (%)	73.10	208.14	N/A	1.54

Table 30: Matrix effect, recovery, and process efficiency in plasma samples.

These results demonstrated large differences in the matrix effect for phenylalanine and tyrosine. Isotope-labelled standards were being utilised for these compounds and should correct for these changes in matrix effect.

The matrix effect results for homogentisate demonstrated a large amount of ion suppression (matrix effect 2.50%) and this compound was not visible in the sample spiked before extraction. This meant it was not possible to establish the recovery or process efficiency for this compound. It is known that this compound is unstable in plasma unless samples are deproteinised immediately, particularly due to the slightly basic environment of plasma[124,129]. Although these samples were promptly deproteinated following addition of homogentisate standards it was believed that the known decrease in homogentisate concentrations in non-deproteinated plasma samples was responsible for these results. Time of Flight mass spectrometry (ToF-MS) was performed on homogentisate by interfacing the Aquity® UPLC system with a Xevo G2-XS Quadrapole Time-of-Flight Mass Spectrometer (both Waters, Milford, MA, USA). This provided greater mass resolution than the previous mass spectrometer. ToF-MS analysis of homogentisate standards on full scan mode revealed the precise m/z of this compound to be 167.0392 at a retention time of 4.26 minutes. To investigate the effect of pH on stability of homogentisate plasma samples were spiked with 10µM homogentisate and treated as follows:

i. Plasma +10μM spike only.

ii. Plasma + 10μM spike with 0.1g ascorbic acid.

iii. Plasma + 10μM spike with 0.1% formic acid.

iv. Plasma + 10μM spike with 0.1% ammonium hydroxide.

All results were compared to a 10μM homogentisate spike, and matching samples water with 10μM spike were analysed for each condition. Results are shown below:

Sample	Homogentisate Peak Area	Stability (vs Standard)
Standard	54001 ± 2836	N/A
Plasma only	8775 ± 1616	16.3%
Water + Ascorbic Acid	3177 ± 1719	5.9%
Plasma +Ascorbic Acid	1320 ± 304	2.4%
Water + Formic Acid	63010 ± 10467	100%
Plasma + Formic Acid	61190 ± 8248	100%
Water + AmmOH	0	0
Plasma + AmmOH	0	0

Table 31: Details of homogentisate peak areas and stability (relative to standard solution) with different sample treatments. Addition of formic acid provided the greatest stability.

These experiments demonstrated that homogentisate had the greatest stability when 0.1% formic acid was added to plasma. Unspiked plasma samples were treated with 0.1% formic acid following immediate deproteinisation. Even with this treatment homogentisate was below the limit of detection in these unspiked samples. When ammonium hydroxide was added homogentisate was below the limit of detection in all spiked samples likely due to homogentisate being unstable in a basic environment[129]. Spiked samples of plasma with 0.1% formic acid, and 0.1% ammonium hydroxide

were then re-analysed using tandem mass spectrometry (MS/MS). Subtraction of the base peak intensity was used to identify peaks present in the ammonium hydroxide sample, which were not present in those treated with formic acid. This was to establish if it was possible to identify the breakdown product of homogentisate. There was one additional peak identified at retention time 4.19 minutes (mass 151.058) which may have represented a breakdown product but this result was not reproducible and it was not possible to definitively identify the breakdown product of homogentisate.

Hydroxyphenylpyruvate also demonstrated very poor recovery and process efficiency. Phenylpyruvates are known to oxidise to form aldehydes and it is believed that this was responsible for these results[130]. This reaction was investigated using derivitisation with 2,4-dinitrophenylhydrazine (DNPH) which is a selective reagent for aldehyde and ketone groups. It was calculated that following derivitisation the single DNPH adduct for hydroxyphenylpyruvate would be mass 301 Da, and the double adduct would be 480 Da. Plasma samples were spiked with 100µM hydroxyphenylpyruvate and 50µL of DNPH in HCl added. Samples were left to derivitise for 1 hour at room temperature. Analysis of these samples revealed a peak at m/z 301 at a retention time of 6.28 minutes. This was believed to represent the aldehyde oxidation product of hydroxyphenylpyruvate.

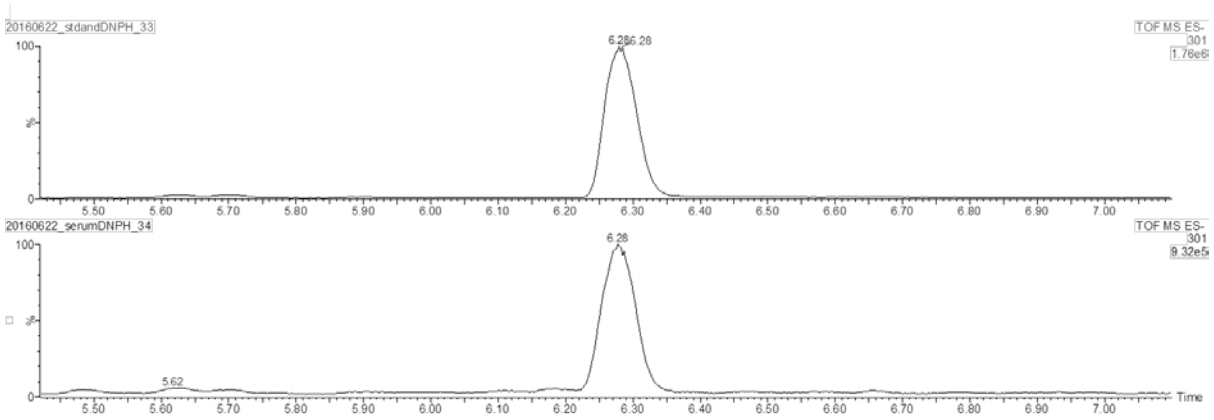


Figure 36: Peak at 6.28 minutes when scanning for m/z 301 in hydroxyphenylpyruvate standards and plasma derivitised with DNPH.

2.4.4 Conclusions

These optimisation experiments have produced an effective and accurate method for quantification of tyrosine in gastric content with a limit of quantification of 1µM. This method is used later in Section 4.4 for quantification of tyrosine in gastric content.

It was not possible to develop a suitable method for quantification of homogentisate within plasma samples as this compound appeared to be converted to an alternative compound within plasma. It was not possible to definitively identify this breakdown product. Previous methods that have successfully quantified homogentisate in serum have utilised samples from patients with alkaptonuria, where the concentration of homogentisate would be anticipated to be greatly elevated relative to normal subjects[124]. These studies also used immediate deproteinisation of blood samples although this did not appear to help homogentisate stability in the experiments conducted here.

The primary aim of this work in plasma was to produce a method for homogentisate quantification. As this was not possible no further plasma experiments were undertaken using LC-MS. LC-MS was therefore only utilised for tyrosine quantification in gastric content.

CHAPTER 3 - AMINO ACID METABOLISM IN OESOPHAGO-GASTRIC CANCER

3.1 Nano-electrospray Ionisation Mass Spectrometry Dried Blood Spot Analysis

3.1.1 Objective

This experiment aimed to utilise nano-electrospray ionisation mass spectrometry analysis of dried blood spot samples to measure intermediary metabolites of aromatic amino acid breakdown.

3.1.2 Introduction

The analysis of dried blood spots was first undertaken in 1963 for the detection of phenylketonuria in newborns[131]. Dried blood spot analysis has since become the mainstay of new-born screening programmes, and has been used for diagnosis of multiple inherited metabolic disorders including tyrosinaemia[132], homocysteinuria[133], congenital adrenal hyperplasia[134], and maple syrup disease[135]. Dried blood spot analysis has also been widely used for therapeutic drug monitoring[136]. This sampling method offers multiple advantages to traditional venous blood sampling as it is less invasive, and can potentially be collected from a finger or heel prick. It requires smaller blood volumes (less than 100µl) and offers simple storage and sample transfer protocols as most samples can be stored at room temperature[137].

Dried blood spot samples are collected by applying blood directly to filter card in order to homogenously and symmetrically fill a predefined circle. Samples are then allowed to dry at room temperature for 2-3 days[136]. Moisture can induce bacterial growth so all samples are stored with desiccant, and depending on analyte stability can be stored for many months or even years[138].

New-born screening programmes most commonly use electrospray tandem mass spectrometry (ESI-MS/MS) analysis coupled to liquid chromatography for compound separation[139,140]. However, nano-electrospray ionisation mass spectrometry has previously been used for metabonomic screening of dried blood spot samples[141]. The advantages of this methodology include shorter analysis times, simplified data analysis and improved reproducibility[141].

This section analysed dried blood spot samples from oesophago-gastric cancer patients using nano-electrospray ionisation mass spectrometry via the previously validated methodology[141]. This experiment aimed to map the pathway of aromatic amino acid breakdown by measuring phenylalanine and tyrosine as well as the intermediary metabolites of aromatic amino acid breakdown (hydroxyphenylpyruvate, homogentisate, maleylacetoacetate and fumarylacetoacetate).

3.1.3 Methods

Local ethics committee approval was obtained for this experiment (ICHTB HTA Licence: 12275; REC Wales Approval: 12/WA/0196; Tissue bank approval number R14118).

Patient recruitment

Patients were identified through the North West London Oesophago-gastric Cancer Unit and the endoscopy unit at St Mary's Hospital Paddington (Imperial College London). All patients had been referred for an upper gastrointestinal endoscopy or were scheduled to undergo surgical resection for oesophago-gastric cancer. All patients completed a health questionnaire at the time of sample collection that provided comprehensive information on their medical history, current medications, smoking status and alcohol consumption. Exclusion criteria included patients with known liver disease or those with any other form of cancer (other than oesophago-gastric cancer). All patients underwent an upper gastrointestinal endoscopy or surgery on the day of sample collection. Patients with biopsy confirmed oesophago-gastric cancer were allocated to the 'cancer cohort'. All individuals with a normal result on OGD or benign disease of the upper gastrointestinal tract (for example gastritis, oesophagitis or peptic ulcer disease) were allocated to the 'control cohort'. Written informed consent was obtained from all patients prior to participant enrolment.

Sample collection

All patients were fasted for a minimum of six hours prior to blood sample collection as per standard protocol prior to surgery or OGD. Blood samples were collected and applied directly to Whatman 903 filter paper (GE Life Sciences, Little Chalfont, BUCKS, UK) and allowed to dry for 48 hours. Samples

were then stored with desiccant. A separate aliquot from each blood sample was collected for haematocrit measurement.

Quality control samples were taken as multiple blood spots from a single blood sample. A proportion of quality control samples were divided into differing quantities (5% of total blood spot, 20%, 50% and 100%) to assist with peak identification.

Sample Preparation

A 96-well filter plate was washed using 100µL methanol (HPLC grade - Sigma Aldrich, Gillingham, Dorset, UK) and centrifuged for two minutes at 2200g. Dried blood spot samples (diameter 6mm) were weighed and then placed in the 96-well filter plate in predefined positions with three blood spot samples being analysed from each participant. These individual spots were positioned in a randomised order. Extraction was performed using 200µL of methanol (HPLC grade containing isotope labelled standards of D5 phenylalanine (5µM), D4 tyrosine (5µM) (both Sigma Aldrich, Gillingham, Dorset, UK) and $C_{13}6$ homogentisate (12µM) (Toronto Research Chemicals, Toronto, Canada)). Extraction was performed for 30 minutes at room temperature followed centrifugation for two minutes at 2200g. The methanolic extracts were then diluted with 50µL of water (HPLC grade - Sigma Aldrich, Gillingham, Dorset, UK) and the plate sealed prior to mass spectrometry analysis.

Sample analysis

Mass spectrometry analysis was performed using the Thermo Exactive® mass spectrometer (ThermoScientific, Waltham, MA, USA) equipped with the Advion TriVErsa NanoMate® ion source (Advion, Ithaca, NY, USA). Total sample analysis time was 1.5 minutes with 45 seconds in negative ion mode and 45 seconds in positive ion mode with automatic polarity switching.

Data analysis was performed using Excalibur® (ThermoScientific, Waltham, MA, USA) software. Compounds of interest were identified and intensity of each peak recorded. Peak intensity was then normalised to the relevant isotope-labelled internal standard for each compound as well as sample

haematocrit value. Haematocrit normalisation was performed according to the previously described formula: Peak intensity/(1-Haematocrit value)[142]. Mean normalised peak intensities (N.P.I) were calculated for each patient from the three dried blood spot samples which were analysed for each patient. Univariate statistical analysis was performed using SPSS v23 (IBM, Armonk, NY, USA). Peak areas were initially calculated using Origin (OriginLab, Northampton, MA, USA) to correlate results from peak area and intensity. Peak areas for all samples were also calculated using MATLAB® (Mathworks Inc. Natick, MA, USA).

3.1.4 Results

Peak Identification

Phenylalanine

Phenylalanine (chemical formula $C_9H_{11}NO_2$) was visible in negative ion mode at the m/z 164.0702.

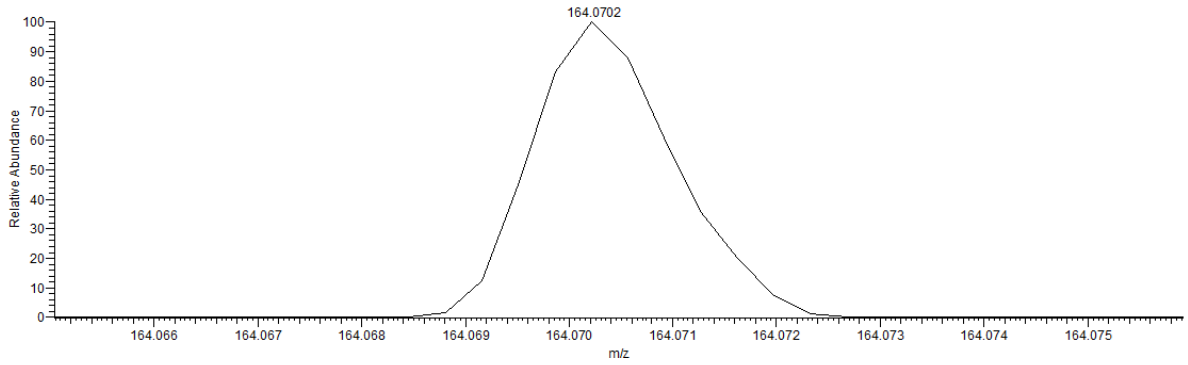


Figure 37: Phenylalanine peak at m/z 164.0702.

Analysis of differing quantities of quality control samples (5%, 20%, 50%, and 100%) demonstrated a linear increase in peak intensity (R-squared value 0.9807) indicating this was a true peak.

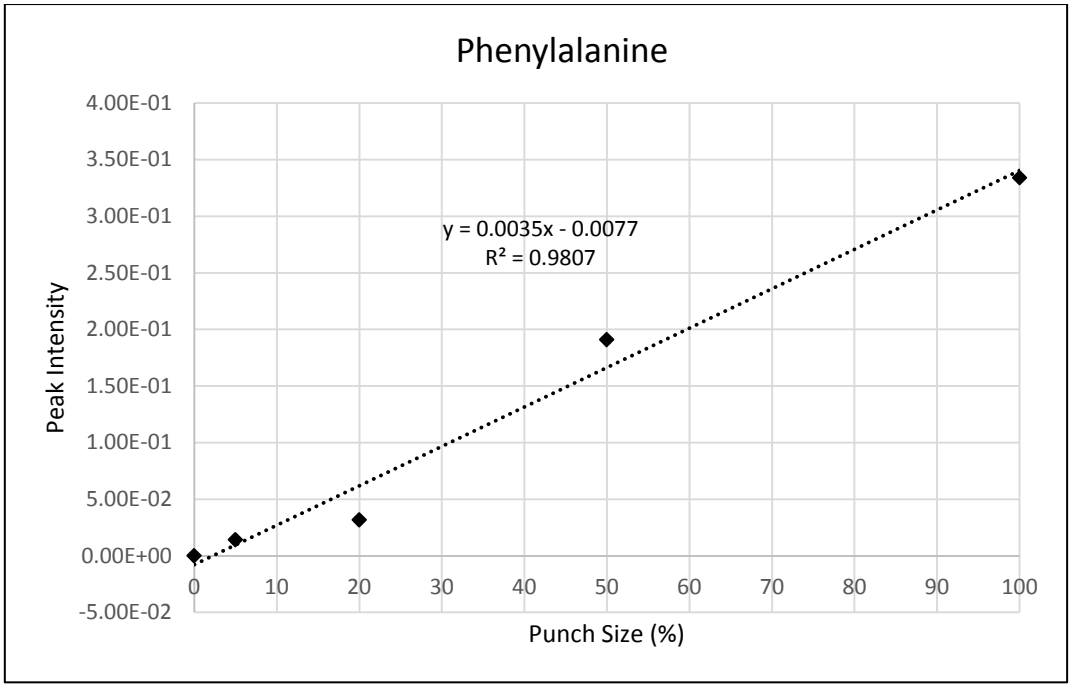


Figure 38: Correlation of peak intensity to punch size demonstrated linearly increasing peak intensity with increasing punch size indicating phenylalanine was a true peak.

Tyrosine

Tyrosine (chemical formula $C_9H_{11}NO_3$) was visible in negative ion mode at the m/z 180.0653.

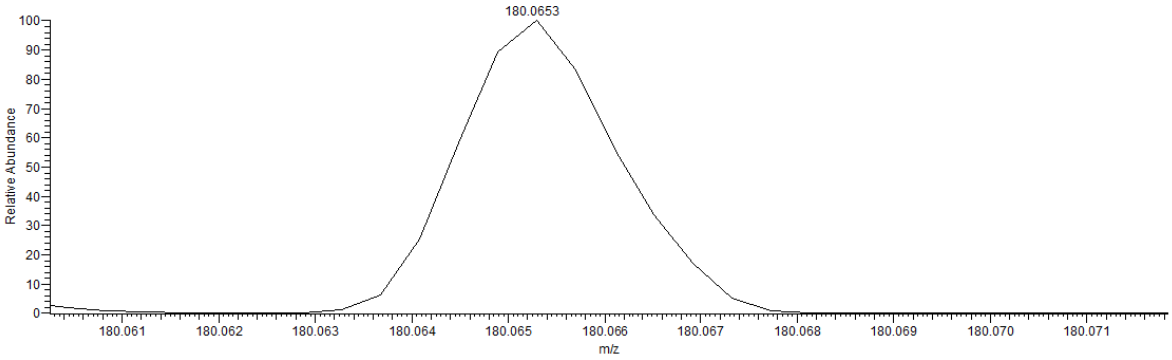


Figure 39: Tyrosine peak visible at m/z 180.0653.

Tyrosine also demonstrated linearly increasing peak intensity with increasing quantity of quality control sample (R-squared 0.9819)

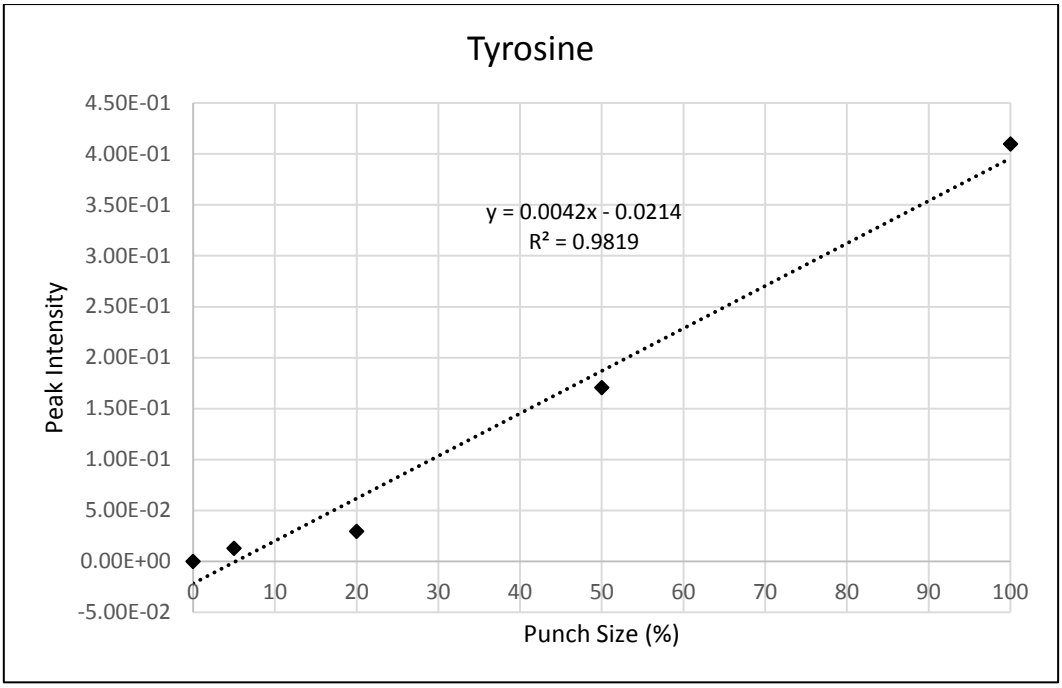


Figure 40: Good correlation between peak intensity and punch size for tyrosine.

Homogentisate

Homogentisate (chemical formula $C_8H_8O_4$) was visible in negative ion mode at the m/z 167.0336.

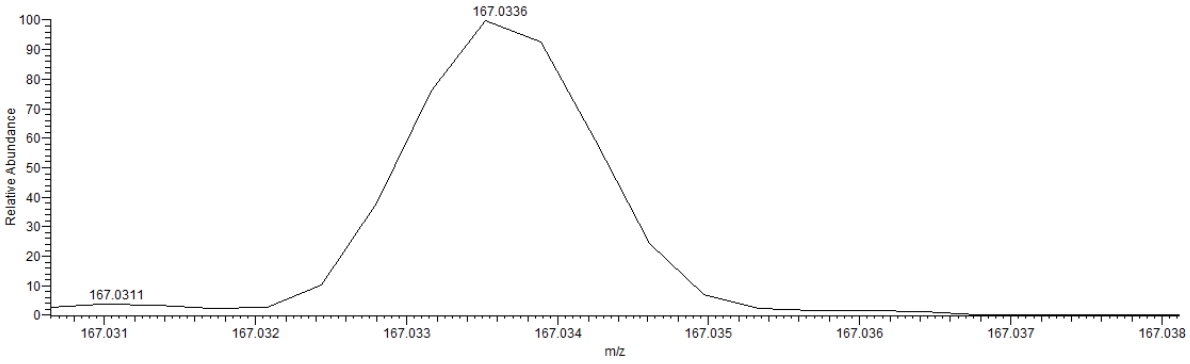


Figure 41: Homogentisate peak visible at 167.0336.

Homogentisate peak area also increased with increasing quantities of quality control sample although this was not as linear as for phenylalanine or tyrosine (R-squared value for homogentisate 0.8436). However, as the value considered acceptable for a true peak was taken to be 0.8 homogentisate was still considered to be a valid peak.

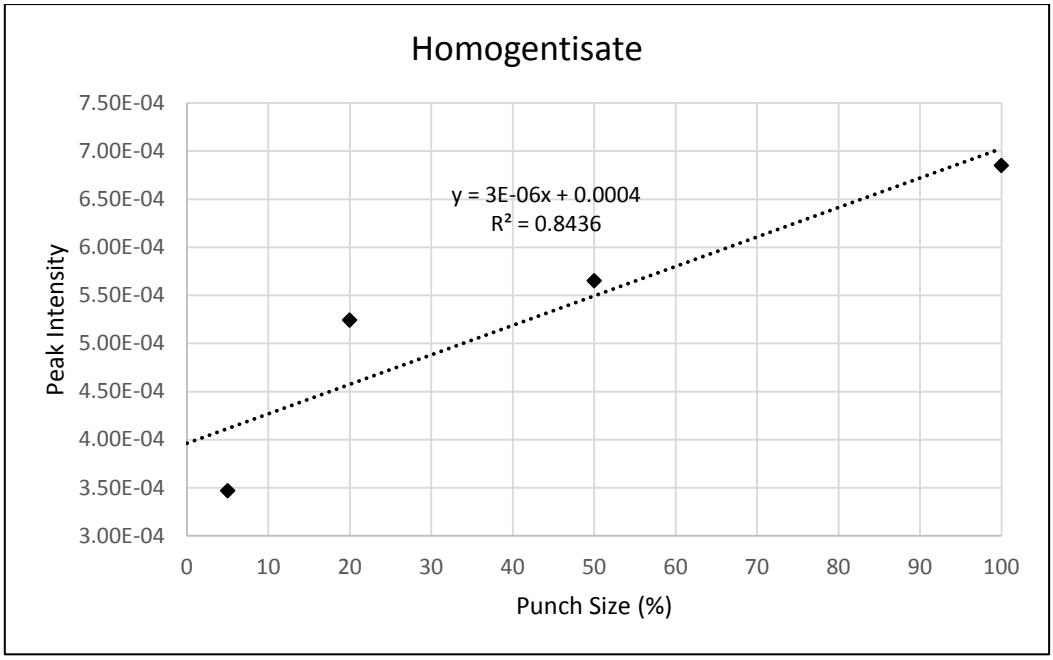


Figure 42: Homogentisate peak intensity to punch size correlation demonstrated R-squared above 0.8.

Hydroxyphenylpyruvate

A peak believed to be hydroxyphenylpyruvate (chemical formula $C_9H_8O_4$) was visible at 179.0336.

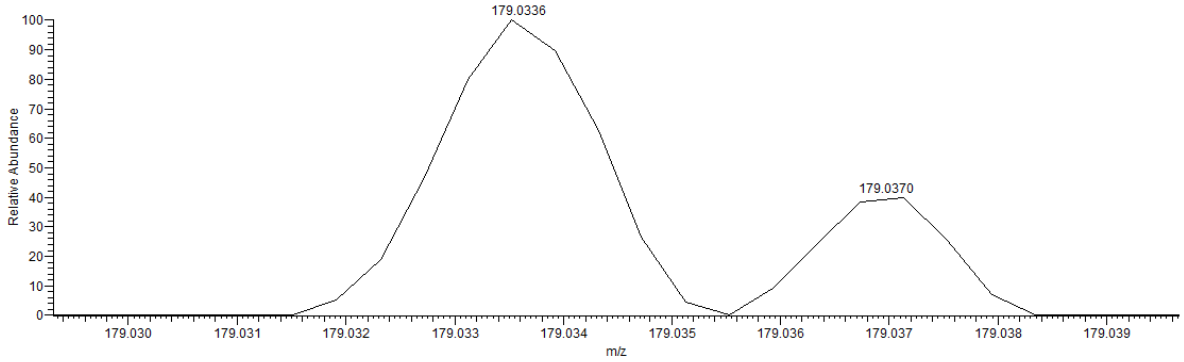


Figure 43: Peak at m/z 179.0336.

However, the analysis of hydroxyphenylpyruvate peak intensity with increasing quality control amounts was poor (R-squared 0.3523) and this was not considered to be a true peak, Hydoxyphenylpyruvate was therefore not considered further in this analysis.

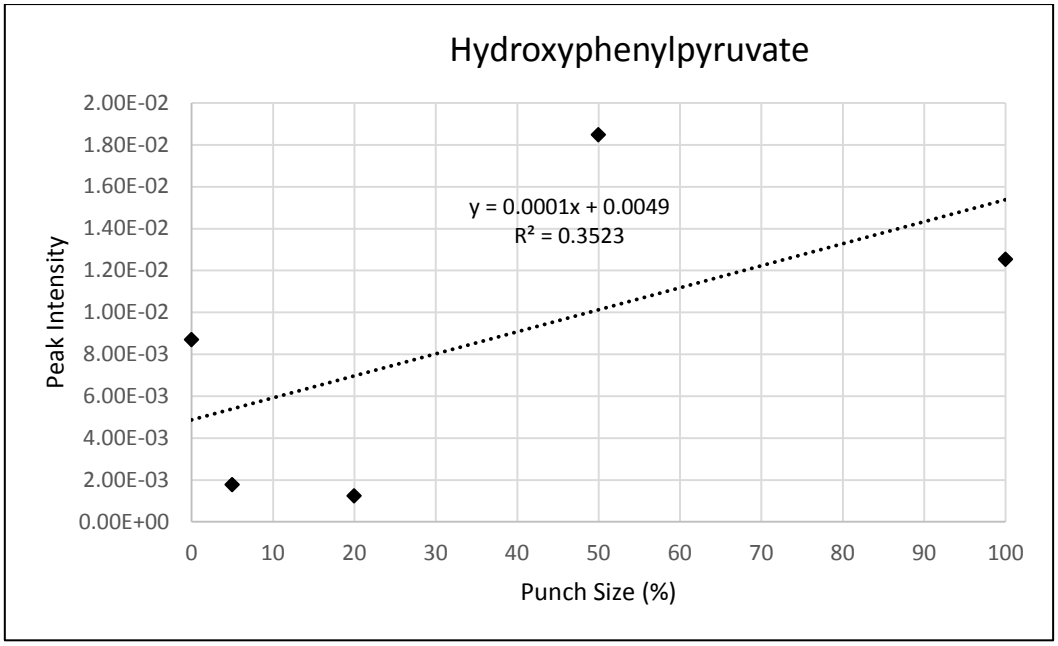


Figure 44: No correlation between peak intensity and punch size for hydroxyphenylpyruvate.

Maleylacetoacetate

Maleylacetoacetate (chemical formula $C_8H_8O_6$) was not visible in either positive or negative ion mode and was therefore not considered further in this analysis.

Fumarylacetoacetate

Fumarylacetoacetate (chemical formula $C_8H_8O_6$) was also not visible in either positive or negative ion mode and was therefore not considered further in this analysis.

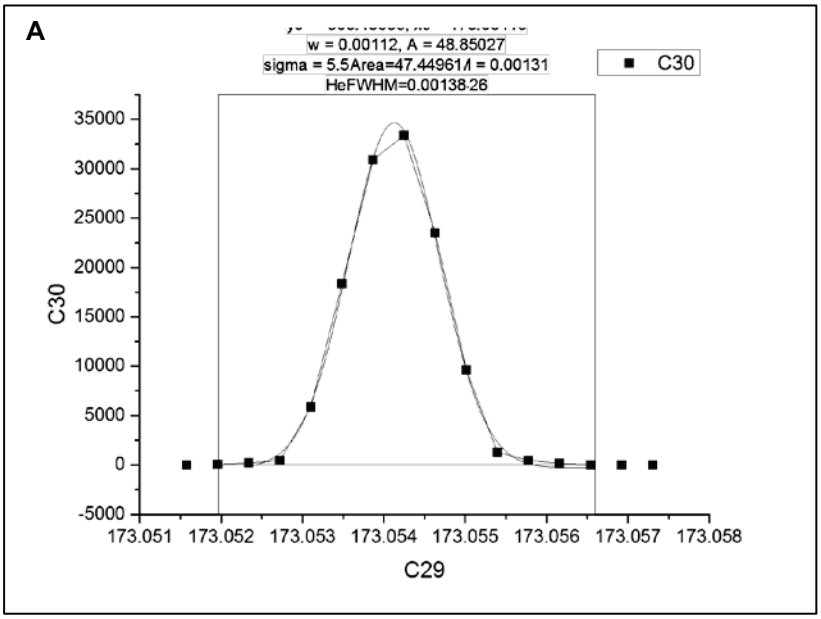
Isotope Labelled Standards

Isotope-labelled standards were identified at the following m/z values:

- D5 Phenylalanine – 169.1020.
- D4 Tyrosine – 184.0661
- C_{13}6 homogentisate – 173.0540

Intensity vs Area

Peak areas were initially calculated for each of the internal standards used. There was good correlation between peak area and peak intensity as shown in figure 45.



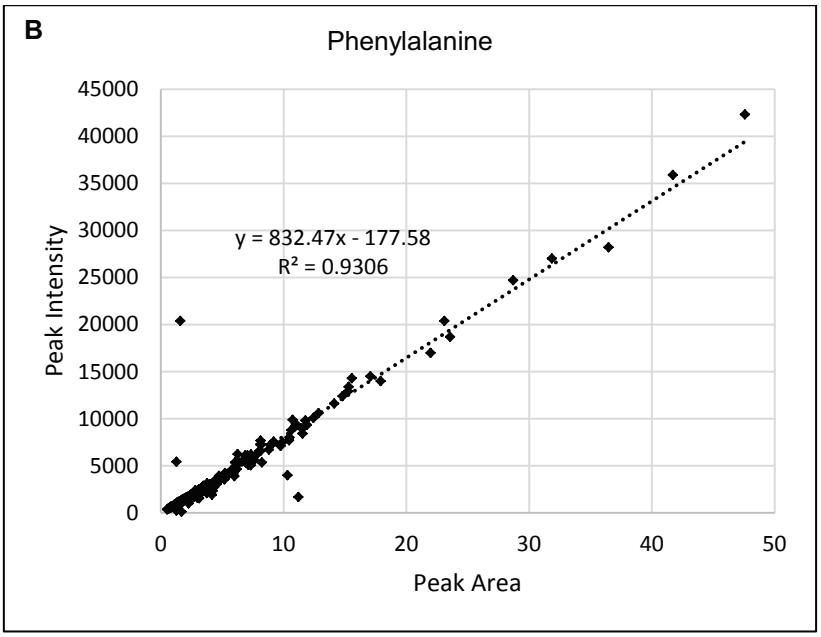
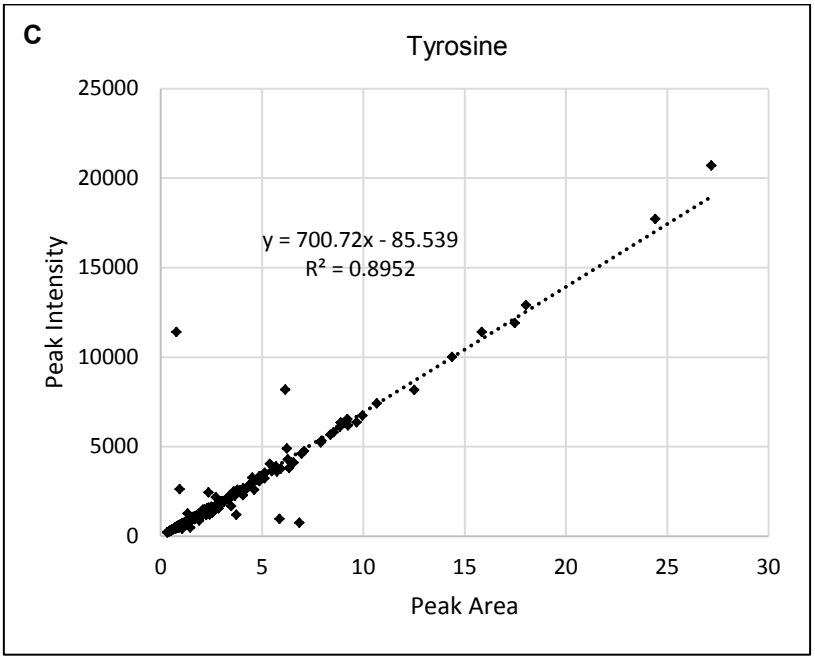


Figure 45*: A - Calculation of peak area via peak integration. B – Good correlation for phenylalanine between peak area and intensity.*



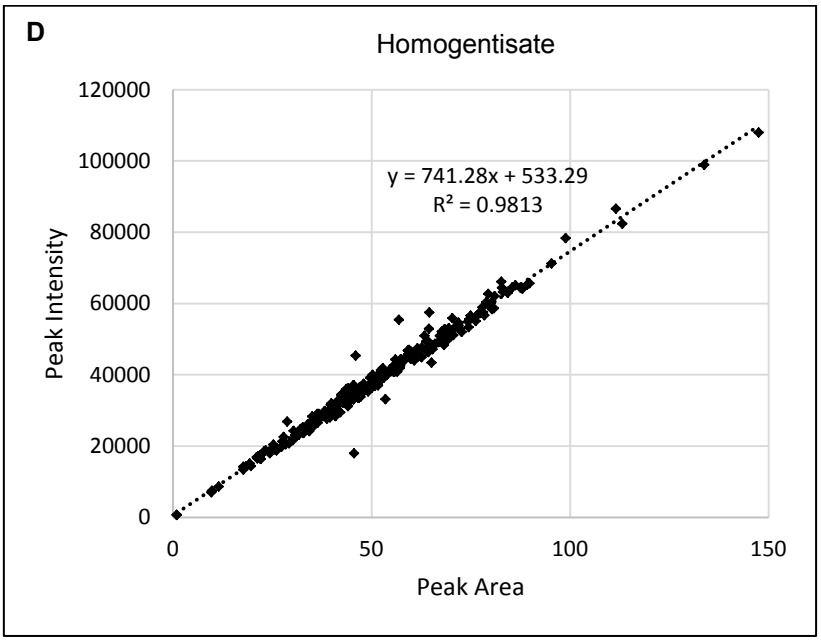


Figure 45 continued: Good correlation between peak intensity and area for tyrosine (C) and homogentisate (D).

These results demonstrated good correlation between peak intensity and peak area. Peak intensity was used for analysis in the remainder of these results.

Normalisation to Haematocrit and Blood Spot Weight

Punch weight was compared to haematocrit value to establish if punch weight could be used as a surrogate for haematocrit in blood spot analysis. The correlation between punch weight and haematocrit was poor as shown in figure 46. Therefore, haematocrit (rather than punch weight) was used as the normalisation measure for the remainder of this analysis.

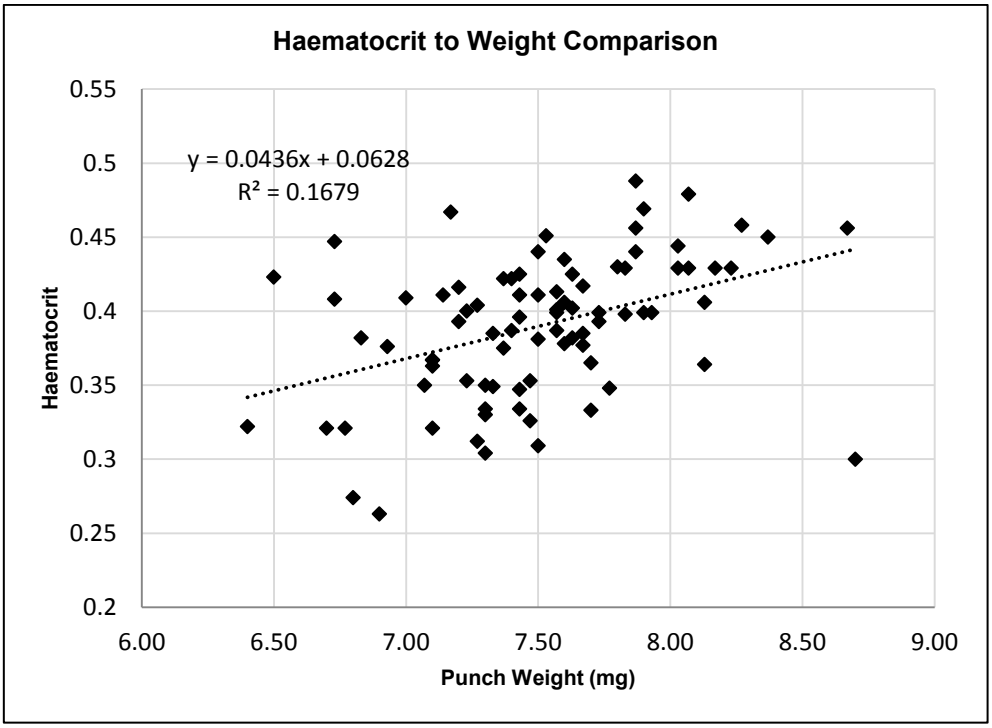


Figure 46: Poor correlation between punch weight and patient haematocrit.

Patient Demographics

In total there were 49 oesophago-gastric cancer cases collected and 37 samples from control patients with normal upper gastrointestinal tract or benign disease of the upper gastrointestinal tract. Demographic details are shown in table 32.

	Control (n=37)	Cancer (n=49)	Chi-Squared (p)
Age (Median)	61 (34-89)	70 (34-94)	0.006 (MWU)
Male	25 (68%)	37 (76%)	0.416
Caucasian	26 (70%)	38 (77%)	0.444
PPI Use	27 (72%)	29 (59%)	0.979
Aspirin Use	8 (22%)	10 (24%)	0.864
Hypertension	9 (24%)	19 (39%)	0.047
Diabetes	3 (8%)	8 (16%)	0.118
Statin Use	7 (19%)	12 (24%)	0.350
Non-Smoker	21 (57%)	24 (49%)	0.976
Alcohol under 21 units per week	32 (86%)	38 (78%)	0.444
ASA 1 or 2	31 (83%)	30 (61%)	0.544

Table 32: Demographic details for patients from who dried blood spot samples were collected.

The control and cancer groups were generally well matched. The control cohort patients were younger than the cancer cohort (Median age 61 in control cohort vs 70 in cancer cohort (MWU 0.006)). There were also significantly more cancer patients who suffered with hypertension (39% in cancer group, 24% in controls (Chi-Squared p=0.047). There were no other significant differences between the groups.

Of the cancer cases 11/49 (22%) had T1/2 stage disease, and the remaining 38 (78%) had T3/4 stage disease. Thirty-five patients (71%) had lymph node involvement, and 7 patients (14%) had metastatic disease spread.

Overall

When all 49 oesophago-gastric cancer cases were compared directly to the 37 control patients the following median normalised peak intensities (N.P.I) were calculated (peak intensities normalised to isotope labelled internal standard and haematocrit value):

	Control (n=37) (N.P.I.)	**Cancer (n=49) (N.P.I.)**	**Mann Whitney U Test**
Phenylalanine	0.837 (IQR: 0.730 to 1.08)	0.698 (IQR: 0.601 to 0.948)	P = 0.009
Tyrosine	1.287 (IQR: 0.909 to 1.686)	1.167 (IQR 0.835 to 1.549)	P = 0.355
Homogentisate	0.0162 (IQR: 0.0118 to 0.0233)	0.0114 (IQR 0.0089 to 0.0141)	P = 0.001

Table 33: Overall normalised peak intensities (N.P.I.) for cancer and control cohorts.

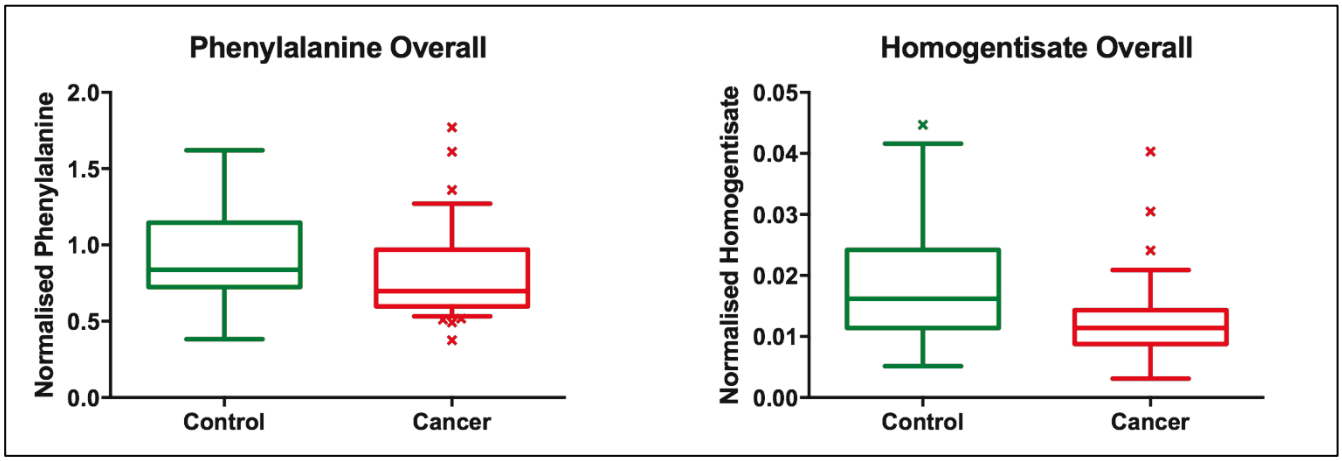


Figure 47: Boxplots of median normalised peak intensities for phenylalanine and homogentisate in control and cancer samples.

These results have demonstrated a significant decrease in both phenylalanine, and homogentisate concentrations in the cancer patients compared to controls.

Effect of Neoadjuvant Chemotherapy

From the oesophago-gastric cancer cohort 33 patients had not received any neo-adjuvant chemotherapy, whilst 16 had completed neo-adjuvant chemotherapy prior to sample collection. When these groups were compared to each other (along with the control group) the following normalised median peak intensities were calculated for each sub-group:

	Control (n=37) (N.P.I.)	**Pre-Chemotherapy (n=33) (N.P.I.)**	**Post-Chemotherapy (n=16) (N.P.I)**	**Kruskal-Wallis Test**
Phenylalanine	0.837 (IQR: 0.730 to 1.08)	0.715 (IQR: 0.582 to 1.001)	0.657 (IQR: 0.641 to 0.732)	P = 0.13
Tyrosine	1.287 (IQR: 0.909 to 1.686)	1.154 (IQR: 0.801 to 1.339)	1.449 (IQR: 0.835 to 1.852)	P = 0.329
Homogentisate	0.0162 (IQR: 0.0118 to 0.0233)	0.0114 (IQR: 0.0087 to 0.0140)	0.0115 (IQR: 0.0093 to 0.014)	P = 0.005

Table 34: Sub-group analysis of patient who had not received any neoadjuvant chemotherapy (pre-chemo) and those who had completed chemotherapy (post-chemo).

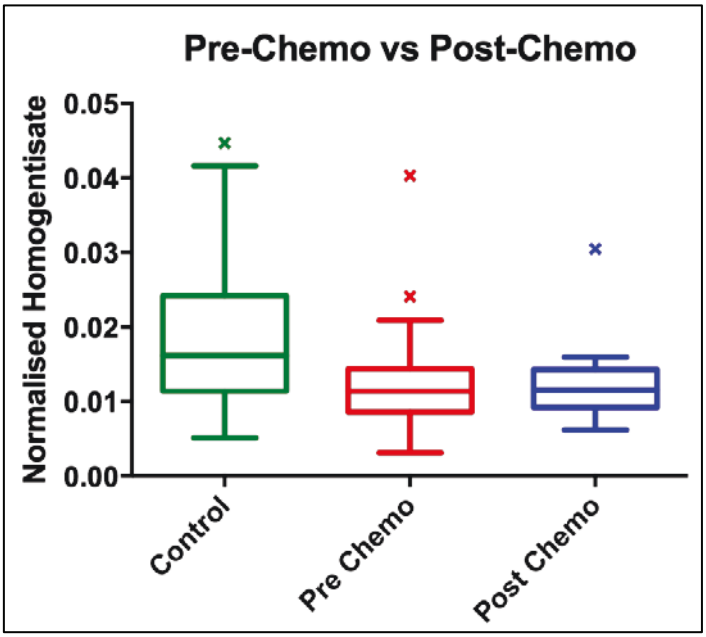


Figure 48: Boxplot of homogentisate normalised peak intensities for control samples and cancer patients pre- and post-chemotherapy.

Oesophageal vs Gastric Tumours

From the oesophago-gastric cancer cohort 31 patients had oesophageal adenocarcinoma or tumours at the gastro-oesophageal junction (Siewert 1 & 2). 18 patients had adenocarcinoma of the stomach (including Siewert type 3). The following median normalised peak intensities were calculated for each sub-group:

	Control (n=37) (N.P.I.)	**Oesophageal (n=31) (N.P.I.)**	**Gastric (n=18) (N.P.I)**	**Kruskal-Wallis Test**
Phenylalanine	0.837 (IQR: 0.730 to 1.08)	0.716 (IQR: 0.646 to 0.992)	0.698 (IQR: 0.594 to 0.872)	0.035
Tyrosine	1.287 (IQR: 0.909 to 1.686)	1.167 (IQR: 0.91 to 1.629)	1.154 (IQR: 0.801 to 1.41)	0.622
Homogentisate	0.0162 (IQR: 0.0118 to 0.0233)	0.0126 (IQR: 0.0095 to 0.0147)	0.0106 (IQR: 0.0086 to 0.0127)	0.004

Table 35: Sub-group analysis of oesophageal and gastric patients separately.

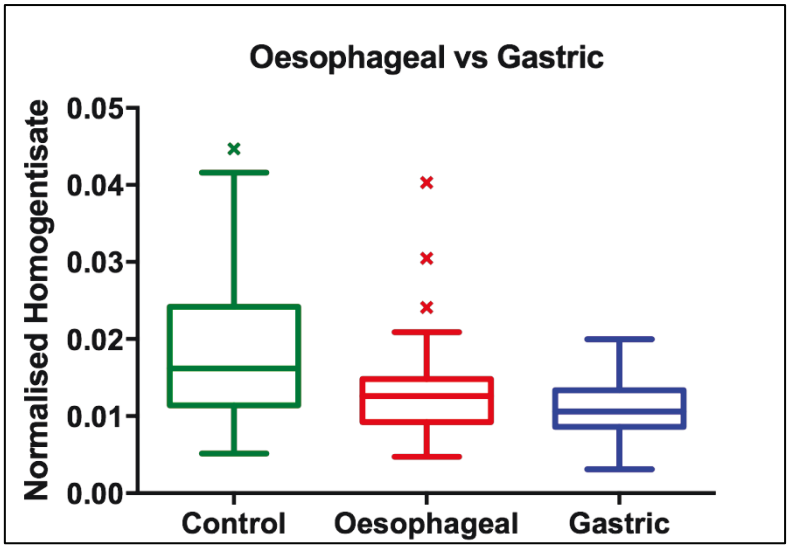


Figure 49: Boxplot of homogentisate normalised peak intensity for oesophageal and gastric adenocarcinoma patients separately.

Disease Stage

Of the cancer cases 11/49 (22%) had T1/2 stage disease, and the remaining 38 (78%) had T3/4 stage disease. Thirty-five patients (71%) had lymph node involvement. Forty-two patients (86%) had no metastatic spread (M0) and 7 patients (14%) had metastatic disease spread at presentation (M1). Results for normalised peak intensity divided by disease stage characteristics are shown below:

	Control (n=37) (N.P.I.)	**T-Stage 1/2 (n=11) (N.P.I.)**	**T-Stage 3/4 (n=18) (N.P.I)**	**Kruskal-Wallis Test**
Phenylalanine	0.837 (IQR: 0.730 to 1.08)	0.711 (IQR: 0.567 to 0.959)	0.697 (IQR: 0.639 to 0.930)	0.034
Tyrosine	1.287 (IQR: 0.909 to 1.686)	0.962 (IQR: 0.749 to 1.319)	1.243 (IQR: 0.860 to 1.673	0.228
Homogentisate	0.0162 (IQR: 0.0118 to 0.0233)	0.0117 (IQR: 0.0083 to 0.0135)	0.0112 (IQR: 0.0092 to 0.0144)	0.005

Table 36: Patients divided by T-stage.

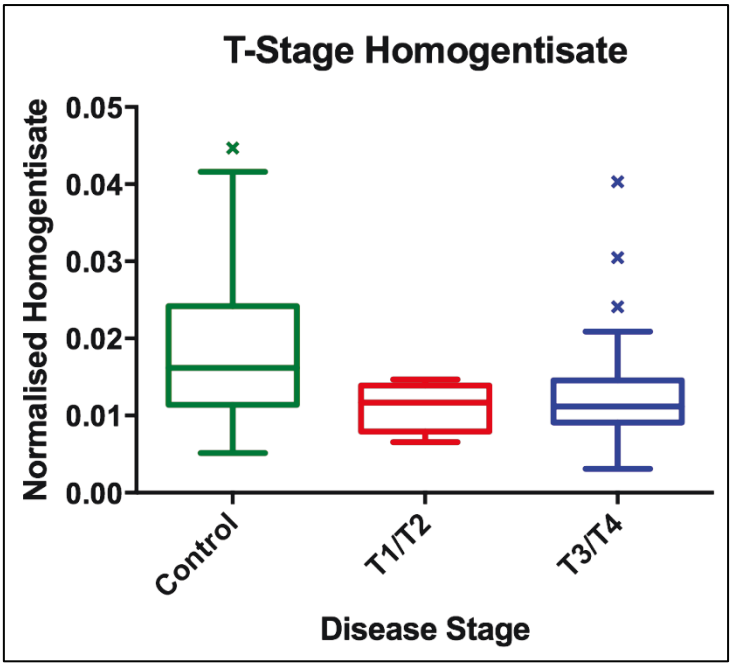


Figure 50: Boxplot of normalised homogentisate intensity for cancer patients divided according to early stage disease (T1/2) or later stage disease (T3/4).

These results showed that changes in phenylalanine and homogentisate peak intensities appeared to be independent of tumour stage. In this relatively small cohort of T1/2 stage cases (n=11) there appeared to be a significant reduction of homogentisate concentration relative to controls in these early stages of disease.

Table 37 provides data for patients subdivided according to the presence or absence of spread to lymph nodes. Table 38 separates patients according to the presence of absence of metastatic spread.

	Control (n=37) (N.P.I.)	**No Nodal Spread (n=14) (N.P.I.)**	**Positive Nodal Spread (n=35) (N.P.I)**	**Kruskal-Wallis Test**
Phenylalanine	0.837 (IQR: 0.730 to 1.08)	0.720 (IQR: 0.600 to 0.940)	0.696 (IQR 0.619 to 0.920)	0.032
Tyrosine	1.287 (IQR: 0.909 to 1.686)	1.051 (IQR: 0.772 to 1.332)	1.232 (IQR 0.872 to 1.717)	0.264
Homogentisate	0.0162 (IQR: 0.0118 to 0.0233)	0.0120 (IQR: 0.0097 to 0.0137)	0.0106 (IQR: 0.0087 to 0.0146)	0.032

Table 37: Patients separated according to the presence or absence of spread to lymph nodes.

	Control (n=37) (N.P.I.)	**M0 (n=11) (N.P.I.)**	**M1 (n=38) (N.P.I)**	**Kruskal-Wallis Test**
Phenylalanine	0.837 (IQR: 0.730 to 1.08)	0.705 (IQR: 0.639 to 0.982)	0.667 (IQR: 0.563 to 0.757)	0.019
Tyrosine	1.287 (IQR: 0.909 to 1.686)	1.21 (IQR: 0.857 to 1.561)	1.010 (IQR: 0.744 to 1.271)	0.385
Homogentisate	0.0162 (IQR: 0.0118 to 0.0233)	0.0115 (IQR: 0.0093 to 0.0140)	0.0089 (IQR: 0.0058 to 0.0174)	0.005

Table 38: Patients divided according to the presence or absence of metastatic spread.

These results demonstrated that the changes in homogentisate and phenylalanine peak intensity appeared to be independent of the presence of absence of lymph node involvement or metastatic disease spread.

3.1.5 Discussion

The results of this study have demonstrated that concentrations of phenylalanine and homogentisate are reduced in oesophago-gastric cancer patients relative to controls. The reduction in homogentisate concentration was more marked than that for phenylalanine. These changes were similar for both oesophageal and gastric cancer cases and seemed to be independent of whether patients had received neo-adjuvant chemotherapy. These changes appeared to occur in early stages of disease with a median normalised peak intensity for homogentisate of 0.0117 in T1/2 stage disease and 0.0122 in T3/4 stage disease (Controls: 0.0162 Kruskal-Wallis test p=0.005).

Malnutrition of the oesophago-gastric cancer patients may have been a contributing factor leading to reduced phenylalanine concentrations in these patients. Due to the obstructive nature of advanced oesophageal cancer up to 79% of patients develop a degree of malnutrition prior to diagnosis[65,66]. Malnourished patients also develop a hypermetabolic state with increased hepatic gluconeogenesis and protein catabolism. Phenylalanine is an essential amino acid which can only be obtained from the diet, and therefore blood concentrations could be influenced by reduced oral intake. However, the results for homogentisate cannot be explained by reduced dietary intake of amino acids alone as the entirety of the aromatic amino acid pathway was not down-regulated. Tyrosine concentrations showed no difference between the groups. Tyrosine is an upstream metabolite from homogentisate in aromatic amino acid breakdown indicating there was dysfunctional metabolism at some point in the breakdown pathway between these two metabolites. This dysregulation would explain the reduced homogentisate concentrations seen here, and normal tyrosine concentrations indicate that malnutrition cannot be the sole contributing factor to these findings. Another factor which indicates that the biological mechanism responsible for these changes is more complex than simply malnutrition is that homogentisate and phenylalanine appeared down-regulated in early stage

disease. At this stage of disease malnutrition would not necessarily have become a significant factor for these patients. However, there were limited numbers of patients in the early stage disease group (T1/2 disease – 11 patients; T3/4 disease – 38 patients) which makes it challenging to draw firm conclusions regarding changes in homogentisate concentration in the early stages of oesophago-gastric cancer from these results.

Phenylalanine hydroxylase activity is known to be dysfunctional in inflammation or malignancy[45,46]. This may provide a potential explanation for reduced phenylalanine concentrations identified here as this enzyme is responsible for conversion of phenylalanine to tyrosine. No detailed investigation of changes in activity of enzymes responsible for aromatic amino acid breakdown has been undertaken in oesophago-gastric cancer patients. Given the results demonstrated here the following sections have undertaken a detailed investigation of enzyme activity with a particular focus upon enzymes related to tyrosine and homogentisate metabolism. These specific enzymes are tyrosine aminotransferase (conversion of tyrosine to hydroxyphenylpyruvate), hydroxyphenylpyruvate dioxygenase (hydroxyphenylpyruvate to homogentisate) and homogentisate 1, 2 dioxygenase (homogentisate to maleylacetoacetate).

In this study all results were normalised to sample haematocrit value using a previously described method[142]. The presence of red blood cells within the matrix significantly affects the spreading/imbibition kinetics of the blood sample upon the porous filter paper[143,144]. Increasing haematocrit concentrations have been shown to result in significantly increased concentrations of amino acids within blood spots[145]. This is believed to be because at low haematocrit the total blood volume needed to fill a given area is smaller than at high haematocrit, due to alterations in droplet spreading. The same study demonstrated that punches taken from the periphery of a blood spot have a higher concentration of amino acids than those taken centrally[145]. In the experiment presented here all punches were taken from the centre of the blood spot to account for this factor.

It was attempted to correlate punch weight to haematocrit value to establish if this could be used as a surrogate for haematocrit. There was no clear correlation between these two factors. It has also been previously demonstrated that sample volume does not influence the weight of punched out disks[146].

Therefore weight does not appear to be a useful measure of haematocrit, or sample volume in dried blood spot analysis. For these reasons all samples in this experiment were normalised to patient haematocrit value rather than punch weight.

Limitations of this study include the fact that it was not possible to identify other intermediary metabolites of aromatic amino acid breakdown using nano-electrospray ionisation mass spectrometry. This means it was not possible to get direct information regarding the concentrations of metabolites immediately upstream (hydroxyphenylpyruvate) and downstream (maleylacetoacetate) from homogentisate. Alterations in the concentration of these metabolites may have helped to more clearly establish the trend in metabolite changes in this section of the aromatic amino acid breakdown pathway. The use of high resolution mass spectrometry means that it was possible to identify the metabolite which corresponds to the same m/z as homogentisate (167.0336 in negative ion mode) with great certainty. Due to the lack of chromatographic separation it was not possible to differentiate this from other compounds with the same chemical composition as homogentisate ($C_8H_8O_4$) and therefore the same exact mass. It was planned to confirm compound identity using liquid-chromatography mass spectrometry from plasma samples collected from the same cohort of patients (which were collected at the same time-point as dried blood spots). However, due to the difficulties with homogentisate measurement in plasma samples (described in Section 2.4) this was not possible.

The control cohort did contain significantly younger patients compared to the cancer cohort (Median age controls 61; Cancer patients 70, MWU p =0.006). Although every effort was made to match control and cancer patients during sample collection this is likely a function of the fact that a large proportion of patients attending for upper gastrointestinal endoscopy are younger than the majority of those being diagnosed with upper gastrointestinal cancer. It was felt necessary to collect samples from endoscopy as it provided direct visualisation of the upper gastrointestinal tract (to confirm if any upper gastrointestinal disease was present) and also provided a convenient, ethically appropriate, time-point for sample collection as many patients would be having an intravenous cannula inserted prior to their endoscopy and would have fasted prior to the investigation. A larger proportion of the cancer cohort suffered with hypertension (likely to also be a function of their increased age) but the groups were otherwise well matched.

3.1.6 Conclusion

This experiment has utilised dried blood spot analysis with nano-electrospray ionisation mass spectrometry to establish that phenylalanine and homogentisate concentrations are lower in oesophago-gastric cancer patients relative to controls.

The results of this experiment were then utilised in the following sections to inform a targeted molecular investigation of the enzymes responsible for aromatic amino acid breakdown, with particular focus upon those directly responsible for homogentisate metabolism.

3.2 In Silico Analysis

3.2.1 Objectives

This section aimed to utilise publically available genome-wide gene profiling expression datasets to establish enzyme targets to account for changes in aromatic amino acid metabolism in oesophago-gastric cancer patients.

3.2.2 Introduction

The previous experiment demonstrated differences in the concentrations of phenylalanine and homogentisate in dried blood spot samples from oesophago-gastric cancer patients compared to controls. This adds to previous evidence from other studies that have identified alterations in aromatic amino acid metabolism in oesophago-gastric cancer patients[147]. However, the biological mechanism responsible for these changes remains unclear.

Prior to beginning targeted biological analysis of enzymes related to this pathway it is necessary to clearly define these biological targets, and establish if there is any difference in gene expression in currently available datasets. In silico analysis of genome-wide gene profiling datasets has been used to establish expression differences in the genes which regulate these enzymes responsible for aromatic amino acid breakdown. Specific enzymes of interest examined using in silico analysis were selected based upon the findings of the previous experiment which identified reduced homogentisate concentrations from the dried blood spot samples of oesophago-gastric cancer patients. Enzymes directly related to homogentisate metabolism include hydroxyphenylpyruvate dioxygenase (responsible for homogentisate production from hyrdroxyphenylpyruvate) and homogentisate 1,2 dioxygenase (responsible for homogentisate breakdown).

3.2.3 Methods

Publically available genome-wide gene profiling expression datasets for oesophago-gastric cancer patients were examined. Only datasets which included oesophageal or gastric adenocarcinoma tissue samples, with control samples consisting of equivalent healthy tissue were included. Three datasets were identified for oesophageal cancer patients[148–150], and two for gastric cancer patients[151,152]. Expression profiling for each of the enzymes related to aromatic amino acid breakdown was evaluated in each dataset for adenocarcinoma and healthy tissues. Relative fold change was calculated for enzymes in each dataset. This would establish changes in enzyme expression in oesophageal and gastric adenocarcinoma within each dataset. Univariate statistical analysis was undertaken using SPSS v23 (IBM, Armonk, NY, USA).

3.2.4 Results

The oesophageal cancer datasets included a total of 104 oesophageal adenocarcinoma tissue samples and 53 normal oesophageal squamous epithelium samples. The gastric cancer datasets included a total of 75 gastric adenocarcinoma tissue samples, with matched areas of healthy gastric mucosa for each sample.

Results of fold change and univariate comparison between the two groups for oesophageal datasets are shown below in table 39. Positive fold change indicates increased gene expression in cancer samples, and negative fold change indicates reduced gene expression in cancer compared to healthy tissues.

	Kim et al[148]		*Wang et al*[149]		*Kimchi et al*[150]	
	Fold Change	**MWU (p)**	**Fold Change**	**MWU (p)**	**Fold Change**	**MWU (p)**
PAH	+0.01	0.010	+1.31	0.405	+1.62	0.130
TAT	+0.01	0.101	+1.13	0.851	+0.05	0.959
HPD	+0.05	0.014	+0.66	0.728	-0.33	0.105
HGD	+0.23	<0.001	+2.14	<0.001	+1.02	0.038
MAAI	-0.02	0.009	+3.42	<0.001	-0.42	0.328
FAH	+0.03	0.008	+70.64	0.294	+0.08	0.798

Table 39: Fold change analysis (relative to normal squamous oesophageal mucosa) for oesophageal adenocarcinoma samples in each relevant dataset.

The most consistent result for oesophageal cancer datasets was up-regulation of homogentisate 1,2 dioxygenase in oesophageal adenocarcinoma samples relative to squamous mucosa. This up-regulation was highly significant in two datasets (MWU p <0.001). Other results were more variable between each of the three datasets, and there was no clear pattern in gene expression for the other enzymes related to this pathway.

Results of fold change and univariate statistical analysis for relevant pathway enzymes in gastric cancer datasets is shown below in table 40.

	Cheng et al[152]		*Holbrook et al*[151]	
	Fold Change	**MWU (p)**	**Fold Change**	**MWU (p)**
PAH	+0.66	0.048	+0.53	0.021
TAT	-0.06	0.167	-0.08	0.726
HPD	-0.02	0.788	+0.20	0.705
HGD	-0.18	0.005	-0.15	0.221
MAAI	-0.08	0.001	-0.27	0.001
FAH	+0.01	0.979	+0.10	0.393

Table 40: Fold change analysis (relative to normal gastric mucosa) for gastric adenocarcinoma samples in each relevant dataset.

These results demonstrated that phenylalanine hydroxylase activity was up-regulated in gastric cancer samples in both datasets. Maleylacetoacetate isomerase was down-regulated significantly in both datasets ($p<0.001$). The change in homogentisate 1,2 dioxygenase in oesophageal cancer datasets appeared to be reversed with a trend towards down-regulation of this enzyme in gastric adenocarcinoma samples ($p = 0.005$ in one dataset).

3.2.5 Discussion

Analysis of these publically available gene expression datasets has demonstrated that homogentisate 1,2 dioxygenase appears to be up-regulated in oesophageal adenocarcinoma samples relative to squamous oesophageal mucosa. This enzyme is responsible for homogentisate breakdown. Up-regulation could lead to increased breakdown of homogentisate and provide a biological explanation for the reduced homogentisate concentrations identified in dried blood spot analysis of oesophageal adenocarcinoma patients in Section 3.1.

The finding of homogentisate 1,2 dioxygenase up-regulation was not replicated in gastric cancer datasets where this enzyme appeared to be down-regulated. Phenylalanine hydroxylase appeared

up-regulated in these gastric adenocarcinoma samples, and maleylacetoacetate isomerase was down-regulated.

3.2.6 Conclusion

Up-regulation of homogentisate 1,2 dioxygenase may provide a biological explanation for reduced homogentisate concentrations found in dried blood spot analysis. This finding was not replicated in gastric cancer datasets, but significant changes to genes relating to other enzymes within this pathway were identified. These changes have been further investigated using quantitative polymerase chain reaction (qPCR) in Section 3.3, and correlated to immunohistochemistry in Section 3.4.

3.3 Quantitative PCR

3.3.1 Objectives

This experiment has utilised reverse transcription quantitative polymerase chain reaction (qPCR) to measure gene expression of enzymes related to aromatic amino acid metabolism in oesophageal cancer cells and oesophageal adenocarcinoma tissue samples. Enzyme activity in cancer tissues has been compared to that for adjacent normal oesophageal squamous mucosa. Gastric adenocarcinoma tissue samples have also been analysed to assess differences between oesophageal and gastric adenocarcinoma.

3.3.2 Introduction

As has been previously described in Section 1.6, aromatic amino acid metabolism is known to be dysfunctional in oesophago-gastric cancer[147]. However, the biological mechanism responsible for these changes remains unknown, and no targeted investigation of the enzymes regulating this metabolic pathway has been previously undertaken. Section 3.1 has identified that homogentisate and phenylalanine concentrations are reduced in the dried blood spots of oesophago-gastric cancer patients. Section 3.2 has used genome profiling datasets to provide a preliminary analysis of gene expression for relevant pathway enzymes. These results have identified potential molecular targets for dysfunctional aromatic amino acid metabolism, in particular homogentisate 1,2 dioxygenase in oesophageal adenocarcinoma. This enzyme is responsible for homogentisate breakdown and up-regulation could provide an explanation for the reduced homogentisate concentrations identified in the dried blood spots of these patients.

This experiment has utilised reverse-transcription qPCR to identify changes in the expression of enzymes responsible for the breakdown of aromatic amino acids. Reverse-transcription PCR works by initially converting RNA extracted from tissue samples into cDNA followed by exponential amplification in a PCR reaction. For qPCR, amplified DNA is fluorescently labelled to facilitate detection and quantification. The qPCR process consists of a series of temperature changes which

are repeated multiple times (thermal cycles). During each cycle initial denaturation of the cDNA double strand occurs at around 95°C. This is followed by primer annealing and cDNA extension. This process is repeated 30-50 times for completion of the PCR process.

In this experimental section qPCR has been used to quantify gene expression of relevant pathway enzymes in squamous oesophageal cells (HET-1A) and oesophageal adenocarcinoma cell lines (OE33 and OE19). This technique was then used to quantify gene expression in oesophageal and gastric adenocarcinoma tissues relative to matched healthy mucosa samples.

3.3.3 Methods

Local ethics committee approval was obtained for this experiment (ICHTB HTA Licence: 12275; REC Wales Approval: 12/WA/0196)

Cell Line Samples

The following commercially available cell lines were utilised for analysis:

i. OE19 (oesophageal adenocarcinoma)
ii. OE33 (oesophageal adenocarcinoma)
iii. HET-1A (normal oesophageal squamous).

Identity of all cell lines was independantly validated prior to analysis. Cells were grown for 72h to 90% confluence. Cells were then tripsinised and centrifuged to produce a cell pellet which was used for RNA extraction.

Tissue Samples

Tissue samples from 36 oesophageal adenocarcinoma patients and 16 gastric adenocarcinoma patients were collected from patients undergoing surgical resection of oesophago-gastric cancer. Matched samples of healthy tissue samples away from the area of the tumour (either squamous oesophageal mucosa or normal gastric mucosa) were collected from patients at the same time-point. Tissue samples were immediately frozen in liquid nitrogen and stored at -80°C prior to analysis.

H&E slides were produced from each tissue sample prior to sample preparation. Tissue types were confirmed with a Consultant Histopathologist prior to analysis.

RNA Purification and cDNA synthesis

Tissue samples or cell pellets were homogenised in TRIzol® (Thermo Fisher Scientific, Waltham, MA, USA) via manual homogenisation followed by being placed in a tissue homogeniser (Retsch, Dusseldorf, Germany) at 25 revolutions per second for 1 minute. Chloroform was then added and samples centrifuged. The supernatant was removed and RNA purified using the RNeasy® kit (Qiagen, Hilden, Germany). cDNA was then produced from these samples using a reverse transcription kit (Qiagen, Hilden, Germany).

cDNA samples were added to a 384-well plate with an appropriate mixture containing SYBR-green® and primers for the relevant enzymes to be examined (Phenylalanine hydroxylase (PAH); Tyrosine aminotransferase (TAT); Hydroxyphenylpyruvate dioxygenase (HPD); Homogentisate 1,2 dioxygenase (HGD); Maleylacetoacetate isomerase (MAAI); Fumarylacetoacetate hydrolase (FAH) - All Qiagen, Hilden, Germany). qPCR was performed using an Applied Biosystems 7900HT instrument (Applied Biosystems, Foster City, CAL, USA) to establish the cycle-time to reach the relevant threshold value. Inter-plate controls were analysed with all samples. The intitial thermal cycling programme consisted of 50°C for 2 minutes, followed by 10 minutes at 95°C to prepare primers. The thermal cycler then completed 40 cycles of 95°C for 15 seconds followed by 1 minute at 60°C. House-keeper genes (GAPDH and HPRT1) were analysed for each sample and all results normalised to these threshold values.

Results were expressed as fold change for cancer tissues or cell samples relative to the result for the matched healthy mucosa from the same patient or HET-1A cells. A fold change result above one represented up-regulation in cancer tissues and below one represented down-regulation. A siginificant fold change result is generally considered a fold change greater than 5 or below 0.2. Results from cancer and healthy mucosa were also analysed as expression per 1000 GAPDH to facilitate univariate statistical analysis using SPSS v23 (IBM, Armonk, NY, USA).

3.3.4 Results

Cell Line Analysis

Fold change in enzyme acitivity for OE33 and OE19 cell lines (relative to HET-1A cells) is shown below in table 41 and figure 51. Fold change of one indicates expression equivalent to that for HET-1A cells. Fold change above one indicates overexpression and below one indicates downregulation of expression.

Enzyme	**OE33 Fold Change relative to HET1A**	**OE19 Fold Change relative to HET1A**
PAH	1.67	0.33
TAT	0.43	0.39
HPD	0.0029	0.00081
HGD	11.05	390.23
MAAI	0.06	0.15
FAH	0.78	0.18

Table 41: Fold change for OE33 and OE19 cells relative to HET1A.

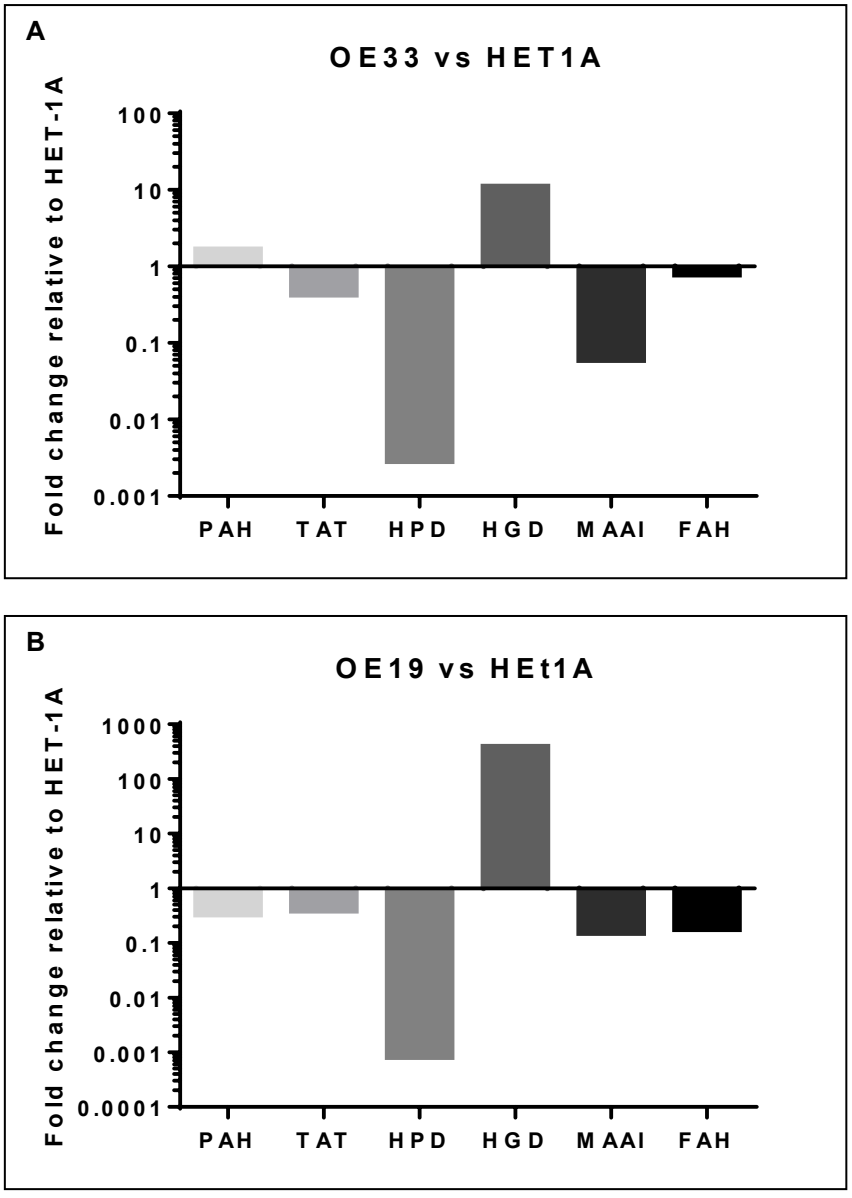


Figure 51: Fold change in OE33 (A) and OE19 (B) cell enzyme activity expressed relative to HET-1A cell enzyme activity. PAH – Phenylalanine hydroxylase; TAT – tyrosine aminotransferase; HPD – 4-Hydroxyphenylpyruvate dioxygenase; HGD – Homogentisate 1,2 dioxygenase; MAAI – maleylacetoacetate isomerase; FAH – fumarylacetoacetate isomerase.

These results demonstrate a large reduction in 4-hydroxyphenylpyruvate dioxygenase activity in both oesophageal cancer cells lines compared to the normal squamous cell line. This was an over 1000-fold reduction in the OE19 cell line (fold change 0.0008). There was also a significant increase in homogentisate 1,2 dioxygenase activity in both oesophageal cancer cell lines relative to normal

oesophageal squamous cells (HET-1A) (Fold change 390.23 for OE19 cells and 11.05 in the OE33 cells).

Oesophageal Cancer Tissue Samples

Tissue samples from 36 oesophageal adenocarcinoma patients were analysed and compared to results from matched healthy oesophageal squamous mucosa samples from the same patient.

The median age of these patients was 64.5 and 75% were male. Thirty six percent (13/36) had T1/2 stage disease and 64% (23/36) had stage T3/4 disease. Sixty-six percent had disease spread to lymph nodes.

Results of fold change analysis are shown below in table 42.

Enzyme	Median Fold Change	IQR
PAH	17.74	3.05 – 103.48
TAT	3.24	1.08 – 10.63
HPD	0.42	0.052 – 3.14
HGD	62.96	11.84 – 1860.95
MAAI	0.70	0.32 – 1.05
FAH	0.86	0.51 – 1.94

Table 42: Details of qPCR fold-change results for oesophageal adenocarcinoma patients.

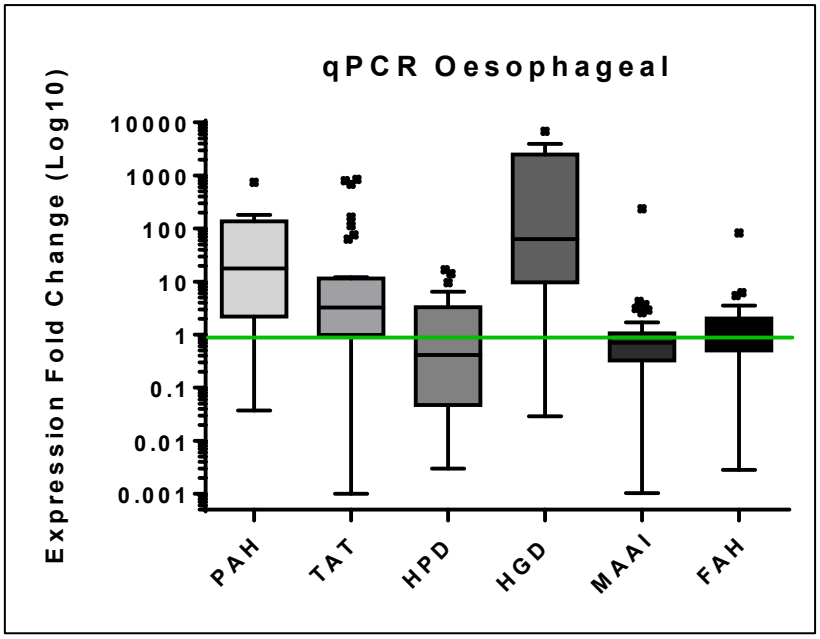


Figure 52: Boxplot of relative fold change for each enzyme. The green line represents a value of 1 indicating expression of normal mucosa for that enzyme relative to which cancer sample fold change was calculated.

These results have demonstrated a clear up-regulation in homogentisate 1,2 dioxygenase activity within oesophageal adenocarcinoma tissues (fold change 62.96). There was also an increase in phenylalanine hydroxylase activity in these tissues (fold change 17.74). There was a trend towards an increase in tyrosine aminotransferase activity (fold change 3.24) and decrease in hydroxyphenylpyruvate dioxygenase activity (fold change 0.42).

Analysis of this data according to median expression per 1000 GAPDH (which facilitated univariate statistical analysis) is shown below in table 43.

Enzyme	Normal oesophageal mucosa (Median copies /1000 GAPDH)	Oesophageal adenocarcinoma (Median copies/1000 GAPDH)	MWU
PAH	0.02 (IQR 0.00 – 0.11)	0.17 (IQR 0.02 – 0.61)	<0.0001
TAT	0.61 (IQR 0.08 – 17.54)	3.05 (IQR 0.54 – 45.76)	0.032
HPD	0.9 (IQR 0.02 – 0.24)	0.03 (IQR 0.01 – 0.18)	0.324
HGD	0.06 (IQR 0.02 – 0.14)	5.72 (IQR 0.92 – 52.56)	<0.0001
MAAI	12.3 (IQR 7.89 – 28.71)	12.09 (IQR 6.81 – 27.62	0.770
FAH	3.99 (IQR 1.32 – 5.85)	3.23 (IQR 1.81 – 6.62)	0.551

Table 43: Normal oesophageal mucosa and oesophageal adenocarcinoma results presented as expression per 1000 GAPDH.

These results confirmed that the up-regulation in homogentisate 1,2 dioxygenase activity was highly statistically significant ($p<0.0001$). Up-regulation of phenylalanine hydroxylase and tyrosine aminotransferase was also significant.

Gastric Cancer Tissue Samples

Tissue samples from 17 gastric adenocarcinoma patients were analysed along with matched healthy gastric mucosa for comparison.

The median age was 71 and 41% were male (7/17). Twenty four percent (4/17) had T1/2 disease and 71% (12/17) had stage T3/4 disease. Nine patients (53%) had lymph node involvement.

Results of relative fold change in gastric adenocarcinoma tissues (compared to healthy gastric mucosa) for each enzyme are shown below in table 44.

Enzyme	Median Fold Change	IQR
PAH	5.47	0.07 – 55.93
TAT	0.97	0.60 – 13.40
HPD	0.21	0.09 – 0.28
HGD	0.32	0.13 – 0.70
MAAI	0.29	0.17 – 0.59
FAH	0.38	0.29 – 0.96

Table 44: Relative fold change results for gastric adenocarcinoma tissue compared to healthy gastric mucosa.

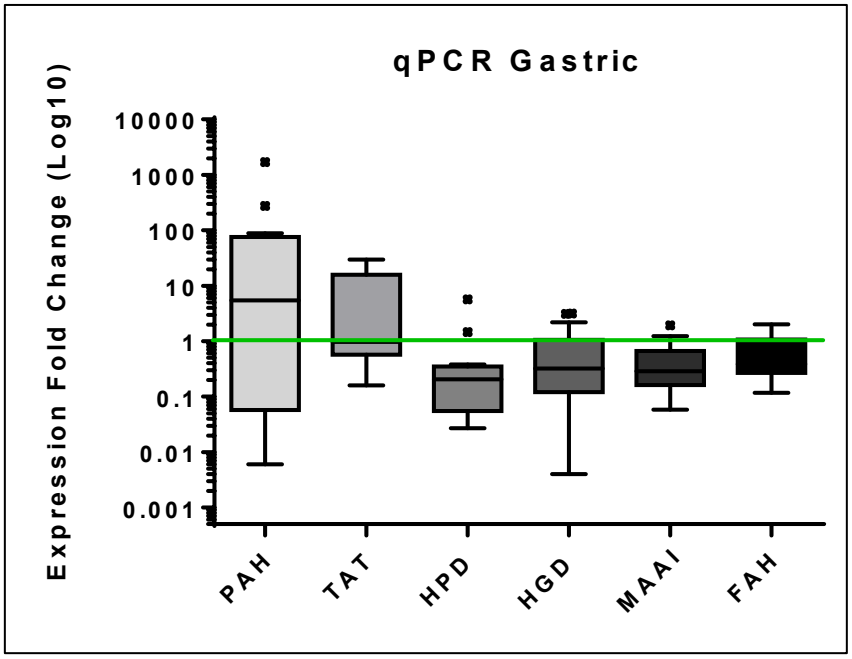


Figure 53: Boxplot of relative fold change for each enzyme related to aromatic amino acid breakdown.

These results have demonstrated that hydroxyphenylpyruvate dioxygenase appears down-regulated in gastric cancer. There also appears to be a trend towards down-regulation of homogentisate 1,2 dioxygenase (up-regulated in oesophageal adenocarcinoma), maleylacetoacetate isomerase and fumarylacetoacetate isomerase.

Results for gastric normal mucosa and adenocarcinoma tissues presented as median expression per 1000 GAPDH are shown in table 45.

Enzyme	Normal gastric mucosa (Median/1000 GAPDH)	Gastric adenocarcinoma (Median/1000 GAPDH)	MWU
PAH	0.21 (IQR 0.02 – 1.09)	0.33 (IQR 0.06 – 1.27)	0.474
TAT	0.93 (IQR 0.71 – 2.81)	5.36 (IQR 0.69 – 16.57)	0.205
HPD	0.40 (IQR 0.14 – 0.64)	0.07 (IQR 0.03 – 0.18)	0.049
HGD	118.67 (IQR 80.88 – 191.71)	47.93 (IQR 17.85 – 92.72)	0.005
MAAI	70.511 (IQR 42.22 – 92.21)	28.62 (IQR 11.37 – 37.66)	<0.001
FAH	9.36 (IQR 5.27 – 13.45)	4.31 (IQR 3.14 – 5.62)	0.004

Table 45: Normal gastric mucosa and gastric adenocarcinoma results presented as expression per 1000 GAPDH.

These results demonstrate that although down-regulation of hydroxyphenylpyruvate dioxygenase activity was statistically significant, this was borderline (p = 0.049). There was statistically significant down-regulation of all enzymes downstream to homogentisate in this pathway (homogentisate 1,2 dioxygenase, maleylacetoacetate isomerase and fumarylacetotacetate isomerase).

Comparison of Homogentisate 1,2 Dioxygenase Activity in Oesophageal and Gastric Cancer

Representative boxplots of homogentisate 1,2 dioxygenase activity in normal and cancer tissues for both oesophageal and gastric cancer are shown in figure 54.

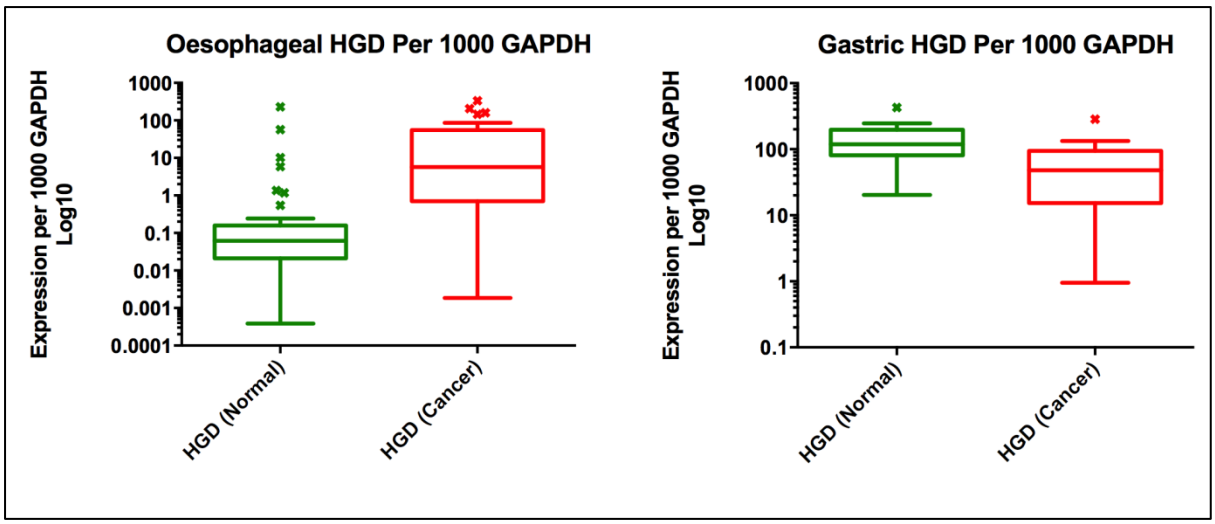


Figure 54: Homogentisate 1,2 dioxygenase activity in oesophageal and gastric tissues demonstrated contrasting findings with up-regulation in oesophageal cancer and down-regulation in gastric cancer.

3.3.5 Discussion

Findings from qPCR of oesophageal cancer patients has confirmed results of in silico analysis with significant up-regulation of homogentisate 1,2 dioxygenase (fold change 62.96, MWU $p<0.0001$ when analysed per 1000 GAPDH). This correlated with findings in oesophageal cell lines where homogentisate 1,2 dioxygenase was up-regulated. This change in homogentisate 1,2 dioxygenase activity was reversed in gastric cancer patients where it was down-regulated (fold change 0.32, MWU $p=0.049$). This also mirrored the results predicted from in silico analysis.

Other findings from oesophageal cancer patients included a significantly increased fold change for phenylalanine hydroxylase activity (fold change 17.74, MWU $p <0.001$). However, this result appeared to be largely driven by very low gene expression within normal tissues (only 0.02 per 1000 GAPDH, with lack of any amplification in many samples) and expression in adenocarcinoma tissues was also low (0.17 per 1000 GAPDH).

Therefore this result must be interpreted cautiously. Tyrosine aminotransferase was also up-regulated in oesophageal cancer patients (fold change 3.24, MWU $p = 0.032$).

Results from gastric cancer patients demonstrated down-regulation of hydroxyphenylpyruvate dioxygenase. This enzyme is responsible for homogentisate production and provides a potential alternate explanation for reduced homogentisate in dried blood spot samples from these patients. Also of note is that there was down-regulation of all enzymes regulating aromatic amino acid breakdown downstream to homogentisate in gastric cancer patients. This may indicate a complete breakdown of the enzymatic pathway in this area. Unfortunately as it was not possible to measure any metabolites downstream to homogentisate using nano-electrospray ionisation mass spectrometry it is not possible to identify how these changes in enzyme expression relate to systemic concentrations of these metabolites.

3.3.6 Conclusions

This experiment has demonstrated significant changes in gene expression relating to enzymes which regulate aromatic amino acid breakdown in oesophageal and gastric cancer. Results have demonstrated up-regulation of the enzyme responsible for homogentisate breakdown (homogentisate 1,2 dioxygenase) in oesophageal cancer patients. This enzyme was down-regulated in gastric cancer patients but the enzyme responsible for homogentisate production (hydroxyphenylpyruvate dioxygenase) was also down-regulated. This indicates there may be an alternative biological mechanism to explain the finding of reduced homogentisate in blood spot analysis for oesophageal and gastric cancer patients.

3.4 Immunohistochemistry

3.4.1 Objectives

Immunohistochemistry has been performed on oesophageal and gastric adenocarcinoma tissues for the relevant enzymes responsible for breakdown of aromatic amino acids in order to provide further information regarding the functional expression of these enzymes within tissues. This experiment aimed to cross-validate the findings of qPCR in Section 3.3.

3.4.2 Introduction

The previous experimental sections have established that homogentisate concentrations are reduced in dried blood spots of oesophago-gastric cancer patients, and have identified a potential biological mechanism to explain this finding in oesophageal and gastric cancer.

In order to ascertain how these genetic changes affect protein expression in tissues it was necessary to cross-validate these findings using immunohistochemistry. This aimed to provide further insight into the biological mechanism responsible for dysfunctional aromatic amino acid metabolism in oesophageal and gastric cancer patients.

3.4.3 Methods

Local ethical approval was granted for this experiment through the Histopathology Department at St Mary's Hospital, Imperial College London.

Immunohistochemistry antibodies were obtained for each enzyme of interest (tyrosine aminotransferase (Rabbit monoclonal antibody), hydroxyphenylpyruvate dioxygenase (Rabbit monoclonal antibody), homogentisate 1,2 dioxygenase (Rabbit monoclonal antibody), and fumarylacetoacetate isomerase (Rabbit polyclonal antibody) (All Abcam, Cambridge, UK),

phenylalanine hydroxylase, (Rabbit polyclonal antibody; Sigma Aldrich, Gillingham, Dorset, UK) and maleylacetoacetate isomerase (Mouse monoclonal antibody; Santa Cruz Biotech, Dallas California). Suitability of each antibody was tested upon appropriate positive control samples (kidney or liver tissue samples depending on antibody).

Hemotoxylin and eosin staining was performed for each section being used for immunohistochemistry staining and all slides were reviewed by a Consultant Histopathologist to confirm areas of cancer and healthy tissue. Areas of normal tissue within the same slide were used as controls for immunohistochemistry scoring.

Following immunohistochemistry areas of cancer and normal tissue for each slide had an H-score calculated to give a total maximum score of 300[153]. This scoring method was performed by scoring areas of the slide according to staining intensity relating to 0 (negative), 1 (weak), 2 (intermediate) and 3 (strong staining). The average percentage area of each staining intensity was calculated and the following formula applied:

IHA H-Score = (% of cells at intensity category 1x1) + (% of cells at intensity category 2 x 2) + (% of cells at intensity category 3 x 3).

An H-score of 0 – 300 was then obtained where 300 was equal to 100% of tumour cells staining strongly.

3.4.4 Results

The following sample numbers were analysed for each enzyme of interest:

- Phenylalanine hydroxylase: n = 19 (14 oesophageal, 5 gastric).
- Tyrosine aminotransferase: n = 37 (30 oesophageal, 7 gastric).
- Hydroxyphenylpyruvate dioxygenase: n = 38 (30 oesophageal, 8 gastric).
- Homogentisate 1,2 dioxygenase n =37 (29 oesophageal, 9 gastric).
- Maleylacetoacetate isomerase n = 17 (8 oesophageal, 9 gastric).
- Fumarylacetoacetate isomerase n = 17 (8 oesophageal, 9 gastric).

Oesophageal Cancer

Representative staining for each enzyme in oesophageal cancer is shown in figure 55.

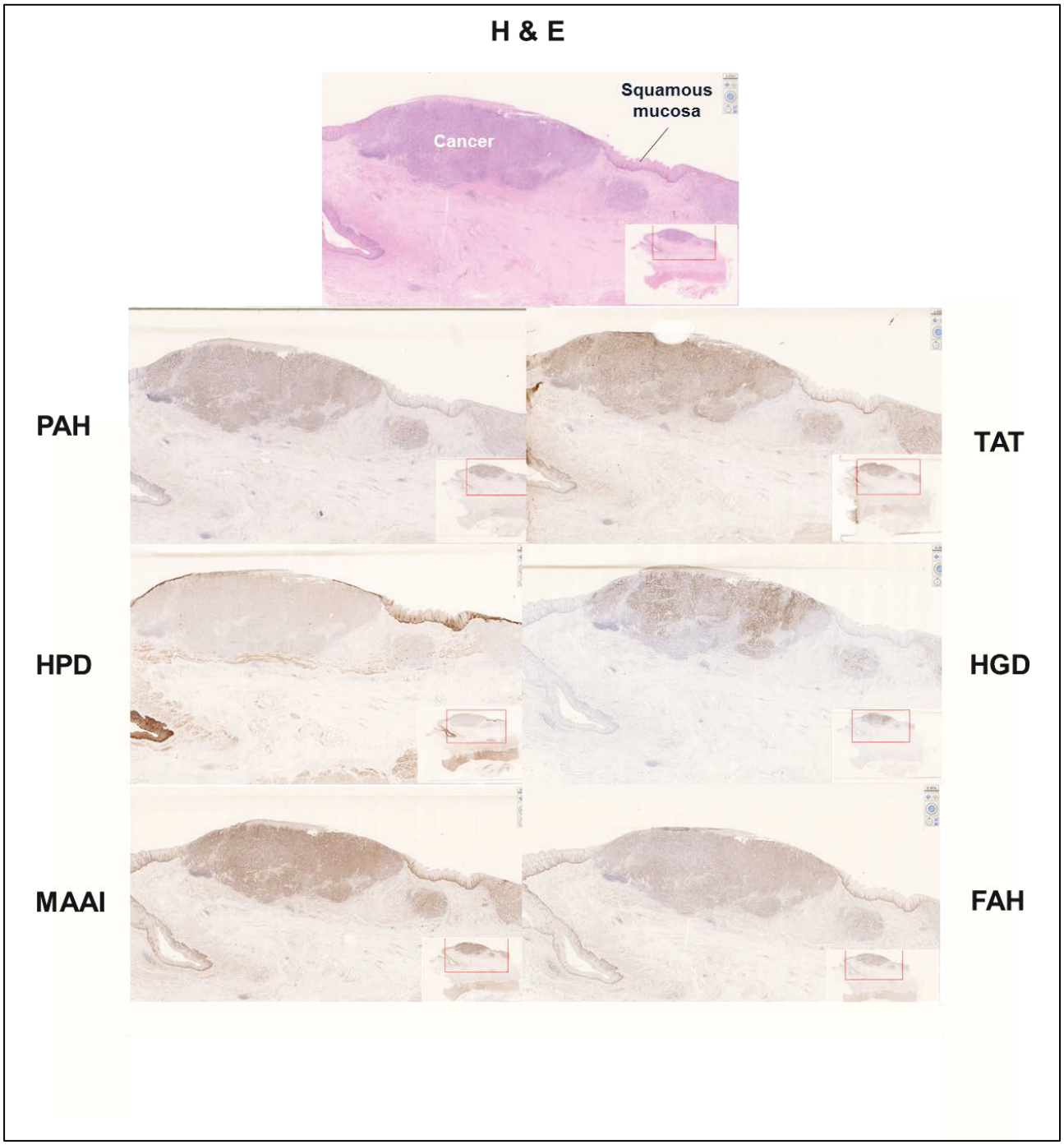


Figure 55: Representative staining for each enzyme in an oesophageal cancer case.

H-score results for oesophageal cases are shown in table 46:

Enzyme	Normal oesophageal mucosa (Median H-Score)	Oesophageal adenocarcinoma (Median H-Score)	MWU
PAH (n=14)	25 (IQR 0 – 105)	80 (IQR 22.5 – 120)	0.252
TAT (n=30)	42.5 (IQR 0 – 67.5)	177.5 (IQR 106.25 – 240)	<0.001
HPD (n=30)	132.5 (IQR 100 – 185)	42.5 (IQR 25 – 73.75)	<0.001
HGD (n=29)	0 (IQR 0)	100 (IQR 40 – 160)	<0.001
MAAI (n=8)	140 (IQR 105 – 155)	175 (IQR 131 – 200)	0.281
FAH (n=8)	105 (57.5 – 130)	145 (50 – 165)	0.574

Table 46: H-score assessment of each enzyme in normal oesophageal mucosa and oesophageal adenocarcinoma.

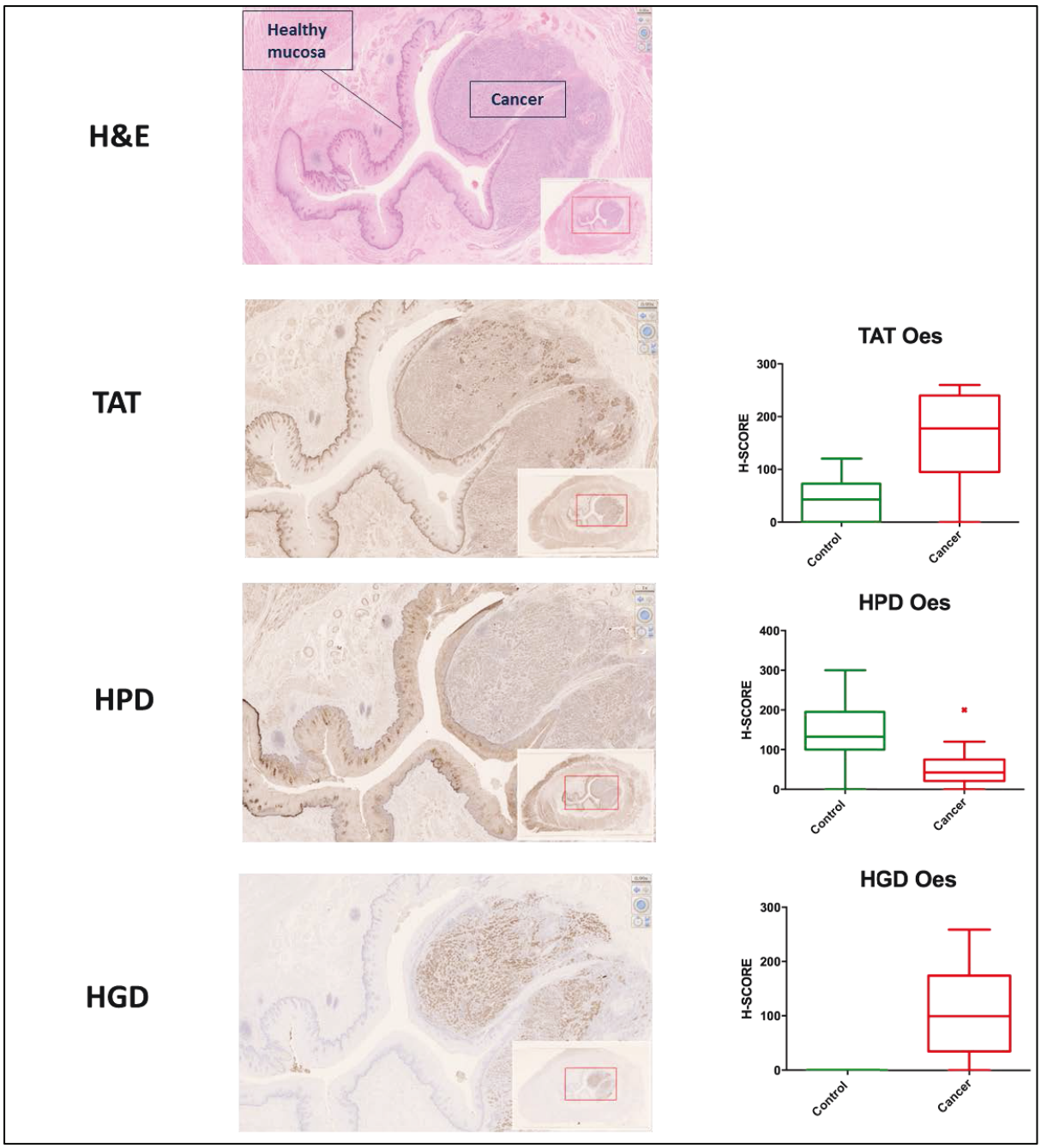


Figure 56: Boxplots of H-score for TAT, HPD and HGD in oesophageal cancer with representative staining.

These results demonstrated up-regulation of tyrosine aminotransferase and homogentisate 1,2 dioxygenase in cancer tissues. There was no expression of homogentisate 1,2 dioxygenase in normal squamous mucosa, but staining was present in 26/29 oesophageal adenocarcinoma samples. There was also reduced staining of hydroxyphenylpyruvate dioxygenase in areas of oesophageal adenocarcinoma.

Gastric Cancer

Gastric mucosa demonstrated large amounts of non-specific staining. This lead to intense staining that did not represent enzyme expression but rather non-specific staining. Results were therefore interpreted with great care, and in many slides there was no normal mucosa for comparison due to the large amount of non-specific staining.

H-score results for gastric cancer cases are shown in table 47:

Enzyme	**Normal gastric mucosa (Median H-Score)**	**Gastric adenocarcinoma (Median H-Score)**	**MWU**
PAH (n=5)	15 (IQR 0 – 53.75)	0 (IQR 0 – 50)	0.905
TAT (n=7)	80 (IQR 75 – 85)	140 (IQR 117.5 – 185)	0.222
HPD (n=8)	90 (IQR 85 – 105)	30 (IQR 15 – 42.5)	0.024
HGD (n=9)	40 (IQR 15 – 105)	80 (IQR 0 – 160)	1
MAAI (n=9)	110 (IQR 100 – 140)	140 (IQR 120 – 200)	0.414
FAH (n=9)	80 (IQR 60 – 140)	175 (IQR 117.5 – 210)	0.482

Table 47: H-Score assessment of each enzyme in normal gastric mucosa and gastric adenocarcinoma

The only significant result in gastric cancer tissues was reduced expression of hydroxyphenylpyruvate dioxygenase in gastric cancer tissues relative to normal gastric mucosa (MWU p = 0.024).

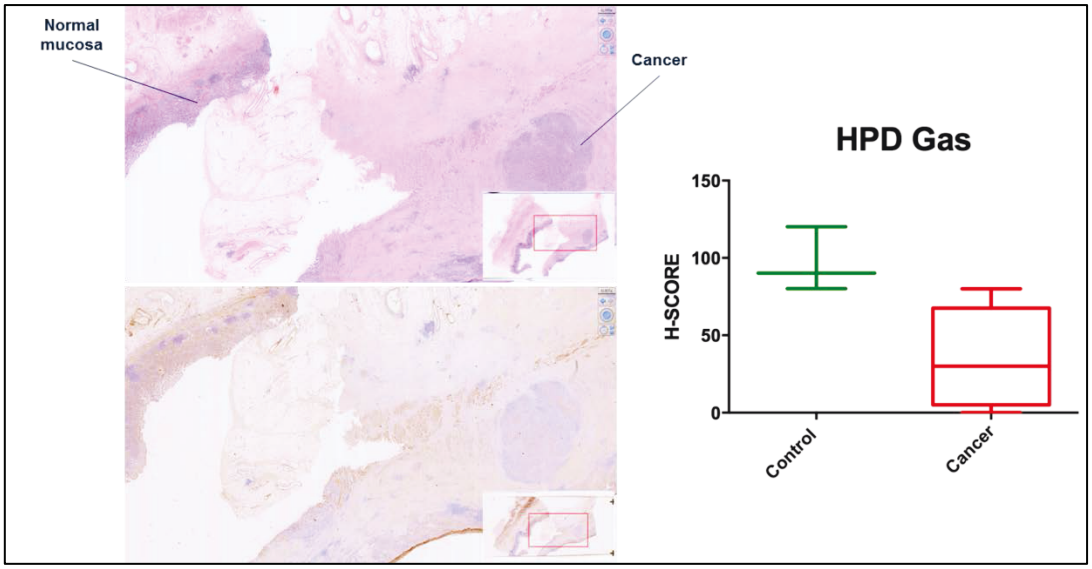


Figure 57: Boxplot of HPD in gastric cancer with representative staining.

3.4.5 Discussion

Immunohistochemistry analysis has validated the findings of previous in silico and qPCR analysis by identifying increased homogentisate 1,2 dioxygenase activity in oesophageal cancer tissues. There was no staining for homogentisate 1,2 dioxygenase in any normal oesophageal mucosa samples whereas staining was present in 26/29 oesophageal adenocarcinoma samples. Immunohistochemistry also revealed increased activity of tyrosine aminotransferase in oesophageal adenocarcinoma, which correlated well with qPCR findings. An additional finding from immunohistochemistry was significantly reduced staining of hydroxyphenylpyruvate dioxygenase in oesophageal adenocarcinoma. In qPCR this enzyme was down-regulated (fold change 0.42) but this result was not statistically significant. In immunohistochemistry the median H-score for hydroxyphenylpyruvate dioxygenase in normal oesophageal mucosa was 132.5 compared to 42.5 in adenocarcinoma tissues (MWU p <0.0001). A correlation between immunohistochemistry and qPCR results for each enzyme related to aromatic amino acid breakdown is shown below in figure 58.

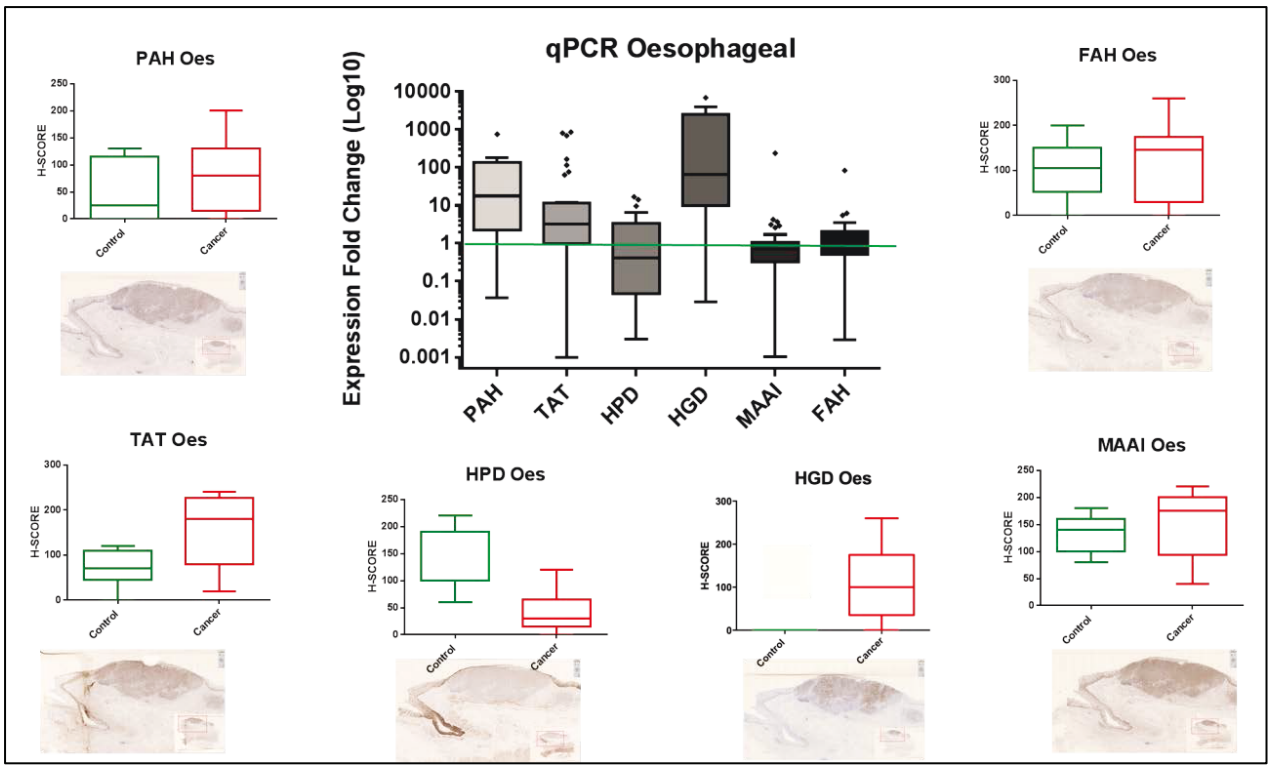


Figure 58: Correlation between qPCR fold change results and immunohistochemistry H-score analysis for each relevant enzyme in oesophageal cancer. Representative staining is also presented.

Findings of immunohistochemistry in gastric cancer samples were more challenging to interpret due to non-specific staining of gastric normal mucosa. This is a known issue for immunohistochemistry of gastrointestinal tract tissues[154]. However, these results still demonstrated that hydroxyphenylpyruvate dioxygenase was down-regulated in cancer samples compared to controls (H-Score 30 vs 90 respectively; MWU p=0.024). This correlated well with qPCR findings in gastric cancer patients where this enzyme was also found to be down-regulated (Fold change 0.21; MWU p=0.049). A correlation between immunohistochemistry and qPCR results for each enzyme in gastric cancer patients is shown in figure 59:

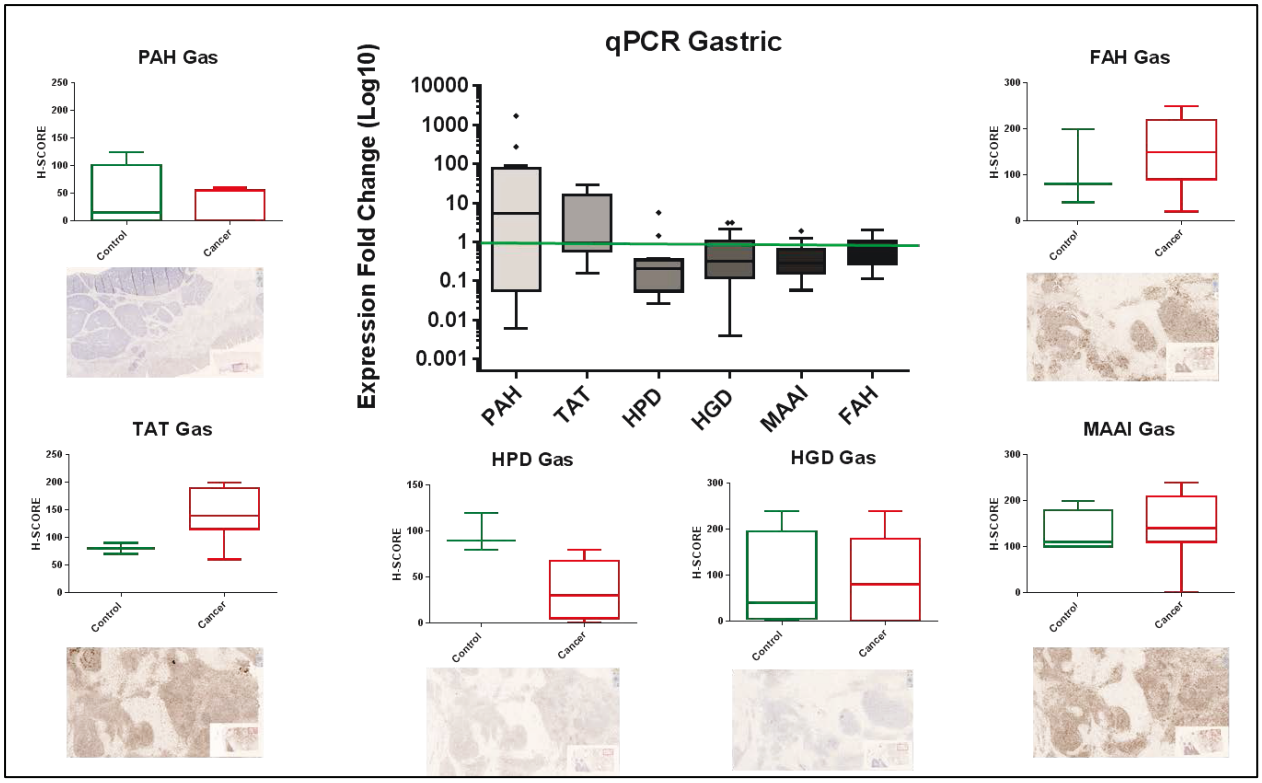


Figure 59: Correlation between qPCR fold change results and immunohistochemistry H-score analysis for each relevant enzyme in gastric cancer. Representative staining also presented.

3.4.6 Conclusions

Immunohistochemistry has validated findings of qPCR in oesophageal cancer patients with up-regulation of homogentisate 1,2 dioxygenase and tyrosine aminotransferase. Immunohistochemistry also identified that hydroxyphenylpyruvate dioxygenase appeared to be down-regulated in oesophageal cancer tissues.

In gastric cancer tissues the qPCR finding of down-regulation of hydroxyphenylpyruvate dioxygenase activity in cancer was also cross-validated in immunohistochemistry. The down-regulation of other enzymes identified as down-regulated by qPCR in gastric tissues (homogentisate 1,2 dioxygenase, maleylacetoacetate isomerase, and fumarylacetoacetate hydrolase) was not confirmed with immunohistochemistry.

3.5 Conclusions of Amino Acid Experimental Section

These experiments have utilised dried blood spot analysis to identify metabolic changes related to aromatic amino acid breakdown in oesophago-gastric cancer patients. This information has guided a targeted molecular investigation of this metabolic pathway using qPCR and immunohistochemistry. This methodology of using metabolic data to inform an investigation of specific biological pathways has recently been suggested as a novel use for metabonomic data which may provide greater insight into mechanisms of disease[155].

A summary of the findings of this experimental section in oesophageal and gastric cancer is presented in figure 60 and 61:

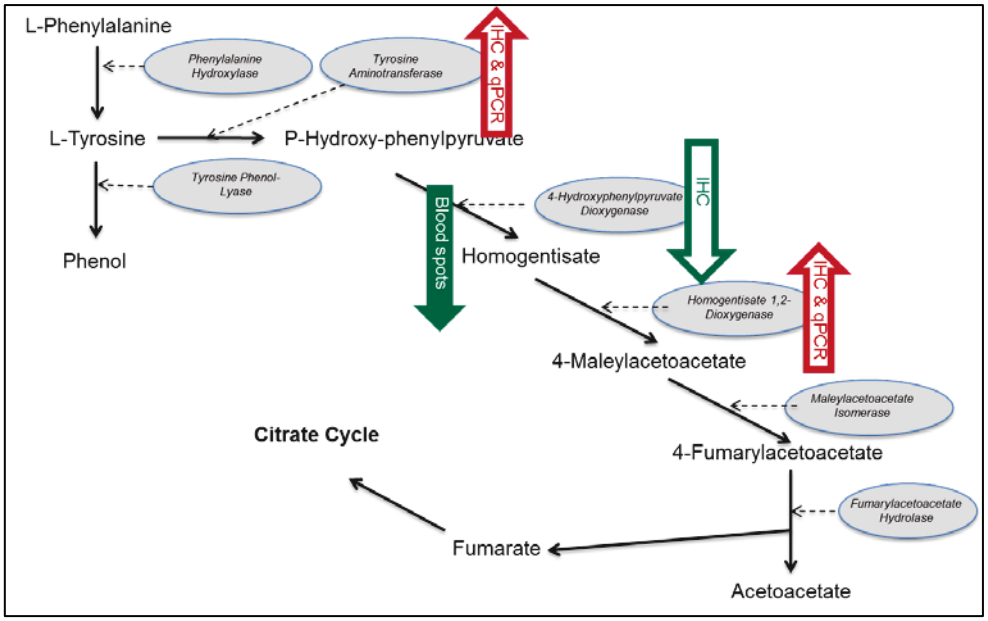


Figure 60: Findings in oesophageal cancer patients with reduced phenylalanine and homogentisate on dried blood spot analysis. Tyrosine aminotransferase and homogentisate 1,2 dioxygenase were up-regulated in qPCR and immunohistochemistry and hydroxyphenylpyruvate dioxygenase down-regulated on immunohistochemistry.

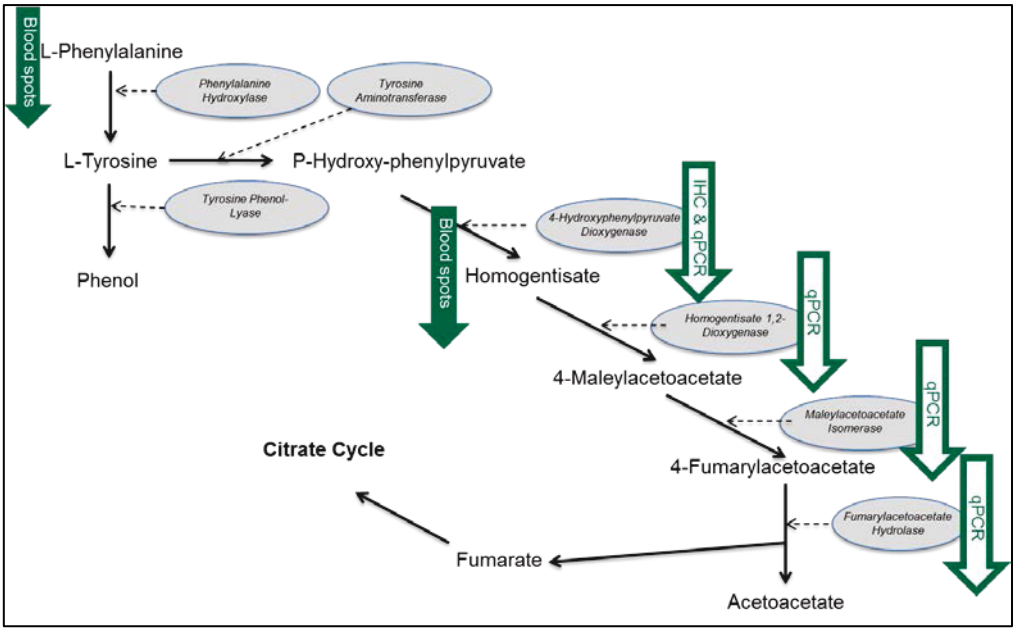


Figure 61: Gastric cancer patients also had reduced phenylalanine and homogentisate on dried blood spot analysis. All pathway enzymes after hydroxyphenylpyruvate dioxygenase were down-regulated on qPCR but this was only cross-validated in hydroxyphenylpyruvate dioxygenase on immunohistochemistry.

These overall findings provide alternate potential explanations for reduced homogentisate concentrations in oesophageal and gastric cancer patients (Median normalised homogentisate peak intensity: Control – 0.0162; Oesophageal cancer – 0.0126; Gastric cancer – 0.0106; Kruskal Wallis Test p=0.004).

In oesophageal cancer patients it seems that up-regulation of homogentisate 1,2 dioxygenase is likely to be the greatest contributing factor leading to reduced homogentisate concentrations. This enzyme is responsible for homogentisate breakdown and was up-regulated in both qPCR (Fold change 62.96, MWU p<0.001) and immunohistochemistry (H-score 100 in cancer samples vs 0 in normal oesophageal mucosa (MWU p<0.001)). Although this appears to be the strongest contributing factor to reduced homogentisate concentrations in these patients, down-regulation of hydroxyphenylpyruvate dioxygenase may also play a role. This enzyme is responsible for homogentisate production. There was a trend towards down-regulation of this enzyme on qPCR (fold change 0.42) but this was not significant. However, immunohistochemistry revealed strong down-regulation of this enzyme in oesophageal cancer tissues (median H-score in normal oesophageal mucosa was 132.5 compared to 42.5 in adenocarcinoma tissues (MWU p <0.0001). Therefore the biological mechanism responsible for reduced homogentisate concentrations in dried blood spot analysis appears to be multi-factorial. There are multiple relevant changes to the section of this metabolic pathway relating to homogentisate production and breakdown in oesophageal cancer patients.

In gastric cancer patients, homogentisate 1,2 dioxygenase was down-regulated in qPCR analysis. Therefore, it does not seem that increased breakdown of homogentisate by this enzyme is responsible for the finding of reduced homogentisate in gastric cancer as is the case in oesophageal cancer. However, the enzyme responsible for homogentisate production (hydroxyphenylpyruvate dioxygenase) was down regulated in qPCR (Fold change 0.21; MWU p=0.049), and immunohistochemistry for these gastric cancer patients (H-Score: Cancer - 30; Control - 90; MWU p=0.024). This indicates that reduced production of homogentisate from hydroxyphenylpyruvate is likely the predominant factor influencing reduced homogentisate concentrations in gastric cancer. qPCR also demonstrated significant down-regulation of homogentisate 1,2 dioxygenase,

maleylacetoacetate isomerase and fumarylacetoacetate hydrolase, which may indicate complete dysregulation of this metabolic pathway downstream to homogentisate. However, these findings were not cross-validated with immunohistochemistry.

In addition to reduced homogentisate concentrations, dried blood spot analysis also identified reduced concentrations of phenylalanine (Median normalised phenylalanine peak intensity: Control – 0.837; Cancer – 0.698; MWU p=0.009). The enzyme responsible for conversion of phenylalanine to tyrosine (phenylalanine hydroxylase) was up-regulated in qPCR for oesophageal adenocarcinoma patients (fold change 17.74, MWU p <0.001). However, it was felt this result was likely due to complete absence of enzyme activity in normal oesophageal tissues, and this enzyme was not found to be significantly upregulated using immunohistochemistry (Median H-score: Squamous oesophageal mucosa – 25; Oesophageal adenocarcinoma – 80; MWU p=0.252). This indicates that there is no clear enzymatic explanation for reduced phenylalanine concentrations in oesophago-gastric cancer.

The primary aim of this experimental section was to establish whether changes in amino acid metabolism (in particular tyrosine) could be related to increased phenol production identified in the exhaled breath and urine of oesophago-gastric cancer patients[25,26]. This primarily relates to direct conversion of tyrosine to phenol via the action of *tyrosine phenol lyase*[42]. There was no significant increase in tyrosine concentrations in dried blood spot analysis (median normalised tyrosine peak intensity: Control - 1.287; Cancer – 1.167; MWU p=0.355). Increased tyrosine concentrations would have potentially led to more tyrosine being released into the gastric content to be acted upon by *tyrosine phenol-lyase* to produce phenol. However, this does not necessarily indicate that the two pathways are not related. Oesophageal cancer patients demonstrated significant up-regulation of tyrosine aminotransferase in qPCR (Fold change 3.24, MWU p=0.032) and immunohistochemistry (Median H-score: Squamous oesophageal mucosa – 42.5; Oesophageal adenocarcinoma – 177.5 (MWU p<0.001). This enzyme converts tyrosine to hydroxyphenylpyruvate and increased activity of this would lead to increased quantities of tyrosine entering this metabolic pathway of tyrosine breakdown. Given that there was no difference in tyrosine concentration between cancer and control groups (rather than reduced tyrosine as would be expected with increased tyrosine aminotransferase

activity), this may indicate that there is surplus tyrosine which may also be released by the tumour into the gastrointestinal tract and acted upon by *tyrosine phenol lyase* to produce phenol.

The relationship between phenol metabolism and tyrosine breakdown has been investigated further in the next experimental section.

CHAPTER 4 - PHENOL METABOLISM IN OESOPHAGO-GASTRIC CANCER

4.1 Urine GC-MS

4.1.1 Objective

This experiment aimed to establish changes in urinary phenol and cresol concentration in relation to oesophago-gastric cancer.

4.1.2 Introduction

Phenol and cresol have previously been proposed as urinary markers of gastrointestinal cancer[26,67,84,85]. Previous studies investigating oesophago-gastric cancer have identified that phenol concentrations were significantly lower within the urine of oesophago-gastric cancer patients when measured using SIFT-MS[26]. Urinary phenol has also been investigated as a marker of breast cancer, renal cell carcinoma and other malignant conditions[34,85,156].

None of these previous studies has taken dehydration status into account when presenting results. It has been established that it is necessary to normalise all compound concentrations to urinary concentration in order to account for patient dehydration status[86,155]. This factor may have a significant influence upon measured VOC concentration.

This experiment planned to cross-validate the previous findings which demonstrated reduced urinary phenol concentrations in oesophago-gastric cancer patients[26]. This experiment has utilised the headspace SPME GC-MS method for phenol quantification developed in Sections 2.1 and 2.2. This analytical technique provided more robust compound identification (over SIFT-MS) via the use of chromatographic separation. This also enabled isomeric differentiation of cresols and ethylphenols to establish which isomers of these compounds are present within urine. All results were normalised to urinary creatinine in order to account for patient dehydration status.

4.1.3 Methods

Local ethics committee approval was obtained for this experiment (ICHTB HTA Licence: 12275; REC Wales Approval: 12/WA/0196; Tissue bank approval number R14118).

Urine samples were collected from 52 patients with oesophago-gastric cancer and 52 controls. Controls included 25 patients with upper gastrointestinal symptoms who had a normal or benign disease of the upper gastrointestinal tract at endoscopy. The control group also included 27 self-reported healthy volunteers who had no upper gastro-intestinal symptoms. All patients were fasted for a minimum of 6 hours prior to sample collection. All subjects were asked to provide a mid-stream urine sample collected into a sterile 60ml universal container.

Three millilitres of each sample was separated for urinary creatinine measurement prior to GC-MS sample preparation. This allowed results to be normalised to urinary creatinine to account for dehydration status of patients.

As urinary phenol is bound to glucuronic acid and sulfate all samples underwent deconjugation prior to analysis. Five millilitres of urine was added to a 20ml SPME vial with screw cap and PTFE septum (Chromacol, Welwyn Garden City, UK) and was acidified with 80µL concentrated hydrochloric acid (to buffer to pH 2). D6 phenol was added as isotope labelled standard (concentration 1µg/ml – Sigma Aldrich, Gillingham, Dorset, UK), along with 0.4g of sodium chloride. These urine samples were placed in sealed vials and heated to 90°C for 90 minutes for deconjugation. Vials were allowed to cool and remained sealed until analysis.

Analysis was undertaken using the GC-MS method described in Section 2.1 and the following SPME parameters which were optimised in Section 2.2: Extraction temperature: 60°C; Equilibration time: 10 minutes; SPME extraction time: 60 minutes. All samples were analysed as technical triplicates.

Calibration curves were produced using standard solutions of phenol, p-cresol, m-cresol, 2-ethylphenol, 3-ethylphenol, 4-ethylphenol (All Sigma Aldrich, Gillingham, Dorset, UK) at varying

concentrations (0.1µg/ml, 0.25µg/ml, 0.5µg/ml, 1µg/ml, 2µg/ml, 5µg/ml, 10µg/ml, 20µg/ml) all containing 1µg/ml D6 phenol. Quality control samples consisted of the 1µg/ml calibration point which was analysed at various time points during sample analysis.

Data analysis was performed using Turbomass® (Perkin Elmer, Seer Green, BUCKS, UK) for mass spectrum analysis and peak integration. Quantification was performed by calculating the ratio of compound peak area to that of internal standard in each sample. Calibration curve slope calculations were then used to provide the concentration of each compound. Univariate statistical analysis was performed using SPSS v23 (IBM, Armonk, NY, USA). Binary logistic regression was utilised in order to produce Receiver Operating Characteristic (ROC) curves also using SPSS v23 (IBM, Armonk, NY, USA).

4.1.4 Results

Patient Demographics

Patient demographics are shown in table 48:

	Control (n=52)			Cancer (n=52)	Chi-Squared (p)
	Overall Control (n=52)	**Positive Control (n=25)**	**Healthy Volunteer (n=27)**	**Cancer (n=52)**	**Overall Control Group vs Cancer**
Age (Median)	34 (27-77)	54 (27-77)	30 (27 – 65)	62 (47-79)	<0.001 (MWU)
Male	33 (63%)	15 (60%)	18 (67%)	40 (77%)	0.181
Caucasian	37 (71%)	14 (56%)	23 (85%)	45 (87%)	0.088
PPI Use	10 (19%)	10 (40%)	0 (0%)	33 (63%)	<0.001
Aspirin Use	2 (4%)	2 (8%)	0 (0%)	1 (2%)	0.547
Hypertension	9 (17%)	8 (32%)	1 (4%)	9 (17%)	0.965
Diabetes	4 (8%)	4 (16%)	0 (0%)	4 (8%)	0.978
Statin Use	4 (8%)	3 (12%)	1 (4%)	8 (15%)	0.233
Non-Smoker	47 (90%)	20 (80%)	27 (100%)	22 (42%)	<0.001
Alcohol under 21 units per week	49 (94%)	22 (88%)	27 (100%)	41 (79%)	0.014
ASA 1 or 2	49 (94%)	22 (88%)	27 (100%)	42 (81%)	0.024

Table 48: Demographic details for patients included in urinary analysis.

These results demonstrated some significant differences between the control and cancer cohorts. The control group patients were significantly younger, largely due to the younger age of the healthy volunteers. The positive control and cancer cohorts were more evenly matched for age (Median age in positive control cohort – 54; Cancer cohort – 62). There was significantly less use of proton pump inhibitors (PPI) in the control cohort. This was largely due to the healthy volunteers comprising asymptomatic patients who were not taking PPI to control upper gastrointestinal symptoms. The positive control and cancer cohorts both had greater rates of PPI use (40% and 63% respectively). There were significantly more smokers in the cancer cohort and a greater proportion of these patients

drank more than 21 units of alcohol per week. There were more patients who were ASA 1 or 2 in the control group but again results were similar between the cancer and positive control cohorts (88% of positive control group ASA 1/2 compared to 81% in cancer cohort).

Urinary concentration

Median urinary creatinine across all samples was 12.8mmol/L. Urinary creatinine ranged from 1.9mmol/L to 34.8mmol/L. Each creatinine concentration was converted to grams of creatinine per litre using the known molecular weight of creatinine (113.12). This calculation allowed for results to be expressed as milligrams of phenol/cresol per gram of creatinine (mg/g).

Overall Analysis

Phenol was identified in all patient urine samples that were analysed. P-cresol was identified above the limit of detection in 101/104 samples. No other cresols or ethylphenols were identified above the limit of detection. Results for phenol and p-cresol concentration in control and cancer patients are shown below in table 49:

	Control (n= 52) (mg/g creatinine)	**Cancer (n = 52) (mg/g creatinine)**	**Mann Whitney U Test**
Phenol	0.42 (IQR 0.27 – 1.30)	0.90 (IQR 0.39 – 2.22)	0.033
p-Cresol	2.29 (IQR 0.98 – 9.19)	4.59 (IQR 3.05 – 10.47)	0.024

Table 49: Phenol and p-cresol concentrations in control and cancer patient cohorts.Results expressed as milligrams of phenol or p-cresol per gram (mg/g) of creatinine.

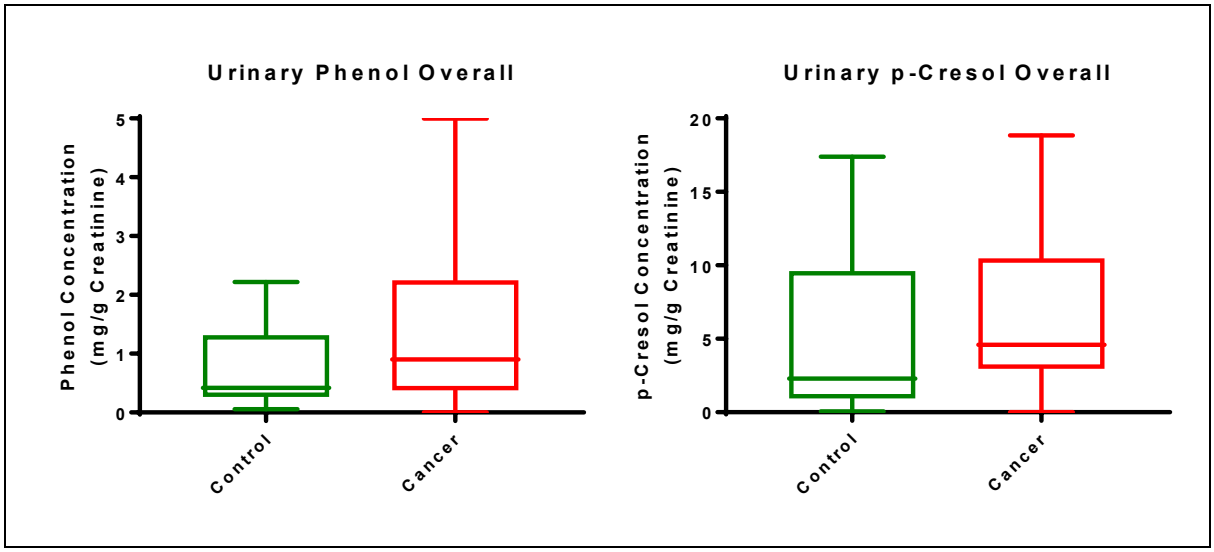


Figure 62: Urinary phenol and p-cresol in control and cancer cohorts.

Median concentration within the control cohort was 0.42mg/g creatinine (IQR 0.27 to 1.30). Phenol concentration was significantly higher within the cancer cohort (0.90mg/g creatinine (IQR 0.39 to 2.22) (MWU 0.033). p-Cresol was also significantly elevated within the cancer cohort (4.59mg/g creatinine (IQR 3.05 – 10.47)) compared to the control cohort (2.29 mg/g creatinine (IQR 0.98 – 9.19) (MWU 0.024). However, when positive control patients (with benign disease of the upper gastrointestinal tract) were compared directly to the cancer cohort no significant difference in phenol or p-cresol concentration was identified (Phenol – Positive Controls 0.84mg/g creatinine; Cancer 0.89mg/g creatinine (MWU = 0.626); p-Cresol – Positive Controls 4.46 mg /g creatinine, Cancer 4.57mg/g creatinine (MWU = 0.279). However, phenol and p-cresol concentrations were particularly low in the asymptomatic healthy volunteer patients (Phenol concentration 0.33mg/g creatinine (MWU vs cancer cohort p=0.004); p-Cresol concentration 2.03mg/g creatinine (MWU vs cancer cohort p=0.006)). When asymptomatic healthy volunteer patients were compared directly to cancer patients and those with benign disease of the upper gastrointestinal tract, these differences remained significant as shown in table 50.

	Healthy Volunteer (n= 27) (mg/g creatinine)	Benign Controls (n = 25) (mg/g creatinine)	Cancer (n=52) (mg/g creatinine)	Kruskal Wallis Test
Phenol	0.33 (IQR 0.22 – 0.63)	0.84 (IQR 0.34 – 1.58)	0.90 (IQR 0.39 – 2.22)	0.011
p-Cresol	2.03 (IQR 0.97 – 5.30)	4.45 (IQR 1.28 – 10.34)	4.59 (IQR 3.05 – 10.47)	0.034

Table 50: Comparison of phenol and p-cresol concentration in healthy volunteers, symptomatic benign controls and cancer patients.

Effect of Tumour Site (Oesophageal Versus Gastric)

Median concentrations of phenol were significantly higher in gastric cancer samples (2.07mg/g creatinine) compared to both oesophageal cancer patients (0.87mg/g creatinine) and the overall control group (0.42mg/g creatinine) (Kruskal Wallis Test 0.044). Concentrations of p-cresol were also significantly elevated in the gastric cancer group (p-cresol concentrations (all mg/g creatinine: Gastric cancer – 6.38; Oesophageal cancer 4.10; All controls 2.29 (Kruskal Wallis Test 0.035).

	Control (n= 52) (mg/g creatinine)	Oesophageal (n = 36) (mg/g creatinine)	Gastric (n=16) (mg/g creatinine)	Kruskal Wallis Test
Phenol	0.42 (IQR 0.27 – 1.30)	0.87 (IQR 0.42 – 1.96)	2.07 (IQR 0.31 – 5.04)	0.044
p-Cresol	2.29 (IQR 0.98 – 9.19)	4.10 (IQR 1.85 - 8.97)	6.38 (IQR 3.35 – 13.57)	0.035

Table 51: Results divided by disease type.

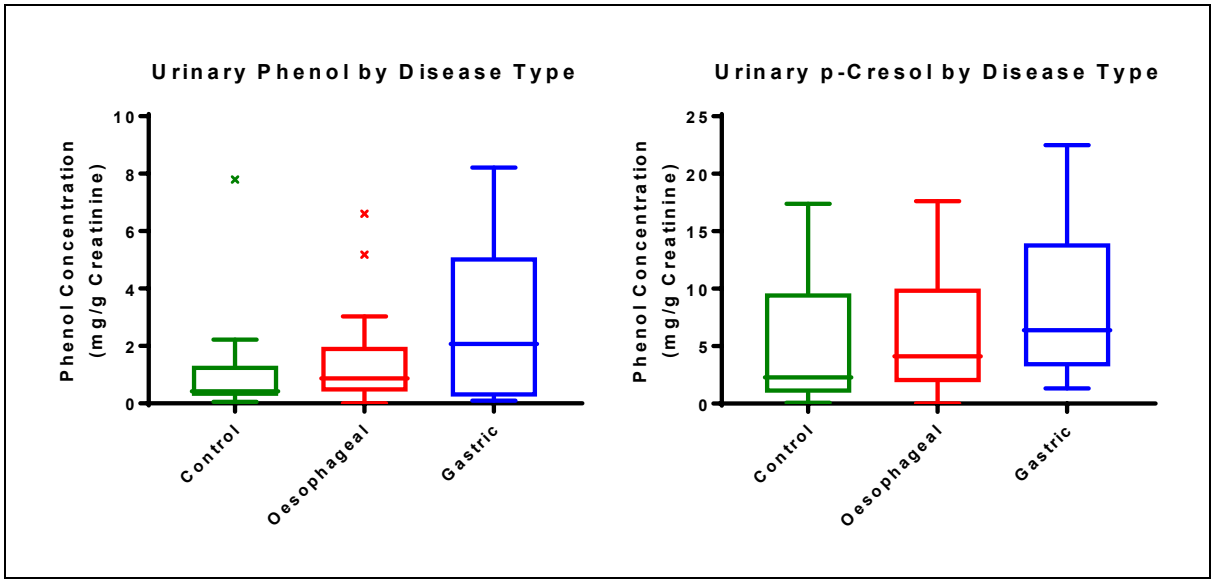


Figure 63: Urinary phenol and p-cresol concentrations in oesophageal and gastric cancer patients separately.

When gastric cancer patients only were compared to the positive control group alone there was no significant elevation of phenol or p-cresol (Phenol concentration – Positive controls 0.84mg/g creatinine; Gastric cancer 2.07 mg/g creatinine (MWU p = 0.292); p-cresol concentration – Positive controls 4.46mg/g creatinine; Gastric cancer 6.38 mg/g creatinine (MWU p = 0.100)).

Effect of Neoadjuvant Chemotherapy

Of the cancer cohort 25 patients had not received any neoadjuvant chemotherapy prior to sample collection, whereas 28 patients had received chemotherapy. Use of chemotherapy did not appear to significantly affect concentrations of phenol or p-cresol as shown in table 52.

	Pre-Chemo (n = 25) (mg/g creatinine)	**Post Chemo (n=27) (mg/g creatinine)**	**MWU (p)**
Phenol	0.57 (IQR 0.39 – 2.18)	0.96 (IQR 0.40 – 2.33)	0.656
p-Cresol	6.38 (IQR 3.17 – 10.47)	4.09 (IQR 2.74 – 10.45)	0.487

Table 52: Urinary phenol and p-cresol concentration subdivided according to whether patients had received neo-adjuvant chemotherapy.

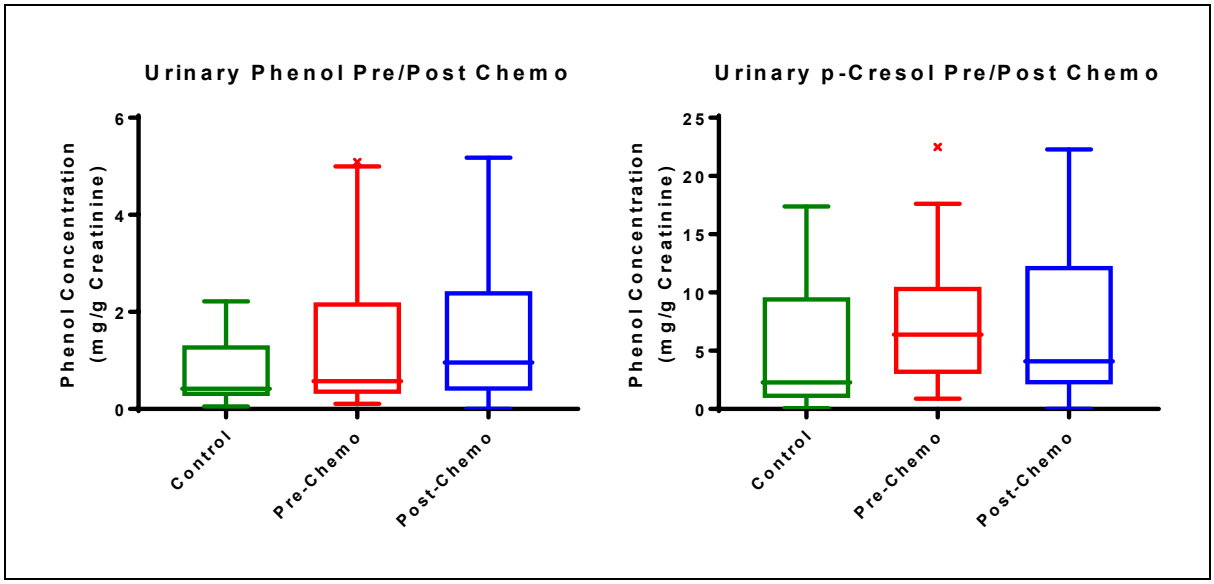


Figure 64: Results for neoadjuvant naïve patients (Pre-Chemo) compared to those who had completed chemotherapy and control patients.

Effect of Disease Stage

Dividing patients according to whether they had early stage (T1/2 n=9) or late stage disease (T3/4 n=44) showed no significant difference between these groups as demonstrated in table 53:

	T1/2 (n = 9) (mg/g creatinine)	**T3/4 (n=43) (mg/g creatinine)**	**MWU**
Phenol	0.50 (IQR 0.44 – 1.50)	0.90 (IQR 0.35 – 2.23)	0.943
p-Cresol	6.91 (IQR 3.05 – 10.49)	4.56 (IQR 3.01 – 9.92)	0.460

Table 53: Results divided according to tumour stage.

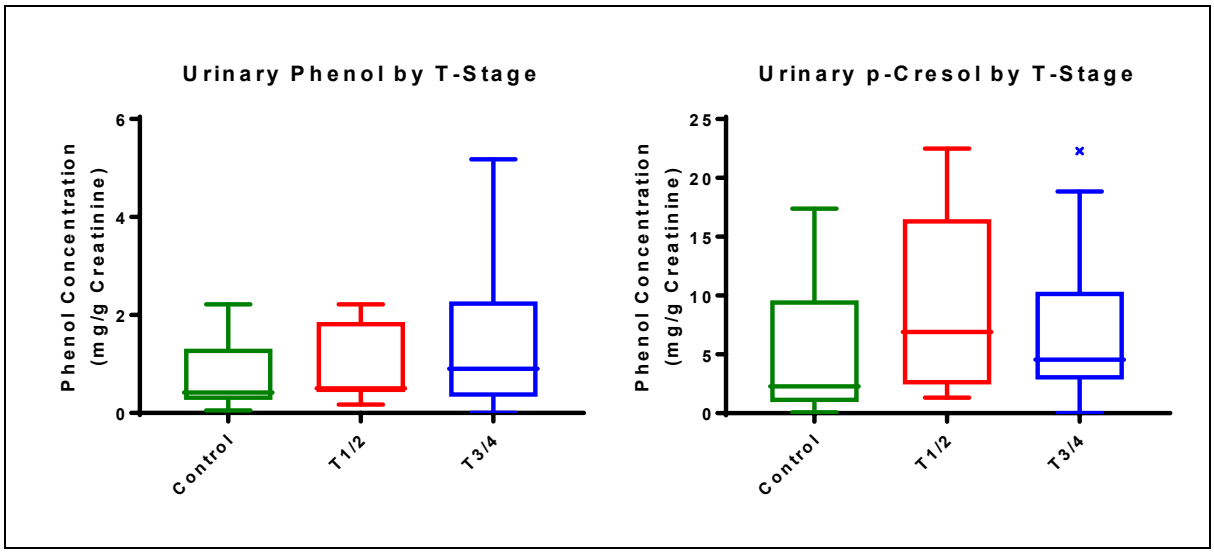


Figure 65: Results divided by tumour stage.

Thirty-five patients within the cancer cohort had lymph node involvement at the time of sampling, and 18 patients had no nodal involvement. There was no significant difference in phenol or p-cresol concentration between these two groups as demonstrated in table 54.

	No Nodal Involvement (n = 18) (mg/g creatinine)	Nodal Involvement (n=34) (mg/g creatinine)	MWU
Phenol	1.14 (IQR 0.37 – 4.51)	0.88 (IQR 0.40 – 2.02)	0.388
p-Cresol	4.48 (IQR 2.94 – 12.52)	4.59 (IQR 3.14 – 9.92)	0.881

Table 54: Results sub-divided according to nodal involvement.

Urinary Phenol and p-Cresol as a Diagnostic Test

To assess the suitability of urinary phenol and p-cresol analysis as a combined diagnostic test of oesophago-gastric cancer, binary logistic regression was undertaken and receiver operating characteristics (ROC) curves calculated. ROC curves are demonstrated in figure 66. Oesophago-gastric cancer cases were compared to all controls (A) and to healthy volunteers only (B).

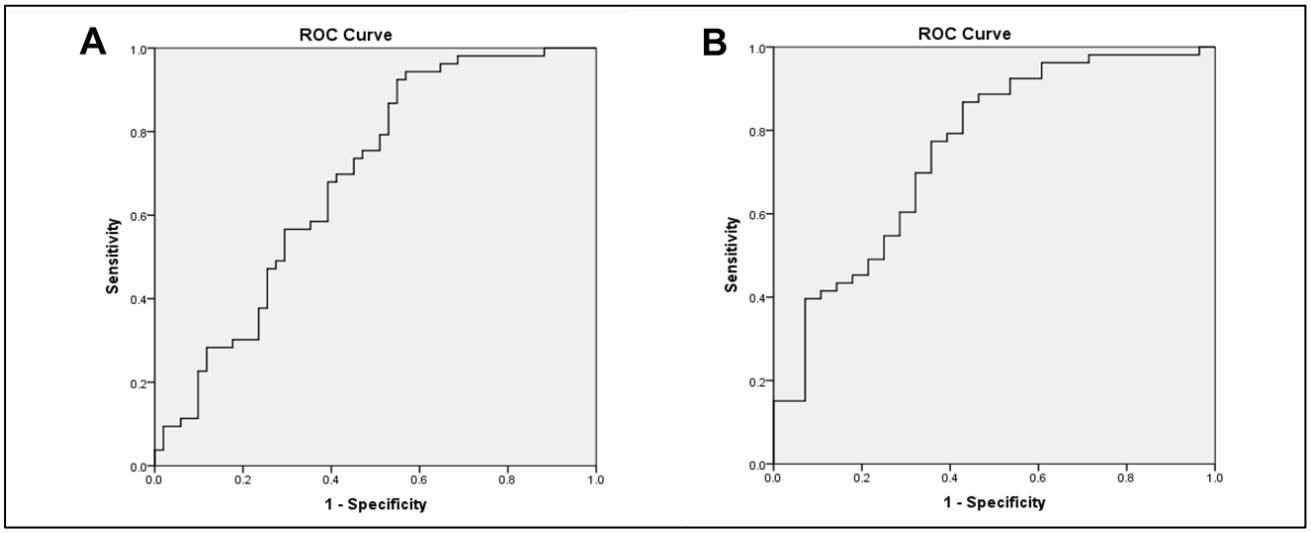


Figure 66: ROC curves for oesophago-gastric cancer patients versus all controls (A – Area under curve 0.687) and against healthy volunteers only (B – Area under curve 0.755).

In general a good test is considered to have an area under the ROC curve of at least 0.8. When oesophago-gastric cancer patients were compared to all controls, the area under the ROC curve was only 0.687. When oesophago-gastric cancer cases were compared to healthy volunteers only, the area under the ROC curve rose to 0.755. This gave a sensitivity of 86.8% but specificity of only 57.1%. When healthy volunteers were compared to cancer patients and benign controls (combined as one 'symptomatic group') the area under the ROC curve was 0.734.

4.1.5 Discussion

This experiment has established that phenol and p-cresol concentrations are significantly elevated in the urine of oesophago-gastric cancer patients relative to controls (median phenol concentration 0.90mg/g creatinine in cancer patients versus 0.42mg/g creatinine in controls (MWU p = 0.033); Median p-cresol concentration 4.59mg/g creatinine in cancer cohort versus 2.29mg/g creatinine in controls (MWU 0.024)). Phenol and p-cresol concentrations were significantly higher in gastric cancer patients compared to the oesophageal cancer cases and controls. Urinary phenol and p-cresol concentration were not affected by use of neoadjuvant chemotherapy, disease stage or nodal involvement.

This result of increased urinary phenol in cancer patients conflicts with previous studies that have demonstrated that phenol concentration was decreased within the urine of oesophago-gastric cancer patients[26]. In the present study urinary concentration was accounted for by normalising all results to urinary creatinine concentration and expressing concentrations of compounds as milligrams per gram (mg/g) of creatinine. Patient dehydration status could significantly affect urinary concentration, and concentration of volatile compounds was dependent upon this factor. Therefore, the difference in the findings between this experiment and previous studies is believed to be due to the effect of normalisation of results to urinary creatinine.

Although this study demonstrated significant differences between cancer and control patients this appeared to be in large part due to low concentrations of phenol and p-cresol in the healthy volunteer group (Median phenol concentration 0.33mg/g creatinine (0.90mg/g creatinine in cancer group (MWU

p=0.004)) ; p-Cresol concentration 2.03mg/g creatinine (4.59mg/g creatinine in cancer cohort (MWU p=0.006))). This group contained a significantly younger population who did not have any symptoms of upper gastrointestinal disease. Because positive control samples were collected at the time of upper gastrointestinal endoscopy these patients had some form of upper gastrointestinal symptoms or disease which had led to the need for endoscopy. There was no significant difference between the urinary phenol and p-cresol concentrations of the positive control and cancer groups. Therefore urinary phenol and p-cresol analysis does not seem able to differentiate between patients with benign diseases of the upper gastrointestinal tract and those with oesophago-gastric cancer. When urinary phenol and p-cresol were used in a binary logistic regression model these compounds were not able to accurately discriminate between oesophago-gastric cancer patients and controls (area under the ROC curve 0.687).

In univariate analysis there did appear to be a significant difference between healthy volunteers and those suffering with oesophago-gastric cancer or other benign conditions of the upper gastrointestinal tract. When oesophago-gastric cancer patients were compared to healthy volunteers in a binary logistic regression model diagnostic accuracy improved (area under the ROC curve 0.755) although this still failed to reach the criteria to be considered a 'good test' (area under the ROC curve 0.8). The area under the ROC curve was similar when benign and malignant disease were combined as one 'symptomatic group' (0.734). This indicates that although concentration of these compounds may be significantly different between cancer patients and healthy volunteers they cannot necessarily be used alone as a diagnostic test in urine analysis. However, these compounds may be more useful as part of a panel of other compounds in order form a diagnostic discrimination model to identify the presence of either benign or malignant disease of the upper gastrointestinal tract. Phenol and cresol were previously utilised in such a manner when they were included as part of a diagnostic model of oesophago-gastric cancer using exhaled breath[25]. They were utilised alongside ten other volatile organic compounds (pentanoic acid, hexanoic acid, ethyl phenol, butanal, pentanal, hexanal, hepatanal, octanal, nonanal and decanal) to produce a diagnostic model with an area under the ROC curve of over 0.9[25]. Therefore it may be possible to utilise urinary phenol and p-cresol analysis as part of a diagnostic discrimination model comprising a panel of compounds capable of identifying those patients requiring upper gastrointestinal endoscopy for diagnosis of benign or malignant disease.

Although there was no significant effect of disease stage upon urinary phenol or p-cresol concentration this may have been related to the small number of patients with early stage disease. Only 9 patients (17%) in this analysis had early stage disease (T1/T2) at the time of presentation. This is typical of patients with oesophago-gastric cancer who tend to present with late stage disease[3]. Further evaluation of phenol and p-cresol in the early stages of disease may help to establish its usefulness as a biomarker of early-stage disease or changes in urinary concentration of these compounds with increasing disease burden.

4.1.6 Conclusion

This experiment has demonstrated that urinary phenol and p-cresol concentrations are elevated in oesophago-gastric cancer patients relative to healthy volunteers. There was no significant difference between cancer patients and positive controls that had been referred for upper gastrointestinal endoscopy.

4.2 Plasma GC-MS

4.2.1 Objective

This experiment aimed to establish the presence of phenol and p-cresol within plasma samples, and whether concentrations of these compounds are significantly elevated in oesophago-gastric cancer patients.

4.2.2 Introduction

The previous section has established that when corrected for patient dehydration status urinary concentrations of phenol and p-cresol appear to be elevated in oesophago-gastric cancer patients relative to healthy volunteers. It has also been previously demonstrated using SIFT-MS that phenol and cresol are present at increased concentrations within the exhaled breath of these patients[25,36]. This highlights the potential of these compounds as non-invasive biomarkers of this disease in exhaled breath or urine. However, if phenol or p-cresol are produced within the tumour or surrounding microenvironment it is necessary for these compounds to be transported via the blood to the lungs or kidneys for excretion[157]. As part of establishing the biological mechanism responsible for the production of these compounds it is necessary to identify whether they are being transported within the systemic circulation as this would be necessary to explain their appearance in exhaled breath or urine.

This section has analysed phenol and p-cresol concentrations within plasma samples in order to establish whether these compounds are being transported within the systemic circulation. It also aimed to ascertain whether concentrations of these compounds are elevated within the plasma of oesophago-gastric cancer patients. This was undertaken using the plasma preparation and solid-phase extraction method developed for direct injection GC-MS in Section 2.3, as well as the GC-MS method developed in Section 2.1. As phenol and p-cresol are typically transported in the blood conjugated to glucuronic acid or sulphate, plasma samples underwent deconjugation prior to analysis[110].

4.2.3 Methods

Local ethics committee approval was obtained for this experiment (ICHTB HTA Licence: 12275; REC Wales Approval: 12/WA/0196; Tissue bank approval number R15065).

Blood samples were collected from 29 histologically confirmed cancer cases (15 oesophageal and 14 gastric) and 15 healthy control samples (diagnosed with healthy or benign disease of the upper gastrointestinal tract at upper gastrointestinal endoscopy). All patients were starved for a minimum of six-hours prior to sample collection. Whole blood was collected into EDTA tubes and centrifuged at 2500g for 10 minutes. The supernatant plasma was collected and stored at -80°C prior to analysis.

As phenol and p-cresol are typically transported in the blood conjugated to glucuronic acid or sulphate, plasma samples required deconjugation prior to analysis[110]. One millilitre of plasma was incubated with 20µl beta-glucuronidase from *Helix pomatia* (Sigma Aldrich, Gillingham, Dorset, UK) at 37°C for 30 minutes (Please see Section 2.3 for optimisation of plasma deconjugation).

De-proteinisation occurred by adding 400µl of deconjugated plasma to 1200µl of HPLC grade methanol Sigma Aldrich, Gillingham, Dorset, UK) and centrifuging at 18000g for 15 minutes at 4°C. 990µl of this sample was then collected for analysis and 10µl of D6 Phenol (Concentration 100µg/ml) added to give a final internal standard concentration of 1µg/ml. These samples then underwent solid phase extraction according to the protocol developed in Section 2.3. One millilitre of methanolic plasma extract was diluted with 3ml 0.05M hydrochloric acid and 46ml of HPLC grade water (both Sigma Aldrich, Gillingham, Dorset, UK). Solid phase extraction tubes (BondElut PPL – Agilent Technologies, Santa Clara, CA, USA) were conditioned with dichloromethane, methanol, and water with 0.05M hydrochloric acid prior to loading of samples. The wash step consisted of 3ml of 5% methanol followed by compound elution with 3ml of acetone. Acetone elutes were evaporated to 1ml under nitrogen prior to analysis on GC-MS using the previously described direct injection method for phenol measurement (Sections 2.1 and 2.3). All samples were analysed as technical triplicates.

Calibration curves were produced using standard solutions of phenol at various concentrations (0.01µg/ml, 0.025µg/ml, 0.05µg/ml, 0.1µg/ml, 0.25µg/ml, 0.5µg/ml, 1µg/ml, 2µg/ml) all containing 1µg/ml of Phenol D6 as internal standard. Quality control samples consisted of the 1µg/ml calibration point which was analysed at various time points during sample analysis.

Data analysis was performed using Turbomass® (Perkin Elmer, Seer Green, BUCKS, UK) for mass spectrum analysis and peak integration. Quantification was performed by calculating the ratio of compound peak area to that of internal standard in each sample. Calibration curve slope calculations were then used to provide concentration of each compound. Univariate statistical analysis was performed using SPSS v23 (IBM, Armonk, NY, USA)

4.2.4 Results

Patient demographics

Patient demographics are shown in table 55.

	Control (n=15)	Cancer (n=29)			Chi-Squared (p)
	Control (n=15)	Oesophageal (n=15)	Gastric (n=14)	Overall (n=29)	Control vs Overall Cancer
Age (Median)	62 (38-77)	68 (48-80)	71.5 (34-86)	71 (34-86)	0.110 (MWU)
Male	8 (53%)	11 (73%)	9 (64%)	20 (69%)	0.307
Caucasian	11 (73%)	14 (93%)	8 (57%)	22 (76%)	0.854
PPI Use	8 (53%)	9 (60%)	8 (57%)	17 (59%)	0.737
Aspirin Use	3 (20%)	2 (13%)	2 (14%)	4 (14%)	0.594
Hypertension	4 (27%)	4 (27%)	8 (57%)	12 (41%)	0.336
Diabetes	0	1 (7%)	3 (21%)	4 (14%)	0.131
Statin Use	2 (13%)	4 (27%)	6 (43%)	10 (34%)	0.135
Non-Smoker	10 (67%)	7 (47%)	8 (57%)	15 (52%)	0.343
Alcohol under 21 units per week	12 (80%)	14 (93%)	13 (93%)	27 (93%)	0.194
ASA 1 or 2	12 (80%)	10 (67%)	9 (64%)	19 (66%)	0.318

Table 55: Demographic details of control and cancer patients undergoing plasma analysis.

The control and cancer cohorts were well matched with no significant differences between the demographics of the two groups.

Phenol Concentration

Total phenol concentration was significantly elevated in oesophago-gastric cancer cases relative to controls (Cancer cohort - 0.051µg/ml (0.024 – 0.086); Control cohort - 0.034µg/ml (0.014 – 0.061) (MWU p=0.021). Dividing the cancer cohort into two cohorts (oesophageal and gastric) revealed that

phenol concentration was elevated in both groups (Oesophageal – 0.051µg/ml (0.024 -0.077); Gastric 0.049µg/ml (0.027 – 0.086).

	Control (n=15)	**Oesophageal (n=15)**	**Gastric (n=14)**	**Kruskal-Wallis**
Phenol Concentration (µg/ml)	0.034 (IQR 0.32 – 0.45)	0.051 (IQR 0.047 – 0.057)	0.049 (IQR 0.041 – 0.055)	0.030

Table 56: Details of phenol concentration in the control, oesophageal cancer and gastric cancer groups.

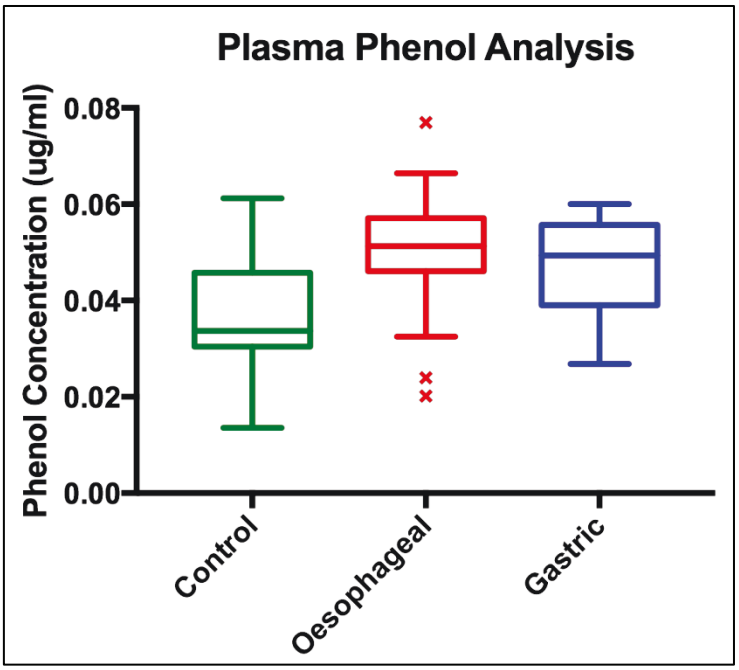


Figure 67: Boxplot of plasma phenol concentration across the three groups.

P-Cresol Concentration

P-Cresol levels were below the limit of detection (0.005µg/ml) in all samples analysed.

4.2.5 Discussion

This experiment has demonstrated that phenol is present within the plasma of oesophago-gastric cancer patients and controls. Plasma p-cresol levels were below the limit of detection in all samples.

Phenol concentration was increased within the plasma of oesophago-gastric cancer patients relative to controls (Cancer cohort - 0.051µg/ml (0.024 – 0.086); Control cohort - 0.034µg/ml (0.014 – 0.061) (MWU p=0.021)). This discovery provides evidence that phenol is being transported within the systemic circulation of these patients, and is at higher concentrations than that identified within the plasma of control patients. This finding provides a potential mechanism for transport of phenol from the tumour microenvironment to the kidneys or lungs for excretion in urine or exhaled breath. In order to explain the previous findings of elevated concentrations of phenol within urine (Section 4.1) and exhaled breath of oesophago-gastric patients in a previous study[25], it is necessary for phenol to be transported within the blood in this manner. This result supports the hypothesis that phenol produced locally at the site of the tumour can be transported within the circulation for excretion by the lungs or kidneys.

4.2.6 Conclusion

This experiment has established that plasma phenol concentrations are significantly elevated in oesophageal and gastric cancer cases relative to controls. This finding provides a potential mechanism for transport of this compound within the systemic circulation from the tumour site to the lungs or kidneys for excretion.

4.3 Tissue GC-MS

4.3.1 Objective

This experiment aimed to establish phenol concentrations within gastric cancer tissues and identify any differences between cancer and healthy tissue.

4.3.2 Introduction

The previous section has established that phenol and p-cresol are elevated within the urine of oesophago-gastric cancer cases, and these compounds are known to be elevated in exhaled breath of these patients[25]. Section 4.2 has provided evidence of increased blood phenol concentrations in these patients providing a potential transport mechanism from the area of the tumour itself to the kidneys or lungs for excretion. However, it is yet to be established whether oesophago-gastric adenocarcinoma tissues produce increased quantities of phenol relative to normal mucosa. The conversion of tyrosine to phenol is modulated by bacteria[42]. Therefore it is most likely that this compound would be identified within gastric cancer tissues which may be in direct contact with bacteria within gastric juice which is known to contain a diverse range of bacterial species[158].

This section has measured phenol concentrations within gastric cancer tissue samples and normal stomach mucosa in order to establish if phenol concentrations are increased within gastric cancer tissues. Previous studies measuring volatile compounds from stomach tissues have utilised large tissue weights (up to 2g)[114]. The available sample set contained much smaller tissue samples (10-30µg). Therefore rather than using HS-SPME analysis as in previous studies a specific method was developed in Section 2.3 for tissue homogenisation, solid phase extraction, and direct liquid injection GC-MS for phenol analysis. This method has been utilised in this experiment.

4.3.3 Methods

Local ethics committee approval was obtained for this experiment (ICHTB HTA Licence: 12275; REC Wales Approval: 12/WA/0196; Tissue bank approval number R15065).

Tissue samples from 5 gastric cancer patients were collected immediately following gastrectomy. Gastric cancer tissue and healthy matched mucosa (at least 10cm away from the area of the tumour) were collected from each patient and immediately placed in liquid nitrogen then stored at -80°C prior to analysis.

Before sample processing H&E slides were produced from each sample and tissue types confirmed with a Consultant Histopathologist.

During sample preparation tissue samples were weighed and then placed in liquid nitrogen within a mortar and a pestle used to powder the tissue. Powdered samples were placed into a 2ml vial and suspended in 1ml HPLC grade methanol (Sigma Aldrich, Gillingham, Dorset, UK). A ball-bearing was inserted and tissue homogenisation completed using a tissue homogeniser (Retsch, Dusseldorf, Germany – 30 cycles per second for 1 minute). Samples were centrifuged and the supernatant removed. A 1µg/ml spike of phenol D6 was then inserted to each sample as internal standard. Samples then underwent solid-phase extraction (as described in Section 2.3) to produce eluted compounds suspended in 1ml of acetone. Analysis was performed using the direct liquid injection GC-MS method described in Section 2.1 and 2.3. All samples were analysed as analytical triplicates.

Calibration curves were created using standard solutions of phenol, p-cresol, m-cresol, 2-ethylphenol, 3-ethylphenol, 4-ethylphenol (All Sigma Aldrich, Gillingham, Dorset, UK) at varying concentrations (0.005µg/ml 0.01µg/ml, 0.025 µg/ml, 0.05µg/ml, 0.1µg/ml, 0.25µg/ml, 0.5µg/ml, 1µg/ml, and 2µg/ml) in acetone. All calibration points contained 1µg/ml D6 phenol. Quality control samples consisted of the 1µg/ml calibration point which was analysed at various time points during sample analysis.

Data analysis was performed using Turbomass® (Perkin Elmer, Seer Green, BUCKS, UK) for mass spectrum analysis and peak integration. Quantification was performed by calculating the ratio of compound peak area to that of internal standard in each sample. Calibration curves slope calculations were then used to provide concentration of each compound. Univariate statistical analysis was performed using SPSS v23 (IBM, Armonk, NY, USA).

4.3.4 Results

Median patient age was 50 (range 33 to 67). All patients had T3/4 gastric cancer and four patients had nodal involvement. Two patients were using proton pump inhibitors at the time of sampling.

Sample weights were low with a median weight of 10µg in the cancer cohort (range 8 to 13µg) and median weight of 15µg in the control group (8 to 25µg).

Phenol was identified above the limit of detection in all normal stomach samples and 4 out of 5 gastric cancer samples. Median concentration of phenol was 0.023µg/ml in the cancer samples (range 0.013 to 0.031µg/ml). The concentration in the normal gastric mucosa was similar (Median 0.021µg/ml, range 0.011 to 0.035µg/ml). Following correction for sample weight results demonstrated that the median concentration of phenol in cancer samples (Median 0.15µg phenol per µg of tissue (range 0.11 – 0.28)), was not significantly different to that of normal tissue samples (Median 0.31µg phenol per µg tissue (range 0.11 – 0.88) (MWU = 0.548)).

4.3.5 Discussion

Although phenol was identified above the limit of quantification in the majority of samples analysed (9 out of 10), concentrations were close to the limit of quantification with all between 0.010µg/ml and 0.035µg/ml. This may be caused by loss of this volatile compound during sample preparation. All possible precautions were taken to prevent loss of volatiles with all tissue powdered within liquid nitrogen prior to homogenisation in methanol. It is also possible that the low concentrations recovered were due to the small tissue sample weights. During tissue collection it was not possible to collect

larger sample weights as it was imperative that tissue sampling for research purposes did not impact upon the histopathology examination of the patient's resected surgical specimen which would potentially affect their clinical management. Therefore, larger tissue samples could not be collected.

These results have demonstrated no difference in phenol concentration between gastric cancer tissues and matched normal gastric mucosa from the same patients. This may indicate that conversion of tyrosine to phenol does not occur within the area of the tumour itself. It may well be that this reaction is occurring in an adjacent environment such as gastric juice where the bacteria present could be responsible for production of this compound.

4.3.6 Conclusion

Although this experiment has identified the presence of phenol within tissue samples no difference in phenol concentration has been identified in gastric cancer tissues samples compared to healthy gastric mucosa. This may indicate that conversion of tyrosine to phenol is occurring within an area other than the tumour itself, and gastric juice has been investigated in the next section to establish if this reaction is occurring within this biological matrix.

4.4 Gastric Content Analysis

4.4.1 Objective

This experiment aimed to establish whether phenol concentrations are increased within the gastric content of gastric cancer cases. Phenol concentrations have been correlated with tyrosine concentration in the same samples to establish if there is a relationship between the concentrations of these two compounds.

4.4.2 Introduction

Previous sections have established that phenol was identified at increased concentrations in the urine and plasma of oesophago-gastric cancer patients relative to controls. This corresponds to findings of previous studies where increased phenol concentrations formed part of a diagnostic model for oesophago-gastric cancer in exhaled breath[25].

Although phenol concentrations appear to be systemically elevated in these patients the mechanism of production of this compound remains unclear. Phenol can be produced from tyrosine via the action of the bacterial enzyme *tyrosine phenol lyase*[42]*.* Phenol was not identified as being significantly elevated within gastric cancer tissues samples. However, as the conversion of tyrosine to phenol is reliant upon the action of bacteria, it may be more likely that this compound would be seen within gastric juice rather than cancer tissues. Previous studies analysing gastric juice have established that phenol is the volatile organic compound which appears most frequently in gastric content samples collected from oesophago-gastric cancer patients[159]. Methyl-phenol (cresol) has also been previously demonstrated to be at significantly increased concentrations in the gastric juice of oesophago-gastric cancer patients relative to controls[35].

Tyrosine concentrations are known to be increased within the gastric juice of gastric cancer patients[39,40]. This potentially indicates that tyrosine released from a gastric tumour could be converted

to phenol within the stomach (via the action of bacteria within gastric content) leading to phenol production.

This experiment has measured concentrations of phenol within gastric content samples from gastric cancer patients and controls. Tyrosine concentrations have been measured in the same samples to establish if there is a correlation between tyrosine and phenol concentrations within gastric content.

4.4.3 Methods

Local ethics committee approval was obtained for this experiment (ICHTB HTA Licence: 12275; REC Wales Approval: 12/WA/0196; Tissue bank approval number R14118).

Sample Collection

All samples were collected from patients undergoing upper gastrointestinal endoscopy (OGD) with all patients being fasted for a minimum of six hours prior to collection (as per standard protocol for this investigation). Patients undergoing assessment of a known gastric adenocarcinoma were allocated to the cancer cohort. Those undergoing this test for investigation of upper gastrointestinal symptoms that were found to have a normal upper gastrointestinal tract or benign disease of the upper gastrointestinal tract were allocated to the control cohort.

During this procedure the endoscope is passed through the mouth into the oesophagus and then through to the stomach. At this point it is possible to collect any gastric content present through a suction channel into a sterile, disposable suction jar (Covidien, Minneapolis, MN, USA). This collection was performed prior to any washing being performed from the endoscope. Samples collected into the suction jar were transferred to a Nalgene vial (ThermoScientific, Waltham, MA, USA) and stored at -80°C prior to analysis.

Buffering of pH

Samples were thawed and starting pH measured using a pH meter (Hanna Instruments Ltd, Leighton Buzzard, UK). All samples were then buffered to pH 2 by addition of hydrochloric acid or ammonium

hydroxide to each sample. To ensure equal dilution of all samples an equivalent total volume was added to each sample with the remainder consisting of HPLC grade water (Sigma Aldrich, Gillingham, Dorset, UK). Following buffering 1ml aliquots of each sample were taken for LC-MS analysis, and the remainder used for HS-SPME GC-MS analysis.

GC-MS Analysis

Samples for GC-MS analysis were divided into 5ml aliquots in 20ml glass vials with magnetic caps and PTFE septum (Chromacol, Welwyn Garden City, HERTS, UK). Four-hundred micrograms of sodium chloride was added to each sample as per Section 2.2. Isotope labelled D6 phenol (Sigma Aldrich, Gillingham, Dorset, UK) was added as internal standard (Final concentration of D6 phenol 0.5µg/ml). Vials were sealed and samples underwent HS-SPME GC-MS analysis as detailed in Sections 2.1 and 2.2. All samples were analysed as technical triplicates.

Calibration curves were produced using standard solutions of phenol, p-cresol, m-cresol, 2-ethylphenol, 3-ethylphenol, 4-ethylphenol (All Sigma Aldrich, Gillingham, Dorset, UK) at varying concentrations (0.01µg/ml, 0.025 µg/ml, 0.05µg/ml, 0.1µg/ml, 0.25µg/ml, 0.5µg/ml, 1µg/ml, 2µg/ml, 5µg/ml, 10µg/ml, 20µg/ml) all containing 0.5µg/ml D6 phenol. Quality control samples consisted of the 1µg/ml calibration point which was analysed at various time points during sample analysis.

LC-MS Analysis

Gastric content sample preparation for LC-MS was undertaken as per Section 2.4. All samples were analysed as technical triplicates. 250µl Of gastric juice was mixed with 750µl methanol and 10µg of D4 tyrosine added as internal standard (Sigma Aldrich, Gillingham, Dorset, UK). Samples were then centrifuged at 18000g for 10 minutes. 200µl Of supernatant was removed and evaporated to dryness and reconstituted in 1000µl HPLC grade water. This five-time dilution was performed to prevent the chromatography column and detector becoming overloaded with tyrosine and gave a final internal standard concentration of 2µg/ml. Samples were thoroughly mixed and centrifuged prior to analysis using the LC-MS method for tyrosine quantification detailed in Section 2.4. Calibration curves were built using tyrosine standards at various concentrations (0.05µg/ml, 0.1µg/ml, 0.5µg/ml, 1µg/ml,

2µg/ml, 5µg/ml, 10µg/ml, 20µg/ml, and 50µg/ml) each with 2µg/ml of D4 tyrosine as internal standard. Quality control samples consisted of the 2µg/ml calibration point which was analysed at various time points during sample analysis.

Data Analysis

GC-MS data analysis was performed using Turbomass® (Perkin Elmer, Seer Green, BUCKS, UK) for mass spectrum analysis and peak integration. LC-MS data analysis was performed using MassLynx® (Waters, Milford, MA, USA). For both GC-MS and LC-MS data quantification was performed by calculating the ratio of compound peak area to that of internal standard in each sample. Calibration curves slope calculations were then used to provide the concentration of each compound. Univariate statistical analysis was performed using SPSS v23 (IBM, Armonk, NY, USA)

4.4.4 Results

Gastric content samples were collected from 15 gastric cancer patients, and 14 controls with normal upper gastrointestinal tract or benign disease of the upper gastrointestinal tract. Of the gastric cancer cases the majority of cases had advanced disease with 14/15 having T-Stage T3/T4 disease and 13/15 having lymph node involvement. Demographic details for each group are shown below in table 57.

	Control (n=14)	Cancer (n=15)	Chi-Squared (p)
Age (Median)	55.5 (35 – 86)	66 (34 – 78)	0.505 (MWU)
Male	7 (50%)	12 (80%)	0.089
Caucasian	9 (64%)	6 (40%)	0.191
PPI Use	7 (50%)	11 (73%)	0.196
Aspirin Use	0	1 (7%)	0.326
Hypertension	2 (14%)	4 (27%)	0.411
Diabetes	1 (7%)	5 (33%)	0.082
Statin Use	1 (7%)	1 (7%)	0.960
Non-Smoker	3 (21%)	5 (33%)	0.474
Alcohol under 21 units per week	12 (86%)	9 (60%)	0.122
ASA 1 or 2	11 (79%)	10 (67%)	0.474

Table 57: Patient details with no significant demographic differences between the control and cancer patient groups.

There was no significant difference in pH of samples between the cancer (median pH 4.1, range 1.44 – 7.88) and the control groups (median pH 4.43, range 1.79 – 7.28).

Phenol was successfully identified above the limit of quantification in all 29 samples being analysed. The median phenol concentration in the cancer cohort was 0.06μg/ml and within the control cohort this was 0.03μg/ml (MWU p = 0.201). Although the difference in phenol concentration between the two groups was not significant there was a much greater range in phenol concentration in the cancer group compared to controls (0.01 – 3.06μg/ml and 0.01 – 0.073μg/ml respectively) (Figure 68). Those patients with an entirely normal upper gastrointestinal tract (n=7) had the same median phenol concentration as patients with benign upper gastrointestinal disease (n=7) (both 0.03μg/ml). There

was no significant difference in phenol concentration between the normal group and cancer cohort (MWU p=0.395).

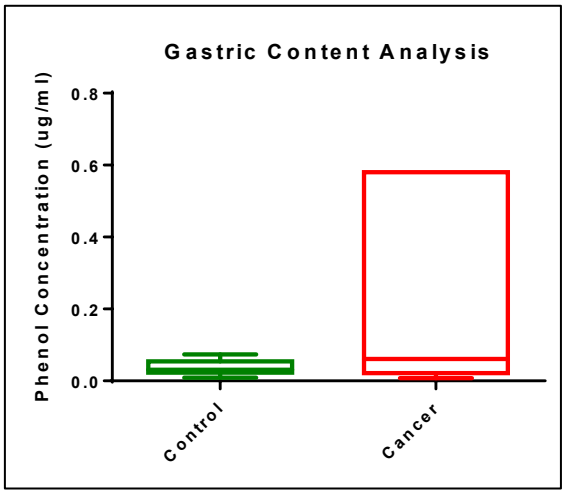


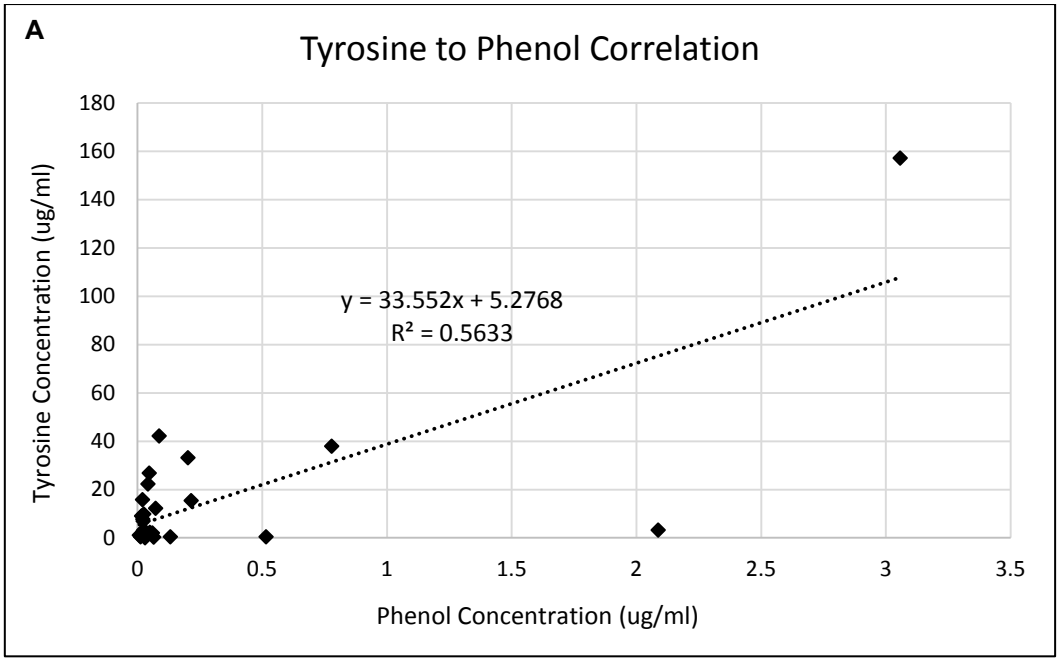
Figure 68: Boxplot showing no difference in median phenol concentration in cancer and control samples.

P-cresol was below the limit of detection in all samples. No other phenolic compounds were identified in these samples.

LC-MS Analysis of Tyrosine in Gastric Content

Tyrosine was identified above the limit of quantification in 24 out of 28 samples. One sample contained tyrosine well above tested dynamic range – Concentration 157µg/ml (upper tested limit of dynamic range 50µg/ml). This sample (from a gastric cancer patient) also contained highest phenol concentration from all samples tested (3.06µg/ml)

When this sample removed from analysis (as it was above dynamic range for tyrosine quantification) there was no clear relationship between phenol and tyrosine concentration. Figure 69 A & B shows the correlation between tyrosine and phenol concentration when this sample is included (Figure 69A) and excluded (Figure 69B).



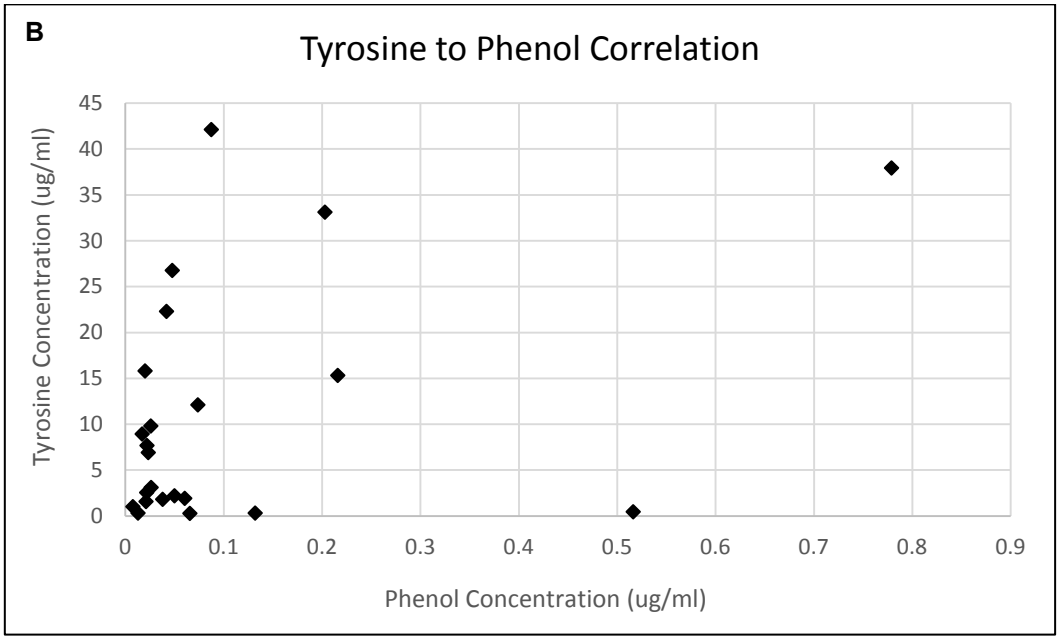


Figure 69: A: When all samples were included there appeared to be a weak correlation between tyrosine and phenol concentration. B: When the sample beyond the dynamic range of tyrosine LC-MS method was excluded this relationship was lost. There appeared to be no clear correlation between tyrosine and phenol concentration.

Samples were also analysed to compare tyrosine concentrations in gastric juice of cancer and control patients. Tyrosine was identified above the limit of quantification in all cancer samples. Tyrosine was below the limit of quantification in 4 out of 14 of the control group samples. Median concentration of tyrosine in the control group (4.56µg/ml (IQR 0.07 – 11.55µg/ml) was similar to that in the gastric cancer patients (3.11µg/ml (IQR 1.42 – 19.05µg/ml)) (MWU 0.354).

4.4.5 Discussion

In this cohort of patients it has been possible to consistently identify the presence of phenol within gastric content of both healthy patients and those with gastric cancer. Although there was no significant difference in phenol concentration between cancer cases and controls, the presence of phenol within gastric content raises the possibility of bacterial interaction with tyrosine within the stomach being responsible for phenol production in both healthy and diseased states.

A potential limitation of gastric content analysis is that the formulation of this bio-fluid is non-uniform and it is comprised of contributions from swallowed saliva, gastric secretions and reflux of fluid from the small intestine. This potential difference in the biological makeup of gastric content between patients is evidenced by the differences in starting pH for the samples analysed in this series (range cancer cases 1.44 – 7.88; control cases 1.79 – 7.28). In analysis of other biofluids such as urine it is possible to normalise metabolite concentrations to a standard biological measure (usually urinary creatinine with metabolite concentrations reported as concentration per gram of creatinine as in Section 4.1). This is not possible in gastric content analysis as no such uniform standardisation measure exists. The potential biological differences in sample make-up mean that interpretation of absolute concentrations of volatile metabolites must be undertaken with great care. This can cause particular difficulties when interpreting subtle differences in concentrations where the exact make-up of the sample may significantly influence results. It is currently not possible to circumvent the differences in biological makeup of this sample matrix and therefore interpretation of volatile concentrations between patients is challenging.

One potential methodology to circumvent these issues with sample makeup is to correlate compound concentrations with those of other metabolites within the same sample. This was attempted in this experiment to correlate tyrosine and phenol concentrations within the same gastric juice samples. Based upon samples within the tested dynamic range of these methods there was no clear correlation between tyrosine and phenol concentrations. This indicates that although both of these compounds are present within gastric juice their metabolism may not be directly related. However, many of the samples analysed contained very low concentrations of phenol which were close to the limit of detection of this GC-MS method (All samples above limit of quantification, but 22/29 samples had a phenol concentration below 0.1µg/ml). Due to this it may be difficult to definitively establish that phenol concentration is not correlated to that of tyrosine within gastric content based upon these results alone. One sample which contained very high concentration of tyrosine (157µg/ml) also contained the highest concentration of phenol in this series (3.06µg/ml). This may indicate that phenol production may only occur in the presence of very high tyrosine concentrations within the stomach. However, as this was the only sample with concentrations of either compound within these ranges it is not possible to draw any firm conclusions from this single sample.

In this cohort of patients the tyrosine concentration in gastric juice of gastric cancer patients was similar to that of control patients (Cancer cohort - 3.11µg/ml; Control cohort - 4.56µg/ml; MWU = 0.354). In previous studies the concentration of tyrosine within the gastric juice of control patients was similar to that identified in the current analysis (Control group in *Deng et al.* 3.8µg/ml[39]). However, this study by *Deng et al.* identified much higher concentrations of tyrosine within the gastric content of gastric cancer patients (Advanced gastric cancer patients – 18.3µg/ml; Early gastric cancer patients 19.4µg/ml[39]) than those seen in the present analysis (Median 3.11µg/ml (IQR 1.42 – 19.05µg/ml)). Based on the results of this small cohort of cancer patients in the current study (n=15) it is not possible to explain these differences.

Previous studies have identified that phenol is the most common volatile compound identified in gastric content samples from oesophago-gastric cancer patients[159]. This finding was re-enforced by the current results where phenol was identified in all patient samples (both healthy and control). However, it was not possible to identify p-cresol above the limit of detection in any of the samples

analysed in the current study. No other phenolic compounds (cresols or ethylphenols) were identified in any of the samples analysed. Previous studies of gastric juice using SIFT-MS have identified cresols (methylphenols) at higher concentrations in the gastric juice of gastric cancer patients relative to controls[35]. Due to the lack of isomeric differentiation with SIFT-MS it was not possible to establish which isomer of cresol was responsible for this difference. However, in the present analysis all cresols were below the limit of detection in all samples.

Gastric content is a challenging biofluid for analysis as it is not possible to standardise results to a uniform biological marker. Due to the variation in sample make-up quantitative analysis of results from individual samples is potentially flawed. Therefore this biological surrogate may be more accurately utilised for compound identification rather than absolute quantification. Therefore the fact that phenol and tyrosine were demonstrated to exist simultaneously within this biofluid is potentially of great interest and the potential for phenol to be produced from tyrosine within gastric content has been further investigated in the following sections.

4.4.6 Conclusion

Phenol and tyrosine were consistently identified within gastric content in both healthy and gastric cancer patients. There was no significant difference in either phenol or tyrosine concentration between these two groups. There was no clear correlation between the concentrations of these two compounds within these samples. However, due to the potential variation in the biological make-up of gastric juice samples, accurate quantitative analysis is challenging. Therefore, the identification of phenol and tyrosine within this biofluid is a significant finding and the relationship between these two compounds has been further investigated in the following sections.

4.5 Enrichment of Gastric Juice with Deuterated Tyrosine

4.5.1 Objective

This experiment aimed to establish if addition of deuterium-labelled tyrosine to gastric juice leads to the formation of equivalently deuterium-labelled phenol.

4.5.2 Introduction

The previous experiment has demonstrated the presence of phenol within gastric content samples. It is known that bacteria are responsible for production of phenol within the colon via fermentation of tyrosine by the enzyme *tyrosine phenol lyase*[42]. Gastric juice is known to contain a diverse range of bacteria[158], but it is unknown whether this reaction occurs within the stomach. The presence of phenol within gastric content may indicate that this compound is being produced from tyrosine within gastric juice. Previous research has demonstrated increased concentrations of tyrosine within stomach content of gastric cancer patients[39,40]. Although these results were not reproduced in the previous section, tyrosine has consistently been identified within gastric juice. Bacteria which are known to convert tyrosine to phenol include *Fusobacteria*[37,38]*, Clostridium*[91]*, and Escherichia*[99]*.* Each of these bacteria have been identified within the stomach at a genus level[95–98], indicating the potential of stomach bacteria to convert tyrosine to phenol.

Tyrosine labelled with four deuteriums has a molecular weight which is four international units heavier than tyrosine. When the deuteriums are attached to the benzene ring conversion of this deuterium-labelled tyrosine by *tyrosine phenol lyase* would produce deuterium-labelled phenol as exemplified in figure 70.

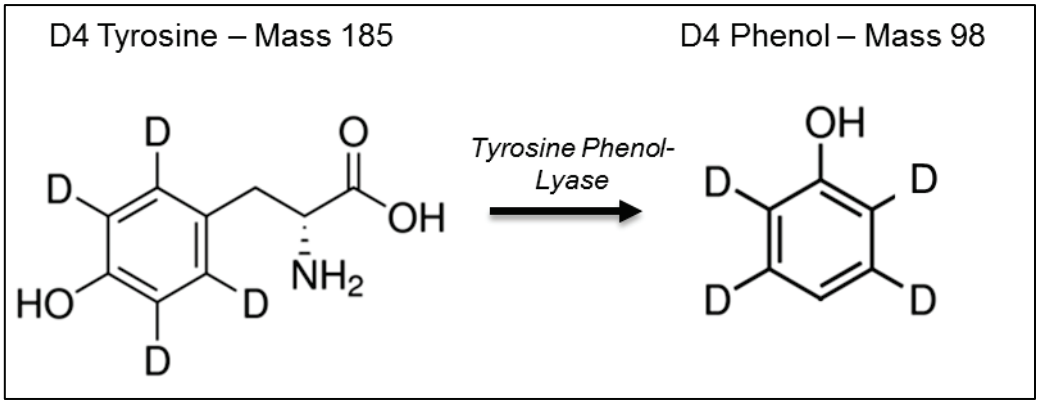


Figure 70: Conversion of D4 tyrosine to D4 phenol.

This deuterium-labelled D4 phenol would have an m/z of 98 rather than the usual m/z for phenol of 94. During GC-MS analysis it was possible to monitor the m/z 98 ion to establish the presence or absence of D4 labelled phenol in gastric juice samples which are enriched with D4 labelled tyrosine.

This experiment established whether adding deuterium-labelled D4-tyrosine to gastric content leads to the production of deuterium-labelled D4-phenol.

4.5.3 Methods

Local ethics committee approval was obtained for this experiment (ICHTB HTA Licence: 12275; REC Wales Approval: 12/WA/0196; Tissue bank approval number R14118).

Deuterium-labelled D4 tyrosine (Sigma Aldrich, Gillingham, Dorset, UK) was made up in HPLC-grade water to a concentration of 1mg/ml. A working solution of D6 phenol was made to a concentration of 100µg/ml in HPLC-grade water as internal standard (final internal standard concentration 1µg/ml - This compound was analysed separately to confirm there was no significant contribution to the 98 m/z ion from this compound).

Gastric content samples from 13 individual patients were divided into 3ml aliquots 20ml glass vials with magnetic caps and PTFE septum (Chromacol, Welwyn Garden City, HERTS, UK). Individual samples from each patient were separately divided into the ‘D4 tyrosine enriched’ and ‘unenriched cohorts’.

Samples to be D4 tyrosine enriched had 2ml of the D4 tyrosine solution added to the 3ml of gastric content. Samples in the 'unenriched' cohort had 2ml of HPLC grade water added to them. All samples were incubated at 37°C for 24 hours. Samples had 0.4g of sodium chloride and 1µg/ml of D6 phenol (both Sigma Aldrich, Gillingham, Dorset, UK) added as internal standard immediately prior to analysis.

Samples were analysed using the targeted phenol HS-SPME GC-MS method as detailed in Section 2.1 and 2.2. The m/z for D4-phenol (98) was added to the selective ion recording mass spectrometry method. SPME extraction was performed for 60 minutes at 60°C, and the injector temperature was 220°C. All samples were analysed as technical triplicates.

Calibration curves were produced using standard solutions of phenol (m/z 94) at various concentrations (0.01µg/ml, 0.025µg/ml, 0.05µg/ml, 0.1µg/ml, 0.25µg/ml, 0.5µg/ml, 1µg/ml, 2µg/ml) all containing 1µg/ml of Phenol D6 as internal standard. Quality control samples consisted of the 1µg/ml calibration point which was analysed at various time points during sample analysis.

Data analysis was performed using Turbomass® (Perkin Elmer, Seer Green, BUCKS, UK) for mass spectrum analysis and peak integration. Quantification was performed by calculating the ratio of compound peak area to that of internal standard in each sample. Calibration curves slope calculations were then used to provide concentration of each compound. Univariate statistical analysis was performed using SPSS v23 (IBM, Armonk, NY, USA)

4.5.4 Results

There was no evidence of any D4 phenol within any of the unenriched samples (see figure 71). D4 phenol (as indicated by the presence of a peak for m/z 98 at the same retention time as phenol) was visible in all enriched samples (see figure 71). D4 phenol was above the limit of quantification in all enriched samples.

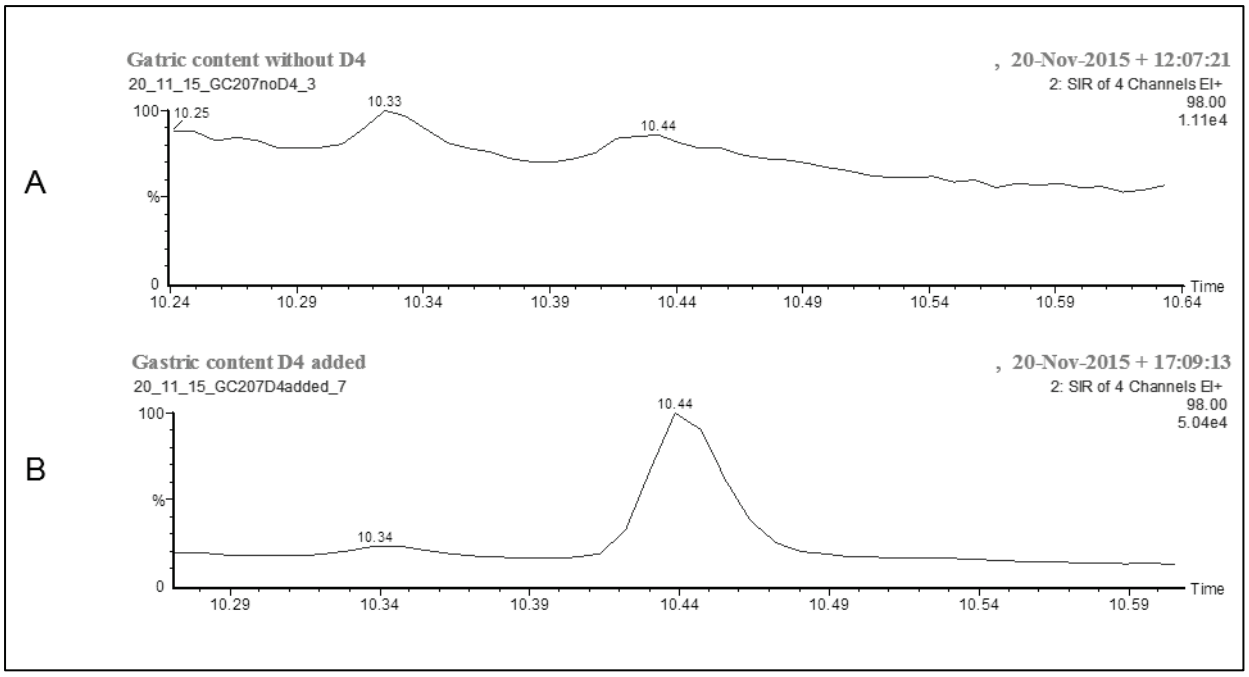


Figure 71: A – Selected ion recording for m/z 98 demonstrated no peak in unenriched samples. B – Peak visible at 10.44 minutes (m/z 98) in D4 tyrosine enriched samples indicating the presence of D4 phenol.

Details of D4 phenol concentration (mean with standard deviation) in each sample are provided in table 58.

Patient	Un-enriched D4 Phenol Concentration (µg/ml)	Enriched D4 Phenol Concentration (µg/ml)
1	Below LOD	0.0130 +/- 0.0001
2	Below LOD	0.0168 +/- 0.0001
3	Below LOD	0.0223 +/- 0.0005
4	Below LOD	0.0180 +/- 0.0006
5	Below LOD	0.0173 +/- 0.0001
6	Below LOD	0.0207 +/- 0.0002
7	Below LOD	0.0366 +/- 0.0107
8	Below LOD	0.0237 +/- 0.0007
9	Below LOD	0.0212 +/- 0.0004
10	Below LOD	0.0208 +/- 0.0004
11	Below LOD	0.0194 +/- 0.0001
12	Below LOD	0.0209 +/- 0.0001

Table 58: Details of D4 phenol production from D4 tyrosine in each patient. D4 phenol was below the limit of detection (LOD) for all unenriched samples but visible in all samples enriched with D4 tyrosine.

4.5.5 Discussion

Unenriched samples have demonstrated no evidence of the 98 m/z ion at the known retention time for phenol. In samples enriched with D4 tyrosine this peak was present at 10.44 minutes when scanning for m/z 98. This indicates that this ion was being produced from D4 labelled tyrosine within gastric content. This m/z and retention time corresponds to that expected for D4 labelled phenol. Therefore it appears that D4-labelled phenol is being produced within gastric content samples enriched with D4-labelled tyrosine. As phenol-producing bacteria are known to exist within the stomach[95–98], it seems probable that these bacteria are responsible for this production of D4-labelled phenol from D4-labelled

tyrosine. However, based upon these results it is not possible to definitively establish whether this conversion is due to bacterial activity within gastric juice.

4.4.6 Conclusion

These results have demonstrated that D4-phenol was absent in unenriched gastric content samples but was identified in all sample enriched with D4-tyrosine. This provides proof-of-principle evidence that tyrosine could be being converted to phenol within gastric juice. However, more evidence is necessary to establish the presence of phenol-producing bacteria within the stomach. The next section has investigated the presence of phenol-producing bacteria within gastric samples.

4.6 Identification of Phenol-Producing Bacteria within the Stomach.

4.6.1 Objectives

This experiment aimed to utilise 16S bacterial sequencing of stomach tissues to identify the presence of bacteria which potentially contain the *tyrosine phenol-lyase* gene.

4.6.2 Introduction

The role of the colonic microbiota in phenol production from tyrosine has long been established[42]. It has long been established that bacterial colonisation of the stomach by the organism *Helicobacter Pylori* is linked to gastric cancer risk [94]. Beyond the presence of this organism it has been demonstrated that the stomach microbiome is dominated by organisms from the bacterial phyla of *Proteobacteria, Firmicutes, Actinobacteria* and *Bacteroidetes*[95,96,98]. Bacteria which are known to contain the *tyrosine phenol-lyase* enzyme include *Fusobacteria*[37,38]*, Clostridium*[91]*, and Escherichia*[99]*.* Each of these bacteria have been identified within the stomach at a genus level[95–98], This increasing knowledge of bacterial presence within the stomach may provide a potential mechanism of phenol production in these patients via bacterial action upon tyrosine found within the gastric juice of cancer patients[39,40]. The bacterial constitution of the stomach can also vary in the presence of gastric cancer[97]. This variation could contribute towards increased phenol production in oesophago-gastric cancer patients as has been demonstrated in urine (Section 4.1), plasma (Section 4.2) and exhaled breath[25].

This section has utilised 16S bacterial sequencing to identify the presence of bacteria within the stomach which contain the *tyrosine phenol-lyase* gene, and therefore have the potential to convert tyrosine to phenol within the stomach.

4.6.3 Methods

Local ethics committee approval was obtained for this experiment (ICHTB HTA Licence: 12275; REC Wales Approval: 12/WA/0196; Tissue bank approval number R15097).

Samples were collected from *Helicobacter Pylori* negative patients undergoing surgical resection of gastric adenocarcinoma. Tissue samples were collected from gastric adenocarcinoma and matched healthy mucosa from the same patients (collected at least 10cm away from the tumour). Samples were immediately placed in liquid nitrogen and stored at -80°C prior to analysis.

During DNA extraction tissue samples were processed using the PowerLyzer© PowerSoil DNA Isolation kit (MoBio Laboratories, Qiagen, Hilden, Germany). Tissue samples were weighed and placed in a homogenisation tube with buffering solutions. Homogenisation was performed using the PowerLyzer© bead beater (Qiagen, Hilden, Germany) at 8000rpm for three minutes. Samples were then centrifuged at 14,000g for 10 minutes to pellet cell debris. The supernatant was transferred to a micro-centrifuge tube and protein precipitation solution added and incubated at 20°C for 10 minutes. Samples were centrifuged again at 14,000g for 10 minutes. The supernatant was added to binding matrix and incubated for 5 minutes then transferred to a SPIN™ filter and centrifuged at 14,000g for five minutes. This process was repeated twice. Buffer was then added to the SPIN™ filter and centrifuged. The SPIN™ tube was dried at room temperature for 10 minutes. Elution buffer was then added to the SPIN™ filter and incubated at 55°C for five minutes. The sample was then centrifuged at 14,000g for 2 minutes to elute DNA.

Successfully extracted DNA then underwent real time quantitative PCR to amplify the 16S gene followed by metataxonomic analysis on the Illumina MiSeq platform (San Diego, CA, USA). Data analysis was undertaken with Mothur (University of Michigan, available from http://www.mothur.org/). All samples with a final sequence number below 1000 were excluded from further analysis. Bacteria which have the potential to contain the *tyrosine phenol-lyase* gene were identified using the KEGG dataset[37,38] and other available literature.

4.6.4 Results

Eleven samples had sequence numbers over 1000 (6 cancer samples, and 5 samples of matched healthy stomach mucosa). The median patient age was 65 (Range 50-81). Two patients had a history of using proton pump inhibitors. All patients had advanced disease stages either with T3/4 disease or nodal involvement.

Consistent with previous studies the dominant bacterial phyla within the stomach were *Firmicutes and Bacteroidetes*. Genus level analysis revealed the presence of a number of bacteria which are known to contain the *tyrosine phenol-lyase* enzyme (*Fusobacteria, Clostridium, and Escherichia*). All eleven samples contained one or more type of phenol-producing bacteria. *Clostridium* was present in all samples, *Escherichia* in six samples (55%), and *Fusobacteria* in five (45%). The median percentage of bacteria which potentially contained the *tyrosine phenol-lyase* gene was 4.87% (range 2.17% to 7.46%). There was no difference in the median percentage of *tyrosine phenol lyase* containing bacteria in gastric cancer samples (3.96%) and healthy mucosa (4.87%, MWU p =1).

4.6.5 Discussion

This experiment has provided evidence that bacteria containing the *tyrosine phenol lyase* gene are present within the stomach microbiome. These included *Clostridium, Escherichia* and *Fusobacteria*. The presence of these bacteria within the stomach microbial community indicates that there is the potential for tyrosine to be converted to phenol within the stomach via bacterial action. Both phenol and tyrosine have been demonstrated to be present within gastric content samples in Section 4.4. The presence of tyrosine provides a potential substrate for these bacteria to act upon to produce phenol within gastric juice. This reaction was demonstrated to be occurring within gastric juice in Section 4.5 where D4-labelled tyrosine was being converted to equivalently D4-labelled phenol. The identification of bacteria with the potential to facilitate this reaction (which contain the *tyrosine phenol-lyase* gene) has provided the necessary evidence to establish that stomach bacteria have the potential to modulate the conversion of tyrosine to phenol within the stomach.

This conversion of tyrosine to phenol within the stomach is reliant upon the gastric microbiome including bacteria which contain the *tyrosine phenol-lyase* gene. In the small set of patients included in the present analysis, all eleven patient samples contained one or more phenol-producing bacteria. However, the composition of the gastric microbiome can be influenced by a number of factors and specifically changes in pH are known to influence the gastric microbiota[160]. Patients with symptoms of upper gastrointestinal disease are commonly prescribed proton pump inhibitors to reduce acid secretion. These medications increase stomach pH and have been associated with greater microbial diversity within the stomach[161,162]. Gastric cancer patients have also been shown to have a higher stomach pH than healthy controls (6.6 vs 2.9, MWU $p < 0.001$)[163]. Cultures from patients with gastric cancer harbour higher numbers of micro-organisms and more anaerobic bacteria (e.g.:*Clostridia* and *Bacteroidetes*) than those from normal mucosa[160]. In canines, proton pump inhibitor use leads to an increased relative abundance of *Fusobacteria*[164]. These results may indicate that rises in intra-gastric pH may lead to an increase in phenol producing bacteria within the stomach. Although no significant differences between proportions of phenol-producing bacteria were demonstrated in the present study, the number of patient samples analysed was small, and larger studies would be necessary to draw more definitive conclusions regarding changes in bacterial make-up relating to gastric cancer.

This study has demonstrated the presence of bacteria which contain the *tyrosine phenol lyase* gene within a small set of gastric cancer samples and matched normal mucosa. This provides further evidence that the stomach microbiome has the potential to convert tyrosine to phenol in addition to the results of Section 4.5 where deuterium-labelled tyrosine was converted to deuterium-labelled phenol. The action of these bacteria may be responsible for the production of phenol within the gastric content which was demonstrated in Section 4.4. However, based on these results alone it is only possible to state that these bacteria appear to be present within the stomach. Although they contain the relevant gene, and have the potential to facilitate this reaction, it is not possible to definitively establish that they are biologically active.

4.6.6 Conclusions

This experiment has demonstrated the presence of *Clostridia, Escherichia* and *Fusobacteria* within the stomach microbiome. All of these bacteria contain the *tyrosine phenol-lyase* gene and have the potential to convert tyrosine to phenol within the stomach.

4.7 Conclusions of Phenol Experimental Section

This section of experiments has established the presence of bacteria containing the *tyrosine phenol lyase* gene within the stomach. This indicates that the bacteria within the stomach have the potential to convert tyrosine to phenol. This explains the results of Section 4.5 which indicated that deuterium-labelled tyrosine was converted to phenol within gastric juice. The presence of phenol within gastric juice was confirmed although this did not appear to be correlated to tyrosine concentration. Once produced within the stomach phenol appears to be transported within the systemic circulation due to the fact that plasma concentrations of phenol were increased in oesophago-gastric cancer patients relative to control patients. Phenol within the systemic circulation can then transported to the kidneys or lungs for excretion. Phenol was identified at increased concentrations within the urine of oesophago-gastric cancer patients relative to asymptomatic healthy volunteers, and has previously been validated as a non-invasive marker of oesophago-gastric cancer in exhaled breath[25].

The present analysis has provided a global profile of phenol production, transport and excretion throughout the body in healthy patients and those suffering with oesophago-gastric cancer. This helps to further our understanding of phenol production in this disease, and provides a biological explanation for the increased concentrations of phenol identified in urine as part of the current work, and also within exhaled breath[25]. Although p-cresol was identified to be elevated within the urine of oesophago-gastric cancer patients this compound was not identified above the limit of detection in other biofluids of oesophago-gastric cancer or healthy patients.

CHAPTER 5 - SUMMARY, CONCLUSIONS AND FUTURE WORK

This thesis has undertaken a systematic investigation of phenylalanine and tyrosine metabolism in oesophago-gastric cancer. It has also investigated how this metabolic pathway may relate to phenol production in these patients.

Homogentisate metabolism has been demonstrated to be dysfunctional within oesophago-gastric cancer patients. There was a systemic reduction in homogentisate concentrations within dried blood spot samples of oesophago-gastric cancer patients and controls. Corresponding changes in enzyme expression have been demonstrated to explain these differences using qPCR and immunohistochemistry. Specifically, homogentisate 1,2 dioxygenase (the enzyme responsible for homogentisate breakdown) was upregulated in oesophageal adenocarcinoma tissues, whilst hydroxyphenylpyruvate dioxygenase (responsible for converting hydroxyphenylpyruvate to homogentisate) was downregulated in gastric cancer.

It will be necessary for future work to validate the metabolic effect of the identified changes in enzyme expression in order to establish if these changes directly lead to reduced systemic concentrations of homogentisate. This work package would initially involve analysing metabolic changes in cultures of oesophageal and gastric cancer cells. Although the stability of homogentisate within cell culture medium would need to be assessed, spiking of cell culture medium with large concentrations of homogentisate would potentially circumvent the issues identified in the present analysis of patient plasma samples where homogentisate concentrations were below the limit of detection due to compound stability. It could be possible to use LC-MS to identify changes in homogentisate concentration in these different cell types. It would be anticipated that when oesophageal cancer cells (where homogentisate 1,2 dioxygenase is upregulated relative to normal oesophageal cells) are allowed to metabolise added homogentisate for a defined period of time, lower final concentrations of homogentisate would be seen relative to normal oesophageal cells treated under the same conditions. In gastric cancer cells (where homogentisate 1,2 dioxygenase was not upregulated) there is unlikely to be any differences in homogentisate concentration between normal and cancer cells when this compound is added to cell cultures. However, spiking gastric cancer cells with hydroxyphenylpyruvate would not lead to increased homogentisate production as it would in normal stomach mucosal cells (due to reduced activity of hydroxyphenylpyruvate dioxygenase activity in

gastric cancer cells). Following these initial assessments in cell-cultures, perturbation experiments could be used to 'knock in' or knock out' these relevant genes and assess functional response. This would involve assessing cell proliferation and behaviour following perturbation of the genes related to function of these enzymes. Animal models could also be utilised to assess the effect of these perturbed cell lines upon overall tumour metabolism. Mice models that are homogentisate 1,2 dioxygenase (HGD) deficient have previously been produced for assessment of alkaptonuria[62]. Use of these HGD-deficient mice would prevent any breakdown of homogentisate which may occur systemically either in the liver or kidneys. If a flank oesophageal tumour were given to these HGD-deficient mice this could be used to establish the contribution of the tumour alone to overall homogentisate metabolism. This could be compared to HGD-deficient control mice (without flank tumours), as well as 'wild-type' mice (not HGD deficient) with and without oesophageal flank tumours. This would establish the differences in overall systemic metabolism of homogentisate relating to the tumour itself and whether there are generalised changes in systemic metabolism of homogentisate relating to the presence of oesophageal tumours. This body of work would aim to further our understanding of how aromatic amino acid (and specifically homogentisate) metabolism is disturbed in oesophago-gastric cancer.

Future work will also need to assess function of enzymes related to homogentisate metabolism within areas Barrett's Oesophagus as this is a premalignant condition leading to the development on oesophageal adenocarcinoma. This would establish whether the changes seen in enzyme activity are a graduated change with a step-wise relationship of increasing alterations in activity of homogentisate 1,2 dioxygenase related to cancer development.

This work investigating homogentisate metabolism may lead to the development of novel non-invasive biomarkers for early detection of disease. In addition this work could lead to the future development of therapies which are able to target specific sections of this metabolic pathway for treatment of oesophageal or gastric cancer. A recent review has highlighted the need for identification of more effective and less toxic therapies for oesophageal cancer[165], and given the findings of this project these enzymes may represent one potential future therapeutic target.

The present work has also identified increased concentrations of phenol and p-cresol within the urine of oesophago-gastric cancer patients. Although phenol and p-cresol concentrations were significantly different between asymptomatic healthy volunteers and patients with oesophago-gastric cancer, these results did not reach the relevant threshold for a 'good test' in binary logistic regression modelling. Therefore should urine be used as a potential non-invasive test for diagnosis of oesophago-gastric cancer it would not be possible to use phenol and p-cresol alone for diagnosis. These compounds would need to be used as part of a panel of other compounds in order to improve diagnostic accuracy. Aldehydes and fatty acids have previously been used as part of a diagnostic model for this disease in urine[26], and it may be possible to combine these compounds to improve sensitivity and specificity of this test. Large scale clinical validation studies of urinary analysis for diagnosis of oesophago-gastric cancer using a panel of biomarkers (including phenol, p-cresol, aldehyde and fatty acids) are necessary in order to establish the effectiveness of this potential diagnostic test.

The presence of increased phenol concentrations within plasma has provided a transport mechanism by which phenol may be transferred within the systemic circulation to the lungs or kidneys for excretion. This discovery has been critical for the validation of exhaled breath or urine analysis for phenol concentration in the diagnosis of oesophago-gastric cancer. Once these compounds are produced in the area local to the tumour they must be transported in the systemic circulation for excretion by the lungs or kidneys. Identifying phenol at increased concentration within plasma samples has provided validity for this hypothesis that volatile compounds can be transported to distant parts of the body for excretion, where they can then be detected in exhaled breath or urine. Future studies should look to explore the relationship between concentrations of phenolic compounds in breath, urine and plasma samples taken at the same timepoint from an individual patient. This would establish the transfusion gradient of these compounds between the systemic circulation, lungs and kidneys.

This work has also established the presence of phenol-producing bacteria within the stomach, and identified that tyrosine appears to be converted to phenol within gastric juice. To definitively establish the presence and functional action of the *tyrosine phenol-lyase* gene within the stomach it will be necessary to develop an assay to measure this enzyme. This could be performed using qPCR for this

enzyme in stomach tissues samples or gastric juice. However, this technique is challenging as the genetic sequence of this enzyme is not well-preserved across bacterial phylum and different genera. This means a single qPCR primer cannot be built to incorporate all forms of this gene in different bacteria. Another potential approach may be to attempt to isolate or purify the *tyrosine phenol-lyase* protein, and determine the primary amino acid sequence of the enzyme to help identify the responsible microbe for production of this enzyme. It will be possible to apply these approaches to stomach tissue samples as well as gastric juice samples. This would establish whether the effect of tyrosine phenol-lyase is greatest within the stomach mucosal tissues or gastric juice itself.

Previous evidence has identified increased concentrations of tyrosine within gastric content[39,40]. Although these results were not reproduced in the present study, increased release of tyrosine into gastric content from the tumour would provide a potential source of this compound for *tyrosine phenol-lyase* to act upon within gastric juice. This would provide a potential explanation for the increased concentrations of phenol identified within plasma and urine as part of this work, and previous changes identified within exhaled breath[25]. In order to definitively establish whether tyrosine is being actively released from the tumour into the intraluminal gastrointestinal tract it would be necessary to 'track' tyrosine from the tumour and map it's course through the body. Radio-labelled amino acids have previously been developed and utilise the concept that tumours demonstrate increased uptake of amino acids due to changes in the transporter mechanism[166,167]. These markers are widely used in assessment of neurological tumours[168–171], but have also been demonstrated to be useful in assessment of prostate cancer[172], neuroendocrine tumours[173], and secondary liver metastases[174]. The utilisation of radiolabelled tyrosine markers with cross-sectional imaging such as computerised tomography (CT) would provide the ability to map tyrosine uptake by the tumour and subsequently identify its final course and whether this compound is shed into the intra-luminal gastrointestinal tract.

The overall aim of this work was to establish the mechanism responsible for phenol production in oesophago-gastric cancer patients and how this is linked to aromatic amino acid metabolism. It has been possible to use results of high-resolution mass spectrometry to inform a targeted molecular investigation of dysfunctional aromatic amino acid metabolism in oesophago-gastric cancer. This has

identified dysregulation of the enzymes responsible for aromatic amino acid breakdown. It was also possible to identify the presence of phenol-producing bacteria within the stomach, and demonstrate that tyrosine was being converted to phenol within gastric juice. A global profile of phenol concentration within multiple body compartments was also provided, with elevated concentrations of phenol within urine and plasma samples of oesophago-gastric cancer patients.

This work has helped to establish the potential mechanism responsible for phenol production in oesophago-gastric cancer. In doing so it has been possible to:

- Provide biological validation for the use of phenol as a marker of oesophago-gastric cancer in exhaled breath. By establishing the validity of this compound as a non-invasive marker of this disease this work will assist the introduction of exhaled breath testing into clinical practice for assessment of oesophago-gastric cancer risk.
- Provide an insight into the mechanisms responsible for dysfunctional aromatic amino acid metabolism in oesophago-gastric cancer. This work could potentially lead to the development of novel therapeutic targets for this disease in the future.

In summary, this work has identified specific sections of the aromatic amino acid breakdown pathway that are dysfunctional in oesophageal and gastric cancer patients. Tyrosine appears to be converted to phenol by bacteria within the stomach, and this compound is then transported within the blood to be excreted in urine or exhaled breath. This work provides greater insight into phenol production in the context of oesophago-gastric cancer and gives a biological explanation for the use of phenol as a non-invasive marker of this disease. Use of non-invasive biomarkers for early diagnosis of oesophago-gastric cancer will help facilitate diagnosis of this condition in early stages of disease. This will increase the number of patients who can be treated with curative intent and thereby improve survival.

REFERENCES

1. Torre LA, Bray F, Siegel RL, Ferlay J, Lortet-tieulent J, Jemal A. Global Cancer Statistics, 2012. CA a cancer J Clin. 2015;65(2):87–108.
2. Arnold M, Soerjomataram I, Ferlay J, Forman D. Global incidence of oesophageal cancer by histological subtype in 2012. Gut. 2015;64(3):381–7.
3. Chadwick G, Varagunam M, Brand C, Cromwell D, Maynard M, Riley S, et al. National Oesophago- Gastric Cancer Audit 2016. The Royal College of Surgeons England. 2016 [Last accessed 02/09/2017]. Available from: http://www.hqip.org.uk/public/cms/253/625/19/633/NationalOGCAuditReport2016.pdf?realName=ix9HOH.pdf&v=0
4. Hvid-Jensen F, Pedersen L, Drewes AM, Sørensen HT, Funch-Jensen P, Heart TN. Incidence of adenocarcinoma among patients with Barrett's esophagus. N Engl J Med. 2011 Oct 13;365(15):1375–83.
5. Dulai GS, Guha S, Kahn KL, Gornbein J, Weinstein WM. Preoperative prevalence of Barrett's esophagus in esophageal adenocarcinoma: a systematic review. Gastroenterology. 2002 Jan;122(1):26–33.
6. Bytzer P, Christensen PB, Damkier P, Vinding K, Seersholm N. Adenocarcinoma of the esophagus and Barrett's esophagus: a population-based study. Am J Gastroenterol. 1999 Jan;94(1):86–91.
7. Conio M, Blanchi S, Lapertosa G, Ferraris R, Sablich R, Marchi S, et al. Long-term endoscopic surveillance of patients with Barrett's esophagus. Incidence of dysplasia and adenocarcinoma: a prospective study. Am J Gastroenterol. 2003 Sep;98(9):1931–9.
8. Lagergren J, Bergström R, Lindgren A, Nyrén O. Symptomatic Gastroesophageal Reflux as a Risk Factor for Esophageal Adenocarcinoma. N Engl J Med; 1999 Mar 18;340(11):825–31.
9. Winters C, Spurling TJ, Chobanian SJ, Curtis DJ, Esposito RL, Hacker JF, et al. Barrett's esophagus. A prevalent, occult complication of gastroesophageal reflux disease. Gastroenterology. 1987 Jan;92(1):118–24.
10. Picardo SL, Maher SG, O'Sullivan JN, Reynolds J V. Barrett's to oesophageal cancer sequence: a model of inflammatory-driven upper gastrointestinal cancer. Dig Surg. 2012;29(3):251–60.
11. Hoyo C, Cook MB, Kamangar F, Freedman ND, Whiteman DC, Bernstein L, et al. Body mass index in relation to oesophageal and oesophagogastric junction adenocarcinomas: a pooled analysis from the International BEACON Consortium. Int J Epidemiol. 2012 Dec;41(6):1706–18.
12. Kubo A, Cook MB, Shaheen NJ, Vaughan TL, Whiteman DC, Murray L, et al. Sex-specific associations between body mass index, waist circumference and the risk of Barrett's oesophagus: a pooled analysis from the international BEACON consortium. Gut. 2013 Dec;62(12):1684–91.
13. Lagergren J. Influence of obesity on the risk of esophageal disorders. Nat Rev Gastroenterol Hepatol. 2011 Jun;8(6):340–7.
14. Kamangar F, Dores GM, Anderson WF. Patterns of cancer incidence, mortality, and prevalence across five continents: defining priorities to reduce cancer disparities in different geographic regions of the world. J Clin Oncol. 2006 May 10;24(14):2137–50.
15. Plummer M, Franceschi S, Vignat J, Forman D, de Martel C. Global burden of gastric cancer attributable to *Helicobacter pylori*. Int J Cancer. 2015 Jan 15;136(2):487–90.
16. Cancer incidence for common cancers. Cancer Research UK; [Last accessed 02/09/2017]. Available from: http://www.cancerresearchuk.org/cancer-info/cancerstats/incidence/commoncancers/
17. Keeble S, Abel GA, Saunders CL, McPhail S, Walter FM, Neal RD, et al. Variation in promptness of presentation among 10,297 patients subsequently diagnosed with one of 18 cancers: evidence from a National Audit of Cancer Diagnosis in Primary Care. Int J cancer. 2014 Sep 1;135(5):1220–8.
18. Tentzeris V, Lake B, Cherian T, Milligan J, Sigurdsson A. Poor awareness of symptoms of oesophageal cancer. Interact Cardiovasc Thorac Surg. 2011 Jan;12(1):32–4.
19. Lyratzopoulos G, Neal RD, Barbiere JM, Rubin GP, Abel GA. Variation in number of general practitioner consultations before hospital referral for cancer: findings from the 2010 National Cancer Patient Experience Survey in England. Lancet Oncol. 2012;13(4):353–65.
20. Arvanitakis C, Nikopoulos A, Giannoulis E, Theoharidis A, Georgilas V, Fotiou H, et al. The impact of early or late diagnosis on patient survival in gastric cancer in Greece.

Hepatogastroenterology. 1992 Aug;39(4):355–7.
21. NICE. Suspected cancer recognition and referral: site or type of cancer - NICE Pathways. 2016; [Last accessed 02/09/2017]; Available from https://www.nice.org.uk/guidance/ng12
22. Mehta SP, Bailey D, Davies N. Comparative outcome of oesophagogastric cancer in younger patients. Ann R Coll Surg Engl. 2010 Sep;92(6):515–8.
23. Miyamoto A, Kuriyama S, Nishino Y, Tsubono Y, Nakaya N, Ohmori K, et al. Lower risk of death from gastric cancer among participants of gastric cancer screening in Japan: A population-based cohort study. Prev Med (Baltim). 2007;44(1):12–9.
24. Lagergren J, Ye W, Bergström R, Nyrén O, WJ B, CC B, et al. Utility of Endoscopic Screening for Upper Gastrointestinal Adenocarcinoma. JAMA. American Medical Association; 2000 Aug 23;284(8):961.
25. Kumar S, Huang J, Abbassi-Ghadi N, Mackenzie HA, Veselkov KA, Hoare JM, et al. Mass Spectrometric Analysis of Exhaled Breath for the Identification of Volatile Organic Compound Biomarkers in Esophageal and Gastric Adenocarcinoma. Ann Surg. 2015 Jan 8;262(6):981–90.
26. Huang J, Kumar S, Abbassi-Ghadi N, Spaněl P, Smith D, Hanna GB. Selected ion flow tube mass spectrometry analysis of volatile metabolites in urine headspace for the profiling of gastro-esophageal cancer. Anal Chem. 2013 Mar 19;85(6):3409–16.
27. Amal H, Leja M, Funka K, Skapars R, Sivins A, Ancans G, et al. Detection of precancerous gastric lesions and gastric cancer through exhaled breath. Gut. 2016 Mar;65(3):400–7.
28. Dweik RA, Amann A. Exhaled breath analysis: the new frontier in medical testing. J Breath Res. NIH Public Access; 2008 Sep;2(3).
29. Pauling L, Robinson AB, Teranishi R, Cary P. Quantitative analysis of urine vapor and breath by gas-liquid partition chromatography. Proc Natl Acad Sci U S A. 1971 Oct;68(10):2374–6.
30. Phillips M, Gleeson K, Hughes JM, Greenberg J, Cataneo RN, Baker L, et al. Volatile organic compounds in breath as markers of lung cancer: a cross-sectional study. Lancet. 1999 Jun 5;353(9168):1930–3.
31. Phillips M, Altorki N, Austin JHM, Cameron RB, Cataneo RN, Greenberg J, et al. Prediction of lung cancer using volatile biomarkers in breath. Cancer Biomark. 2007 Jan;3(2):95–109.
32. Hakim M, Broza YY, Barash O, Peled N, Phillips M, Amann A, et al. Volatile organic compounds of lung cancer and possible biochemical pathways. Chem Rev. 2012 Nov 14;112(11):5949–66.
33. Spanel P, Smith D, Holland TA, Al Singary W, Elder JB. Analysis of formaldehyde in the headspace of urine from bladder and prostate cancer patients using selected ion flow tube mass spectrometry. Rapid Commun Mass Spectrom. 1999 Jan;13(14):1354–9.
34. Silva C, Passos M, Câmara J. microextraction, mass spectrometry and metabolomic approaches for detection of potential urinary cancer biomarkers—A powerful strategy for breast cancer diagnosis. Talanta. Elsevier B.V.; 2012 Jan 30;89:360–8.
35. Kumar S, Huang J, Cushnir J. Selected Ion Flow Tube-MS Analysis of Headspace Vapor from Gastric Content for the Diagnosis of Gastro-Esophageal Cancer. Anal Chem. 2012; 84(21): 9550-7.
36. Kumar S, Huang J, Abbassi-ghadi N, Patrik S, Smith D, Hanna GB. Selected Ion Flow Tube Mass Spectrometry Analysis of Exhaled Breath for Volatile Organic Compound Profiling of Esophago-Gastric Cancer. Anal Chem. 2013;85(12):6121–8.
37. Kanehisa M, Goto S. KEGG: kyoto encyclopedia of genes and genomes. Nucleic Acids Res. 2000 Jan 1;28(1):27–30.
38. Kanehisa M, Sato Y, Kawashima M, Furumichi M, Tanabe M. KEGG as a reference resource for gene and protein annotation. Nucleic Acids Res. 2016 Jan 4;44(D1):D457-62.
39. Deng K, Lin S, Zhou L, Li Y, Chen M, Wang Y, et al. High levels of aromatic amino acids in gastric juice during the early stages of gastric cancer progression. PLoS One. 2012 Jan;7(11):e49434.
40. Deng K, Lin S, Zhou L, Geng Q, Li Y, Xu M, et al. Three aromatic amino acids in gastric juice as potential biomarkers for gastric malignancies. Anal Chim Acta. Elsevier B.V.; 2011 May 23;694(1–2):100–7.
41. Kakihara Y, Ichihara K. Studies of phenol formation. I. Method of the determination of phenol and its microbial formation from tyrosine and tyrosine derivatives. Med J Osaka Univ. 1953;
42. Bone E, Tamm A, Hill M. The production of urinary phenols by gut bacteria and their possible role in the causation of large bowel cancer. Am J Clin Nutr. 1976 Dec;29(12):1448–54.
43. Womack M, Rose W. Feeding experiments with mixtures of highly purified amino acids: VI The relation of pehnylalanine and tyrosine to growth. J Biol Chem. 1934;

44. Lichter-Konecki U, Hipke C, Konecki D. Human Phenylalanine Hydroxylase Gene Expression in Kidney and Other Nonhepatic Tissues. Mol Genet Metab. 1999;316:308–16.
45. Neurauter G, Grahmann A V, Klieber M, Zeimet A, Ledochowski M, Sperner-unterweger B, et al. Serum phenylalanine concentrations in patients with ovarian carcinoma correlate with concentrations of immune activation markers and of isoprostane-8. Cancer Lett. Elsevier Ireland Ltd; 2008;272(1):141–7.
46. Ploder M, Neurauter G, Spittler A, Schroecksnadel K, Roth E, Fuchs D. Serum phenylalanine in patients post trauma and with sepsis correlate to neopterin concentrations. 2008;303–7.
47. Al Hafid N, Christodoulou J. Phenylketonuria: a review of current and future treatments. Transl Pediatr.; 2015 Oct;4(4):304–17.
48. Matalon R, Michals K. Phenylketonuria: screening, treatment and maternal PKU. Clin Biochem; 1991 Aug;24(4):337–42.
49. Scott CR. The genetic tyrosinemias. Am J Med Genet - Semin Med Genet. 2006 May 15;142 C(2):121–6.
50. Sniderman King L, Trahms C, Scott CR. Tyrosinemia Type I. GeneReviews(®). University of Washington, Seattle; 1993. [Last accessed 02/09/2017]. Available from: https://www.ncbi.nlm.nih.gov/books/NBK1515/
51. Davit-Spraul A, Romdhane H, Poggi-Bach J. Simple and fast quantification of nitisone (NTBC) using liquid chromatography-tandem mass spectrometry method in plasma of tyrosinemia type 1 patients. J Chromatogr Sci. 2012 May;50(5):446–9.
52. Lindstedt S, Holme E, Lock EA, Hjalmarson O, Strandvik B. Treatment of hereditary tyrosinaemia type I by inhibition of 4-hydroxyphenylpyruvate dioxygenase. Lancet (London, England). 1992 Oct 3;340(8823):813–7.
53. Hall MG, Wilks MF, Provan WM, Eksborg S, Lumholtz B. Pharmacokinetics and pharmacodynamics of NTBC (2-(2-nitro-4-fluoromethylbenzoyl)-1,3-cyclohexanedione) and mesotrione, inhibitors of 4-hydroxyphenyl pyruvate dioxygenase (HPPD) following a single dose to healthy male volunteers. Br J Clin Pharmacol. 2001 Aug;52(2):169–77.
54. Cerone R, Holme E, Schiaffino M, Caruso U, Maritano L, Romano C. Tyrosinemia type III: diagnosis and ten-year follow-up. Acta Paediatr.; 1997 Sep;86(9):1013–5.
55. Garrod AE. The Incidence of Alkaptonuria: A Study in Chemical Individuality. Lancet. 1902;ii:1616–20.
56. La Du BN, Zannoni VG, Laster L, Seegmiller JE. The nature of the defect in tyrosine metabolism in alcaptonuria. J Biol Chem. 1958 Jan;230(1):251–60.
57. O'brien WM, La Du BN, Bunim JJ. Biochemical, pathologic and clinical aspects of alcaptonuria, ochronosis and ochronotic arthropathy. Am J Med. Elsevier; 1963 Jun;34(6):813–38.
58. Phornphutkul C, Introne W PM et al. Alkaptonuria Natural History of Alkaptonuria. N Engl J Med. 2002;347(26).
59. Keller JM, Macaulay W, Nercessian OA, Jaffe IA. New developments in ochronosis: review of the literature. Rheumatol Int.; 2005 Mar 21;25(2):81–5.
60. Helliwell TR, Gallagher JA, Ranganath L. Alkaptonuria – a review of surgical and autopsy pathology. Histopathology. 2008 Mar 10;53(5):503–12.
61. Ranganath LR, Jarvis JC, Gallagher J a. Recent advances in management of alkaptonuria. J Clin Pathol. 2013;66:367–73.
62. Taylor AM, Preston AJ, Paulk NK, Sutherland H, Keenan CM, Wilson PJM, et al. Ochronosis in a murine model of alkaptonuria is synonymous to that in the human condition. Osteoarthr Cartil.; 2012 Aug;20(8):880–6.
63. Liesenfeld DB, Habermann N, Owen RW, Scalbert A, Ulrich CM. Review of mass spectrometry-based metabolomics in cancer research. Cancer Epidemiol Biomarkers Prev. 2013 Dec;22(12):2182–201.
64. Lai H-S, Lee J-C, Lee P-H, Wang S-T, Chen W-J. Plasma free amino acid profile in cancer patients. Semin Cancer Biol. 2005 Aug;15(4):267–76.
65. Bozzetti F, Migliavacca S, Scotti A, Bonalumi MG, Scarpa D, Baticci F, et al. Impact of cancer, type, site, stage and treatment on the nutritional status of patients. Ann Surg. 1982 Aug;196(2):170–9.
66. Riccardi D, Allen K. Nutritional Management of Patients With Esophageal and Esophagogastric Junction Cancer. Cancer Control. 1999 Jan;6(1):64–72.
67. Cheng Y, Xie G, Chen T, Qiu Y. Distinct urinary metabolic profile of human colorectal cancer. J Proteome Res. 2012; 11 (2), 1354-1363.
68. Whiting P, Rutjes A. QUADAS-2: A revised tool for the quality assessment of diagnostic

accuracy studies. Ann Intern Med. 2011;155(4):529–36.
69. Whiting P. Sources of Variation and Bias in Studies of Diagnostic Accuracy. Ann Intern Med. American College of Physicians; 2004 Feb 3;140(3):189.
70. Zhang X, Xu L, Shen J, Cao B, Cheng T. Metabolic signatures of esophageal cancer : NMR-based metabolomics and UHPLC-based focused metabolomics of blood serum. Biochim Biophys Acta.; 2013;1832(8):1207–16.
71. Zhang J, Bowers J, Liu L, Wei S, Gowda GAN, Hammoud Z, et al. Esophageal cancer metabolite biomarkers detected by LC-MS and NMR methods. PLoS One; 2012 Jan;7(1):e30181.
72. Miyagi Y, Higashiyama M, Gochi A, Akaike M, Ishikawa T, Miura T, et al. Plasma free amino acid profiling of five types of cancer patients and its application for early detection. PLoS One. 2011 Jan;6(9):e24143.
73. Ikeda A, Nishiumi S, Shinohara M, Yoshie T, Hatano N, Okuno T, et al. Serum metabolomics as a novel diagnostic approach for gastrointestinal cancer. Biomed Chromatogr. 2012 May;26(5):548–58.
74. Naini a B, Dickerson JW, Brown MM. Preoperative and postoperative levels of plasma protein and amino acid in esophageal and lung cancer patients. Cancer. 1988 Jul 15;62(2):355–60.
75. Norton JA, Gorschboth CM, Wesley RA, Burt ME, Brennan MF. Fasting plasma amino acid levels in cancer patients. Cancer. 1985 Sep 1;56(5):1181–6.
76. Lian W, Ma DJ, Xu X, Chen Y, Wu YL. Rapid high-performance liquid chromatography method for determination of tryptophan in gastric juice. J Dig Dis. 2012 Feb;13(2):100–6.
77. Segawa K, Nakazawa S, Tsukamoto Y, Yamaguchi H, Goto H, Kurita Y. Amino acid patterns in human gastric juice in health and gastric disease. Jpn J Med. 1985 Aug;24(3):244–9.
78. Abasov I. Chromatographic analysis of free amino acids of gastric juice in patients with cancer and other stomach diseases. J Gastroenterol. 1969;5:269–73.
79. Hasim A, Ma H, Mamtimin B, Abudula A, Niyaz M, Zhang L-W, et al. Revealing the metabonomic variation of EC using ^{1}H-NMR spectroscopy and its association with the clinicopathological characteristics. Mol Biol Rep. 2012 Sep;39(9):8955–64.
80. Davis VW, Schiller DE, Eurich D, Sawyer MB. Urinary metabolomic signature of esophageal cancer and Barrett's esophagus. World J Surg Oncol. World Journal of Surgical Oncology; 2012;10(1):1.
81. Song H, Wang L, Liu H-L, Wu X-B, Wang H-S, Liu Z-H, et al. Tissue metabolomic fingerprinting reveals metabolic disorders associated with human gastric cancer morbidity. Oncol Rep. 2011 Aug;26(2):431–8.
82. Wu H, Xue R, Lu C, Deng C, Liu T, Zeng H, et al. Metabolomic study for diagnostic model of oesophageal cancer using gas chromatography/mass spectrometry. J Chromatogr B. 2009;877(27):3111–7.
83. Hirayama A, Kami K, Sugimoto M, Sugawara M, Toki N, Onozuka H, et al. Quantitative metabolome profiling of colon and stomach cancer microenvironment by capillary electrophoresis time-of-flight mass spectrometry. Cancer Res. 2009 Jun 1;69(11):4918–25.
84. Qiu Y, Cai G, Su M, Chen T, Liu Y, Xu Y, et al. Urinary metabonomic study on colorectal cancer. J Proteome Res. 2010;9(3):1627–34.
85. Silva CL, Passos M, Câmara JS. Investigation of urinary volatile organic metabolites as potential cancer biomarkers by solid-phase microextraction in combination with gas chromatography-mass spectrometry. Br J Cancer. 2011 Dec 6;105(12):1894–904.
86. Sovova K, Wiggins T, Markar SR, Hanna GB, Kumar S, Huang J, et al. Quantification of phenol in urine headspace using SIFT-MS and investigation of variability with respect to urinary concentration. Anal Methods. The Royal Society of Chemistry; 2015;7(12):3409–16.
87. Schettgen T, Alt A, Dewes P, Kraus T. Simple and sensitive GC/MS-method for the quantification of urinary phenol, o- and m-cresol and ethylphenols as biomarkers of exposure to industrial solvents. J Chromatogr B Analyt Technol Biomed Life Sci. 2015 Jul 15;995–996:93–100.
88. Kawamura I, Moldawer LL, Keenan RA, Batist G, Bothe A, Bistrian BR, et al. Altered Amino Acid Kinetics in Rats with Progressive Tumor Growth Altered Amino Acid Kinetics in Rats with Progressive Tumor Growth1. 1982;824–9.
89. Engbring JA, Kleinman HK. The basement membrane matrix in malignancy. J Pathol. 2003 Jul;200(4):465–70.
90. Seftor REB, Seftor EA, Koshikawa N, Meltzer PS, Gardner LMG, Bilban M, et al. Cooperative Interactions of Laminin 5 γ 2 Chain , Matrix Metalloproteinase-2 , and Membrane Type-1-Matrix / Metalloproteinase Are Required for Mimicry of Embryonic Vasculogenesis by

Aggressive Melanoma Embryonic Vasculogenesis by Aggressive Melanoma 1. Cancer Res. 2001;61:6322–7.
91. Elsden SR, Hilton MG, Waller JM. The end products of the metabolism of aromatic amino acids by Clostridia. Arch Microbiol. 1976 Apr 1;107(3):283–8.
92. Scanlan PD, Shanahan F, Clune Y, Collins JK, O'Sullivan GC, O'Riordan M, et al. Culture-independent analysis of the gut microbiota in colorectal cancer and polyposis. Environ Microbiol. 2008;10(3):789–98.
93. Correa P. Human gastric carcinogenesis: a multistep and multifactorial process--First American Cancer Society Award Lecture on Cancer Epidemiology and Prevention. Cancer Res. 1992 Dec 15;52(24):6735–40.
94. Uemura N, Okamoto S, Yamamoto S, Matsumura N, Yamaguchi S, Yamakido M, et al. Helicobacter pylori infection and the development of gastric cancer. N Engl J Med. 2001 Sep 13;345(11):784–9.
95. Bik EM, Eckburg PB, Gill SR, Nelson KE, Purdom EA, Francois F, et al. Molecular analysis of the bacterial microbiota in the human stomach. Proc Natl Acad Sci U S A. 2006 Jan 17;103(3):732–7.
96. Andersson AF, Lindberg M, Jakobsson H, Bäckhed F, Nyrén P, Engstrand L. Comparative analysis of human gut microbiota by barcoded pyrosequencing. PLoS One. 2008 Jan;3(7):e2836.
97. Eun CS, Kim BK, Han DS, Kim SY, Kim KM, Choi BY, et al. Differences in gastric mucosal microbiota profiling in patients with chronic gastritis, intestinal metaplasia, and gastric cancer using pyrosequencing methods. Helicobacter. 2014 Dec;19(6):407–16.
98. Maldonado-Contreras A, Goldfarb KC, Godoy-Vitorino F, Karaoz U, Contreras M, Blaser MJ, et al. Structure of the human gastric bacterial community in relation to Helicobacter pylori status. ISME J. 2011 Apr;5(4):574–9.
99. Enei H, Matsui H, Yamashita K, Okumura S, Yamada H. Distribution of tyrosine phenol lyase in microorganisms. Agric Biol Chem. 1972;36(11):1861–8.
100. Gall A, Fero J, McCoy C, Claywell BC, Sanchez CA, Blount PL, et al. Bacterial Composition of the Human Upper Gastrointestinal Tract Microbiome Is Dynamic and Associated with Genomic Instability in a Barrett's Esophagus Cohort. PLoS One. 2015;10(6):e0129055.
101. Liu N, Ando T, Ishiguro K, Maeda O, Watanabe O, Funasaka K, et al. Characterization of bacterial biota in the distal esophagus of Japanese patients with reflux esophagitis and Barrett's esophagus. BMC Infect Dis. 2013;13:130.
102. Pei Z, Bini EJ, Yang L, Zhou M, Francois F, Blaser MJ. Bacterial biota in the human distal esophagus. Proc Natl Acad Sci U S A. 2004 Mar 23;101(12):4250–5.
103. Smith D, Spanel P. Selected ion flow tube mass spectrometry (SIFT-MS) for on-line trace gas analysis. Mass Spectrom Rev. 2005;24(5):661–700.
104. Arthur CL, Pawliszyn J. Solid phase microextraction with thermal desorption using fused silica optical fibers. Anal Chem. American Chemical Society; 1990 Oct;62(19):2145–8.
105. Spietelun A, Pilarczyk M, Kloskowski A, Namieśnik J. Current trends in solid-phase microextraction (SPME) fibre coatings. Chem Soc Rev. 2010 Nov;39(11):4524–37.
106. Gionfriddo E, Souza-Silva ÉA, Pawliszyn J. Headspace versus direct immersion solid phase microextraction in complex matrixes: investigation of analyte behavior in multicomponent mixtures. Anal Chem. 2015 Aug 18;87(16):8448–56.
107. Kataoka H, Lord HL, Pawliszyn J. Applications of solid-phase microextraction in food analysis. J Chromatogr A. 2000;880(1):35–62.
108. Eisert R, Levsen K. Solid-phase microextraction coupled to gas chromatography: A new method for the analysis of organics in water. J Chromatogr A. 1996 May;733(1–2):143–57.
109. Buchholz KD, Pawliszyn J. Optimization of solid-phase microextraction conditions for determination of phenols. Anal Chem. American Chemical Society; 1994 Jan;66(1):160–7.
110. de Loor H, Bammens B, Evenepoel P, De Preter V, Verbeke K, Mahadevan MS, et al. Gas chromatographic-mass spectrometric analysis for measurement of p-cresol and its conjugated metabolites in uremic and normal serum. Clin Chem. 2005 Aug;51(8):1533–5.
111. Toriba A, Homma C, Kita M, Uozaki W, Boongla Y, Orakij W, et al. Simultaneous determination of polycyclic aromatic hydrocarbon quinones by gas chromatography-tandem mass spectrometry, following a one-pot reductive trimethylsilyl derivatization. J Chromatogr A. 2016 Aug 12;1459:89–100.
112. Cudjoe E, Bojko B, Togunde P, Pawliszyn J. In vivo solid-phase microextraction for tissue bioanalysis. Bioanalysis. 2012 Nov;4(21):2605–19.
113. Bojko B, Gorynski K, Gomez-Rios GA, Knaak JM, Machuca T, Spetzler VN, et al. Solid phase

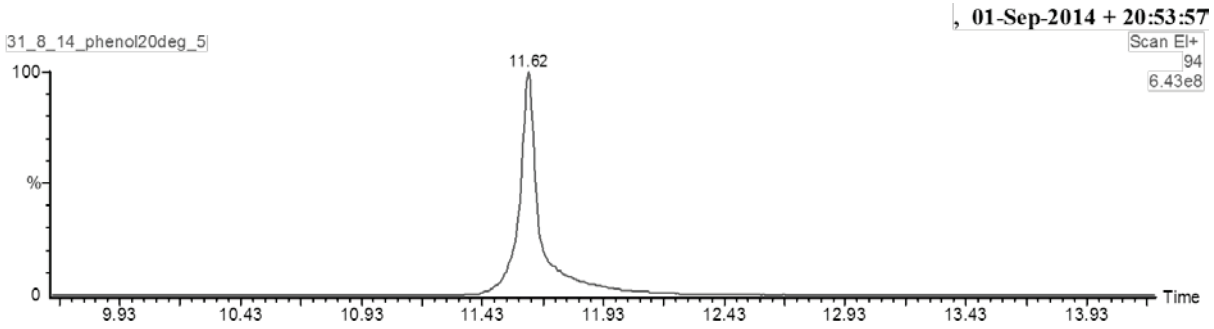
microextraction fills the gap in tissue sampling protocols. Anal Chim Acta. 2013 Nov 25;803:75–81.
114. Buszewski B, Ulanowska A, Ligor T, Jackowski M, Kłodzińska E, Szeliga J. Identification of volatile organic compounds secreted from cancer tissues and bacterial cultures. J Chromatogr B Analyt Technol Biomed Life Sci. 2008 Jun 1;868(1–2):88–94.
115. Sigma Aldrich. Guide to Solid Phase Extraction [Last accessed 02/09/2017]. Available from: http://www.sigmaaldrich.com/Graphics/Supelco/objects/4600/4538.pdf
116. Restek Solvent Expansion Calculator [Last accessed 02/09/2017]. Available from: http://www.restek.com/images/calcs/calc_backflash.htm
117. Munch JW. Determination of Phenols in Drinking Water. US Environ Prot Agency, Washingt DC EPA/815/R-00/014. 2000;(April):1–46.
118. Hušek P. Rapid derivatization and gas chromatographic determination of amino acids. J Chromatogr A. Elsevier; 1991 Aug;552:289–99.
119. Salazar C, Armenta JM, Cortés DF, Shulaev V. Combination of an AccQ·Tag-ultra performance liquid chromatographic method with tandem mass spectrometry for the analysis of amino acids. Methods Mol Biol. 2012;828:13–28.
120. Sharma G, Attri SV, Behra B, Bhisikar S, Kumar P, Tageja M, et al. Analysis of 26 amino acids in human plasma by HPLC using AQC as derivatizing agent and its application in metabolic laboratory. Amino Acids. 2014 May;46(5):1253–63.
121. Wang H, McNeil YR, Yeo TW, Anstey NM. Simultaneous determination of multiple amino acids in plasma in critical illness by high performance liquid chromatography with ultraviolet and fluorescence detection. J Chromatogr B Analyt Technol Biomed Life Sci. 2013 Dec 1;940:53–8.
122. Xie Y, Li Z. Determination of 18 Types of Amino Acids in the Serum of Ischemic Stroke Patients by High Performance Liquid Chromatography-diode Array Detector Derivatized with 6-Aminoquinolyl-N-hydroxysuccinimidyl Carbamate. Cell Biochem Biophys. 2015 Sep;73(1):111–5.
123. Hesse A, Weller MG. Protein Quantification by Derivatization-Free High-Performance Liquid Chromatography of Aromatic Amino Acids. J Amino Acids. 2016;2016:8.
124. Hughes AT, Milan AM, Davison AS, Christensen P, Ross G, Gallagher JA, et al. Serum markers in alkaptonuria: simultaneous analysis of homogentisic acid, tyrosine and nitisinone by liquid chromatography tandem mass spectrometry. Ann Clin Biochem. 2015;52(Pt 5):597–605.
125. Hughes A, Milan A, Christensen P, Ross G, Davison A, Gallagher J, et al. Urine homogentisic acid and tyrosine: Simultaneous analysis by liquid chromatography tandem mass spectrometry. J Chromatogr B Anal Technol Biomed Life Sci. Elsevier B.V.; 2014;963:106–12.
126. Annesley TM. Ion suppression in mass spectrometry. Clin Chem. 2003 Jul;49(7):1041–4.
127. Gosetti F, Mazzucco E, Zampieri D, Gennaro MC. Signal suppression/enhancement in high-performance liquid chromatography tandem mass spectrometry. J Chromatogr A. 2010 Jun 18;1217(25):3929–37.
128. Matuszewski BK, Constanzer ML, Chavez-Eng CM. Strategies for the assessment of matrix effect in quantitative bioanalytical methods based on HPLC-MS/MS. Anal Chem. 2003 Jul 1;75(13):3019–30.
129. Bory C, Boulieu R, Chantin C, Mathieu M. Homogentisic acid determined in biological fluids by HPLC. Clin Chem. 1989 Feb;35(2):321–2.
130. Pitt BM. Oxidation of phenylpyruvates to aromatic aldehydes and oxalate. Nature. 1962 Oct 20;196:272–3.
131. Guthrie R, Susi A. A Simple Method for Detecting Phenylketonuria in Large Populations of Newborn Infants. Pediatrics. 1963 Sep;32:338–43.
132. la Marca G, Malvagia S, Materazzi S, Della Bona ML, Boenzi S, Martinelli D, et al. LC-MS/MS method for simultaneous determination on a dried blood spot of multiple analytes relevant for treatment monitoring in patients with tyrosinemia type I. Anal Chem. 2012 Jan 17;84(2):1184–8.
133. Bártl J, Chrastina P, Krijt J, Hodík J, Pešková K, Kožich V. Simultaneous determination of cystathionine, total homocysteine, and methionine in dried blood spots by liquid chromatography/tandem mass spectrometry and its utility for the management of patients with homocystinuria. Clin Chim Acta. 2014 Nov 1;437:211–7.
134. Monostori P, Szabó P, Marginean O, Bereczki C, Karg E. Concurrent Confirmation and Differential Diagnosis of Congenital Adrenal Hyperplasia from Dried Blood Spots: Application of a Second-Tier LC-MS/MS Assay in a Cross-Border Cooperation for Newborn Screening.

Horm Res pædiatrics. 2015;84(5):311–8.
135. Jeong J-S, Sim H-J, Lee Y-M, Yoon H-R, Kwon H-J, Hong S-P. Chromatographic diagnosis of maple syrup urine disease by measuring the L-alloisoleucine/L-phenylalanine ratio in dried blood spots. J Chromatogr B Analyt Technol Biomed Life Sci. 2011 Jul 15;879(22):2171–4.
136. Edelbroek PM, van der Heijden J, Stolk LML. Dried blood spot methods in therapeutic drug monitoring: methods, assays, and pitfalls. Ther Drug Monit. 2009 Jun;31(3):327–36.
137. Li W, Tse FLS. Dried blood spot sampling in combination with LC-MS/MS for quantitative analysis of small molecules. Biomed Chromatogr. 2010 Jan;24(1):49–65.
138. Török D, Mühl A, Votava F, Heinze G, Sólyom J, Crone J, et al. Stability of 17alpha-hydroxyprogesterone in dried blood spots after autoclaving and prolonged storage. Clin Chem. Clinical Chemistry; 2002 Feb;48(2):370–2.
139. Rashed MS. Clinical applications of tandem mass spectrometry: ten years of diagnosis and screening for inherited metabolic diseases. J Chromatogr B Biomed Sci Appl. 2001 Jul 5;758(1):27–48.
140. Chace DH. Mass spectrometry in newborn and metabolic screening: historical perspective and future directions. J Mass Spectrom. 2009 Feb;44(2):163–70.
141. Dénes J, Szabó E, Robinette SL, Szatmári I, Szőnyi L, Kreuder JG, et al. Metabonomics of newborn screening dried blood spot samples: a novel approach in the screening and diagnostics of inborn errors of metabolism. Anal Chem. 2012 Nov 20;84(22):10113–20.
142. Eyles D, Anderson C, Ko P, Jones A, Thomas A, Burne T, et al. A sensitive LC/MS/MS assay of 25OH vitamin D3 and 25OH vitamin D2 in dried blood spots. Clin Chim Acta. 2009 May;403(1–2):145–51.
143. Chao TC, Trybala A, Starov V, Das DB. Influence of haematocrit level on the kinetics of blood spreading on thin porous medium during dried blood spot sampling. Colloids Surfaces A Physicochem Eng Asp. 2014 Jun;451:38–47.
144. Chao TC, Arjmandi-Tash O, Das DB, Starov VM. Spreading of blood drops over dry porous substrate: Complete wetting case. J Colloid Interface Sci. Elsevier Inc.; 2015;446:218–25.
145. Holub M, Tuschl K, Ratschmann R, Strnadová KA, Mühl A, Heinze G, et al. Influence of hematocrit and localisation of punch in dried blood spots on levels of amino acids and acylcarnitines measured by tandem mass spectrometry. Clin Chim Acta. 2006;373(1):27–31.
146. Hoogtanders K, van der Heijden J, Christiaans M, Edelbroek P, van Hooff JP, Stolk LML. Therapeutic drug monitoring of tacrolimus with the dried blood spot method. J Pharm Biomed Anal. 2007 Jul 27;44(3):658–64.
147. Wiggins T, Kumar S, Markar SR, Antonowicz S, Hanna GB. Tyrosine, Phenylalanine, and Tryptophan in Gastroesophageal Malignancy: A Systematic Review. Cancer Epidemiol Biomarkers Prev. 2015 Jan;24(1):32–8.
148. Kim SM, Park Y-Y, Park ES, Cho JY, Izzo JG, Zhang D, et al. Robust prognostic biomarkers for esophageal adenocarcinoma identified by analysis of tumor transcriptome. PLoS One. 2010;5(11):e15074.
149. Wang Q, Ma C, Kemmner W. Wdr66 is a novel marker for risk stratification and involved in epithelial-mesenchymal transition of esophageal squamous cell carcinoma. BMC Cancer. 2013;13:137.
150. Kimchi ET, Posner MC, Park JO, Darga TE, Kocherginsky M, Karrison T, et al. Progression of Barrett's metaplasia to adenocarcinoma is associated with the suppression of the transcriptional programs of epidermal differentiation. Cancer Res. 2005 Apr 15;65(8):3146–54.
151. Holbrook JD, Parker JS, Gallagher KT, Halsey WS, Hughes AM, Weigman VJ, et al. Deep sequencing of gastric carcinoma reveals somatic mutations relevant to personalized medicine. J Transl Med. 2011;9:119.
152. Cheng L, Wang P, Yang S, Yang Y, Zhang Q, Zhang W, et al. Identification of genes with a correlation between copy number and expression in gastric cancer. BMC Med Genomics. 2012;5:14.
153. Detre S, Saclani Jotti G, Dowsett M. A "quickscore" method for immunohistochemical semiquantitation: validation for oestrogen receptor in breast carcinomas. J Clin Pathol. 1995 Sep;48(9):876–8.
154. Hasui K, Murata F. A new simplified catalyzed signal amplification system for minimizing non-specific staining in tissues with supersensitive immunohistochemistry. Arch Histol Cytol. International Society of Histology and Cytology; 2005;68(1):1–17.
155. Johnson CH, Ivanisevic J, Siuzdak G. Metabolomics: beyond biomarkers and towards mechanisms. Nat Rev Mol Cell Biol. 2016 Jul;17(7):451–9.
156. Wang D, Wang C, Pi X, Guo L, Wang Y, Li M, et al. Urinary volatile organic compounds as

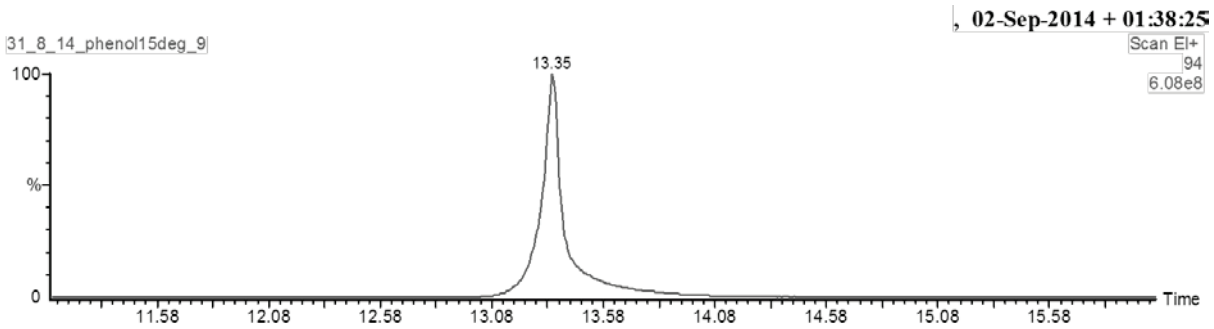
potential biomarkers for renal cell carcinoma. Biomed reports. 2016 Jul;5(1):68–72.
157. Haick H, Broza YY, Mochalski P, Ruzsanyi V, Amann A. Assessment, origin, and implementation of breath volatile cancer markers. Chem Soc Rev. 2014 Dec 4;43(5):1423–49.
158. Sung J, Kim N, Kim J, Jo HJ, Park JH, Nam RH, et al. Comparison of Gastric Microbiota Between Gastric Juice and Mucosa by Next Generation Sequencing Method. J cancer Prev. 2016 Mar;21(1):60–5.
159. Kumar S. Mass Spectrometric Analysis of Volatile Organic Compounds in Oesophago-Gastric Cancer. Imp Coll London - PhD Thesis. 2014.
160. Wu WM, Yang YS, Peng LH. Microbiota in the stomach: new insights. J Dig Dis. 2014;15(2):54–61.
161. Adamsson I, Nord CE, Lundquist P, Sjöstedt S, Edlund C. Comparative effects of omeprazole, amoxycillin plus metronidazole versus omeprazole, clarithromycin plus metronidazole on the oral, gastric and intestinal microflora in Helicobacter pylori-infected patients. J Antimicrob Chemother. Oxford University Press; 1999 Nov;44(5):629–40.
162. Mowat C, Williams C, Gillen D, Hossack M, Gilmour D, Carswell A, et al. Omeprazole, Helicobacter pylori status, and alterations in the intragastric milieu facilitating bacterial N-nitrosation. Gastroenterology. Elsevier; 2000 Aug;119(2):339–47.
163. Lu P-J, Hsu P-I, Chen C-H, Hsiao M, Chang W-C, Tseng H-H, et al. Gastric juice acidity in upper gastrointestinal diseases. World J Gastroenterol. 2010 Nov 21;16(43):5496–501.
164. Garcia-Mazcorro JF, Suchodolski JS, Jones KR, Clark-Price SC, Dowd SE, Minamoto Y, et al. Effect of the proton pump inhibitor omeprazole on the gastrointestinal bacterial microbiota of healthy dogs. FEMS Microbiol Ecol. 2012;80(3):624–36.
165. Zhang L, Ma J, Han Y, Liu J, Zhou W, Liu H, et al. Targeted therapy in esophageal cancer. Expert Rev Gastroenterol Hepatol. 2016;10(5):595–604.
166. Ganapathy V, Thangaraju M, Prasad PD. Nutrient transporters in cancer: Relevance to Warburg hypothesis and beyond. Pharmacol Ther. 2009;121(1):29–40.
167. Huang C, McConathy J. Fluorine-18 labeled amino acids for oncologic imaging with positron emission tomography. Curr Top Med Chem. 2013;13(8):871–91.
168. Chen W. Clinical applications of PET in brain tumors. J Nucl Med. 2007 Sep;48(9):1468–81.
169. Pauleit D, Stoffels G, Bachofner A, Floeth FW, Sabel M, Herzog H, et al. Comparison of (18)F-FET and (18)F-FDG PET in brain tumors. Nucl Med Biol. 2009 Oct;36(7):779–87.
170. Gempt J, Bette S, Ryang Y-M, Buchmann N, Peschke P, Pyka T, et al. 18F-fluoro-ethyl-tyrosine positron emission tomography for grading and estimation of prognosis in patients with intracranial gliomas. Eur J Radiol. 2015 May;84(5):955–62.
171. Bette S, Gempt J, Delbridge C, Kirschke JS, Schlegel J, Foerster S, et al. Prognostic Value of O-(2-[18F]-Fluoroethyl)-L-Tyrosine-Positron Emission Tomography Imaging for Histopathologic Characteristics and Progression-Free Survival in Patients with Low-Grade Glioma. World Neurosurg. 2016 May;89:230–9.
172. Schuster DM, Savir-Baruch B, Nieh PT, Master VA, Halkar RK, Rossi PJ, et al. Detection of recurrent prostate carcinoma with anti-1-amino-3-18F-fluorocyclobutane-1-carboxylic acid PET/CT and 111In-capromab pendetide SPECT/CT. Radiology. 2011 Jun;259(3):852–61.
173. Jager PL, Chirakal R, Marriott CJ, Brouwers AH, Koopmans KP, Gulenchyn KY. 6-L-18F-fluorodihydroxyphenylalanine PET in neuroendocrine tumors: basic aspects and emerging clinical applications. J Nucl Med. 2008 Apr;49(4):573–86.
174. Kodaira S, Nakajima T, Arisaka Y, Tokue A, Higuchi T, Tsushima Y. Advantages of L-3-[(18)F] fluoro-alpha-methyl tyrosine over 2-[(18)F]-fluoro-2-deoxyglucose in detecting liver metastasis during positron emission tomography scan. Springerplus. 2016;5:618.

APPENDIX 1: SUPPLEMENTARY FIGURES

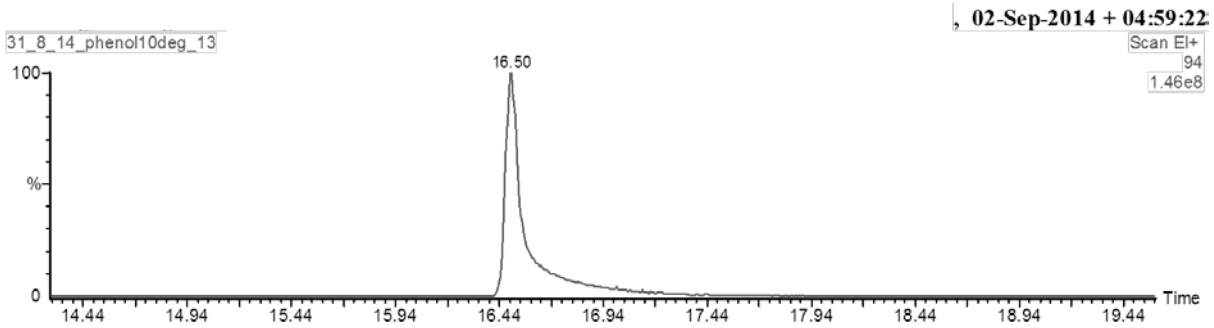
A



B

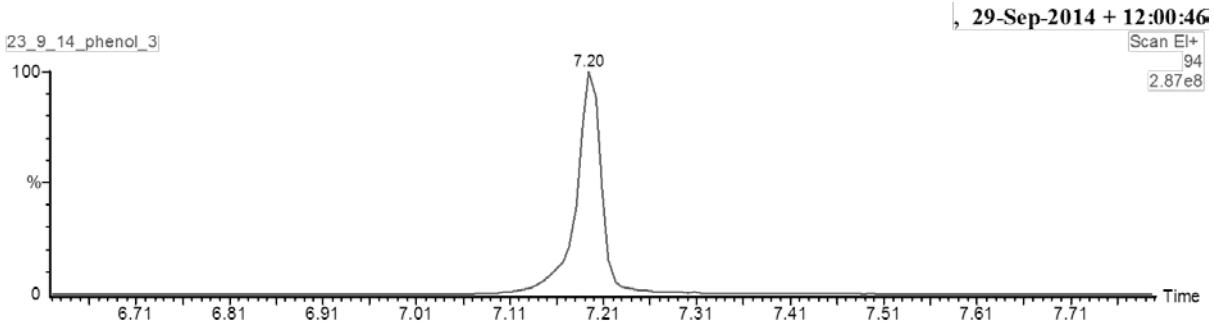


C

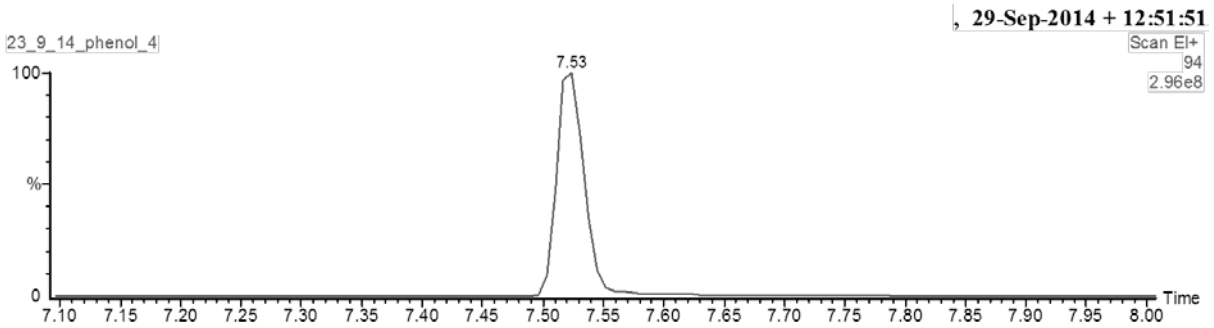


Supplementary Figure 1: Peak shape for phenol with temperature ramp set to 20°C per minute (A), 15°C per minute (B) and 10°C per minute (C).

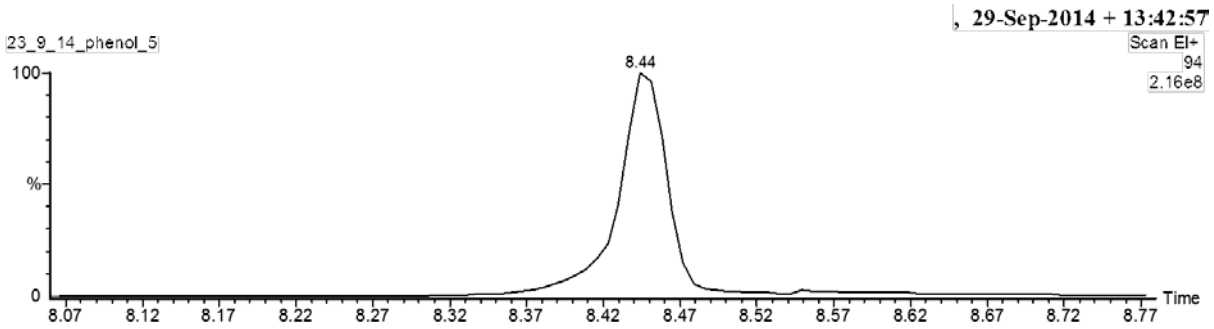
A



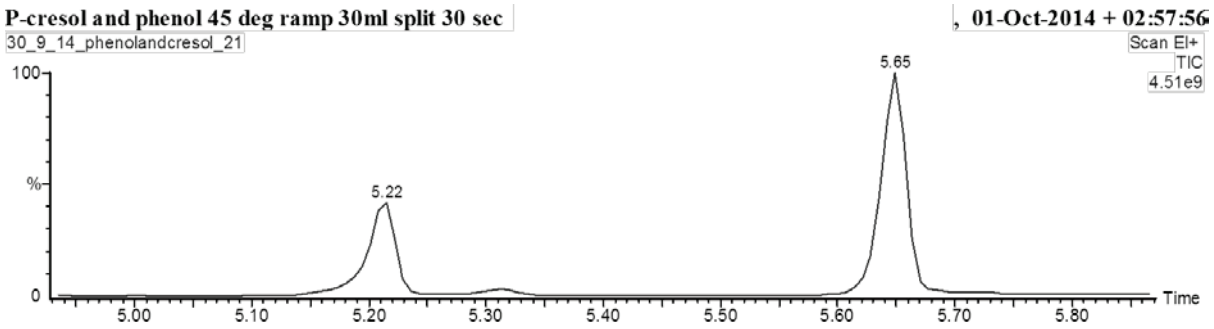
B



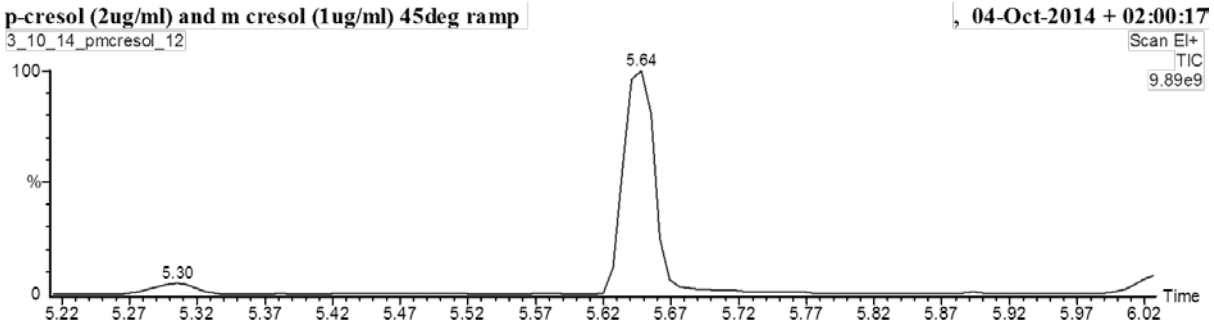
C



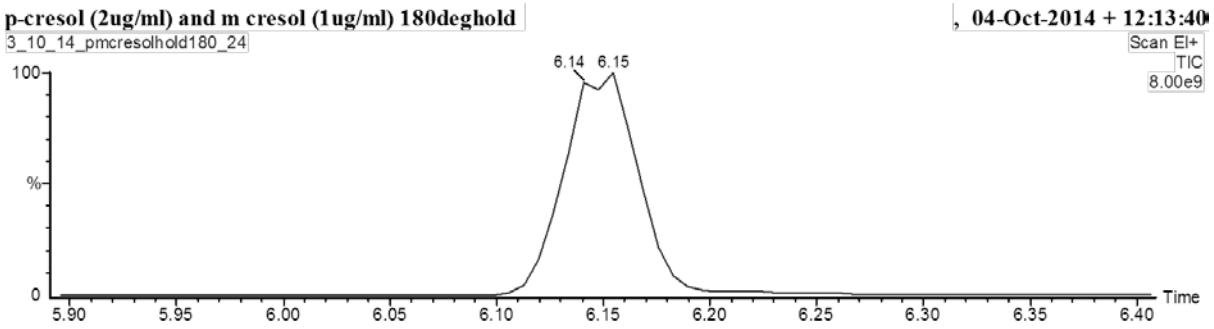
<u>Supplementary Figure 2:</u> Peak shape for phenol with temperature ramp set to 45°C per minute (A), 40°C per minute (B) and 30°C per minute (C).



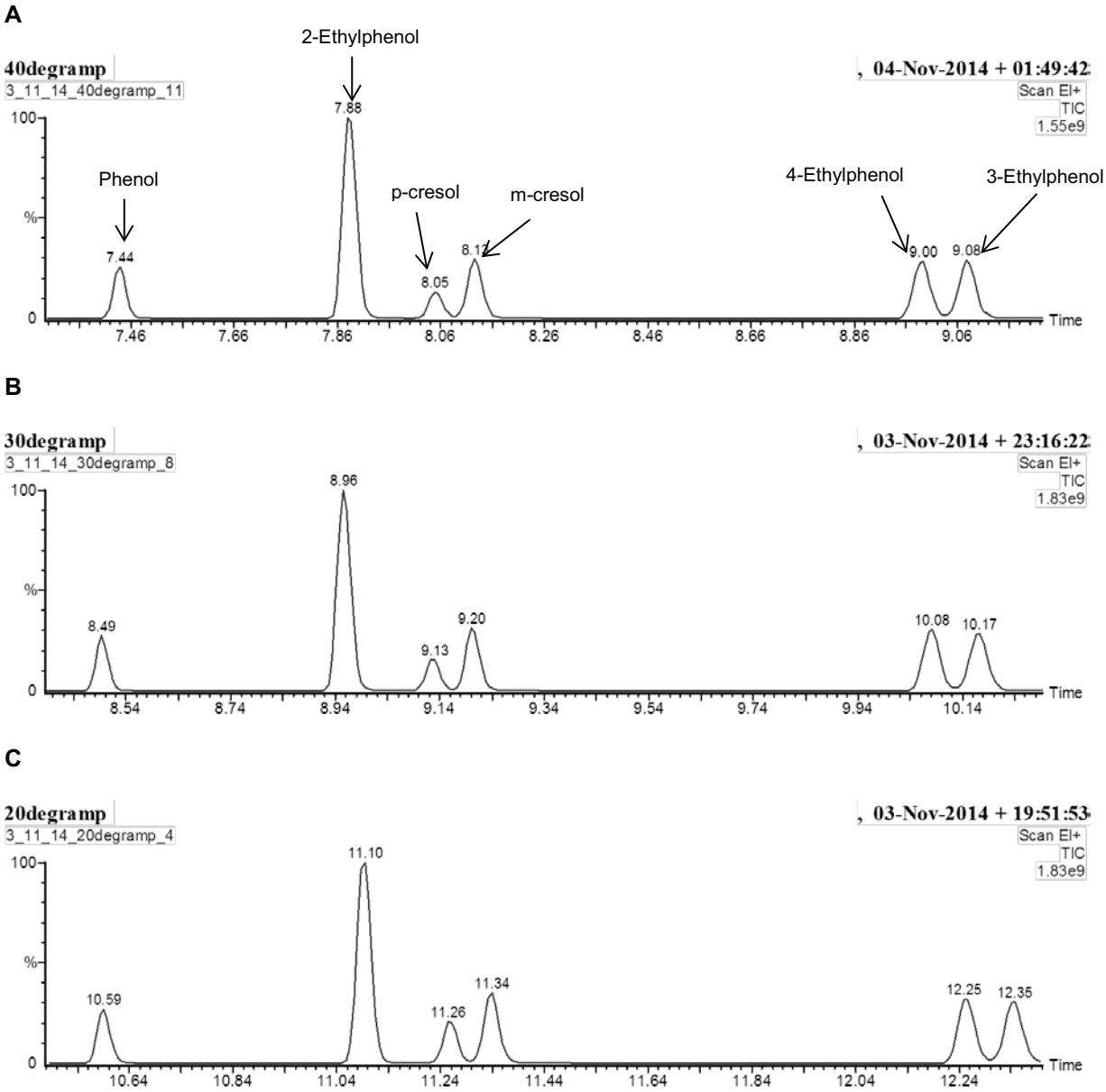
Supplementary Figure 3: *Peaks of phenol (5.22) and p-cresol (5.65) on this temperature programme.*



Supplementary Figure 4: *p and m-cresol eluting together at 5.64 minutes on this temperature programme.*

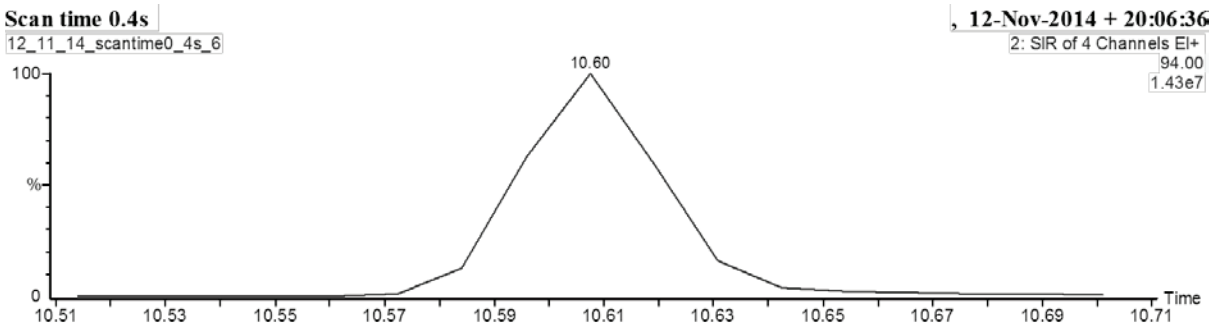


Supplementary Figure 5: *p and m-cresol still eluting together at 6.14/5 minutes.*

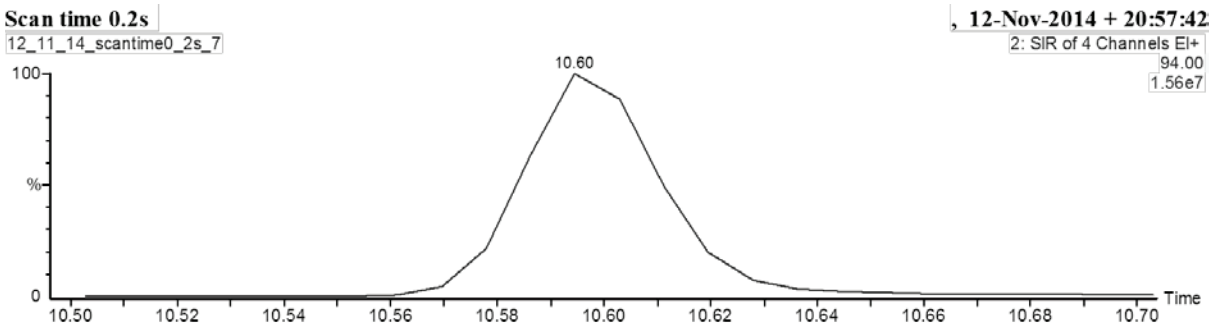


Supplementary Figure 6: Phenolic compound elution for 40°C/min ramp (A), 30°C/min ramp (B), and 20°C/min ramp (C).

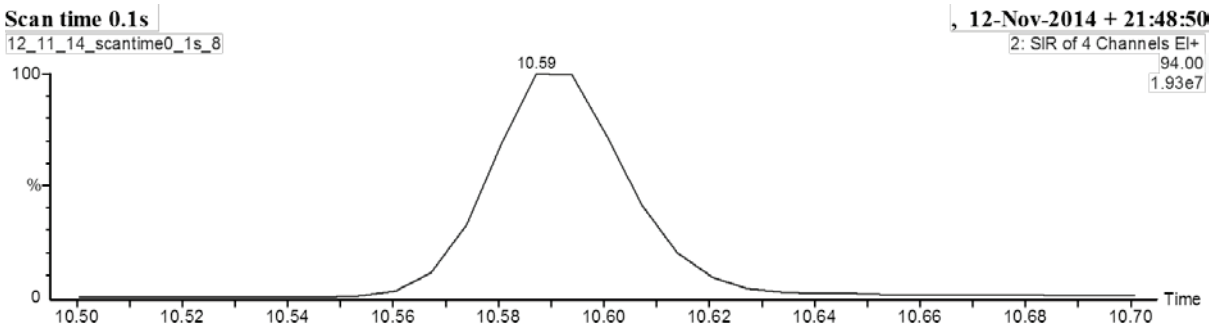
A



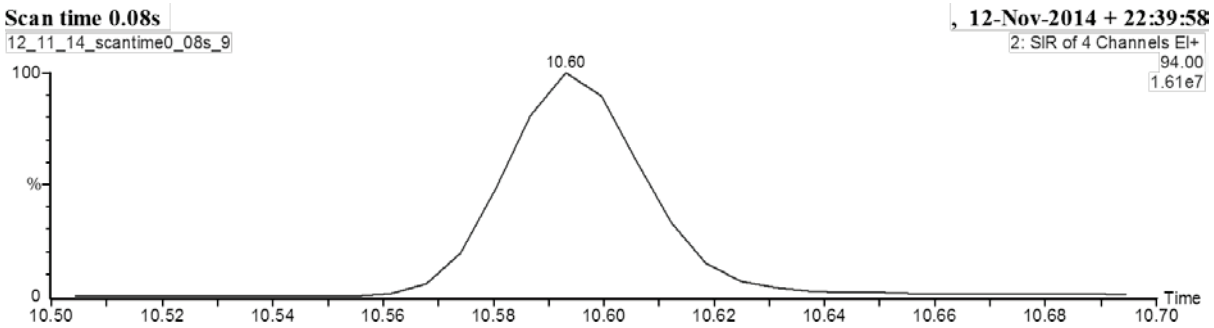
B



C

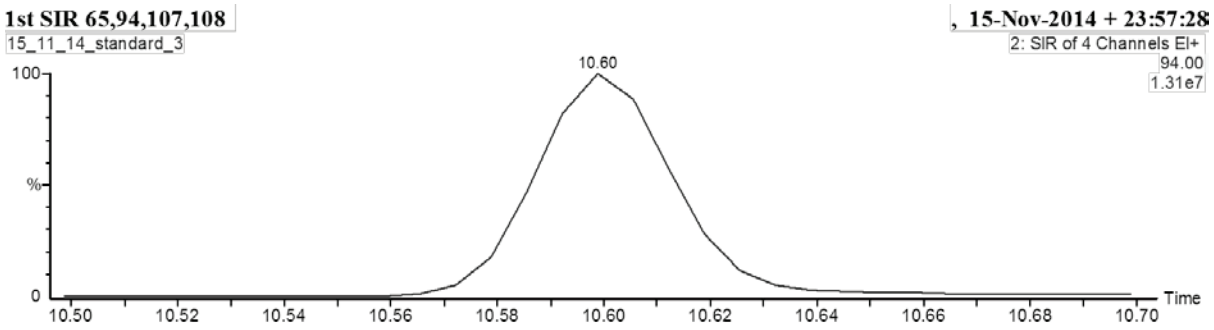


D

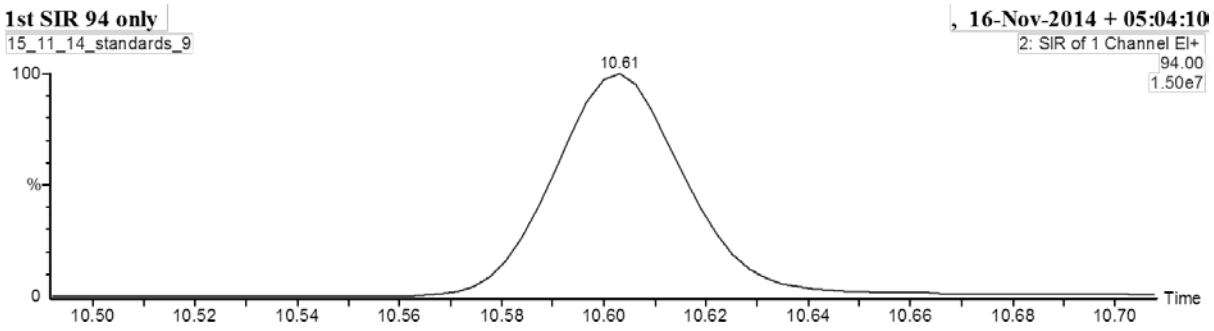


Supplementary Figure 7: Phenol peak shape on full scan mode with scan time of A: 0.4s; B: 0.2s; C: 0.1s; D: 0.08s.

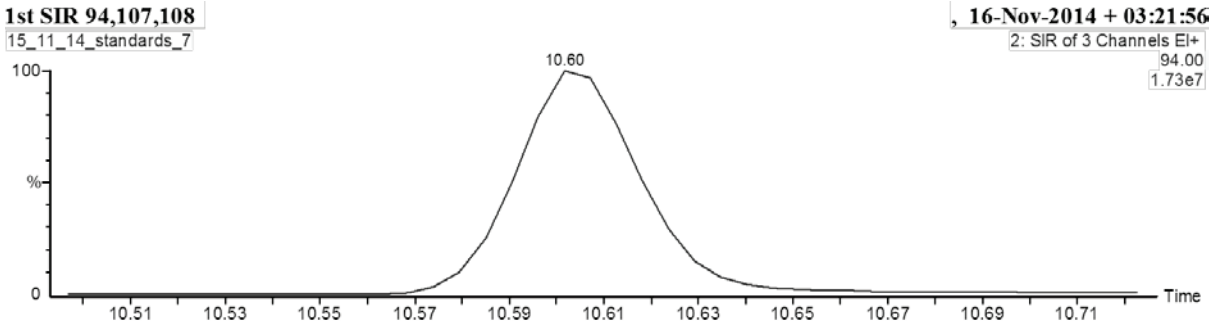
A



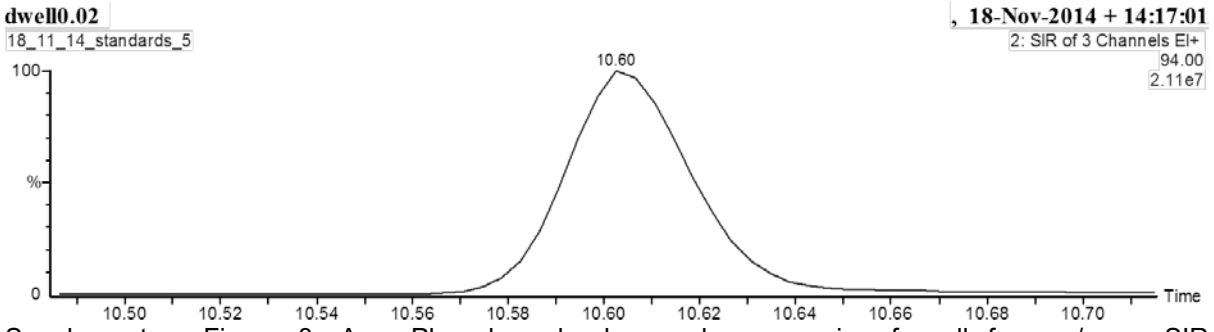
B



C



D

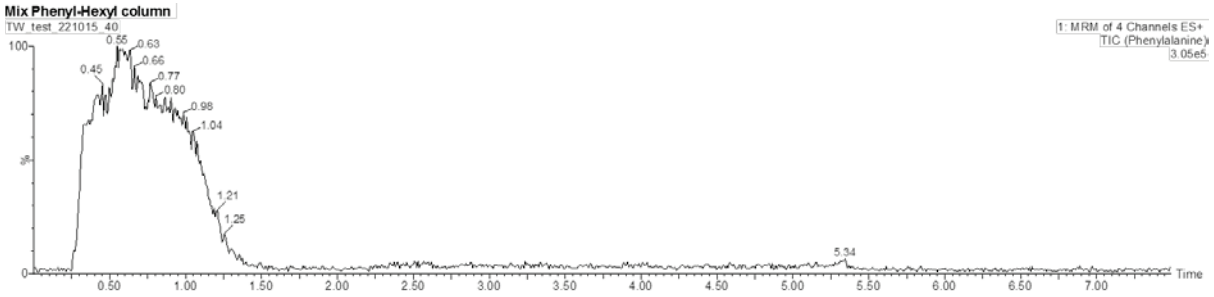


Supplementary Figure 8: A – Phenol peak shape when scanning for all four m/z on SIR (65,94,107,108); B – Scanning for 94 ion only; C – Scanning for m/z 94,107 and 108; D – Reduced dwell-time to 0.02s.

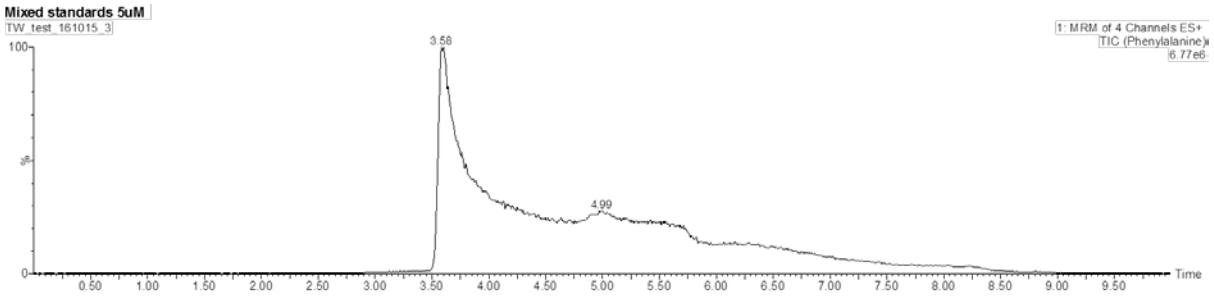
A

Time	Flow rate	A (%) (Water)	B (%) (Acetonitrile)
0	0.3	96	4
1	0.3	96	4
3	0.3	10	90
5	0.3	10	90
5.3	0.3	96	4
8	0.3	96	4

B



Supplementary Figure 9: A: Mobile phase gradient details for analysis with phenyl-hexyl column. B: Representative chromatogram showing lack of retention of phenylalanine with this column.



<u>Supplementary Figure 10:</u> Poor peak shape for phenylalanine with methanol as mobile phase B.

APPENDIX 2: SUPPLEMENTARY TABLE

Time	Flow rate	A (%) (Water)	B (%) (Acetonitrile)
0	0.3	3	97
2	0.3	3	97
5	0.3	50	50
7	0.3	50	50
7.1	0.3	3	97
9	0.3	3	97

Supplementary Table 1: Mobile phase gradient details for assessment of HILIC column.

APPENDIX 3: ETHICAL APPROVALS

Imperial College Healthcare Tissue Bank
Department of Surgery and Cancer,
Hammersmith Hospital,
Du Cane Road,
London W12 0HS
Tel: +44 7711 701382
Email: gerry.thomas@imperial.ac.uk

ICHTB HTA licence: 12275
REC Wales approval: 12/WA/0196

Professor George Hannah

Academic Surgical Department
10th Floor
QEQM Building
St Mary's Hospital
London
W2 1NY

1st January 2015

Dear George,

Re: Tissue Bank application number Project R14118; Investigation of phenol and aromatic amino acid metabolism in gastro-oesophageal cancer patients.

I am pleased to confirm that the Tissue Management Committee of the ICHTB has approved your application for access.

In order to satisfy HTA tracking requirements, would you please ensure the samples you use are reported to the tissue bank via the online database and sub-collection, along with any publications you produce, that should contain the acknowledgment wording as per the signed MTA.

Yours sincerely,

Professor Gerry Thomas
DI, Hammersmith HTA Research Licence.

Imperial College Healthcare Tissue Bank
Department of Surgery and Cancer,
Hammersmith Hospital,
Du Cane Road,
London W12 0HS
Tel: +44 7711 701382
Email: gerry.thomas@imperial.ac.uk

ICHTB HTA licence: 12275
REC Wales approval: 12/WA/0196

Professor George Hanna
Academic Surgical Department
10th Floor
QEQM Building
St. Mary's Hospital
London
W2 1NY

28th August 2015

Dear George,

Re: Tissue Bank application number Project R15065; Investigation of phenol and aromatic amino acid metabolism in gastro-oesophageal cancer patients.

I am pleased to confirm that the Tissue Management Committee of the ICHTB has approved your application for access.

In order to satisfy HTA tracking requirements, would you please ensure the samples you use are reported to the tissue bank via the online database and sub-collection, along with any publications you produce, that should contain the acknowledgment wording as per the signed MTA.

Yours sincerely,

Professor Gerry Thomas
DI, Hammersmith HTA Research Licence.

Imperial College Healthcare Tissue Bank
Department of Surgery and Cancer,
Charing Cross Hospital,
Fulham Palace Road,
London W6 8RF
Tel: 0208 311 7173
Email: tissuebank@imperial.ac.uk

ICHTB HTA licence: 12275
REC Wales approval: 12/WA/0196

Professor G. Hanna
Academic Surgical Department
10th Floor
QEQM Building
St. Mary's Hospital
London
W2 1NY

19/October /2016

Dear Prof Hanna,

Re: Tissue Bank application number R15097-1A; modified on 07/10/2016
Project title: Investigation of phenol and aromatic amino acid metabolism in gastro-oesophageal cancer patients

I am pleased to confirm that the Tissue Management Committee of the ICHTB has approved your amended application for access, modification include *analysis of sample in conjunction with Ingenza Ltd.* (duration 24 months)

In order to satisfy HTA tracking requirements, would you please ensure the samples you use are reported to the tissue bank via the online database and sub-collection, along with any publications you produce, that should contain the acknowledgment wording as per the signed MTA.

Yours sincerely,

Professor Gerry Thomas
DI, HTA Research Licence.

Cc: TM/tissue bank file